Supplementary Material to paper 'Estimating actual, potential, reference crop and pan evaporation using standard meteorological data: A pragmatic synthesis'

Thomas A McMahon, Murray C Peel, Lisa Lowe, R Srikanthan, Tim R McVicar

This supplementary material consists of a list of symbols and variables used in the paper and in the following 21 appendices. **Appendix S1** discusses data used or referred to in the appendices. **Appendix S2** addresses the computation of some common meteorological variables and **Appendix S3** outlines the computation of net solar radiation. The application of the evaporation models, Penman and Penman-Monteith, is discussed in **Appendices S4 and S5**. Computation of Class-A pan evaporation by the PenPan model is outlined in **Appendix S6**. Actual evaporation estimates using Morton, and Advection-Aridity and like models are discussed in **Appendices S7 and S8**. **Appendix S9** describes the computation of potential evaporation by several other models. Two methods to estimate deep lake evaporation where advected energy and heat storage should be accounted for are outlined in **Appendix S10** and **Appendix S11** describes the application of four methods to estimate shallow lake evaporation. The next four appendices deal with evaporation from lakes covered by vegetation (**Appendix S12**), estimating potential evaporation in rainfall-runoff modelling (**Appendix S13**), estimating evaporation from intercepted rainfall (**Appendix S14**) and estimating bare soil evaporation (**Appendix S15**). In **Appendix S16** there is a discussion of Class-A pan evaporation equations and pan coefficients. **Appendix S17** includes a summary of published evaporation estimates. **Appendix S18** is a summary of a comparison of evaporation estimates by 14 models for six sites across Australia. Detailed worked examples for most models are carried out in **Appendix S19**. **Appendix S20** is a Fortran 90 listing of Morton's WREVAP program and **Appendix S21** is a worked example of Morton's CRAE, CRWE and CRLE models within the WREVAP framework.

List of Supplementary Material

Figure S2 Plot showing Priestley-Taylor pan coefficients against mean annual unscreened Class-A pan evaporation based on six years of climate station data in Jordon (Weiβ and Menzel, 2008)

Figure S3 Comparison of monthly PenPan evaporation and Class-A pan evaporation for 68 Australian climate stations

List of variables and symbols in the paper and supplementary appendices excluding Appendices S20 and S21

Variable/symbol	Description	Units*
Symbols		
AA	Advection-Aridity model	symbol
AWBM	Rainfall-runoff model	symbol
AWS	Automatic Weather Station	symbol
BC	Blaney-Criddle evapotranspiration model	symbol
BS	Brutsaert-Strickler evaporation model	symbol
CR	Complementary Relationship	symbol
CRAE	Complementary Relationship Areal Evapotranspiration	symbol
CRLE	Complementary Relationship Lake Evaporation	symbol
CRWE	Complementary Relationship Wet-surface Evaporation	symbol
ET	Evapotranspiration	symbol
FAO56 RC	FAO-56 Reference Crop model	symbol
GG	Granger-Gray evaporation model	symbol
HS	Hargreaves-Samani evapotranspiration model	symbol
M	Month	symbol
Mo	Morton evaporation model	symbol
Ma	Makkink evaporation equation	symbol
modH	Modified Hargreaves evaporation model	symbol
PM	Penman-Monteith evapotranspiration model	symbol
PET	Potential evapotranspiration	symbol
PT	Priestley-Taylor evaporation model	symbol
P48	Penman equation with 1948 wind function	symbol
P56	Penman equation with 1956 wind function	symbol
SILO	An enhanced Australian climate database	symbol
SW	Shuttleworth-Wallace model	symbol
SHE	Système Hydrologique Européen rainfall-runoff model	symbol
SIMHYD	Rainfall-runoff model	symbol
SWAT	Soil and Water Assessment Tool	symbol
Th	Thornthwaite evapotranspiration model	symbol
TIN	Triangular irregular networks	symbol

Tu	Turc evaporation model	symbol
WREVAP	Program combining three Morton models CRAE, CRWE and CRLE	symbol
Variables		
A	Evaporating area	m^2
A_L	Lake area (in Kohler and Parmele (1967) procedure)	km^2, (m^2)
A_W	Net water advected energy during Δt (net inflow from inflows and outflows of water)	mm day^{-1}
A_e	Available energy (sensible and latent heat) above canopy	MJ m^{-2} day^{-1}
A_p	Gradient in Equation (S13.1)	undefined
A_w	Net water advected energy during Δt	mm day^{-1}
A_s	Surface area of the lake	m^2
A_{ss}	Available energy at sub-strate	MJ m^{-2} day^{-1}
A_{i+1} , A_i	Area of adjacent layers	m^2
a	Coefficient	undefined
a_p	Constant in PenPan equation	dimensionless
a_s	Constant for Ångström –Prescott formula	dimensionless
a_{Th}	Exponent in Thornthwaite 1948 procedure	undefined
a_o	Constant	dimensionless
b	Coefficient or slope of the regression between two variables	undefined
b_0	Constant , or constant in CRAE and CRWE models	dimensionless
b_s	Constant for Ångström –Prescott formula	dimensionless
b_{var}	Working variable	undefined
b_1, b_2	Empirical coefficients for Morton's procedure	W m^{-2}
B	Bowen Ratio	dimensionless
B_p	Intercept in Equation (S13.1)	undefined
C	Constant = 13 m	m
C_{HS}	Hargreaves-Samani working coefficient	undefined
C_o	Cloud cover	oktas
C_{ca} , C_{su}	Working variables	undefined
C_{ret}	Amount of water retained on the canopy	mm
c	Parameter in linear Budyko-type relationship	undefined
c_a	Specific heat of air	MJ kg^{-1}°C^{-1}

C_f	Fraction of cloud cover	dimensionless
c_o	Constant	dimensionless
c_s	Volumetric heat capacity of soil	MJ m^{-3} °C^{-1}
C_u	Wind function coefficient	undefined
c_w	Specific heat of water	MJ kg^{-1} °C^{-1}
C_D	Number of tenths of the sky covered by cloud	dimensionless
C_{atm}	Atmospheric conductance	m s^{-1}
C_{can}	Canopy conductance	m s^{-1}
C_{emp}	Empirical coefficient	undefined
D	Day or dimensionless relative drying power	dimensionless
DoY	Day of Year	dimensionless
D_p	Dimensionless relative drying power	dimensionless
d	Zero plane displacement height	m
$daymon$	Number of days in month	day
d_r	Relative distance between the earth and the sun	undefined
d_s	Effective soil depth	m
d_o	Constant	dimensionless
E	Surface evaporation	mm day^{-1}
$Elev$	Elevation above sea level	m
E_{Act}	Actual evaporation rate	mm day^{-1}
E_{EQ}	Equilibrium evaporation rate	mm day^{-1}
E_{Mak}	Makkink potential evaporation	mm day^{-1}
E_{PenPan}	Modelled Class-A (unscreened) pan evaporation	mm day^{-1}
E_i	Lake evaporation on day i	mm day^{-1}
E_{pa}	Working variable	undefined
$EP2$, $EP3$, $EP5$	Various definitions of potential evaporation	undefined
E_{SW}	Shuttleworth-Wallace combined evaporation from vegetation and soil	mm day^{-1}
$E_{PT}(T_e)$	Wet-environment evaporation estimated by Priestley-Taylor at T_e	mm day^{-1}
$E_{Pen,j}$	Penman estimate of evaporation for specific period	mm/unit time
E_{DL}	Evaporation from a deep lake	mm day^{-1}
E_L	Lake evaporation large enough to be unaffected by the upwind transition	mm day^{-1}
E_{McJ}	Evaporation from a water body using McJannet et al (2008a)	mm day^{-1}

E_{PT}	Priestley-Taylor potential evaporation	mm day^{-1}
$E_{Pan,j}$	Monthly (daily) Class-A pan data in month (day) *j*	mm/unit time
E_{Pan}	Daily Class-A pan evaporation	mm day^{-1}
E_{Pen}	Penman potential evaporation	mm day^{-1}
E_{PenOW}	Penman open-surface water evaporation	mm day^{-1}
E_{Pot}	Potential evaporation (in the land environment) or pan-size wet surface evaporation	mm day^{-1}
E_{SL}	Shallow lake evaporation	mm month^{-1}
E_s	Evaporation component due to net heating	mm day^{-1}
E_{can}	Transpiration from canopy	mm day^{-1}
E_{soil}	Soil evaporation	mm day^{-1}
E_{water}	Evaporation from standing water	mm day^{-1}
$\bar{E}_{Trans}$	Mean transpiration	mm day^{-1}
$\bar{E}_{Inter}$	Mean interception evaporation	mm day^{-1}
$E_{wetland}$	Evapotranspiration from the wetland	mm day^{-1}
$\bar{E}_{pot}$	Mean annual catchment potential evapotranspiration	mm year^{-1}
$\bar{E}_{Soil}$	Mean soil evaporation	mm day^{-1}
$E_{L,d}$	Daily estimate of lake evaporation from Webb (1966) equation	cm day^{-1}
E'_{pan}	Daily Class-A pan evaporation from Webb (1966) equation	cm day^{-1}
E'_{PenOW}	Open-water evaporation based on modified Penman equation incorporating aerodynamic resistance	mm day^{-1}
$E_{1^{st}}$, $E_{2^{nd}}$	Radiation and aerodynamic terms respectively in the PM model	mm day^{-1}
$\bar{E}_{Th,j}$	Thornthwaite (1948) estimate of mean monthly PET for month *j*	mm month^{-1}
E_{SLx}	Average lake evaporation for a crosswind width of *x* m	mm day^{-1}
$\bar{E}_{Penman}$	Average daily stage 1 evaporation which is assumed to be at or near the rate of Penman evaporation	mm day^{-1}
$\bar{E}_{Act}$	Mean annual catchment evaporation	mm year^{-1}
ET_{Act}	Actual daily evaporation	mm day^{-1}
ET_c	Well-watered crop evapotranspiration in a semi-arid windy environment	mm day^{-1}
ET_{Act}^{BS}	Actual evapotranspiration estimated by Brutsaert-Strickler equation	mm day^{-1}
ET_{Act}^{GG}	Granger-Gray actual evapotranspiration	mm day^{-1}
ET_{Act}^{SJ}	Actual evapotranspiration based on the Szilagyi-Jozsa equation	mm day^{-1}
ET_{BC}	Evaporation based on the Blaney-Criddle method without	mm day^{-1}

	height adjustment	
ET_{BC}^{H}	Evaporation based on the Blaney-Criddle method with height adjustment	mm day^{-1}
ET_{Act}^{Mo}	Morton's estimate of actual areal evapotranspiration	mm day^{-1}
ET_{Pot}^{Mo}	Morton's estimate of potential evapotranspiration	mm day^{-1}
ET_{Wet}^{Mo}	Morton's estimate of wet-environmental areal evapotranspiration	mm day^{-1}
ET_{HS}	Hargreaves-Samani reference crop evapotranspiration	mm day^{-1}
$ET_{Harg,j}$	Modified Hargreaves monthly potential evapotranspiration (month j)	mm month^{-1}
ET_P	Potential evaporation of the land environment	mm day^{-1}
ET_{PET}	Daily potential evaporation	mm day^{-1}
ET_{PM}	Penman-Monteith potential evapotranspiration	mm day^{-1}
ET_{Pot}	Potential evapotranspiration	mm day^{-1}
ET_{RC}	Reference crop evapotranspiration	mm day^{-1}
ET_{RCsh}	Reference crop evapotranspiration for short grass (0.12 m high)	mm day^{-1}
ET_{RCta}	Reference crop evapotranspiration for tall grass (0.5 m high)	mm day^{-1}
ET_{Turc}	Turc's reference crop evapotranspiration	mm day^{-1}
ET_{Wet}	Wet environment areal evapotranspiration	mm day^{-1}
ET_{eqPM}	Daily equivalent Penman-Monteith potential evapotranspiration	mm day^{-1}
$\overline{ET}_{Act}$	Mean annual catchment evapotranspiration	mm year^{-1}
E_a	Aerodynamic component of Penman's equation; regional drying power of atmosphere; evaporative component due to wind	mm day^{-1}
E_{Larea}	Estimate of open-surface water evaporation as a function of lake area	mm day^{-1}
$E_{fw,j}$	Monthly (daily) open water evaporation in month (day) j	mm/unit time
E_{fw}	Daily open water evaporation	mm day^{-1}
E_{ic}	Evaporation from an irrigation channel	mm day^{-1}
$E_{bsoil}(t)$	Cumulative bare soil evaporation up to time t	mm
$E_{stage\ 1}$	Cumulative stage 1 bare soil evaporation	mm
e	Turc-Pike parameter	dimensionless
$e_0, e_1, \dots, e_4$	Coefficients in Blaney-Criddle model	undefined
F	Upwind grass fetch	m
FET	Fetch or length of the identified surface	m
F_{100}	Working variable	undefined

f	Fu-Zhang parameter	dimensionless
$f(\phi)$	Aridity function	undefined
$f(u)$	Wind speed function	units of u
$f(u_2)$	Wind speed function at u_2	units of u_2
$f(u)_{48}$	1948 Penman wind function	units of u
$f(u)_{56}$	1956 Penman wind function	units of u
$f(u)_{LIN}$	Linacre Penman wind function	units of u
$f_{Pan}(u)$	Wind function for Class-A pan	units of u
f_{dir}	Fraction of R_s that is direct	dimensionless
f_v	Vapour transfer coefficient in Morton's procedure	W m^{-2} $mbar^{-1}$
f_Z	Constant in Morton's procedure	W m^{-2} $mbar^{-1}$
G	Soil heat flux	MJ m^{-2} day^{-1}
G_L	Monthly solar and waterborne energy input into lake for Morton's procedure	W m^{-2}
G_w	Daily change in heat storage of water body	MJ m^{-2} day^{-1}
$G_w(t)$	$dH(t)/dt$	MJ m^{-2} day^{-1}
G_{LB}	Available solar and waterborne heat energy at the beginning of the month for Morton's procedure	W m^{-2}
G_{LE}	Available solar and waterborne heat energy at the end of the month for Morton's procedure	W m^{-2}
$G_W^{[t]}$, $G_W^{[t+1]}$	Value of G_W^0 computed $[t]$ and $[t+1]$ months previously for Morton's procedure	W m^{-2}
G_W^0	Solar and waterborne heat input for Morton's procedure	W m^{-2}
GW_{in}	Groundwater inflows to lake	mm day^{-1}
GW_{out}	Groundwater outflows from lake	mm day^{-1}
G_W^t	Delayed energy input into the lake for Morton's procedure	W m^{-2}
G_g	Dimensionless relative evaporation parameter	dimensionless
$\bar{G}$	Mean heat conductance into the soil	MJ m^{-2} day^{-1}
G_j	Coefficient in Equation (S16.4)	undefined
G_{sc}	Solar constant	MJ m^{-2} min^{-1}
$\bar{G}_{DS}$	Mean annual deep seepage	mm $year^{-1}$
g	Working variable	undefined
H	Sensible heat flux	MJ m^{-2} day^{-1}
$\bar{H}$	Mean sensible heat flux	MJ m^{-2} day^{-1}
$H(t)$	Total heat energy content of the lake per unit area of the lake surface at time t	MJ m^{-2}

h	Mean height of the roughness obstacles (including crop)	m
h_w	Water depth	m
h_i, h_{i+1}	Depth of water in lake on day i and day $i+1$ respectively	m
$\bar{h}$	Mean lake depth	m
$\overline{hrday}$	Mean monthly daylight hours in month	hour
i	Monthly heat index	undefined
i, *i-1*	Index for days	undefined
I	Annual heat index	undefined
I_j	Intercept in Equation (S16.4)	undefined
j, *j-1*	Index for months	undefined
K_c	Crop coefficient	dimensionless
K_E	Coefficient that represents the efficiency of the vertical transport of water vapour	m day^2 kg^{-1}
K_{us}	Unsaturated hydraulic conductivity	mm day^{-1}
K_j	Monthly (daily) Class-A pan coefficient	dimensionless
K_{ratio}	Ratio of incoming solar radiation to clear sky radiation	dimensionless
K_{Pan}	Class-A pan coefficient	dimensionless
k	von Kármán’s constant	dimensionless
lat	Latitude	radians
LAI	Leaf area index	m^2 m^{-2}
LAI_{active}	Active (sunlit) leaf area index	m^2 m^{-2}
m	Number of horizontal layers	dimensionless
M	Month of the year	dimensionless
N	Total day length	hour
n	Duration of sunshine hours in a day	hour
P_d	Daily precipitation	mm day^{-1}
PM_{ca}, PM_{su}	Evaporation from respectively a closed canopy and bare substrate	mm day^{-1}
$\bar{P}$	Mean rainfall or mean annual rainfall	mm day^{-1}, mm year^{-1}
P_{i+1}	Rainfall on day $i+1$	mm day^{-1}
P_j	Monthly precipitation in month j	mm month^{-1}
P_{rad}	Pan radiation factor	dimensionless
p	Atmospheric pressure (for Morton’s procedure)	kPa (mbar)
p_s	Sea-level atmospheric pressure	mbar

p_y	Percentage of actual daytime hours for the specific day compared to the day-light hours for the entire year	%
Q_t	Heat flux increase in stored energy	MJ m^{-2} day^{-1}
Q_v	Heat flux advected into the water body	MJ m^{-2} day^{-1}
$\bar{Q}$	Mean runoff or mean annual runoff	mm day^{-1}, mm year^{-1}
Q^*	Net radiation	MJ m^{-2} day^{-1}
Q^*_{wb}	Net radiation at wet-bulb temperature	MJ m^{-2} day^{-1}
RH	Average monthly relative humidity	%
$\bar{R}$	Mean net radiation received	MJ m^{-2} day^{-1}
REW	Readily evaporable water	mm
R_{il}	Incoming longwave radiation	MJ m^{-2} day^{-1}
R_{ol}	Outgoing longwave radiation	MJ m^{-2} day^{-1}
RH_{max}	Maximum daily relative humidity	%
RH_{mean}	Mean daily relative humidity	%
RH_{min}	Minimum daily relative humidity	%
R_a	Extraterrestrial radiation	MJ m^{-2} day^{-1}
R_{NPan}	Net radiation at Class-A pan	MJ m^{-2} day^{-1}
R_{SPan}	Total shortwave irradiance of pan	MJ m^{-2} day^{-1}
R_{il}	Incoming longwave radiation	MJ m^{-2} day^{-1}
R_n	Net radiation at evaporating surface at air temperature (for Morton's procedure)	MJ m^{-2} day^{-1} (W m^{-2})
R_{ne}	Net radiation for the soil-plant surface at T_e for Morton's procedure	W m^{-2}
R_{nl}	Net longwave radiation	MJ m^{-2} day^{-1}
R_{ns}	Net incoming shortwave radiation	MJ m^{-2} day^{-1}
R_{nw}	Net radiation at water surface	MJ m^{-2} day^{-1}
R_{ol}	Outgoing longwave radiation	MJ m^{-2} day^{-1}
R_s	Measured or estimated incoming solar radiation	MJ m^{-2} day^{-1}
R_{so}	Clear sky radiation	MJ m^{-2} day^{-1}
R_n^{can}	Net radiation to canopy	MJ m^{-2} day^{-1}
R_n^{soil}	Net radiation to soil	MJ m^{-2} day^{-1}
R_n^{water}	Net radiation to water based on surface water temperature	MJ m^{-2} day^{-1}
R_n^{w}	Net daily radiation based on water temperature	MJ m^{-2} day^{-1}
R_{ol}^{wa}	Outgoing longwave radiation based on water temperature	MJ m^{-2} day^{-1}
R_{ol}^{wb}	Outgoing longwave radiation based on wet-bulb temperature	MJ m^{-2} day^{-1}

R_{wb}^{*}	Net radiation to water based on wet-bulb temperature	MJ m^{-2} day^{-1}
R^2	Square of the correlation coefficient	dimensionless
RMSE	Root mean square error	various
r_{clim}	Climatological resistance	s m^{-1}
r_a	Aerodynamic or atmospheric resistance to water vapour transport	s m^{-1}
r_c	Bulk stomatal resistance	s m^{-1}
r_l	Bulk stomatal resistance of a well-illuminated leaf	s m^{-1}
r_c^{50}	Aerodynamic resistance for crop height, h	s m^{-1}
r_s	Surface resistance	s m^{-1}
$(r_s)_c$	Surface resistance of a well-watered crop equivalent to FAO crop coefficient	s m^{-1}
R_A	Average monthly extraterrestrial solar radiation	MJ m^{-2} day^{-1}
r_a^a	Aerodynamic resistance between canopy source height and reference level	s m^{-1}
r_a^c	Bulk boundary layer resistance of vegetation elements in canopy	s m^{-1}
r_a^s	Aerodynamic resistance between substrate and canopy source height	s m^{-1}
r_s^c	Bulk stomatal resistance of canopy	s m^{-1}
r_s^s	Surface resistance of substrate	s m^{-1}
S	Proportion of bare soil	dimensionless
S_{con}	Solar constant	MJ m^{-2} day^{-1}
S_O	Mean water equivalent for extraterrestrial solar radiation in month j	mm $month^{-1}$
SEE	Standard error of estimate	units of dependent variable
SM	Soil moisture level	mm
SW_{in}	Surface water inflows to lake	mm day^{-1}
SW_{out}	Surface water outflows from lake	mm day^{-1}
S_c	Storage constant	month
S_{can}	Storage capacity of the canopy	mm
s	Lake salinity for Morton's procedure	ppm
T	Temperature, the generalised Turc-Pike coefficient	°C, undefined
TEW	Total evaporable water	mm
T_a	Air temperature	°C
T_d	Dewpoint temperature	°C

T_e	Equilibrium temperature (at evaporating surface)	°C
T_j	Monthly mean daily air temperature in month j	°C
T_{pan}	Mean daily pan water temperature	°C
T_s	Temperature of the surface or evaporated water	°C
T_w	Temperature of the water	°C
T_{wb}	Wet-bulb temperature	°C
T_{w0}	Temperature from previous time-step	°C
$T_{w,j} - T_{w,j-1}$	Change in surface water temperature from month $j-1$ to month j	°C
T_{L1}, T_{L2}	Average lake temperature at the beginning and end of period	°C
$T_e^{'}$	Working estimate of the equilibrium temperature	°C
T_{gwin}	Temperature of the groundwater inflows to lake	°C
T_{gwout}	Temperature of the groundwater outflows from lake	°C
T_i , T_{i-1}	Average air temperatures on day i and day $i-1$ respectively	°C
$T_{w,i}, T_{w,i-1}$	Surface water temperatures on day i and day $i-1$ respectively	°C
T_{max}	Maximum daily air temperature	°C
T_{min}	Minimum daily air temperature	°C
T_{mean}	Mean daily temperature	°C
T_p	Temperature of precipitation	°C
T_{swin}	Temperature of the surface water inflows to lake	°C
T_{swout}	Temperature of the surface water outflows from lake	°C
$\bar{T}$	Mean monthly air temperature	°C
$\bar{T}_j$	Mean monthly air temperature in month j	°C
$\overline{TD}_j$	Mean monthly difference between mean daily maximum air temperature and mean daily minimum air temperature (month j)	°C
t	Cumulative time of bare soil evaporation	day
t_L	Lake lag time	month
t_1	Length of the stage-1 atmosphere-controlled bare soil evaporation period	day
t_{day}	Local time of day	undefined
t_0	Intermediate variable defined by Equation (S7.15)	month
t_m	Number of days in the month	day
$[t_L]$	Integral component of lag time	month
$T_w(z_i)$, $T_w(z_{i+1})$	Water temperature at depths z_i and z_{i+1}	°C

u	Mean daily wind speed	m day^{-1}
u_2	Average daily wind speed at 2 m height (original Penman 1948 and 1956 and Linacre wind function)	m s^{-1}, (miles day^{-1})
u_{10}	Average daily wind speed at 10 m height	m s^{-1}
u_{Pan}	Average daily wind speed over pan	m s^{-1}
u_z	Average daily wind speed at height z	m s^{-1}
u_*	Friction velocity	m s^{-1}
$\bar{u}$	Mean wind speed	m s^{-1}
VPD	Vapour pressure deficit	kPa
V_i	Volume of each layer	m^3
V_1, V_2	Lake volume at the beginning and end of period	m^3
VPD_2, VPD_{50}	Vapour pressure deficit at 2m and 50 m respectively	kPa
W	Proportion of open water	dimensionless
w	Plant available water coefficient in Zhang 2-parameter model	dimensionless
x	Cross wind width of lake	m
z	Height of wind speed measurement	m
z_e	Depth of surface soil layer	m
$z_{i+1} - z_i$	Thickness of each layer	m
z_2	Height above ground of the water vapour measurement	m
z_1	Height above ground of the wind speed measurement	m
z_h	Height of the humidity measurements	m
z_d	Zero-plane displacement	m
z_m	Height of the instrument above ground	m
z_o	Roughness length or roughness height	m
z_{oh}	Roughness length governing transfer of heat and vapour	m
z_{om}	Roughness length governing momentum transfer	m
z_{ov}	Roughness length governing water transfer	m
α	Albedo of the evaporating surface	dimensionless
α_A	Albedo for Class-A pan	dimensionless
α_{KP}	Proportion of the net addition of energy from advection and storage used in evaporation during Δt	dimensionless
α_{SS}	Albedo of ground surface surrounding evaporation pan	dimensionless
α_{pan}	Proportion of energy exchanged through sides of evaporation pan	dimensionless

α_{PT}	Priestley-Taylor coefficient	dimensionless
γ	Psychrometric constant (for Morton's procedure)	kPa ° C^{-1} (mbar °C^{-1})
Δ	Slope of the saturation vapour pressure curve	kPa °C^{-1}
Δ'	dv_T^*/dT slope of the saturation vapour pressure curve at T	kPa °C^{-1}
ΔH	Change in heat storage (net energy gained from heat storage in the water body)	MJ m^{-2} day^{-1}
ΔQ	Change in stored energy during Δt	mm day^{-1}
ΔS	Change in soil moisture storage or stored water	mm day^{-1}, mm $year^{-1}$
ΔW	Change in heat storage in water column during the current time step	MJ m^{-2} day^{-1}
Δt	Time interval	day
Δ_e	Slope of the saturation vapour pressure curve at temperature T_e for Morton's procedure	mbar °C^{-1}
Δ_w	Slope of the vapour pressure curve at water temperature	kPa °C^{-1}
Δ_{wb}	Slope of the vapour pressure curve at wet-bulb temperature	kPa °C^{-1}
$\Delta(T_e)$	Slope of the vapour pressure curve at temperature T_e	kPa °C^{-1}
$\Delta H_{j,j-1}$	Change in heat storage from month $j-1$ to month j for Vardavas and Fountoulakis (1996) procedure	W m^{-2}
ΔT_{wl}	Change in lake surface water temperature month $j-1$ to month j	°C
Δ_e'	Working estimate of the slope of the saturation vapour pressure curve at T_e for Morton's procedure	mbar °C^{-1}
δ	Solar declination	radians
δh	Difference between heat content of inflows and outflows from lake for Morton's procedure	W m^{-2}
δT_e	A small change in the equilibrium temperature	undefined
δv_e	$= \Delta_e' \delta T_e$	undefined
ε_s	Surface emissivity	dimensionless
ε	Ratio of the temperature variations in the latent heat and sensible heat contents of saturated air	dimensionless
ε_w	Emissivity of water	dimensionless
θ	Sun's altitude	degrees
θ_{FC}	Soil moisture content at field capacity	%
θ_{WP}	Soil moisture content at wilting point	%
λ	Latent heat of vaporisation (for Morton's procedure)	MJ kg^{-1} (W day kg^{-1})
λ_e	Working variable	undefined
ξ	Dimensionless stability factor	dimensionless

τ	Time constant for the storage	day
υ	Kinematic viscosity of air	$m^2\ s^{-1}$
v_4	Afternoon average vapour pressure 4 m above ground for Webb (1966) procedure	mbar
v_a	Mean daily actual vapour pressure at air temperature	kPa
v_d	Vapour pressure at the reference height	kPa
v_a^*	Daily saturation vapour pressure at air temperature (for Morton's procedure)	kPa (mbar)
v_e^*	Saturation vapour pressure at T_e (for Morton's procedure)	kPa (mbar)
v_D^*	Saturation vapour pressure at dew point temperature for Morton's procedure	mbar
v_L^*	Afternoon average lake saturation vapour pressure for Webb (1966) procedure	mbar
v_P^*	Afternoon maximum pan saturation vapour pressure for Webb (1966) procedure	mbar
$(v_a^* - v_a)$	Vapour pressure deficit at air temperature	kPa
v_s^*	Saturation vapour pressure at the water surface	kPa
v_w^*	Saturation vapour pressure at the evaporating surface	kPa
$v_a(T_a)$	Vapour pressure at a given height above the water surface evaluated at the air temperature T_a for Vardavas and Fountoulakis (1996) procedure	mbar
$v_a^*(T_a)$	Saturated vapour pressure at the water surface evaluated at air temperature T_a for Vardavas and Fountoulakis (1996) procedure	mbar
$v_e^{*'}$	Working estimate of the saturation vapour pressure at equilibrium temperature (for Morton's procedure)	mbar
v_T^*	Saturation vapour pressure at temperature, T	mbar
$v_{T_a}^*$	Saturation vapour pressure at air temperature, T_a	kPa
$v_{T_s}^*$	Saturation vapour pressure at surface temperature, T_s	kPa
$\bar{v}_a$	Mean daily actual vapour pressure	kPa
ρ_a	Mean air density at constant pressure	$kg\ m^{-3}$
ρ_w	Density of water	$kg\ m^{-3}$
σ	Stefan-Boltzmann constant (for Morton's procedure)	$MJ\ K^{-4}\ m^{-2}\ day^{-1}$ $(W\ m^{-2}\ K^{-4})$
ϕ	Aridity index	dimensionless
ω_s	Sunset hour angle	radian
Ω	Decoupling coefficient	dimensionless
$\eta_a,\ \eta_c,\ \eta_s$	Working variables	undefined

v^*_{Tmax}	Saturated vapour pressure at Tmax	kPa
v^*_{Tmin}	Saturated vapour pressure at Tmin	kPa

*Where possible a consistent set of units is used throughout the paper and supplementary appendices except for **Appendices S20 and S21** which relate to Morton's (1983a, b and 1986) procedures. In this list of variables where the units are different from the common set, model names or references are included in the description. Non-SI units are either included in parenthesis along with the model name or the relevant reference is included in parenthesis in the description or, if listed separately, the model name or the relevant reference is also included. For some intermediate and working variables and where the source reference has not identified, the units are described as undefined.

Supplementary Material

Appendix S1 Data

In this appendix, five issues are addressed – sources of climate data in Australia, climate data used in the analyses reported in later appendices, remotely sensed actual evapotranspiration, daily and monthly data, and location of meteorological stations relative to the target evaporating site.

Sources of climate data in Australia

1. In Australia at Automatic Weather Stations (AWSs) maintained by the Bureau of Meteorology and other operators, the following data as a minimum are monitored at a short time-step and are recorded as cumulative or average values over a longer interval: rainfall, temperature, humidity, wind speed and direction, and atmospheric pressure. Information is available at:

http://www.bom.gov.au/inside/services_policy/pub_ag/aws/aws.shtml

For Australian at-site daily wind data, it is recommended that, if available, 24-hour wind run data (km day^{-1}) be used and converted to wind speed (m s^{-1}).

2. Class-A pan evaporation data are also measured on a daily basis and, at some locations, the associated temperature and wind at or near the pan water surface are also recorded. A high-quality monthly Class-A pan data set of 60 stations across Australia is listed by Jovanovic et al. (2008). (Lavery et al. (1997) identified for Australia an extended high-quality daily rainfall data set consisting of 379 gauges.)

3. In many parts of the world an alternative approach to using measured data directly is to deploy outputs from spatial interpolation and spatial modelling. If seeking to estimate evaporation at a point or localised area using data from a proximally located meteorological station, at-site data are optimal; however, these do not always exist. Specific to Australia, if seeking an estimate of evaporation for a larger area (e.g., a catchment or an administrative region) then gridded output is available. Donohue et al. (2010a; 2010b) have made available five potential evaporation formulations being: (i) Morton point; (ii) Morton areal; (iii) Penman; (iv) Priestley-Taylor; and (v) Thornthwaite in:

http://www-data.iwis.csiro.au/ts/climate/evaporation/donohue/Donohue_readme.txt.

It should be noted here that R. Donohue (pers. comm.) advised that "the reason Morton point potential values were so high in Donohue et al (2010b) was because, in their modelling of net radiation, they explicitly accounted for actual land-cover dynamics. Donohue et al (2010b) modelled R_s (incoming shortwave radiation) using the Bristow and Campbell (1984) model calibrated to Australian conditions (McVicar and Jupp, 1999), and combined this with remotely sensed estimates of albedo (Saunders, 1990) to model R_{ns} (net incoming shortwave radiation). R_{nl} (net longwave radiation) was modelled according to Allen et al (1998) with soil and vegetation emissivity weighted by their per-pixel fractions determined from remotely sensed data (Donohue et al., 2009). This procedure differs from Morton's (1983a) methodology, developed over 25 years ago, when remotely sensed data were not routinely available, and thus Donohue et al. (2010b) is in contradiction to Morton's (1983a) methodology."

The evaporation formulations in the above web-site are available at 0.05° resolution from 1982 onwards at a daily (mm day^{-1}), a monthly (mm month^{-1}), an annual (mm year^{-1}), or an annual average (mm year^{-1}) time-step. From the same web-site, at the same spatial and temporal resolutions as above, nine variables associated with the surface radiation balance are provided. They are: surface albedo (unitless), fractional cover (unitless), incoming longwave radiation (MJ m^{-2} day^{-1}), incoming shortwave radiation (MJ m^{-2} day^{-1}), outgoing longwave radiation (MJ m^{-2} day^{-1}), outgoing shortwave radiation (MJ m^{-2} day^{-1}), net radiation (MJ m^{-2} day^{-1}), top-of-atmosphere radiation (MJ m^{-2} day^{-1}), and diffuse radiation fraction (unitless). Additionally, the following reference datasets are also available including: wind speed at 2m (TIN-based (Triangular Irregular Networks), units are m s^{-1}), saturated vapour pressure (Pa), vapour pressure deficit (Pa), slope of the saturated vapour pressure curve (Pa K^{-1}), diurnal air temperature range (K), mean air temperature (K), Class-A pan evaporation modelled using the PenPan formulation (mm $period^{-1}$), and FAO-56 Reference Crop evapotranspiration (mm $period^{-1}$). It should be noted that Penman (1948) potential evaporation and PenPan evaporation are calculated with both a TIN-based wind data and a spline-based wind data. The latter for the period from 1 January 1975 can be accessed from (McVicar et al., 2008):

http://www-data.iwis.csiro.au/ts/climate/wind/mcvicar_etal_grl2008/.

We prefer using the spline-based wind data for spatial modelling, and when assessing trends the TIN-based model provided improved results (Donohue et al., 2010b). The FAO-56 Reference Crop (Allen et al., 1998) evapotranspiration only uses the spline-based wind speed data. These data can be linked with basic daily meteorological data (Jones et al., 2009) including: precipitation, maximum air temperature, minimum air temperature, and actual vapour pressure (Pa) which are all available from:

http://www.bom.gov.au/climate/

The vegetation fractional cover data which are also available (Donohue et al., 2008) have been split into its persistent and recurrent components (Donohue et al., 2009); both available from:

http://datanet.csiro.au/dap/public/landingPage.zul?pid=csiro:AVHRR-derived-fPAR)

Thus, there is a now a very powerful resource of freely available data for regional ecohydrological modelling across Australia. There is also available a commercially-based SILO product of many of the key meteorological grids that are required to model evaporation across Australia (Jeffrey et al., 2001).

Data used in later appendices

The data used in the later appendices cover the period from January 1979 to February 2010 and include daily data for Class-A pan evaporation, sunshine hours, maximum and minimum temperature, maximum and minimum humidity and average wind speed. A minimum amount of missing daily temperature (0.37%), relative humidity (0.16%), sunshine hours (0.43%) and wind speed (0.35%) data was infilled for only days in which values were available on adjacent days from which the average was used to infill. Only months with a complete record of all variables were analysed. As a result the average length of station record with all variables is 15.9 years. Some of the analyses in this paper are based on daily data for 68 stations located across Australia (**Figure S1**). Class-A evaporation pan and climate data were obtained from the Climate Information Services, National Climate Centre, Bureau of Meteorology. Of these stations, 39 are part of the high quality Class-A pan evaporation network (Jovanovic et al., 2008, Table 1).

Remotely sensed actual evapotranspiration

Remotely sensed estimates of actual evapotranspiration (usually combining remotely sensed data with some climate data) are becoming more accurate and more accessible to analysts who are not experts in this technology. There are three main approaches to estimate actual evapotranspiration using remote sensing, namely: (i) thermal based methods based on the land surface energy balance (e.g., Sobrino et al. (2005), Kalma et al. (2008), Jia et al. (2009), Elhaddad et al. (2011), and Yang and Wang (2011)); (ii) methods that use the vegetation (and shortwave infrared) indices (e.g., Glenn et al., 2007; 2010; Guerschman et al (2009)); and (iii) hybrid methods that combine the surface temperature and vegetation index (e.g., Carlson, 2007; Tang et al., 2010). Readers wishing to pursue such approaches are referred to the growing volume of material that is accessible in the international literature.

Daily and monthly data

Analyses of most procedures are carried out for a daily and a monthly time-step. In the daily analysis, daily values of maximum and minimum temperature, maximum and minimum relative humidity, sunshine hours and daily wind run are required. For the analysis using a monthly time-step, the average daily values for each month and for each variable are the basis of computation.

Location of meteorological stations relative to the target evaporating site

In discussing evaporation procedures, most writers are silent on where to measure meteorological data to achieve the most accurate estimate of evaporation. For estimating evaporation from lakes using Morton's CRWE or CRLE model, land-based meteorological data can be used (Morton, 1983b, page 82). Furthermore, Morton (1986, page 378) notes that data measured over water have only a "…relatively minor effect…" on the estimate of lake evaporation. Morton (1986, page 378) says the CRAE, which estimate landscape evaporation (see Section 2.5.2), is different because "…the latter requires accurate temperature and humidity data from a representative [land-based] location". (A discussion of Morton's evaporation models is presented in Section 2.5.2 and in **Appendix S7**.)

Based on a 45,790 ha lake in Holland, Keijman and Koopmans (1973) compared Penman (1948) evaporation for seven periods over 32 days with a water balance estimate, an energy budget estimate and observed pan evaporation data, where the meteorological instruments were located on a floating raft. The authors observed that the Penman (1948) lake evaporation estimates are highly correlated and show little bias with the water balance estimates and the energy balance estimates. Based on further analysis, Keijman (1974) concluded that for estimating energy balance at the centre of a lake land-based meteorological measurements downwind from the lake are preferred over measurements upwind.

In a major study of evaporation from Lake Nasser using three floating AWS, Elsawwaf et al. (2010) compared Penman (1956) evaporation with estimates from the Bowen Ratio Energy Budget method. The Penman method exhibited negative bias (Elsawwaf et al., 2010) which is consistent with the Penman (1948) results recorded in Holland. (In **Appendix S4,** the differences expected between Penman (1948) and Penman (1956) are discussed).

Supplementary Material

Appendix S2 Computation of some common variables

This appendix includes equations to estimate common variables used in the evaporation equations. Values of specific constants are listed in **Table S1**.

Mean daily temperature

$$Mean\ daily\ temperature = \frac{T_{max}+T_{min}}{2} \quad \text{(Allen et al., 1998, Equation 9)} \tag{S2.1}$$

where T_{max} and T_{min} are the maximum and minimum air temperatures (°C), respectively, recorded over a 24-hour period.

Wet-bulb temperature

$$T_{wb} = \frac{0.00066\times 100 T_a + \frac{4098 v_a}{(T_d+237.3)^2} T_d}{0.00066\times 100 + \frac{4098 v_a}{(T_d+237.3)^2}} \quad \text{(McJannet et al., 2008b, Equation 25)} \tag{S2.2}$$

where T_{wb} is wet-bulb temperature (°C), T_d is the dew point temperature (°C) and v_a is actual vapour pressure (kPa).

Dew point temperature

$$T_d = \frac{116.9+237.3\ln(v_a)}{16.78-\ln(v_a)} \quad \text{(McJannet et al., 2008b, Equation 26)} \tag{S2.3}$$

Slope of the saturation vapour pressure curve

$$\Delta = \frac{4098\left[0.6108 exp\left(\frac{17.27 T_a}{T_a+237.3}\right)\right]}{(T_a+237.3)^2} \quad \text{(Allen et al., 1998, Equation 13)} \tag{S2.4}$$

where Δ is the slope of the saturation vapour pressure curve (kPa °C^{-1}) at the mean daily air temperature, T_a (°C).

Saturation vapour pressure at temperature, T(°C)

$$v_T^* = 0.6108 exp\left[\frac{17.27T}{T+237.3}\right] \quad \text{(Allen et al., 1998, Equation 11)} \tag{S2.5}$$

where v_T^* is the saturation vapour pressure (kPa) at temperature, T (°C).

Daily saturation vapour pressure

$$v_a^* = \frac{v_a^*(T_{max})+v_a^*(T_{min})}{2} \quad \text{(Allen et al., 1998, Equation 12)} \tag{S2.6}$$

where v_a^* is the daily (24-hour period) saturation vapour pressure (kPa) at air temperature, and where the saturation vapour pressures are evaluated at temperatures (°C) T_{max} and T_{min}.

Mean daily actual vapour pressure

$$v_a = \frac{v_a^*(T_{min})\frac{RH_{max}}{100}+v_a^*(T_{max})\frac{RH_{min}}{100}}{2} \quad \text{(Allen et al., 1998, Equation 17)} \tag{S2.7}$$

where v_a is the mean daily actual vapour pressure (kPa), RH_{max} is the maximum relative humidity (%) in a day, and RH_{min} is the minimum relative humidity (%) in a day.

Mean daily actual vapour pressure using dew point temperature

If daily dew point temperature is known, then daily actual vapour pressure can be estimated thus:

$$v_a = 0.6108 exp\left[\frac{17.27T_d}{T_d+237.3}\right] \quad \text{(Allen et al., 1998, Equation 14)} \qquad \text{(S2.8)}$$

where T_d is the dew point temperature (°C).

Psychrometric constant

$$\gamma = 0.00163\frac{p}{\lambda} \quad \text{(Allen et al., 1998, Equation 8)} \qquad \text{(S2.9)}$$

where γ is the psychrometric constant (kPa °C^{-1}), λ is the latent heat of vaporization = 2.45 MJ kg^{-1} (at 20°C), and p is atmospheric pressure at elevation z m.

Atmospheric pressure

$$p = 101.3\left(\frac{293-0.0065Elev}{293}\right)^{5.26} \quad \text{(Allen et al., 1998, Equation 7)} \qquad \text{(S2.10)}$$

where p is the atmospheric pressure (kPa) at elevation $Elev$ (m) above mean sea level.

Zero-plane displacement (displacement height)

Zero-plane displacement (z_d) (m) can be explained as the height within obstacles, e.g., trees, in which wind speed is zero. Values are listed in **Table S2**. Allen et al. (1998, Box 4) reported that for a natural crop-covered surface and Wieringa (1986, Table 1) noted for an average obstacle height:

$$z_d = \frac{2}{3}h \qquad \text{(S2.11)}$$

where h is the mean height of the roughness obstacles (including vegetation) (m).

Roughness length (height)

Roughness length (z_o) (m) is related to the roughness of the evaporating surface and is the optimal parameter for defining terrain effects on wind (Wieringa, 1986, Table 1). Values are listed in **Table S2**. If values are not available for a particular terrain or surface, the following relationship can be used:

$$z_o \cong \frac{(vegetation\ height)}{10} \qquad \text{(S2.12)}$$

Units of evaporation

Evaporation rates are expressed as depth per unit time, e.g., mm day^{-1}, or the rates can also be expressed as energy flux and, noting that the latent heat of water is 2.45 MJ kg^{-1}, it follows that 1 mm day^{-1} of evaporation is equivalent to 2.45 MJ m^{-2} day^{-1}.

Supplementary Material

Appendix S3 Estimating net solar radiation

This appendix outlines how net radiation is estimated with and without incoming solar radiation data. The method is based on the procedure outlined in Allen et al. (1998, pages 41 to 53).

$$R_n = R_{ns} - R_{nl} \tag{S3.1}$$

where R_n is the net radiation (MJ m^{-2} day^{-1}), R_{ns} is the net incoming shortwave radiation (MJ m^{-2} day^{-1}), and R_{nl} is the net outgoing longwave radiation (MJ m^{-2} day^{-1}).

Net shortwave solar radiation is estimated from the measured incoming solar radiation (R_s) at an Automatic Weather Station and albedo for the evaporating surface as:

$$R_{ns} = (1 - \alpha)R_s \tag{S3.2}$$

where R_s is the measured or estimated incoming solar radiation (MJ m^{-2} day^{-1}), and α is the albedo of the evaporating surface. Several albedo values are listed in **Table S3**.

Except for eight sites in Australia (Roderick et al., 2009a, Section 2.3), measured values of net longwave radiation are not available. Hence, net outgoing longwave radiation is estimated by:

$$R_{nl} = \sigma(0.34 - 0.14\bar{v}_a^{0.5})\left(\frac{(T_{max}+273.2)^4+(T_{min}+273.2)^4}{2}\right)\left(1.35\frac{R_s}{R_{so}} - 0.35\right) \tag{S3.3}$$

noting that $\frac{R_s}{R_{so}} \leq 1$, and where R_{nl} is the net outgoing longwave radiation (MJ m^{-2} day^{-1}), R_s is the measured or estimated incoming solar radiation (MJ m^{-2} day^{-1}), R_{so} is the clear sky radiation (MJ m^{-2} day^{-1}), $\bar{v}_a$ is the mean actual daily vapour pressure (kPa), T_{max} and T_{min} are respectively the maximum and the minimum daily air temperature (°C), and σ is Stefan-Boltzmann constant (MJ K^{-4} m^{-2} day^{-1}).

$$R_{so} = (0.75 + 2\times10^{-5}Elev)R_a \tag{S3.4}$$

where $Elev$ is the ground elevation (m) above mean sea level of the automatic weather station (AWS), and R_a is the extraterrestrial radiation (MJ m^{-2} day^{-1}) which is the solar radiation on a horizontal surface at the top of the earth's atmosphere and is computed by:

$$R_a = \frac{1440}{\pi}G_{sc}d_r^2[\omega_s sin(lat)sin(\delta) + cos(lat)cos(\delta)sin(\omega_s)] \tag{S3.5}$$

where G_{sc} is the solar constant = 0.0820 MJ m^{-2} min^{-1}, d_r is the inverse relative distance Earth-Sun, ω_s is the sunset hour angle (rad), lat is latitude (rad) (negative for southern hemisphere), and δ is the solar declination (rad).

$$d_r^2 = 1 + 0.033cos\left(\frac{2\pi}{365}DoY\right) \tag{S3.6}$$

This equation and Equation (S3.5) are modified from the errata provided with Allen et al. (1998) for their Equation 23. The amended Equation (S3.6) is shown in McCullough and Porter (1971, Equation 2) and amended Equation (S3.5) is shown in McCullough (1968, Equation 3).

$$\delta = 0.409sin\left(\frac{2\pi}{365}DoY - 1.39\right) \tag{S3.7}$$

where DoY is Day of Year (see below).

The sunset hour angle ω_s is estimated from:

$$\omega_s = arcos[-\tan(lat)\tan(\delta)] \tag{S3.8}$$

If measured values of R_s are not available, R_s can be calculated from the Ångström-Prescott equation (see Martinez-Lonano et al. (1984) and Ulgen and Hepbasli (2004) for historical developments and review of the equation) as follows:

$$R_s = \left(a_s + b_s \frac{n}{N}\right) R_a \tag{S3.9}$$

where n is the observed duration of sunshine hours, N is the maximum possible duration of daylight hours, and a_s and b_s are constants. a_s represents the fraction of extraterrestrial radiation reaching earth on sunless days (n = 0) and $a_s + b_s$ is the fraction of extraterrestrial radiation reaching earth on full-sun days (n = N). Where calibrated values of a_s and b_s are not available, values of a_s = 0.25 and b_s = 0.5 are preferred (Fleming et al, 1989, Equation 3; Allen et al., 1998, page 50). A literature review of more than 50 models revealed that many estimates of a_s and b_s, based on a monthly time-step have been developed (Menges et al., 2006, Yang et al, 2006, Roderick, 1999), although only five models are simple linear relationships as in Equation (S3.9). For these five models (Bahel et al., 1986; Benson et al., 1984; Louche et al., 1991; Page, 1961; Tiris et al., 1997 as reported in Menges et al., 2006), the average values of a_s and b_s are, respectively, 0.20 and 0.55. Roderick (1999, page 181) in estimating monthly average daily diffuse radiation for 25 sites in Australia and Antarctica commented that his results were consistent with a_s = 0.23 and b_s = 0.50 based on Linacre (1968) and Stitger (1980). More recently, McVicar et al. (2007, page 202) considered the study by Chen et al. (2004) and adopted a_s = 0.195 and b_s = 0.5125 for their analysis of the middle and lower catchments of the Yellow River. It is recommended, however, that if local calibrated values are available for the study area, these values should be used.

If the number of sunshine hours is unavailable, alternatively cloudiness (in terms of oktas – the number of eights of the sky covered by cloud) may have been measured. Chiew and McMahon (1991) developed the following empirical relationship relating oktas to sunshine hours:

$$n = a_o + b_o C_O + c_o C_O^2 + d_o C_O^3 \tag{S3.10}$$

where n is the estimated sunshine hours, C_O is cloud cover in oktas, and a_o, …, d_o are empirical constants and have been estimated for 26 climate stations across Australia. Values are provided in Chiew and McMahon (1991, Table A1). Errors in ground-based cloud cover estimates are discussed by Hoyt (1977).

The maximum daylight hours, N, is given by:

$$N = \frac{24}{\pi} \omega_s \tag{S3.11}$$

where ω_s is the sunset hour angle (rad).

If sunshine hours or cloudiness are not available for Australia, following Linacre (1993, Equation 20) cloudiness can be estimated from:

$$C_D = 1 + 0.5 logP_j + \left(logP_j\right)^2, P_j \geq 1 \tag{S3.12}$$

$$C_D = 1, P_j < 1 \tag{S3.13}$$

where P_j is the monthly precipitation (mm).

Thus, as an alternative to Equation (S3.9), R_s can be computed from (Linacre (1993, Equation 19):

$$R_s = (0.85 - 0.047C_D)R_a \qquad \text{(S3.14)}$$

where C_D is the number of tenths of the sky covered by cloud, R_a is the extraterrestrial radiation, and R_s is the estimate of the incoming solar radiation.

Estimating separately incoming and outgoing longwave radiation

In some procedures to estimate evaporation e.g., McJannet et al. (2008b) discussed in **Appendix S5**, outgoing longwave radiation needs to be computed separately from incoming longwave radiation rather than being combined as in Equation S3.3. In McJannet et al. (2008b) outgoing longwave radiation is estimated as a function of water surface temperature and separately as a function of wet-bulb temperature.

In Equation (S3.1), R_{ns} is estimated from Equations (S3.2), (S3.5), and (S3.9), and

$$R_{nl} = R_{ol} - R_{il} \qquad \text{(S3.15)}$$

where R_{ol} is the outgoing longwave radiation (MJ m^{-2} day^{-1}), and R_{il} is the incoming longwave radiation (MJ m^{-2} day^{-1}).

Following McJannet et al. (2008b, Equation 13) incoming longwave radiation may be estimated as follows:

$$R_{il} = \left(C_f + (1 - C_f)\left(1 - \left(0.261exp(-7.77 \times 10^{-4}T_a^2)\right)\right)\right)\sigma(T_a + 273.15)^4 \qquad \text{(S3.16)}$$

where R_{il} is the incoming longwave radiation (MJ m^{-2} day^{-1}), T_a is the mean daily air temperature (°C), σ is the Stefan-Boltzman constant (MJ K^{-4} m^{-2} day^{-1}), and C_f is the fraction of cloud cover estimated from (McJannet et al, 208b, Equations 14 and 15):

$$C_f = 1.1 - K_{ratio}, K_{ratio} \leq 0.9 \qquad \text{(S3.17)}$$

$$C_f = 2(1 - K_{ratio}), K_{ratio} > 0.9 \qquad \text{(S3.18)}$$

where $K_{ratio} = \frac{R_s}{R_{so}}$, R_{so} and R_s are estimated from Equations (S3.4) and (S3.9).

Outgoing longwave radiation is estimated as a function of water temperature and/or wet-bulb temperature as follows McJannet at al. (2010, Equations 22 and 29):

$$R_{ol}^{wa} = 0.97\sigma(T_w + 273.15)^4 \qquad \text{(S3.19)}$$

where R_{ol}^{wa} is the outgoing longwave radiation (MJ m^{-2} day^{-1}) based on water temperature, and T_w is the water temperature (°C),

$$R_{ol}^{wb} = \sigma(T_a + 273.15)^4 + 4\sigma(T_a + 273.15)^3(T_{wb} - T_a) \qquad \text{(S3.20)}$$

where R_{ol}^{wb} is the outgoing longwave radiation (MJ m^{-2} day^{-1}) based on wet-bulb temperature, and T_{wb} is the wet-bulb temperature (°C).

Estimating Day of Year (adapted from Allen et al., 1998, page 217)

The Day of Year (DoY) is computed for each day (D) of each month (M) as:

DoY=INTEGER(275*M/9 – 30 + D) – 2 (S3.21)

IF (M < 3) THEN DoY = DoY + 2 (S3.22)

IF(leap year and (M > 2) THEN DoY = DoY + 1 (S3.23)

Note that year 2000 is a leap year, whereas 1900 is not a leap year.

Appendix S4

Penman model

The Penman or combination equation (Penman, 1948, Equation 16) for estimating open-water evaporation is defined as:

$$E_{PenOW} = \frac{\Delta}{\Delta+\gamma}\frac{R_{nw}}{\lambda} + \frac{\gamma}{\Delta+\gamma}E_a \tag{S4.1}$$

where E_{PenOW} is the daily open-water evaporation (mm day^{-1}), R_{nw} is the net radiation at the water surface (MJ m^{-2} day^{-1}), E_a (mm day^{-1}) is a function of wind speed, saturation vapour pressure and average vapour pressure, Δ is the slope of the vapour pressure curve (kPa °C^{-1}) at air temperature, γ is the psychrometric constant (kPa °C^{-1}), and λ is the latent heat of vaporization (MJ kg^{-1}). See Dingman (1992, Section 7.3.5) for a detailed discussion of Penman and evaporation issues in general.

In preparing this supplementary appendix, we were cognisant of de Bruin's (1987) comment. "The result of the [recent] developments … is that Penman's formula experienced a large number of changes in the last decades and that at this very moment tens of different versions of the formula exist. This causes a tremendous confusion." Thus, in the following material we identified several keys features of the Penman equation for inclusion herein.

It is noted in Section 2.1.1 that Equation (S4.1) is based on simplifying assumptions to account for the fact that the temperature of the evaporating surface is unknown. References for readers wishing to follow up on this topic include Monteith (1965), Monteith (1981) and Raupach (2001). Some commentary is provided at the end of this Section.

To estimate R_{nw}, details are given in **Appendix S3**. In estimating R_{nw} an appropriate value of albedo (α) should be used, which depends on the evaporating surface (**Table S3**); for open-water α = 0.08. Although Penman (1948, pages 132 and 137) used 6-day and monthly time-steps in his studies, several analysts have used a daily time-step.

To estimate E_a (mm day^{-1}) in Equation (S4.1), one should use:

$$E_a = f(u)(v_a^* - v_a) \tag{S4.2}$$

where $f(u)$ is the wind function and $(v_a^* - v_a)$ is the vapour pressure deficit (kPa). In this paper, although there are several wind functions available (their application is discussed at the end of this appendix), we have adopted Penman's (1956) equation as standard:

$$f(u) = 1.313 + 1.381u_2 \tag{S4.3}$$

where u_2 is the average daily wind speed (m s^{-1}) at 2 m, and vapour pressure is measured in kPa. (In Australia, wind run is recorded at 9 am as the accumulated value over the previous 24 hours and, therefore, in Equation (S4.3) mean daily wind speed is based on the accumulated 24-hour value.)

Equations for estimating v_a^*, v_a and Δ are set out in **Appendix S2**.

In the Penman equation, it is assumed there is no change in heat storage nor heat exchange with the ground, and no advected energy and, hence, the actual evaporation does not affect the overpassing air (Dingman, 1992, Section 7.3.5). Data required to apply the equation includes solar radiation (or sunshine hours or cloudiness), wind speed, air temperature and relative humidity, all averaged over the time-step adopted.

Adjustment for the height of the wind speed measurement in Penman equation

If wind measurements are not available at 2 m the following equation may be used to adjust u_z. This is important as the wind speed coefficients in Penman have been calibrated for wind speed at 2 m.

$$u_2 = u_z \frac{\ln\left(\frac{2}{z_0}\right)}{\ln\left(\frac{z}{z_0}\right)} \tag{S4.4}$$

where u_2 and u_z are respectively the wind speeds (m s^{-1}) at heights 2 m and z m, and z_0 is the roughness height.

Form of wind function

Over the years Penman and other authors have suggested several forms for the wind function. The form of the original Penman (1948) wind function (using wind speed u_2 in miles day^{-1} and vapour pressure in mm of mercury) is:

$$f(u)_{48} = 0.35(1 + 9.8 \times 10^{-3} u_2) \tag{S4.5}$$

where $f(u)_{48}$ is the 1948 Penman wind function. Some authors (e.g., Szilagyi and Jozsa, 2008, page 173) have labelled this equation as the Rome wind function.

In 1956, Penman (1956) suggested that the original wind function should be reduced to accommodate both the Lake Hefner evaporation results and the original Rothamsted tank evaporation as follows:

$$f(u)_{56} = 0.35(0.5 + 9.8 \times 10^{-3} u_2) \tag{S4.6}$$

where $f(u)_{56}$ is the 1956 Penman wind function.

This equation in which u_2 is in miles per day and the saturation deficit is in units of mm of mercury is equivalent to Equation (S4.3) in which the average daily wind speed u_2 is in m s^{-1} and the vapour pressure deficit is in units of kPa. Based on a study of several reservoirs in Australia and Botswana, Fleming et al. (1989, page 59) adopted this form of the wind function. Shuttleworth (1992, Section 4.4.4) observed that the Penman equation with the original wind function overestimated evaporation from large lakes by 10% to 15%. Linacre (1993, page 243 and Appendix 1) observed from the median of 26 studies he identified and his own analysis of the heat transfer coefficient of water, that the coefficient was in the range 2.3u to 2.6u W m^{-2} K^{-1} (and u in m s^{-1}), which implies that

$$f(u)_{LIN} \text{ is between } 0.31(9.8 \times 10^{-3} u_2) \text{ and } 0.35(9.8 \times 10^{-3} u_2) \tag{S4.7}$$

where $f(u)_{LIN}$ is the Linacre wind function, u_2 is in miles day^{-1} and vapour pressure in mm of mercury for comparison with Equations S4.5 and S4.6.

Based on Brutsaert (1982), Valiantzas (2006, page 695) reported that the 1948 function is used more frequently than the 1956 function in hydrologic applications. However, Cohen et al. (2002, Section 4) reporting Stanhill (1963) noted the 1948 wind function to be unrealistically high. Using the FAO CLIMWAT global data (~5000 stations world-wide), Valiantzas (2006) compared the E_{Pen} values for the three wind functions and found that the following relationships held with an $R^2 = 0.991$:

$$E_{PenOW}|f(u)_{48} \approx 1.06 E_{PenOW}|f(u)_{56} \approx 1.12 E_{PenOW}|f(u)_{LIN} \tag{S4.8}$$

This result approximates our analysis which is based on applying the three wind functions to the 68 Australian stations (**Table S4)** as summarised below:

$$E_{PenOW}|f(u)_{48} \approx 1.11 E_{PenOW}|f(u)_{56} \approx 1.19 E_{PenOW}|f(u)_{LIN} \tag{S4.9}$$

Table S4 also shows a comparison with FAO-56 Reference Crop evapotranspiration and Priestley-Taylor evaporation as well as 10th and 90th percentile values.

Valiantzas (2006, page 696) suggested the 1948 wind function be adopted as standard in the Penman equation, however, noting the comments above by Shuttleworth (1992, Section 4.4.4), Linacre (1993) and Cohen et al (2002), we have adopted the Penman (1956) form of the wind function in this paper. In terms of the units used (vapour pressure in kPa, and mean daily wind speed in m s^{-1}), the ***Penman 1956 wind function*** is:

$$f(u) = 1.313 + 1.381u_2 \tag{S4.10}$$

For comparison, ***Penman's 1948 wind function*** in the same units as Equation (S4.10) (vapour pressure in kPa, and wind speed in m s^{-1}) is:

$$f(u) = 2.626 + 1.381u_2 \tag{S4.11}$$

Penman equation without wind data

Valiantzas (2006, Equation 33) proposed the following equation for situations where no wind data are available:

$$E_{PenOW} \approx 0.047R_S(T_a + 9.5)^{0.5} - 2.4\left(\frac{R_S}{R_a}\right)^2 + 0.09(T_a + 20)\left(1 - \frac{RH_{mean}}{100}\right) \tag{S4.12}$$

where E_{PenOW} is Penman's open-water evaporation (mm day^{-1}), R_s is the measured or estimated incoming solar radiation (MJ m^{-2} day^{-1}), T_a is the mean daily temperature (°C), R_a is the extraterrestrial solar radiation (MJ m^{-2} day^{-1}) and RH_{mean} is the mean daily relative humidity (%). This assumes the albedo for water is 0.08 and the "0.09" in Equation (S4.12) applies to the Penman (1948) wind function. If one uses the Penman (1956) wind function, "0.09" should be replaced by "0.06". Based on six years of daily data from California, Valiantzas (2006) compared Equation (S4.12) with Equation (S4.1) using monthly data and found the modified equation performed satisfactorily (R^2 = 0.983, the long term ratio of "approximate" to "reference" evaporation was 0.995, and SEE = 0.25 mm day^{-1}) compared with the standard Penman equation.

Modifying Penman equation by including aerodynamic turbulence

According to Fennessey (2000), van Bavel (1966) modified the original Penman 1948 equation to take into account boundary layer resistance as follows:

$$E'_{PotOW} = \frac{\Delta}{\Delta+\gamma}\frac{R_n - G}{\lambda} + \frac{\gamma}{\Delta+\gamma}\frac{\rho_a c_a(v_a^* - v_a)}{\lambda r_a} \tag{S4.13}$$

where E'_{PotOW} is the modified Penman open water evaporation (mm day^{-1}) incorporating aerodynamic resistance, ρ_a is the mean air density at constant pressure (kg m^{-3}), c_a is the specific heat of the air (MJ kg^{-1} °C^{-1}), and r_a is an "aerodynamic or atmospheric resistance" to water vapour transport (s m^{-1}). Equation (S4.13) for open water is equivalent to the Penman-Monteith Equation (S5.1) with the surface resistance r_s set to zero.

To estimate aerodynamic resistance, McJannet et al. (2008a) introduced a specific wind function incorporating lake area into the Calder and Neal (1984) aerodynamic resistance equation as follows:

$$r_a = \frac{86400\,\rho_a c_a}{\gamma\left(\frac{5}{A}\right)^{0.05}(3.80 + 1.57u_{10})} \tag{S4.14}$$

where r_a is the aerodynamic resistance over a lake (s m^{-1}), A is the lake area (km^2) ρ_a is the mean air density at constant pressure (1.2 kg m^{-3}), c_a is the specific heat of the air (0.001013MJ kg^{-1} °C^{-1}), γ is the psychrometric constant (0.0668 kPa °C^{-1} at mean sea-level pressure 101.3 kPa), u_{10} is the wind speed (m s^{-1}) at 10 m height, yielding r_a for a lake at sea-level as:

$$r_a = \frac{410}{\left(\frac{5}{A}\right)^{0.05}(1+0.413u_{10})} \tag{S4.15}$$

It is noted here that r_a is a function of wind speed as well as lake area.

Chin (2011, Equation 12) offered an alternative equation to estimate r_a for wind speeds (u_2) (m s^{-1}) measured at 2 m height and for no adjustment for lake area as follows:

$$r_a = \frac{400}{(1+0.536u_2)} \tag{S4.16}$$

Price (1994) estimated r_a for Lake Ontario, Canada during a six-week summer period in 1991. Based on 2015 samples he determined a mean value of r_a = 201 ± 122 s m^{-1}. The wide range of observed values is a function of wind-speed.

Estimating Δ under extreme conditions

McArthur (1992, page 306) explains the assumptions behind Δ in the Penman equation (Equation (S4.1)). Equation (S4.17) provides the physically correct estimate of Δ, which requires knowledge of the evaporating surface temperature (T_s).

$$\Delta = \frac{[v^*_{T_S} - v^*_{T_a}]}{(T_s - T_a)} \tag{S4.17}$$

However, because T_s is generally unknown, Δ is approximated as the slope of the saturated vapour pressure curve at air temperature as follows:

$$\Delta' = \frac{dv^*_T}{dT} \quad \text{evaluated at air temperature } (T_a) \tag{S4.18}$$

In most practical situations Δ′ is an acceptable approximation to Δ when the surface and air temperatures are close (McArthur (1992, page 306)). Under extreme conditions, high aerodynamic resistance, high humidity and low temperature, the surface and air temperatures diverge and this approximation breaks down (Paw U (1992, page 299)) and can lead to under-estimating evaporation by about 10% (Slatyer and McIlroy, 1961; Paw U and Gao, 1988). Milly (1991), McArthur (1992) and Paw U (1992) provide a discussion of alternate procedures to estimate evaporation under such conditions.

Supplementary Material

Appendix S5 Penman-Monteith and FAO-56 Reference Crop models

The Penman-Monteith model defined below is usually adopted to estimate potential evapotranspiration, E_{PM} (mm day^{-1}). The equation is based on Allen et al. (1998, Equation 3):

$$ET_{PM} = \frac{1}{\lambda}\frac{\Delta(R_n - G) + \rho_a c_a \frac{(v_a^* - v_a)}{r_a}}{\Delta + \gamma\left(1 + \frac{r_s}{r_a}\right)} \tag{S5.1}$$

where ET_{PM} is the Penman-Monteith potential evapotranspiration (mm day^{-1}), R_n is the net radiation at the vegetated surface (MJ m^{-2} day^{-1}) incorporating an albedo value appropriate for the evaporating surface (**Table S3**), G is the soil heat flux (MJ m^{-2} day^{-1}), ρ_a is the mean air density at constant pressure (kg m^{-3}), c_a is the specific heat of the air (MJ kg^{-1} °C^{-1}), r_a is an "aerodynamic or atmospheric resistance" to water vapour transport, i.e., from the leaf surface to the atmosphere (s m^{-1}) (Dunin and Greenwood, 1986, page 48), r_s is a "surface resistance" term, that is the resistances from within the plant to the bulk leaf surfaces (s m^{-1}) (Dunin and Greenwood, 1986, page 48), $(v_a^* - v_a)$ is the vapour pressure deficit (kPa), λ is the latent heat of vaporization (MJ kg^{-1}), Δ is the slope of the vapour pressure curve (kPa °C^{-1}) at air temperature, and γ is the psychrometric constant (kPa °C^{-1}). G is defined as (Allen et al., 1998, Equation 41):

$$G = c_s d_s \left(\frac{T_i - T_{i-1}}{\Delta t}\right) \tag{S5.2}$$

where c_s is the volumetric heat capacity of soil (MJ m^{-3} °C^{-1}) (for an average soil moisture $c_s \cong 2.1$, Grayson et al., 1996, page 33), d_s is the effective soil depth (m), T_i and T_{i-1} are the average air temperatures (°C) on day i and i-1 respectively, and Δt is time-step (day).

It is noted in Section 2.1.2 that Equation (S5.1) is based on simplifying assumptions to account for the fact that the temperature of the evaporating surface is unknown. References for readers wishing to follow up on this topic include Monteith (1965), Monteith (1981) and Raupach (2001). An aspect of this issue is discussed in the previous section dealing with Equation (S4.14).

Generally, for daily time-steps G can be assumed to be negligible (Allen et al., 1998, page 68).

Values of aerodynamic resistance and surface (or canopy) resistance

r_a, ***the aerodynamic resistance***, controls the removal of water vapour from the plant surface under neutral stability conditions and is defined for an evaporating surface by Allen et al. (1998, Equation 4) as follows:

$$r_a = \frac{ln\left[\frac{z_m - d}{z_{om}}\right] ln\left[\frac{z_h - d}{z_{oh}}\right]}{k^2 u_z} \tag{S5.3}$$

where z_m is the height of the wind instrument (m), z_h is the height of the humidity measurements (m), d is the zero plane displacement height (m), z_{om} is the roughness length governing momentum transfer (m), z_{oh} is the roughness length governing transfer of heat and vapour (m), k is von Kármán's constant (0.41), and u_z is the wind speed at height z_m (m s^{-1}).

According to Allen et al. (1998, page 21), for a wide range of crops, d and z_{om} can be estimated from the crop height (h) as:

$d = 0.67h$, and (S5.4)

$z_{om} = 0.123h$ (S5.5)

and z_{oh} can be approximated from:

$z_{oh} = 0.1z_{om}$ (S5.6)

Some typical values of r_a are listed in **Table S2**.

According to Chin (2011, Equation 12), Equation (S5.3) and the following Equation (S5.7), which is for water, are conventional practice for the PM equation.

$$r_a = \frac{4.72\left[ln\left(\frac{z_m}{z_o}\right)^2\right]^2}{1+0.54u_z} \quad \text{(S5.7)}$$

where z_m is the height of wind measurements and z_o (roughness length) is:

$$z_o = \frac{(vegetation\ height)}{10} \quad \text{(S5.8)}$$

For water z_o = 0.001 m (**Table S2**).

r_s, the ***surface resistance*** term, in vegetation represents bulk stomatal resistance or canopy resistance, which is a property of the plant type and its water stress level. This term controls the release of water to the plant or soil surface; some typical values of r_s are listed in **Table S2**. For water, r_s = 0.

Again following Allen et al. (1998, Equation 5), an alternative definition of r_s after Szeicz et al. (1969, Equation 9) is:

$$r_s = \frac{r_l}{LAI_{active}} \quad \text{(S5.9)}$$

where r_l is the bulk stomatal resistance of a well-illuminated leaf (s m^{-1}), and LAI_{active} is the active (sunlit) leaf area index (m^2 (of leaf area) m^{-2} (of soil surface)). It is further noted by Allen et al. (1998) that r_l is influenced by climate, water availability and vegetation type. They provide a simple example for a grass reference crop as follows:

$LAI_{active} = 0.5LAI$, and (S5.10)

and a general equation for LAI of grass is:

$LAI = 24h$ (S5.11)

where h is the crop height (m).

Given the stomatal resistance of a single leaf of grass is ~100 s m^{-1} and the crop height is 0.12 m (Allen et al., 1998, page 22), then r_s for a grass reference surface is:

$$r_s = \frac{100}{0.5 \times 24 \times 0.12} = 70\ \text{s m}^{-1} \quad \text{(S5.12)}$$

Dingman (1992, page 296, footnote 9) notes that atmospheric conductance, C_{atm}, is the inverse of aerodynamic resistance:

$$C_{atm} = \frac{1}{r_a} \quad \text{(S5.13)}$$

Also, it is implied from Dingman (1992, page 299) that canopy conductance, C_{can}, is the inverse of surface resistance:

$$C_{can} = \frac{1}{r_s} \quad \text{(S5.14)}$$

Based on data collected in the Amazonian forest, Shuttleworth (1988) proposed that for a dry canopy the surface resistance can be described by the following quadratic function of time of day, with r_s falling to a minimum late morning and rising to a very large value at dusk as follows:

$$r_s = \frac{1000}{12.17 - 0.531(t_{day} - 12) - 0.223(t_{day} - 12)^2} \tag{S5.15}$$

where r_s is surface or canopy resistance (s m^{-1}) and t_{day} is local time of day in hours.

Readers interested in this topic are referred to Sharma (1984), Kelliher et al (1995), Magnani et al. (1998), Silberstein et al. (2003) and Amer and Hatfield (2004).

To understand the relative importance of radiation and atmospheric demand (through the vapour pressure deficit) in the transpiration process, Jarvis and McNaughton (1986, A16) introduced a decoupling coefficient, Ω, (Equation S5.16) which ranges between 0 and 1 and is a measure of the decoupling between the conditions at the surface of a leaf and in the surrounding air:

$$\Omega = \frac{\frac{\Delta}{\gamma} + 1}{\frac{\Delta}{\gamma} + 1 + \frac{r_s}{r_a}} \tag{S5.16}$$

Wallace and McJannet (2010, page 109) explain the significance of Ω as follows. When Ω is small there is a strong coupling between the canopy and the atmosphere and, consequently, canopy conductance, the vapour pressure deficit and wind speed strongly influence transpiration, whereas as Ω approached 1 (complete decoupling) radiation is the dominant factor affecting transpiration. This relationship is explained mathematically by Kumagai et al (2004, Equation 3) as follows:

$$ET_{PM} = \Omega E_{1st} + (1 - \Omega)E_{2nd} \tag{S5.17}$$

where E_{1st} is the radiation (first) term in the PM model (Equation S5.1) and E_{2nd} is aerodynamic (second) term.

FAO-56 Reference Crop Evapotranspiration

If we substitute for r_a and r_s in Equation (S5.1) using the relevant equations in Allen et al. (1998, Equations (3) and (4)) and adopting the properties of the FAO-56 hypothetical crop of assumed height of 0.12 m, a surface resistance of 70 s m^{-1} and an albedo of 0.23, the substitutions yield the familiar FAO-56 Reference Crop evapotranspiration, ET_{RC}, equation (Allen et al., 1998, Equation 6):

$$ET_{RC} = \frac{0.408\Delta(\mathrm{R_n} - \mathrm{G}) + \gamma\frac{900}{\mathrm{T_a}+273}\mathrm{u_2}(v_a^* - v_a)}{\Delta + \gamma(1 + 0.34\mathrm{u_2})} = ET_{RCsh} \tag{S5.18}$$

where ET_{RCsh} is the Reference Crop evapotranspiration for short grass (mm day^{-1}), $\mathrm{u_2}$ is the average daily wind speed (m s^{-1}) at 2 m, and $\mathrm{T_a}$ is the mean daily air temperature (°C). Meyer (1999) discusses the application of the Penman-Monteith equation to inland south-eastern Australia.

ASCE-EWRI Standardized Penman-Monteith Equation

The ASCE-EWRI Standardized Penman-Monteith Equation (S5.19) (ASCE, 2005, Equation 1, Table 1) was developed to estimate potential evapotranspiration from a tall crop with the following characteristics: vegetation height 0.50 m, surface resistance 45 s m^{-1} and albedo of 0.23. The equivalent equation to Equation (S5.18) for tall grass is:

$$ET_{RCta} = \frac{0.408\Delta(\mathrm{R_n}-\mathrm{G})+\gamma\frac{1600}{\mathrm{T_a}+273}\mathrm{u_2}(v_a^*-v_a)}{\Delta+\gamma(1+0.38\mathrm{u_2})} \quad \text{(S5.19)}$$

where ET_{RCta} is the Reference Crop evapotranspiration for tall grass (mm day^{-1}).

Adjustment for height of wind speed measurement in Penman-Monteith and FAO-56 Reference Crop equations

The following equation is to adjust wind speed for instrument height associated with short grassed surfaces (Allen et al., 1998, Equation (47)):

$$u_2 = u_z \frac{4.87}{ln(67.8z-5.42)} \quad \text{(S5.20)}$$

where u_2 and u_z are respectively the wind speeds at heights 2 m and *z* m.

Reference Crop equation without wind data

Valiantzas (2006, Equation 39) proposed the following equation (which is similar to the simplified Penman equation, see Equation (S4.12)), to estimate monthly Reference Crop evapotranspiration for situations where no wind data are available:

$$ET_{RC} \approx 0.038R_S(\bar{T}+9.5)^{0.5} - 2.4\left(\frac{R_S}{R_A}\right)^2 + 0.075(\bar{T}+20)\left(1-\frac{RH}{100}\right) \quad \text{(S5.21)}$$

where ET_{RC} is the Reference Crop estimate of evapotranspiration for short grass (mm day^{-1}), R_S is the measured or estimated average monthly incoming solar radiation (MJ m^{-2} day^{-1}), $\bar{T}$ is the mean monthly air temperature (°C), R_A is the average monthly extraterrestrial solar radiation (MJ m^{-2} day^{-1}) and RH is the mean monthly relative humidity (%). This procedure assumes the albedo = 0.25 (rather than the standard 0.23) for a crop. For 535 northern hemisphere climate stations, monthly estimates of E_{RC} based on Equation (S5.21) were compared with the standard reference crop Equation (S5.18). The approximate model performed very well on a sub-set of 4461 monthly estimates (R^2 = 0.951), the long term ratio of "approximate" to "reference" was 1.03, and SEE = 0.34 mm day^{-1}.

Application of Penman-Monteith to water bodies based on equilibrium temperature

An interesting application of the Penman-Monteith equation (Equation (S5.1) to a range of water bodies (irrigation channels, ponds, lakes, reservoirs streams and floodplains) was carried out by McJannet et al. (2008b) who set r_s = 0 for water bodies (**Table S2**). The approach is outlined in **Appendix S11**.

Shuttleworth-Wallace

To deal with sparse vegetation Shuttleworth and Wallace (1985, Equations 11 to 18) modified the PM model to separate evapotranspiration into soil evaporation and transpiration. Wessel and Rouse (1994) further modified the Shuttleworth-Wallace (SW) model to accommodate evaporation from water surfaces but recommended that this component be not included in the SW approach. The Shuttleworth and Wallace (1985) equations are:

$$E_{SW} = \frac{1}{\lambda}(C_{ca}PM_{ca} + C_{su}PM_{su}) \quad \text{(S5.22)}$$

$$PM_{ca} = \frac{1}{\lambda}\frac{\Delta A_e + \frac{[\rho c_a(v_a^*-v_a)-\Delta r_a^c A_{SS}]}{r_a^a+r_a^c}}{\Delta+\gamma\left[1+\frac{r_s^c}{r_a^a+r_a^c}\right]} \quad \text{(S5.23)}$$

$$PM_{su} = \frac{1}{\lambda}\frac{\Delta A_e + \frac{[\rho c_a(v_a^* - v_a) - \Delta r_a^s(A_e - A_{SS})]}{r_a^a + r_a^s}}{\Delta + \gamma\left[1 + \frac{r_s^s}{r_a^a + r_a^s}\right]} \tag{S5.24}$$

$$C_{ca} = \frac{1}{\left[1 + \frac{\eta_c \eta_a}{\eta_s(\eta_c + \eta_a)}\right]} \tag{S5.25}$$

$$C_{su} = \frac{1}{\left[1 + \frac{\eta_s \eta_a}{\eta_c(\eta_s + \eta_a)}\right]} \tag{S5.26}$$

$$\eta_a = (\Delta + \gamma) r_a^a \tag{S5.27}$$

$$\eta_s = (\Delta + \gamma) r_a^s + \gamma r_s^s \tag{S5.28}$$

$$\eta_c = (\Delta + \gamma) r_a^c + \gamma r_s^c \tag{S5.29}$$

where E_{SW} is the Shuttleworth-Wallace combined evaporation (mm day^{-1}) from the vegetation and the soil, PM_{ca} and PM_{su} are respectively the evaporation (mm day^{-1}) from a closed canopy and from bare substrate, A_e is the available energy (MJ m^{-2} day^{-1}) defined as the above-canopy fluxes of sensible heat and latent heat, and A_{SS} is the energy (MJ m^{-2} day^{-1}) available at the substrate, λ is the latent heat of vaporization (MJ kg^{-1}), Δ is the slope of the vapour pressure curve (kPa °C^{-1}), γ is the psychrometric constant (kPa °C^{-1}), c_a is the specific heat of the air (MJ kg^{-1} °C^{-1}) at air temperature, $(v_a^* - v_a)$ is the vapour pressure deficit (kPa), r_a^a is the aerodynamic resistance between the canopy source height and the reference level (s m^{-1}), r_a^c is the bulk boundary layer resistance of the vegetative elements in the canopy level (s m^{-1}), r_a^s is the aerodynamic resistance between the substrate and canopy source height level (s m^{-1}), r_s^c is the bulk stomatal resistance of the canopy level (s m^{-1}), and r_s^s is the surface resistance of the substrate level (s m^{-1}). Wessel and Rouse (1994, Section 4.1) were unable to determine the soil surface resistance, r_s, and adopted a value of 500 s m^{-1} for their hourly analysis.

It appears that Shuttleworth and Wallace (1985) did not prescribe the appropriate time-step that should be used in their model but Wessel and Rouse (1994) adopted both an hourly and daily time-step in their simulations. Readers interested in applying the SW model should refer to Stannard (1993) and Federer et al. (1996).

Weighted Penman-Monteith

In order to estimate the evaporation from a wetland, Wessel and Rouse (1994, Equation 14) proposed the following weighted Penman-Monteith approach:

$$E_{wetland} = LAI\ E_{can} + S\ E_{soil} + W\ E_{water} \tag{S5.30}$$

where $E_{wetland}$ is the evapotranspiration (mm day^{-1}) from the wetland, E_{can} is the transpiration (mm day^{-1}) from the canopy, E_{soil} is the soil evaporation (mm day^{-1}), E_{water} is the evaporation (mm day^{-1}) from the standing water, LAI is the leaf area index, and S and W are respectively the proportion of total area of bare soil and open water. E_{can}, E_{soil} and E_{water} are the Penman-Monteith estimates of ET for the canopy, soil and water as specified by Drexler et al. (2004, Equations 17 to 19):

$$E_{can} = \frac{1}{\lambda}\frac{\Delta(R_n^{can} - G) + \frac{\rho c_a(v_a^* - v_a)}{r_a}}{\Delta + \gamma\left(1 + \frac{r_c}{r_a}\right)} \tag{S5.31}$$

$$E_{soil} = \frac{1}{\lambda}\frac{\Delta(R_n^{soil} - G) + \frac{\rho c_a(v_a^* - v_a)}{r_a}}{\Delta + \gamma\left(1 + \frac{r_s^s}{r_a}\right)} \tag{S5.32}$$

$$E_{water} = \frac{1}{\lambda}\frac{\Delta\left(R_n^{water} - G\right) + \frac{\rho c_a (v_a^* - v_a)}{r_a}}{\Delta + \gamma} \tag{S5.33}$$

where E_{can}, E_{soil}, and E_{water} are respectively the evaporation (mm day^{-1}) from the canopy, soils and water, R_n^{can}, R_n^{soil}, and R_n^{water} are respectively the net solar radiation (MJ m^{-2} day^{-1}) to the canopy, soil and water, G is the heat flux transfer (MJ m^{-2} day^{-1}) to and from the soil and water, and other variables are defined above.

Matt-Shuttleworth

Shuttleworth and Wallace (2009, page 1904) recommend that the FAO-56 Reference Crop method (Allen et al., 1998) should not be applied to irrigation areas like those in Australia that are semi-arid and windy. They recommend that the Matt-Shuttleworth (M-S) model be adopted in place of the FAO-56 Reference Crop method. The M-S model consists of five steps (details are given in Shuttleworth and Wallace (2009, as Equations 5, 8, 9, and 10):

1. Select the surface resistance for the target crop (from Shuttleworth and Wallace (2009, Table 3). For example, for rye grass the surface resistance is 66 s m^{-1}.
2. Calculate

$$r_{clim} = 86400\,\frac{\rho_a c_a (VPD)}{\Delta R_n} \tag{S5.34}$$

where r_{clim} is termed the climatological resistance (s m^{-1}), ρ_a is the mean air density (kg m^{-3}) at constant pressure, c_a is the specific heat of the air (MJ kg^{-1} °C^{-1}), (VPD) is the vapour pressure deficit (kPa), Δ is the slope of the vapour pressure curve (kPa °C^{-1}) at air temperature, and R_n is the net radiation (MJ m^{-2} day^{-1}) at the vegetated surface. The 86,400 constant converts the radiation energy from MJ m^{-2} day^{-1} to MJ m^{-2} sec^{-1}.

3. Calculate

$$\frac{VPD_{50}}{VPD_2} = \left(\frac{302(\Delta+\gamma)+70\gamma u_2}{208(\Delta+\gamma)+70\gamma u_2}\right) + \frac{1}{r_{clim}}\left[\left(\frac{302(\Delta+\gamma)+70\gamma u_2}{208(\Delta+\gamma)+70\gamma u_2}\right)\left(\frac{208}{u_2}\right) - \left(\frac{302}{u_2}\right)\right] \tag{S5.35}$$

where VPD_{50} and VPD_2 are the vapour pressure deficits (kPa) at 50 m and 2 m height, and u_2 is the mean daily wind speed (m s^{-1}) at 2 m height.

4. Calculate

$$r_c^{50} = \frac{1}{(0.41)^2}\, ln\left[\frac{(50-0.67h)}{(0.123h)}\right] ln\left[\frac{(50-0.67h)}{(0.0123h)}\right] \frac{ln\left[\frac{(2-0.08)}{0.0148}\right]}{ln\left[\frac{(50-0.08)}{0.0148}\right]} \tag{S5.36}$$

where r_c^{50} is the aerodynamic coefficient (s m^{-1}) for crop height (h)

5. Calculate

$$ET_c = \frac{1}{\lambda}\frac{\Delta R_n + \frac{\rho_a c_a u_2 (VPD_2)}{r_c^{50}}\left(\frac{VPD_{50}}{VPD_2}\right)}{\Delta + \gamma\left(1 + \frac{(r_s)_c u_2}{r_c^{50}}\right)} \tag{S5.37}$$

where ET_c is the well-watered crop evapotranspiration in a semi-arid and windy location, λ is the latent heat of vaporization (MJ kg^{-1}), $(r_s)_c$ is the surface resistance (s m^{-1}) of a well-watered crop equivalent to the FAO crop coefficient (Shuttleworth and Wallace, 2009, Table 3), and other variables are defined previously.

At five locations in Australia, Shuttleworth and Wallace (2009) compared water requirements estimated by the Matt-Shuttleworth method with the requirements estimated by

FAO-56 Reference Crop method (Allen et al., 1998, Chapter 4) for irrigated sugar cane, cotton and short pasture. The analysis showed that within a growing season the differences between the two procedures varied considerably. However, over an entire season the M-S evapotranspiration estimate was 3% to 15% higher for sugar cane, 6% higher for cotton and between 0.5% and 2.5% for pasture compared to the FAO-56 method (Shuttleworth and Wallace, 2009, Table 4 and page 1905).

Supplementary Material

Appendix S6 PenPan model

There have been several variations of the Penman equation to model the evaporation from a Class-A evaporation pan. Linacre (1994) developed a physical model which he called the Penpan formula or equation. Rotstayn et al. (2006) coupled the radiative component of Linacre (1994) and the aerodynamic component of Thom et al. (1981) to develop the PenPan model which is defined, using the symbols of Johnson and Sharma (2010), as follows:

$$E_{PenPan} = \frac{\Delta}{\Delta + a_p\gamma}\frac{R_{NPan}}{\lambda} + \frac{a_p\gamma}{\Delta + a_p\gamma} f_{Pan}(u)(v_a^* - v_a) \tag{S6.1}$$

where E_{PenPan} is the modelled Class-A (unscreened) pan evaporation (mm day^{-1}), R_{NPan} is the net radiation (MJ m^{-2} day^{-1}) at the pan, Δ is the slope of the vapour pressure curve (kPa °C^{-1}) at air temperature, γ is the psychrometric constant (kPa °C^{-1}), and λ is the latent heat of vaporization (MJ kg^{-1}), a_p is a constant adopted as 2.4, $v_a^* - v_a$ is the vapour pressure deficit (kPa), and $f_{Pan}(u)$ is defined as (Thom et al., 1981, Equation 34):

$$f_{Pan}(u) = 1.201 + 1.621\, u_2 \tag{S6.2}$$

where u_2 is the average daily wind speed at 2 m height (m s^{-1}).

To estimate R_{NPan}, we refer to Rotstayn et al. (2006, Equations 4 and 5)):

$$R_{NPan} = (1 - \alpha_A)R_{SPan} - R_{nl} \tag{S6.3}$$

$$R_{SPan} = [f_{dir}P_{rad} + 1.42(1 - f_{dir}) + 0.42\alpha_{ss}]R_S \tag{S6.4}$$

where R_{SPan} is the total shortwave radiation (MJ m^{-2} day^{-1}) received by the pan, R_{nl} is the net outgoing longwave radiation (MJ m^{-2} day^{-1}) from the pan, R_S is the incoming solar radiation (shortwave) (MJ m^{-2} day^{-1}) at the surface, f_{dir} is the fraction of R_S that is direct, P_{rad} is a pan radiation factor, α_A is the albedo for a Class-A pan given as 0.14 (Linacre, 1992) as reported by Rotstayn et al. (2006, page 2), and α_{ss} is the albedo of the ground surface surrounding the evaporation pan (**Table S3**). To be consistent with Equation (S3.1) we have assumed the net outgoing longwave radiation R_{nl} as positive. As noted by Roderick et al. (2007, page 1), R_{SPan} > R_S because of the interception of energy by the pan walls.

f_{dir} and P_{rad} are defined as:

$$f_{dir} = -0.11 + 1.31\frac{R_S}{R_a} \tag{S6.5}$$

$$P_{rad} = 1.32 + 4 \times 10^{-4} lat + 8 \times 10^{-5} lat^2 \tag{S6.6}$$

where R_a is the extraterrestrial radiation (MJ m^{-2} day^{-1}), and lat is the absolute value of latitude in degrees.

The equations to estimate R_{nl} are set out in **Appendix S3**. The above analysis is carried out on a monthly time-step.

Application to Australian data

Using the PenPan model (with a_s = 0.23 and b_s = 0.50 as noted in **Appendix S3**), the mean monthly ratio of the PenPan evaporation, adjusted for the bird-screen, to the Class-A pan evaporation over the 68 stations (consisting of approximately 11840 ratios over all months) is 1.078. The monthly evaporation estimates are plotted in **Figure S3**. The performance of the PenPan model in estimating Class-A pan evaporation is satisfactory although the PenPan values are biased towards slightly higher values at lower evaporations. These results compare favourably with PenPan versus Class-A pan evaporation results of Rotstayn et al. (2006, Figure 4), Roderick et al. (2007, Figure 1) and Johnson and Sharma (2010, Figure 1) especially as we use the standard climate data available through the Bureau of Meteorology National Climate Centre and sunshine hours as the basis of estimating solar radiation.

An objective of this supplementary material was to develop for Australia mean monthly evaporation pan coefficients (relating open surface-water based on Penman to Class-A pan evaporation). Confidence in the monthly Penman estimates is based on the fact that the PenPan estimates, which utilise the same climatic data and a similar model structure as for the Penman model, were found to estimate the monthly pan evaporation very satisfactorily. In order to estimate Penman evaporation suitable for computing pan coefficients, we varied a_s and b_s values so that the overall monthly PenPan/Class-A pan ratio for the 68 stations was unity. We argue that the optimised values of a_s = 0.05 and b_s = 0.65 obtained in this way provided realistic monthly Penman values and, therefore, realistic pan coefficients. The mean monthly pan coefficients for the 68 Australian stations are listed in **Table S6.**

Supplementary Material

Appendix S7 Morton models

In 1985, Morton et al. (1985) published the program WREVAP which sets out operational aspects for computing estimates of areal evapotranspiration and lake evaporation. WREVAP contains three models CRAE (Complementary Relationship Areal Evapotranspiration) (Morton, 1983a), CRWE (Complementary Relationship Wet-Surface Evaporation) (Morton, 1983b) and CRLE (Complementary Relationship Lake Evaporation) (Morton, 1986). CRAE computes evapotranspiration for the land-based environment whereas CRWE deals with shallow lakes and CRLE considers deep lakes where water-borne heat input and energy storage are key issues. The three models are shown comparatively in Table 2 and are described in detail below.

In Morton's procedure, measurements of solar radiation are not required but are estimated through sunshine duration. However, if solar radiation data are available they may be used. The climate variables necessary to compute Morton's monthly evaporation are mean monthly maximum and minimum air temperature, dew point temperature (or monthly relative humidity), monthly sunshine duration and mean annual rainfall. For periods shorter than one month, Morton (1983a, page 28) imposed a limit on the shortest time-step for analysis and advocated a minimum of five days. However, for hydrological applications, Morton (1986, page 379) permits daily time-step analysis so long as the daily values are accumulated to a week or longer. But, it is important for lake analysis, described in CRLE below, that the time-step of analysis be one month (Morton (1986, page 379).

Morton (1986, page 378) notes that the CRLE model estimates are sensitive to radiation inputs (or sunshine hours) but insensitive to errors in air temperature and relative humidity inputs, whereas the CRAE model requires accurate air temperature and relative humidity from a representative location. For lakes, land-based meteorological data can be used (Morton, 1983b, page 82). Furthermore, Morton (1986, page 378) notes that data measured over water have only a "…relatively minor effect…" on the estimate of lake evaporation.

CRAE

The CRAE model consists of three components: potential evapotranspiration, wet-environment areal evapotranspiration and actual areal evapotranspiration. A discussion of each component follows.

Estimating potential evapotranspiration (ET_{Pot} in Figure 1)

Morton's approach to estimating potential evapotranspiration for a catchment or a large vegetated surface is to solve the energy-balance and the vapour transfer equations respectively for potential evapotranspiration and the equilibrium temperature:

$$ET_{Pot}^{Mo} = \frac{1}{\lambda}\left(R_n - [\gamma p f_v + 4\epsilon_s \sigma (T_e + 273)^3](T_e - T_a)\right) \quad \text{(S7.1)}$$

$$ET_{Pot}^{Mo} = \frac{1}{\lambda}\left(f_v (v_e^* - v_D^*)\right) \quad \text{(S7.2)}$$

where ET_{Pot}^{Mo} is Morton's estimate of point potential evaporation (mm day^{-1}), R_n is the net radiation (W m^{-2}) for soil-plant surfaces at air temperature, γ is the psychrometric constant (mbar °C^{-1}), p is the atmospheric pressure (mbar), f_v is a vapour transfer coefficient (W m^{-2} mbar^{-1}), ϵ_s is the surface emissivity, σ is the Stefan-Boltzmann constant (W m^{-2} K^{-4}), T_e and T_a are the equilibrium and air temperatures (°C), v_e^* is the saturation vapour pressure (mbar) at T_e, v_D^* is the saturation vapour pressure (mbar) at dew point temperature, and λ is the latent heat of vaporisation (W day kg^{-1}). (Note, the units used in Morton's procedures have been adopted here to ensure that the correct values of the empirical constants are included.)

f_v is given by:

$$f_v = \left(\frac{p_s}{p}\right)^{0.5} \frac{f_Z}{\xi} \tag{S7.3}$$

where p_s and p are the sea-level atmospheric pressure (mbar) and at-site atmospheric pressure (mbar) respectively, f_Z is a constant (W m^{-2} mbar^{-1}), and ξ is a dimensionless stability factor estimated from:

$$\xi = \frac{1}{0.28\left(1+\frac{v_D^*}{v_a^*}\right)+\frac{R_n\Delta}{\left[\gamma p\left(\frac{p_s}{p}\right)^{0.5} b_0 f_Z\left(v_a^*-v_D^*\right)\right]}} \quad \text{noting that } \xi \geq 1 \tag{S7.4}$$

where v_D^* is the saturation vapour pressure (mbar) at dew point temperature, v_a^* is the saturation vapour pressure (mbar) at air temperature, Δ is the slope of the saturation vapour pressure curve (mbar °C^{-1}) at air temperature, and b_0 = 1.0 for the CRAE model (Table 2).

Morton (1983a, Section 5.1) sets out the following procedure to find T_e by iteration, and then E_{Pot}^{MO} can be estimated from Equation (S7.1). Assume a trial value of T_e', which yields Δ_e' and $\delta T_e = T_e - T_e'$, hence $\delta v_e = \Delta_e' \delta T_e$ and $v_e^{*\prime} = v_e^* + \delta v_e$. Equating Equations (S7.1) and (S7.2) and substituting gives:

$$\delta T_e = \frac{\frac{R_n}{f_v}+v_a^*-v_e^{*\prime}+\lambda_e\left(T-T_e'\right)}{\left(\Delta_e'+\lambda_e\right)} \tag{S7.5}$$

where $\lambda_e = \gamma p + \frac{4\epsilon\sigma\left(T_e+273\right)^3}{f_v}$ (S7.6)

and variables are defined previously.

Initially, T_e' is set equal to the air temperature and the iterative procedure continues until δT_e becomes <0.01°C. Further details of the procedure are not included here but a worked example is provided in **Appendix S21**.

Estimating wet-environment areal evapotranspiration (ET_{Wet} in Figure 1)

To estimate the wet-environment areal evapotranspiration, which is equivalent to the conventional definition of potential evapotranspiration, Morton added an empirically derived advection constant (b_1) to the Priestley-Taylor equation (Equation (6) with G = 0) as follows:

$$ET_{Wet}^{Mo} = \frac{1}{\lambda}\left(b_1 + b_2 \frac{R_{ne}}{\left(1+\frac{\gamma p}{\Delta_e}\right)}\right) \tag{S7.7}$$

where ET_{Wet}^{Mo} is the wet-environment areal evapotranspiration (mm day^{-1}), R_{ne} is the net radiation (W m^{-2}) for the soil-plant surface at T_e (°C), Δ_e is the slope of the saturation vapour pressure curve (mbar °C^{-1}) at T_e (°C), b_1 and b_2 are empirical coefficients, and the other variables are as defined previously. Values of b_1 and b_2, which were derived by Morton (1983a, page 25) for representative regions, are set out in Table 2. R_{ne} is estimated as follows (Morton, 1983a, Equation C37):

$$R_{ne} = ET_{Pot}^{Mo} + \gamma p f_v\left(T_e - T_a\right) \tag{S7.8}$$

In their analysis of Australian data, Wang et al. (2001) adopted after calibration f_Z = 29.2 Wm^{-2} mbar^{-1} (Equation (S7.3)) and b_1 and b_2(Equation S7.7) equal to 13.4 Wm^{-2} and 1.13 Wm^{-2} instead of 28 Wm^{-2} mbar^{-1}, 14 Wm^{-2}, and 1.2 Wm^{-2} respectively (Table 2) to give an overall value of the Priestley-Taylor coefficient, α_{PT}, equal to 1.26 rather than Morton's 1.32 value. Chiew and Leahy (2003, Section 2.3) argue that the recalibrated values better represent Australian data. Our analysis for Australia stations (to be reported in later document) confirms that the Wang et al. (2001) calibrated parameters yield more realistic results than those of Morton.

Estimating actual areal evapotranspiration (ET_{Act} in Figure 1)

To estimate Morton's actual areal evapotranspiration (ET_{Act}^{Mo}) (mm day^{-1}), one uses the results from Equations (S7.1) and (S7.7) in the Complementary Relationship as follows:

$$ET_{Act}^{Mo} = 2ET_{Wet}^{Mo} - ET_{Pot}^{Mo} \tag{S7.9}$$

Morton (1983a, page 29) argues that as the models are completely calibrated they are accurate world-wide.

Limitations of CRAE model

Morton (1983a, page 28) points out five limitations of the CRAE model:

1. The model requires accurate measurements of humidity data.
2. The model should not be used for intervals of three days or less, however, as Morton (1983a) notes, so long as the accumulated values for a week or longer are accurate then a daily time-step is acceptable. (For lake evaporation, a monthly time-step should be used (Morton et al., 1985)).
3. The CRAE model should not be used near sharp discontinuities, e.g., near the edge of an oasis.
4. The climatological station should be representative of the area of interest.
5. Because the CRAE model does not use knowledge about the soil-vegetation system, it should not be used to examine the impact of natural or man-made change in the system.

Documentation of CRAE model

Documentation of the detailed steps to apply the CRAE model is given in Morton (1983a), Appendix C, and will not be repeated here. Our **Appendix S21** provides a worked example.

CRWE

In CRWE, the only difference to CRAE is that the radiation absorption and the vapour transfer characteristics reflect the water surface rather than a vegetated surface (Morton, 1983b) (Table 2). The CRWE model provides estimates of lake-size wet surface evaporation from routine climate data observed in the land environment. Furthermore, according to Morton (1986, page 371) monthly evaporation can be accumulated to provide reliable estimates of lake evaporation at the annual time-step for lakes up to approximately 30 m deep. To estimate the evaporation from a shallow lake, Equation (S7.7) is applied with coefficients b_1 and b_2 taking values given in Table 2.

CRLE

In the CRLE model, the computational procedure to estimate lake evaporation is the same as that used in CRWE except that the energy term is net energy available, which depends on solar and water inputs for the current and previous months. In estimating deep lake evaporation on a monthly time-step, where changes in sub-surface heat storage may be important, Morton (1986, page 376) adopts a classical lag and route procedure where the routing is a linear storage function. The 1986 method, which we adopt herein, is different to Morton's (1983b, Section 3) method. In the 1983 method, storage routing is applied to estimates of the shallow lake evaporation, whereas in Morton's (1986) procedure, the solar and water borne inputs are routed and then lake evaporation is estimated. Using Morton's symbols we summarise the four-step procedure of Morton (1986) as follows. Firstly, estimates of the solar and water borne heat input are computed:

$$G_W^0 = (1-\alpha)R_s - R_{nl} + \delta h \qquad \text{(S7.10)}$$

where G_W^0 is the solar and waterborne heat input (W m^{-2}), R_s is the incident global radiation (W m^{-2}), R_{nl} is the net outgoing longwave radiation (W m^{-2}), α is albedo for water, $(1-\alpha Rs$ is the net incoming shortwave radiation (W m^{-2}), and δh, which is usually small, is the difference between heat content of inflows and outflows from the lake (W m^{-2}). However, δh may be important for small lakes that receive cooling water with elevated temperatures, e.g., from a thermal power station or for a small deep lake with seasonal heat input from a large river (Morton, 1986, page 376). Note that Equation (S7.10) is different to Morton (1986, Equation 2) in that he appears not to have included net longwave radiation at this point in the analysis.

Secondly, the delayed energy input is computed from:

$$G_W^t = G_W^{[t_L]} + (t_L - [t_L])\left(G_W^{[t_L+1]} - G_W^{[t_L]}\right) \qquad \text{(S7.11)}$$

where $[t_L]$ and $(t_L - [t_L])$ are the integral and fractional components of the lake lag or delay time, t_L, (months), $G_W^{[t_L]}$ and $G_W^{[t_L+1]}$ are respectively the value (W m^{-2}) of G_W^0 computed for $[t_L]$ and for $[t_L+1]$ months previously.

The third step uses a linear routing procedure to route on a monthly time-step the available input energy, G_W^t, through the storage as follows:

$$G_{LE} = G_{LB} + \frac{G_W^t - G_{LB}}{0.5+S_c} \qquad \text{(S7.12)}$$

$$G_L = 0.5(G_{LE} + G_{LB}) \qquad \text{(S7.13)}$$

where G_L is the monthly lake energy input (W m^{-2}), G_{LB} and G_{LE} are the available solar and waterborne heat energy (W m^{-2}) at the beginning and end of the month respectively, and S_c is the storage coefficient or routing constant (months).

To compute S_c and t_L, the average lake depth and the lake salinity are taken into account as follows:

$$S_c = \frac{t_0}{\left[1+\left(\frac{\bar{h}}{93}\right)^7\right]} \qquad \text{(S7.14)}$$

$$t_0 = 0.96 + 0.013\bar{h} \;\text{ with } 0.039\bar{h} \le t_0 \le 0.13\bar{h} \qquad \text{(S7.15)}$$

$$t_L = \frac{t_0}{\left(1+\frac{s}{27000}\right)^2} \;\text{ with } t \le 6.0 \qquad \text{(S7.16)}$$

where t_0 is the soft water delay time (months), $\bar{h}$ is the average depth of the lake (m), and s is the lake salinity (ppm) (1 ppm ~ 1.56 microS cm^{-1} or EC units).

The final step is to input monthly values of G_L as R_n into Equation S7.1 to estimate deep lake monthly evaporation.

Typically, reservoir evaporation exceeds the evapotranspiration that would have occurred from the inundated area in the natural state. This net evaporation can be estimated as the difference between lake evaporation and actual areal evapotranspiration (Morton, 1986, item 4, page 386).

In Morton's procedure, solar radiation measurements are not required as these are estimated from the other observed climate variables in the model. Chiew and Jayasuriya (1990) and Szilagyi (2001, page 198) indicate that estimates of daily global and net radiation by the Morton (1983a, Appendix C.1.2) procedure are accurate. Some researchers, e.g., Wang et al. (2001) and Szilagyi and Jozsa (2008) have used observed solar radiation data instead of Morton's empirical estimate of R_T, which is equivalent to R_s in this paper.

A listing of a Fortran 90 version of Program WREVAP, which follows closely Morton (1983a, Appendix C) and the routing scheme described in Morton (1986), is provided in **Appendix S20**.

Australian application of the complementary relationship

Wang et al. (2001) used Morton's (1983a) model to produce a series of maps for Australia showing mean monthly areal potential evapotranspiration, point potential evapotranspiration and areal actual evapotranspiration; these terms were adopted by Wang et al (2001). The maps, which are at 0.1°(~10 km) grid resolution, are available at http://www.bom.gov.au/climate/averages and as a hard-copy in Wang et al. (2001). The detailed methodology is described in Chiew et al. (2002). Wang et al. (2001) provides the following guidelines for the application of the maps noting that they should not be used in estimating open water evaporation:

- Areal potential evapotranspiration (equivalent to Morton's wet environment areal evapotranspiration ET_{Wet}^{Mo})
  - Large area with unlimited water supply
  - "Areal" > 1 km^2
  - Upper limit to actual evapotranspiration in rainfall-runoff modelling studies
  - Evapotranspiration from a large irrigation area with no shortage of water
- Point potential evapotranspiration (equivalent to Morton's potential evapotranspiration ET_{Pot}^{Mo})
  - ET from a point with unlimited water supply
  - A small irrigation area surrounded by unirrigated area
  - Approximate preliminary estimate of evaporation from farm dams and shallow water storages

Based on 55 locations across Australia Chiew and Leahy (2003) found that ET_{Pot} could be used as a substitute for Class-A pan evaporation.

Following an extensive analysis of potential evaporation formulations across Australia, Donohue et al. (2010b, page 192) have provided two of the Morton evaporation estimates namely areal potential evapotranspiration and point potential evapotranspiration as daily time-step grids. However, they concluded that the Morton point potential method is unable to reproduce evaporation dynamics observed across Australia and is unsuitable for general use. However, R. Donohue (pers. comm.) advised that "the reason Morton point potential values were so high in Donohue et al. (2010b) was because, in their modelling of net radiation, they explicitly accounted for actual land-cover dynamics. This procedure differs from Morton's

(1983) methodology, developed over 25 years ago, when remotely sensed data were not routinely available, and thus Donohue et al. (2010b) is in contradiction to Morton's (1983) methodology."

Supplementary Material

Appendix S8 Advection-Aridity and like models

Advection-aridity model

Based on the Complementary Relationship, Brutsaert and Strickler (1979, page 445) proposed the Advection-Aridity (AA) model to estimate actual evapotranspiration (ET_{Act}) in which they adopted the Penman equation for potential evapotranspiration (ET_{Pot}) and the Priestley-Taylor equation for the wet-environment (ET_{Wet}). The Complementary Relationship is:

$$ET_{Act} = 2ET_{Wet} - ET_{Pot} \tag{S8.1}$$

and substituting for the Penman (Equation (4)) and Priestley-Taylor (Equation (6)) and rearranging yields:

$$ET_{Act}^{BS} = (2\alpha_{PT} - 1)\frac{\Delta}{\Delta+\gamma}\frac{R_n}{\lambda} - \frac{\gamma}{\Delta+\gamma}f(u_2)(v_a^* - v_a) \tag{S8.2}$$

where ET_{Act}^{BS} is the actual areal evapotranspiration (mm day^{-1}) based on Brutsaert and Strickler (1979), R_n is the net radiation (MJ m^{-2} day^{-1}) at the evaporating vegetative surface, α_{PT} is the Priestley-Taylor parameter, u_2 is the average daily wind speed in m s^{-1}, v_a^* and v_a are respectively the saturation vapour pressure and the vapour pressure of the overpassing air (kPa) at aie temperature, Δ is the slope of the saturation vapour pressure curve at air temperature (kPa °C^{-1}), γ is the psychrometric constant (kPa °C^{-1}) and λ is the latent heat of vaporization (MJ kg^{-1}).

Based on an energy budget for a rural catchment in Holland, Brutsaert and Strickler (1979, page 445) adopted a Priestley and Taylor (1972) constant α_{PT} of 1.28 rather than 1.26 (see Section 2.1.3) and Penman's (1948) wind function $f(u_2)$ as:

$$f(u_2) = 2.626 + 1.381u_2 \tag{S8.3}$$

which, according to Brutsaert and Strickler (1979, page 445), is equivalent to a surface of moderate roughness. In the comparison, R_n was measured by a net radiometer and surface albedo did not need to be assessed. If measured values of R_n are not available the adopted value of albedo should be appropriate for the surface conditions (see **Table S3**).

Brutsaert and Strickler (1979, Figures 1 to 4) tested their model at a daily time-step and observed that integrating the daily ET estimates over three days achieved better agreement with energy budget estimates than single day estimates. Equation (S8.2) sometimes generates negative ET values at the daily time-step.

Hobbins et al. (2001a) applied the AA model of Brutsaert and Strickler (1979) and the CRAE model of Morton (1983a) to 120 minimally impacted U.S. catchments and found the AA model underestimated annual actual evapotranspiration by 10.6% of mean annual precipitation; the CRAE model overestimated annual evapotranspiration by only 2.5% of precipitation (Hobbins et al., 2001a, Abstract). Hobbins et al. (2001b) recalibrated the AA model for a larger data set (139 minimally impacted basins) and adopted monthly regional wind functions, $f(u_2)$. Using α_{PT} = 1.3177 they achieved a more satisfactory result than the original AA model. Another application of the AA model and the Zhang et al. (2001) model is by Brown et al. (2008, Table 1) who examined the spatial distribution of water supply in the United States. Across the U.S., the AA model overestimated the US Geological Survey gauged data by 4% and the Zhang model underestimated the gauged data by 5%.

Monteith (1981, page 24) offers the following comment regarding the Brutsaert and Strickler equation. "The scheme … has the merit of elegance and simplicity but its foundations need strengthening. Apart from the uncertainty which surrounds the value of α and it physical significance, Bouchet's hypothesis of complementarity between actual and potential rates of evaporation needs to be substantiated by an appropriate model of the planetary boundary layer."

Granger-Gray model

To estimate actual evapotranspiration from non-saturated lands, Granger and Gray (1989) developed a modified form of the Penman (1948) equation following Granger (1998) as follows:

$$ET_{Act}^{GG} = \frac{\Delta G_g}{\Delta G_g + \gamma}\frac{R_n - \mathrm{G}}{\lambda} + \frac{\gamma G_g}{\Delta G_g + \gamma}E_a \tag{S8.4}$$

where ET_{Act}^{GG} is the actual evapotranspiration (mm day^{-1}) based on Granger and Gray (1989), R_n is the net radiation (MJ m^{-2} day^{-1}) near the evaporating surface (hence the albedo adopted is for the evaporating surface), G is the heat flux into the soil (MJ m^{-2} day^{-1}), λ is the latent heat of vaporization (MJ kg^{-1}), Δ is the slope of the saturation vapour pressure curve at air temperature (kPa °C^{-1}), and γ is the psychrometric constant (kPa °C^{-1}), E_a is the drying power of the air (Equation S4.2), and G_g is a dimensionless evaporation parameter, which is based on several surface types, and is defined as (Granger, 1998, Equations 6 and 7):

$$G_g = \frac{1}{0.793 + 0.20e^{4.902 D_p}} + 0.006 D_p \tag{S8.5}$$

where D_p, a dimensionless relative drying power, is defined as:

$$D_p = \frac{E_a}{E_a + \frac{R_n - G}{\lambda}} \tag{S8.6}$$

where G is set to zero.

Adopting a daily time-step, Xu and Chen (2005, page 3725) compared, inter alia, Granger-Gray (GG) model with 12 years of daily lysimeter observations located at Mönchengladbach-Rheindahlen meteorological station in Germany and found the GG model performed better than the Brutsaert and Strickler Advection-Aridity model and the Morton CRAE model (Xu and Chen (2005, Abstract).

Szilagyi-Jozsa model

Based on theoretical considerations, Szilagyi (2007) offered an alternative modification of the AA model which was further amended by Szilagyi and Jozsa (2008, Equation (10)) to the following:

$$ET_{Act}^{SJ} = 2E_{PT}(T_e) - E_{Pen} \tag{S8.7}$$

where ET_{Act}^{SJ} is actual evapotranspiration (mm day^{-1}), $ET_{PT}(T_e)$ is wet-environment evaporation (mm day^{-1}) estimated by Priestley-Taylor at T_e (°C), E_{Pen} is potential evapotranspiration (mm day^{-1}) estimated by Penman using the 1948 wind function.

To evaluate T_e, Szilagyi and Jozsa (2008) considered the Bowen Ratio (Bowen, 1926) for a small lake or sunken pan and found the equilibrium surface temperature, T_e, could be estimated iteratively on a daily basis from (Szilagyi and Jozsa, 2008, Equation (8)):

$$\frac{R_n}{\lambda E_{Pen}} = 1 + \frac{\gamma(T_e - T_a)}{v_e^* - v_a} \tag{S8.8}$$

where R_n is the available energy (MJ m^{-2} day^{-1}), E_{Pen} is the Penman evaporation (mm day^{-1}) based on T_a, and T_e and T_a are respectively the equilibrium and air temperatures (°C), v_e^* is the saturation vapour pressure (kPa) at T_e, v_a is the actual vapour pressure (kPa) at T_a, λ is the latent heat of vaporization (MJ kg^{-1}), and γ is the psychrometric constant (kPa °C^{-1}).

Based on daily data and adopting α_{PT} = 1.31 but applying the Complementary Relationship to obtain monthly ET_{Act}^{SJ} values, Szilagyi and Jozsa (2008) tested Equation (S8.7) against actual evaporation estimated by Morton's WREVAP model for 210 SAMSON (Solar and Meteorological Surface Observation Network) stations in the United States and found excellent agreement (R^2 = 0.95) (Szilagyi and Jozsa, 2008, Figure 6). Szilagyi et al (2009, page 574) applied their modified AA model to 25 watersheds, 194 SAMSON sites and 53 semi-arid SAMSON sites and concluded that their modified AA model performed better than the Brutsaert and Strickler (1979) traditional AA model.

In applying Equation (S8.7), a daily time-step is used and an albedo value for the vegetative surface is adopted. We note that when we applied Equation (S8.7) to days of very low net radiation, negative values of evaporation were occasionally estimated, a feature also observed in the Brutsaert and Strickler (1979, page 448) Aridity-Advection model (see **Appendix S18**).

Supplementary Material

Appendix S9 Additional evaporation equations

Although the following empirical equations (except the energy based procedure described at the end of this appendix) have been extensively referenced or widely used in past practice and therefore are included in this paper, we are of the view that the more physically-based equations described earlier are generally more appropriate for estimating evaporation or evapotranspiration. This is particularly so in regions where empirical coefficients have not been derived.

Dalton-type equations

Mass-transfer equations of the following form were first described by John Dalton in 1802 and are known as Dalton-type equations (Dingman, 1992, Section 7.3.2):

$$E = C_{emp} f(u)(v_s^* - v_a) \tag{S9.1}$$

where E is the actual surface evaporation (mm day^{-1}), $f(u)$ is an appropriate wind function, v_s^* is the saturation vapour pressure (kPa) at the evaporating surface, v_a is the atmospheric vapour pressure (kPa), and C_{emp} is an empirical constant. McJannet et al. (2012) reviewed 19 studies for estimating open water evaporation and proposed a wind function (Equation 14) that depends on the area of the evaporating surface (see Section 2.4.2).

Thornthwaite (1948)

In the Thornthwaite evaporation method, the only meteorological data required to compute mean monthly potential evapotranspiration is mean monthly air temperature, The original steps in Thornthwaite's (1948) procedure involved a nomogram and tables, which can be represented by the follow equations (Xu and Singh, 2001, Equations 4a and 4b):

$$\bar{E}_{Th,j} = 16\left(\frac{\overline{hrday}}{12}\right)\left(\frac{daymon}{30}\right)\left(\frac{10\bar{T}_J}{I}\right)^{a_{Th}} \tag{S9.2}$$

where $\bar{E}_{Th,j}$ is the Thornthwaite 1948 estimate of mean monthly potential evapotranspiration (mm month^{-1}) for month j, (j = 1 to 12), $\overline{hrday}$ is the mean daily daylight hours in month j, $daymon$ is the number of days in month j, $\bar{T}_J$ is the mean monthly air temperature (^{o}C) in month j, and I is the annual heat index. The annual heat index is estimated as the sum of the monthly indices:

$$I = \sum_{j=1}^{12} i_j \tag{S9.3}$$

where $i = \left(\frac{\bar{T}_J}{5}\right)^{1.514}$ (S9.4)

and $a_{Th} = 6.75 \times 10^{-7} I^3 - 7.71 \times 10^{-5} I^2 + 0.01792 I + 0.49239$ (S9.5)

It is noted that strict application of Thornthwaite (1948) yields only 12 values of potential evapotranspiration, a mean value for each calendar month. However, in several studies, Thornthwaite's procedure has been modified to allow a time series of daily (Federer et al., 1996; Donohue et al., 2010b) or monthly (Xu and Singh, 2001; Lu et al., 2005; Amatya et al., 1995; Xu and Chen, 2005; Trajkovic and Kolakovic, 2009) potential evaporation values to be computed.

Building on Thornthwaite's (1948) water balance procedure used in his climate classification analysis, Thornthwaite and Mather (1957) developed a procedure for computing a water balance. We suggest readers planning to use the Thornthwaite-Mather method pay attention to Black's (2007) paper in which he notes that there are significant differences between a 1955 version of the methodology and the 1957 version which, according to Black (2007), is the correct procedure. The Thornthwaite and Mather (1957) methodology consists of applying the 1948 procedure in a water balance context. Scozzafava and Tallini (2001) provide an example.

Makkink model

G.F. Makkink, as reported by de Bruin (1981, Equation 5), simplified the Penman (1948) equation by disregarding the aerodynamic term but compensated the evaporation estimate by introducing two empirical coefficients as follows:

$$E_{Mak} = 0.61\left(\frac{\Delta}{\Delta+\gamma}\frac{R_s}{2.45}\right) - 0.12 \qquad \text{(S9.6)}$$

where E_{Mak} is the Makkink potential evaporation (mm day^{-1}), R_s is the solar radiation (incoming shortwave) (MJ m^{-2} day^{-1}) at the water surface, Δ is the slope of the vapour pressure curve (kPa °C^{-1}) at air temperature, and γ is the psychrometric constant (kPa °C^{-1}). According to Rosenberry et al. (2004, Table 1), a monthly time-step is used in the Makkink computations.

FAO-24 Blaney and Criddle (Allen and Pruitt, 1986)

There have been a number of modifications made to the original Blaney (1959) equation for estimating the consumptive use or reference crop evapotranspiration. We outline here the Reference Crop FAO-24 (Allen and Pruitt, 1986; Jensen et al, 1990) version of Blaney and Criddle which is for a grass-related crop evapotranspiration. The method is based on several empirical coefficients which were developed from data measured at adequately watered, agricultural lysimeter sites (Allen and Pruitt, 1986), located in the dry western United States where advection effects were strong (Yin and Brook, 1992).

The FAO-24 Reference Crop version of Blaney-Criddle is defined as (Allen and Pruitt, 1986, Equations 1, 2 and 3; Shuttleworth, 1992, Equation 4.2.45):

$$ET_{BC} = \left(0.0043RH_{min} - \frac{n}{N} - 1.41\right) + b_{var}p_y(0.46T_a + 8.13) \qquad \text{(S9.7)}$$

$$b_{var} = e_0 + e_1 RH_{min} + e_2\frac{n}{N} + e_3 \mathrm{u}_2 + e_4 RH_{min}\frac{n}{N} + e_5 RH_{min}\mathrm{u}_2 \qquad \text{(S9.8)}$$

where ET_{BC} is the Blaney-Criddle Reference Crop evapotranspiration (mm day^{-1}), RH_{min} is the minimum relative daily humidity (%), *n/N* is the measured sunshine hours divided by the possible daily sunshine hours, p_y is the percentage of actual daytime hours for the day compared to the day-light hours for the entire year, T_a is the average daily air temperature (^{o}C), and u_2 is average daily wind speed (m s^{-1}) at 2 m. The recommended values of the coefficients are from Frevert et al. (1983, Table 1) as follows: e_0 = 0.81917, e_1 = -0.0040922, e_2 = 1.0705, e_3 = 0.065649, e_4= -0.0059684, e_5 = -0.0005967. Due to lower minimum daily temperatures at higher elevation (McVicar et al., 2007 Figure 3), Allen and Pruitt (1986) incorporate an adjustment for elevation to the FAO-24 Blaney-Criddle equation for arid and semi-arid regions following Allen and Brockway (1983) as follows:

$$ET_{BC}^{H} = ET_{BC}\left[1 + 0.1\frac{Elev}{1000}\right] \qquad \text{(S9.9)}$$

where ET_{BC}^{H} is the Blaney-Criddle Reference Crop evapotranspiration adjusted for site elevation and $Elev$ is the elevation of the site above mean sea level (m).

Doorenbos and Pruitt (1992, page 4) note that the BC procedure should be used “with scepticism” in equatorial regions (where air temperatures are “relatively constant”), for small islands and coastal areas (where air temperature is affected by sea temperature), for high elevations (due to environmental lapse rate induced low mean daily air temperature) and in monsoonal and mid–latitude regions (with a wide variety of sunshine hours).

It is noted that the original Blaney-Criddle procedure incorporates only monthly temperature data. Consequently, the coefficients e_0, …, e_5 and the climate variables RH_{min}, , T_a, u_2 in Equations (S9.7) and (S9.8), which were based on the crop consumptive use in western United States using the original BC model, will not represent potential evaporation in regions with climates differing from those in western United States. This may explain the Doorenbos and Pruitt (1992) comment in the previous paragraph.

Although the BC method has been used at both a daily and a monthly time-step (Allen and Pruitt, 1986), a monthly period is recommended (Doorenbos and Pruitt, 1992, page 4; Nandagiri and Kovoor, 2006, page 240).

Turc (1961)

The Turc method (Turc 1961) is one of the simplest empirical equations used to estimate reference crop evapotranspiration under humid conditions. (Note that the Turc (1961) equations are very different to those proposed in Turc (1954, 1955).) The Turc 1961 equation, based on daily data, is quoted by Trajković and Stojnić (2007, Equation 1) as:

$$ET_{Turc} = 0.013(23.88R_s + 50)\left(\frac{T_a}{T_a+15}\right) \tag{S9.10}$$

where ET_{Turc} is the reference crop evapotranspiration (mm day^{-1}), T_a is the average air temperature (^{o}C), and R_s is the incoming solar radiation (MJ m^{-2} day^{-1}).

For non-humid conditions (RH < 50%), the adjustment provided by Alexandris et al. (2008, Equation 5b) may be used.

$$ET_{Turc} = 0.013(23.88R_s + 50)\left(\frac{T_a}{T_a+15}\right)\left(1 + \frac{50-RH}{70}\right) \tag{S9.11}$$

where RH is the relative humidity (%).

Because Jensen et al. (1990) identified that the Turc (1961) method performs satisfactorily in humid regions (see Table 5), Trajković and Kolaković (2009) developed an empirical factor to adjust ET_{Turc} for wind speed. Details are given in Trajković and Kolaković (2009).

Hargreaves-Samani (Hargreaves and Samani, 1985)

The Hargreaves-Samani equation (Hargreaves and Samani, 1985, Equations 1 and 2), which estimates reference crop evapotranspiration, is as follows:

$$ET_{HS} = 0.0135C_{HS}\frac{R_a}{\lambda}(T_{max} - T_{min})^{0.5}(T_a + 17.8) \tag{S9.12}$$

where ET_{HS} is the reference crop evapotranspiration (mm day^{-1}), C_{HS} is an empirical coefficient, R_a is the extraterrestrial radiation (MJ m^{-2} day^{-1}), T_{max}, T_{min}, T_a are respectively the maximum, minimum and average daily air temperature (^{o}C). Samani (2000, Equation 3) proposed a modification to the empirical coefficient to reduce the error associated with the estimation of solar radiation as follows:

$$C_{HS} = 0.00185(T_{max} - T_{min})^2 - 0.0433(T_{max} - T_{min}) + 0.4023 \quad \text{(S9.13)}$$

According to Amatya et al. (1995, Table 4), weekly or monthly data should be used in the Hargreaves-Samani model in the computation of reference crop evapotranspiration rates.

Modified Hargreaves

The modified Hargreaves procedure (Droogers and Allen, 2002), as adapted by Adam et al (2006, Equation 6), allows one to estimate the reference crop evapotranspiration without wind data using monthly values of rainfall, air temperature, daily air temperature range, and extra-terrestrial solar radiation as follows:

$$ET_{Harg,j} = 0.0013S_O(T_j + 17.0)(\overline{TD}_j - 0.0123P_j)^{0.76} \quad \text{(S9.14)}$$

where, for a given month j, $ET_{Harg,j}$ is the modified Hargreaves monthly reference crop evapotranspiration (mm day^{-1}), T_j is the monthly mean daily air temperature (°C), $\overline{TD}_j$ is the mean monthly difference between mean daily maximum air temperature and mean daily minimum air temperature (°C) for month j, P_j is the monthly precipitation (mm month^{-1}), and S_O is the mean monthly water equivalent for extraterrestrial solar radiation (mm day^{-1}). If $\overline{TD}_j$ data are unavailable, New et al. (2002) have provided 10′ latitude/longitude gridded mean monthly diurnal air temperature range. Again, following the approach of Adam et al. (2006, Equations 7, 8, 9 and 10), S_O is estimated by:

$$S_0 = 15.392 d_r^2 \left(\omega_s sin(lat) sin(\delta) + cos(lat) cos(\delta) sin(\omega_s)\right) \quad \text{(S9.15)}$$

where lat is the latitude of the location in radians (negative for southern hemisphere), d_r is the relative distance between the earth and the sun, given by:

$$d_r^2 = 1 + 0.033 cos\left(\frac{2\pi}{365} DoY\right) \quad \text{(S9.16)}$$

where DoY is the Day of Year (see **Appendix S3**), ω_s is the sunset hour angle in radians (see Adam et al., 2006, page 22 for boundary conditions) and is given by:

$$\omega_s = arcos(-tan(lat)\tan(\delta)) \quad \text{(S9.17)}$$

and δ is the solar declination in radians given by:

$$\delta = 0.4093 sin\left(\frac{2\pi}{365} DoY - 1.405\right) \quad \text{(S9.18)}$$

Evapotranspiration estimates are based on a monthly time-step.

Application based on energy balance

A very different approach to the application of energy balance is by McLeod and Webster (1996, Equations 8 and 9) who used data from an instrumented irrigation channel to estimate channel evaporation from:

$$E_{ic} = \frac{(R_n + Q_v - Q_t)}{\left(1 + B + \frac{c_w T_s}{\lambda}\right)} \frac{\Delta t}{\lambda} \quad \text{(S9.19)}$$

where E_{ic} is the evaporation from the irrigation channel (mm day^{-1}), R_n is the net radiation on the water surface (MJ m^{-2} day^{-1}), Q_v is the heat flux advected into the water body (MJ m^{-2} day^{-1}), Q_t is the heat flux increase in stored energy (MJ m^{-2} day^{-1}), B is the Bowen Ratio, c_w is specific heat of water (MJ kg^{-1} °C^{-1}), T_s is the temperature of the evaporated water (°C), Δt is time interval over which the fluxes are estimated (day), and λ is the latent heat of vaporisation (MJ kg^{-1}).

Supplementary Material

Appendix S10 Estimating deep lake evaporation

Based on a review of the literature, **Table S5** provides guidelines to define deep and shallow lakes for the purpose of estimating lake evaporation. (The background to **Table S5** is discussed in the **Appendix S11**.)

Kohler and Parmele (1967)

The Penman estimate of open-water evaporation, E_{PenOW}, (Equation (12)) is a starting point to estimate evaporation from a deep lake using the Kohler and Parmele (1967) procedure. To account for water advected energy and heat storage, Kohler and Parmele (1967, Equation 12) recommended the following relationship:

$$E_{DL} = E_{PenOW} + \alpha_{KP}(A_w - \frac{\Delta Q}{\Delta t}) \quad \text{(S10.1)}$$

where E_{DL} is the evaporation from the deep lake (mm day^{-1}), E_{PenOW} is the Penman open-water evaporation (mm day^{-1}), α_{KP} is the proportion of the net addition of energy from advection and storage used in evaporation during Δt, A_w is the net water advected energy during Δt (mm day^{-1}), and $\frac{\Delta Q}{\Delta t}$ is the change in stored energy (mm day^{-1}). Kohler and Parmele (1967, page 1002) illustrated their method adopting Δt = 1 day. The three other terms are complex and following Dingman (1992, Equations 7.38, 7.31 and 7.32 respectively) can be computed from:

$$\alpha_{KP} = \frac{\Delta}{\Delta + \gamma + \frac{4\varepsilon_W \sigma (T_W + 273.2)^3}{\rho_W \lambda K_E u}} \quad \text{(S10.2)}$$

$$A_w = \frac{c_w \rho_w}{\lambda}(P_d T_p + SW_{in} T_{swin} - SW_{out} T_{swout} + GW_{in} T_{gwin} - GW_{out} T_{gwout}) \quad \text{(S10.3)}$$

$$\Delta Q = \frac{c_w \rho_w}{A_L \lambda}(V_2 T_{L2} - V_1 T_{L1}) \quad \text{(S10.4)}$$

where Δ is the slope of the vapour pressure curve (kPa °C^{-1}) at air temperature, ε_W is the effective emissivity of the water (dimensionless), σ is the Stefan-Boltzman constant (MJ m^{-2} day^{-1} K^{-4}), T_w is the temperature of the water (°C), T_p is the temperature of precipitation (°C), c_w is the specific heat of water (MJ kg^{-1} °C^{-1}), P_d is the precipitation rate (mm day^{-1}), λ is the latent heat of vaporization (MJ kg^{-1}), K_E is a coefficient that represents the efficiency of the vertical transport of water vapour (kPa^{-1}), u is mean daily wind speed (m day^{-1}), SW and GW represent surface and ground water inflows and outflows as per subscript (mm day^{-1}) and V's and T's represent respective average lake volumes (m^3) and temperatures (°C), A_L is lake area (m^2), and 1 and 2 identify values at the beginning and end of Δt. Generally, for surface lakes GW will be small with respect to SW and can be ignored, but for a deep void following surface mining, groundwater may need to be assessed. Estimation of K_E (m day^2 kg^{-1}) is based on Equation (S10.5), but may need to be adjusted for atmospheric stability (see Dingman, 1992, Equation 7.2):

$$K_E = 0.622 \frac{\rho_a}{p \rho_W} \frac{1}{6.25\left[ln\left(\frac{z_m - z_d}{z_0}\right)\right]^2} \quad \text{(S10.5)}$$

where ρ_a is the density of air (kg m^{-3}), ρ_w is the density of water (kg m^{-3}), p is the atmospheric pressure (kPa), z_m is the height above ground level (m) at which the wind speed and vapour pressure are measured (m), z_d is the zero-plane displacement (m), and z_0 is the roughness height of the surface (m).

Harbeck (1962) found that lake area accounted for much of the variability in K_E and, as an alternative to Equation (S10.5), K_E can be estimated by (Dingman, 1992, Equation 7-19):

$$K_E = 1.69{\times}10^{-5} A_L^{-0.05} \tag{S10.6}$$

where A_L is the lake area (km^2).

Because changes in daily energy cannot be estimated with sufficient accuracy relative to the other fluxes, Kohler and Parmele (1967, page 1002) based their comparisons on periods of a week to a month, not daily.

Vardavas and Fountoulakis (1996)

The Vardavas and Fountoulakis (1996) method for estimating monthly evaporation from a deep lake, in which seasonal heat storage effects are significant, is based on the Penman equation (Penman, 1948):

$$E_{DL} = \left(\frac{\Delta}{\Delta+\gamma}\right) E_s + \left(\frac{\gamma}{\Delta+\gamma}\right) E_a \tag{S10.7}$$

where E_{DL} is the evaporation (mm day^{-1}) for a deep lake, E_s is the evaporation component (mm day^{-1}) due to net heating, E_a is the evaporation component (mm day^{-1}) due to wind, Δ is the slope of the vapour pressure curve (kPa °C^{-1}) at air temperature, and γ is the psychrometric constant (kPa °C^{-1}).

$$E_s = \frac{1}{\lambda}(R_n + \Delta H) \tag{S10.8}$$

where R_n is the net radiation (MJ m^{-2} day^{-1}) at the water surface, λ is the latent heat of vaporization (MJ kg^{-1}), and ΔH is the net energy gained from heat storage in the water body (MJ m^{-2} day^{-1}).

Following Vardavas and Fountoulakis (1996, Equation 28), ΔH is determined on a monthly basis using:

$$\Delta H_{j,j-1} = -48.6\bar{h}\frac{\Delta T_{wl}}{t_m} \tag{S10.9}$$

where $\Delta H_{j,j-1}$ is the change in heat storage (W m^{-2}) from month j-1 to month j, $\bar{h}$ is the mean lake depth (m), $\Delta T_{wl} = T_{w,j} - T_{w,j-1}$, i.e., the change in surface water temperature (°C) from month j-1 to month j, and t_m is the number of days in the month.

E_a is the wind component defined by Penman (1948) as:

$$E_a = f(\bar{u})[v_a^*(T_a) - v_a(T_a)] \tag{S10.10}$$

where $\bar{u}$ is average daily wind speed (m s^{-1}), $v_a^*(T_a)$ is the saturation vapour pressure (mbar) at the water surface evaluated at air temperature T_a (°C), and $v_a(T_a)$ is the vapour pressure (mbar) at a given height above the water surface evaluated at the air temperature (°C), and

$$f(\bar{u}) = C_u\bar{u} \tag{S10.11}$$

where C_u can be evaluated as set out below. Estimated values of C_u by Vardavas and Fountoulakis (1996, page 144) for four Australian reservoirs (Manton, Cataract, Mundaring and Eucumbene) range from 0.11 to 0.13 mm day^{-1}/(m s^{-1} mbar).

Following Vardavas (1987, Equation 23) C_u can be evaluated from:

$$C_u = \frac{3966}{T_a ln\left(\frac{z_2}{z_{ov}}\right) ln\left(\frac{z_1}{z_{om}}\right)} \tag{S10.12}$$

where T_a is the air temperature (K), z_1 is the height above ground of the wind speed measurement (m), z_2 is the height above ground of the water vapour measurement (m). z_{om}, the momentum roughness (m), and z_{ov}, the roughness length for water vapour (m), are given by:

$$z_{om} = 0.135 \frac{\upsilon}{u_*} \tag{S10.13}$$

$$z_{ov} = 0.624 \frac{\upsilon}{u_*} \tag{S10.14}$$

where υ is the kinematic viscosity of air (m^2 s^{-1}) and is estimated by:

$$\upsilon = 2.964 \times 10^{-7} \frac{T_a^{3/2}}{p} \tag{S10.15}$$

where T_a is the air temperature (K), and p is the atmospheric pressure (kPa).

The friction velocity, u_*, is computed from:

$$\bar{u} = \frac{u_*}{k} ln\left(\frac{z_2 u_*}{0.135 \upsilon}\right) \tag{S10.16}$$

where k is von Kármán's constant, $\bar{u}$ is the mean wind speed (m s^{-1}), z_2 is the height above ground of water vapour measurement (m), and υ is the kinematic viscosity of air (m^2 s^{-1}). u_* can be estimated by a numerical iteration technique, e.g., Newton-Raphson.

Other approaches that may be appropriate

Several approaches that have been included under **Appendix S11** *Estimating shallow lake evaporation* may be appropriate for deep lakes. In particular, McJannet et al. (2008b) procedure has been tested for two deep lakes.

Supplementary Material

Appendix S11 Estimating shallow lake evaporation

Based on a review of the literature, **Table S5** provides guidelines to define deep and shallow lakes for the purpose of estimating lake evaporation. According to Monteith (1981, page 9), it is inappropriate to apply the Penman equation to estimating evaporation from open water bodies that exceed "… a metre or so in depth…" because of the damping due to heat stored in the water. Morton's (1986) analysis indicates "… the CRLE model has little advantage over the CRWE at depths less than 1.5 m". For shallow lakes of 3 m mean depth, de Bruin (1978) and Sacks et al (1994) consider it unnecessary to take account of seasonal heat storage in estimating lake evaporation, whereas Fennessey (2000), in his study of a shallow lake of 2 m mean depth, incorporated monthly heat storage. For a shallow lake (average depth of 0.6 m and characterised by a bottom crust of a thick frozen mud layer) in Hudson Bay, Canada, Stewart and Rouse (1976) incorporated heat flux through the bottom of the lake and the heat capacity of the water.

Based on the above evidence we suggest as a general guide that seasonal heat storage be taken into account for shallow lakes with an average water depth of 2 m or more. For shallow lakes with water depth less than 2 m, we prefer the Penman equation (Equation (12)) with the 1956 wind function..

Shallow lake evaporation by Penman equation based on the equilibrium temperature (Finch, 2001)

To take heat storage into account, Finch (2001) used the concept of equilibrium temperature and tested the accuracy of the method by estimating evaporation from a shallow lake. A description of the model is presented by Keijman (1974) and de Bruin (1982). As noted in Section (2.1.4), the equilibrium temperature is the temperature of the surface water when the net rate of heat exchange at the water surface is zero (Edinger et al., 1968, page 1139). In this context, Sweers (1976, page 377) assumes that, although on clear calm days a water body will exhibit strong temperature gradients near the water surface, the top 0.5 m – 1.0 m or so is well mixed and its mean temperature specifies the surface temperature.

To estimate shallow lake evaporation, Finch (2001) adopted Penman (1948) but incorporated the Sweers (1976, Equation 18) wind function (Equation (S11.2)) and the equilibrium temperature. In the method it is assumed the water column is well mixed and the heat flux at the bed of the water body can be neglected (Finch, 2001, pages 2772). For each daily time-step, the following nine equations are computed:

$$\lambda E = \frac{\Delta(R_n^W - G_W) + \gamma\lambda f(u)(v_a^* - v_a)}{(\Delta+\gamma)} \tag{S11.1}$$

$$\lambda f(u) = 0.864(4.4 + 1.82u) \tag{S11.2}$$

where E is daily lake evaporation (mm day^{-1}), R_n^w is the net daily radiation (MJ m^{-2} day^{-1}) based on the surface water temperature, G_w is the daily change in heat storage (MJ m^{-2} day^{-1}), λ is the latent heat of vaporisation (MJ kg^{-1}), $(v_a^* - v_a)$ is the vapour pressure deficit (kPa) at air temperature, γ is psychrometric constant (kPa K^{-1}), Δ is the slope of the saturation vapour curve (kPa K^{-1}) at air temperature, and u is the mean daily wind speed (m s^{-1}) at 10 m. (Note that many wind measuring instruments are at a height of 2 m rather than 10 m and for those situations the wind speed needs to be adjusted by Equation (S4.4).)

However, before R_n^w and G_w can be estimated the daily surface water temperature of the lake needs to be estimated as follows:

$$T_{w,i} = T_e + (T_{w,i-1} - T_e)e^{\frac{1}{\tau}} \quad \text{(S11.3)}$$

where $T_{w,i}$, $T_{w,i-1}$ are the surface water temperatures (°C) on day i and day $i-1$ respectively, and T_e is the equilibrium temperature (°C) and τ is equilibrium temperature time constant (days). T_e and τ are estimated as follows:

$$T_e = T_{wb} + \frac{R^*_{wb}}{4\sigma(T_{wb}+273.1)^3+\lambda f(u)(\Delta_{\rm wb}+\gamma)} \quad \text{(Finch, 2001, page 2773)} \quad \text{(S11.4)}$$

where R^*_{wb} is the net radiation (MJ m^{-2} day^{-1}) based on wet-bulb temperature (T_{wb}) (°C) and is estimated by:

$$R^*_{wb} = (1-\alpha)R_s + R_{il} - C_f[\sigma(T_a + 273.1)^4 + 4\sigma(T_a + 273.1)^3(T_{wb} - T_a)] \quad \text{(S11.5)}$$

$$\tau = \frac{\rho_w c_w h_w}{4\sigma(T_{wb}+273.1)^3+\lambda f(u)(\Delta_{\rm wb}+\gamma)} \quad \text{(Finch, 2001, page 2772)} \quad \text{(S11.6)}$$

where τ is the equilibrium temperature time constant (days), T_{wb} is the mean daily wet-bulb temperature (°C), R_s is the shortwave solar radiation (MJ m^{-2} day^{-1}), α is the albedo for a water surface (Finch (2001) estimated using Payne (1972)), R_{il} is incoming longwave radiation (MJ m^{-2} day^{-1}), C_f is a cloudiness factor, σ is the Stefan-Boltzman constant (MJ m^{-2} K^{-4} day^{-1}), T_a is mean daily air temperature (°C) at screen height, $\Delta_{\rm wb}$ is the slope of the saturation vapour curve (kPa K^{-1}) at wet-bulb temperature, γ is the psychrometric constant (kPa K^{-1}), ρ_w is the density of water (kg m^{-3}), c_w is the specific heat of water (MJ m^{-2} K^{-4} day^{-1}), and h_w is the depth of the lake (m).

Thus, having an estimate of the surface water temperatures from Equation (S11.3), R^w_n and G_w are estimated from:

$$R^w_n = (1-\alpha)R_s + R_{il} - C_f\left[\sigma(T_a + 273.1)^4 + 4\sigma(T_a + 273.1)^3(T_{w,i-1} - T_a)\right] \quad \text{(S11.7)}$$

$$G_w = \rho_w c_w h_w (T_{w,i} - T_{w,i-1}) \quad \text{(S11.8)}$$

where R^w_n is the net radiation given the surface water temperature, $T_{w,i}$, $T_{w,i-1}$ are the surface water temperature on day i and day $i-1$ respectively.

Next, λE can be estimated using Equation S11.1 and the depth of water h_w on day $i+1$ is estimated as:

$$h_{i+1} = h_i + P_{i+1} - E_i \quad \text{(S11.9)}$$

where P_{i+1} is the rainfall measured on day $i+1$ and E_i is the lake evaporation on day i.

According to deBruin (1982, page 270) because water bodies up to 10 m deep are generally well mixed by wind, the model is of practical significance. The meteorological data are assumed to be land-based (Finch, 2001, page 2771) and the model uses a daily time-step.

The model was applied by Finch (2001) to a small reservoir at Kempton Park, UK resulting in the annual evaporation being 6% lower than the measured value.

Shallow lake evaporation by finite difference model (Finch and Gash, 2002)

Finch and Gash (2002) proposed a finite difference approach as an alternative to estimating shallow lake evaporation. The steps are set out as follows (Finch and Gash, 2002, Figure 1):

1. Estimate $\propto$ (shortwave albedo for the water surface).

2. Set the first estimate of T_w (average water temperature) at the beginning of the current time-step to the value at the end of the previous time-step.
3. Calculate the average T_w.
4. Calculate R_n (net radiation).
5. Calculate $f(u)$ (u is wind speed at a height of 10 m).
6. Calculate λE (latent heat flux) and H (sensible heat flux).
7. Calculate W(change in heat storage in water column during the current time-step).
8. Calculate a new estimate of T_w at the end of the time-step.
9. Is the difference between the last estimate of T_w and the present one < 0.01?
10. If no, return to step 3, otherwise proceed to the next time-step.

The equations to estimate the above variables are as follows (Finch and Gash, 2002):

$$\propto = f(g, \theta) \tag{S11.10}$$

$$g = \frac{R_s}{\frac{S_{con}\, sin\theta}{d_r^2}}[1] \tag{S11.11}$$

$$T_w = T_{w,i-1} + \left(\frac{T_{w,i} - T_{w,i-1}}{2}\right) \tag{S11.12}$$

$$R_{nw} = R_s(1 - \alpha) + R_{il} - C_f\sigma(T_w + 273.1)^4 \tag{S11.13}$$

$$f(u) = \frac{0.216u}{\Delta + \gamma} \text{ for } T_w \leq T_a \tag{S11.14}$$

$$f(u) = \frac{0.216u\left[1 + 10\frac{(T_w - T_a)}{u^2}\right]^{0.5}}{\Delta + \gamma} \text{ for } T_w > T_a \tag{S11.15}$$

$$\lambda E = f(u)(v_w^* - v_d) \tag{S11.16}$$

$$H = \gamma f(u)(T_w - T_a) \tag{S11.17}$$

$$\Delta W = R_n - \lambda E - H \tag{S11.18}$$

$$T_{w,i} = T_{w,i-1} + \frac{\Delta W}{\rho_w c_w h_w} \tag{S11.19}$$

where α is shortwave albedo for the water surface, R_s is the incoming shortwave radiation (MJ m^{-2} d^{-1}), S_{con} is the solar constant = 0.0820 MJ m^{-2} day^{-1}, θ is the Sun's altitude (°), d_r is the ratio of the actual to mean Earth-Sun separation or the inverse relative distance Earth-Sun, T_w is average water temperature (°C), $T_{w,i}$ and $T_{w,i-1}$ are, respectively, the estimated water temperature (°C) at the end of the current and previous periods, T_a is the air temperature (°C) at the reference height, R_{nw} is the net radiation (MJ m^{-2} d^{-1}), R_{il} is incoming longwave radiation (MJ m^{-2} day^{-1}) , C_f is a cloudiness factor, σ is the Stefan-Boltzman constant (MJ m^{-2} K^{-4} day^{-1}), Δ is the slope of the saturation vapour pressure curve at air temperature (kPa K^{-1}), γ is the psychrometric constant (kPa K^{-1}), u is wind speed (m s^{-1}) at a height of 10 m, v_w^* is the saturation vapour pressure at the water temperature (kPa), v_d is the vapour pressure at the reference height (kPa), λE is the latent heat flux (MJ m^{-2} d^{-1}), H is the sensible heat flux (MJ m^{-2} d^{-1}), ΔW is change in heat storage in water column during the current time-step (MJ m^{-2} d^{-1}), ρ_w is the density of water (kg m^{-3}), c_w is the specific heat of water, and h_w is the depth of water (m).

[1] In Equation (S11.11), we have adopted Payne's equation (Payne, 1972, Equation 3; see also Berger et al, 1993, Equation 2) and Simpson and Paulson (1979, Equation 2) in which d_r^2 is used rather than d_r as published in the Finch and Gash (2002) paper.

R_s is either measured solar radiation or estimated from Equation S3.9 and R_{il} may be estimated from Equation (S3.16). Finch and Gash (2002) used Payne (1972, Table 1) to estimate $\propto$ knowing g and θ. g requires d to be estimated which is computed from:

$$d_r^2 = 1 + 0.033cos\left(\frac{2\pi}{365}DoY\right) \tag{S11.20}$$

where DoY is day of year (DoY = 1, 2, …, 365).

θ is estimated as follows (Al-Rawi, 1991, Equation 1):

$$\sin\theta = \cos\ (lat)\cos\ (\delta)\cos\ (\omega_s) + \sin\ (lat)\sin\ (\delta) \tag{S11.21}$$

where lat is latitude in radians, δ is the solar declination angle in radians, and ω_s is the sunset hour angle in radians. δ and ω_s can be estimated from Equations (S9.18) and (S9.17) respectively.

Lake evaporation by Penman-Monteith equation based on the equilibrium temperature (McJannet et al., 2008b)

McJannet et al. (2008b) adopted the Penman-Monteith as the basis of applying the equilibrium temperature to estimate lake evaporation for a range of water bodies – shallow and deep lakes and an irrigation canal. Their approach is similar to that used by Finch (2001). We reproduce below the method proposed and tested by McJannet et al. (2008b). Evaporation is estimated as follows:

$$E_{McJ} = \frac{1}{\lambda}\left(\frac{\Delta_w(Q^* - G_w) + \frac{86400\rho_a c_a(v_w^* - v_a)}{r_a}}{\Delta_w + \gamma}\right) \tag{S11.22}$$

where E_{McJ} is the evaporation from the water body (mm day^{-1}), Q^* is the net radiation (MJ m^{-2} day^{-1}), G_w is the change in heat storage in the water body (MJ m^{-2} day^{-1}), ρ_a is the density of air (kg m^{-3}), c_a is the specific heat of air (MJ kg^{-1} K^{-1}), v_w^* is the saturation vapour pressure at water temperature (kPa), v_a is the daily vapour pressure (kPa) taken at 9:00 am, λ is the latent heat of vaporisation (MJ kg^{-1}), Δ_w is the slope of the saturation water vapour curve at water temperature (kPa °C^{-1}), γ is the psychrometric constant (kPa °C^{-1}), and r_a is the aerodynamic resistance (s m^{-1}) and is defined by Calder and Neal (1984, page 93) and McJannet et al. (2008b, Appendix B, Equation 10) as:

$$r_a = \frac{\rho_a c_a}{\gamma\left(\frac{f(u)}{86400}\right)} \tag{S11.23}$$

where from Sweers (1976, page 398) and modified by McJannet et al. (2008b, Appendix B, Equation 11) and converting units from W m^{-2} mbar^{-1} to MJ m^{-2} kPa-1 day^{-1} yields:

$$f(u) = \left(\frac{5}{A}\right)^{0.05}(3.80 + 1.57u_{10}) \tag{S11.24}$$

where u_{10} is the wind speed (m s^{-1}) at 10 m and A (km^2) is the area of the water body, and other variables are defined previously. (For elongated water bodies, the square of the width was adopted as the area (Sweers, 1976, page 398).)

Q^* in Equation (S11.22) is defined as:

$$Q^* = R_s(1 - \alpha) + (R_{il} - R_{ol}) \tag{S11.25}$$

where R_s is the total daily incoming shortwave radiation (MJ m^{-2} day^{-1}), α is albedo for water (= 0.08), R_{il} is the incoming longwave radiation (MJ m^{-2} day^{-1}), and R_{ol} is the outgoing longwave radiation (MJ m^{-2} day^{-1}).

$$R_{il} = \left(C_f + \left(1 - C_f\right)\left(1 - \left(0.261\, exp(-7.77 \times 10^{-4} T_a^2)\right)\right)\right) \sigma (T_a + 273.15)^4 \quad \text{(S11.26)}$$

where C_f is the fraction of cloud cover, T_a is the mean daily air temperature (°C), and σ is the Stefan-Boltzmann constant (MJ m^{-2} K^{-4} day^{-1}).

$$R_{ol} = 0.97\, \sigma (T_w + 273.15)^4 \quad \text{(S11.27)}$$

where T_w is the water temperature (°C) which will vary for each time-step and must be estimated before Equation (S11.22) can be applied.

Because the heat storage in a water body affects surface water temperatures and, therefore, evaporation, it is necessary to predict heat storage changes over time which depend on the equilibrium temperature (T_e), the time constant for the storage (τ), as well as the water temperature (T_w). Equilibrium temperature is the surface temperature at which the net rate of heat exchange is zero (see Section 2.1.4). Again, following McJannet et al. (2008b, Equation 23), we estimate water temperature, based on de Bruin (1982, Equation 10), from the following equation:

$$T_w = T_e + (T_{w0} - T_e) \exp\left(-\frac{1}{\tau}\right) \quad \text{(S11.28)}$$

where T_{w0} is the water temperature (°C) in the previous time-step, T_e is the equilibrium temperature (°C), and τ is the time constant (day).

Following McJannet et al. (2008b, Equation 5), the time constant (τ) in days is given by (de Bruin, 1982, Equation 4):

$$\tau = \frac{\rho_w c_w h_w}{4\sigma (T_{wb} + 273.15)^3 + f(u)(\Delta_{wb} + \gamma)} \quad \text{(S11.29)}$$

where ρ_w is the density of water (kg m^{-3}), c_w is the specific heat of water (MJ kg^{-1} K^{-1}), h_w is the water depth (m), Δ_{wb} is the slope of the saturation water vapour curve (kPa °C^{-1}) estimated at wet-bulb temperature (T_n) (°C). The water depth h_w could be a time-series if required (see Equation (S11.9).

The equilibrium temperature is estimated from (de Bruin, 1982, Equation 3):

$$T_e = T_{wb} + \frac{Q_{wb}^*}{4\sigma (T_{wb} + 273.15)^3 + f(u)(\Delta_{wb} + \gamma)} \quad \text{(S11.30)}$$

where Q_{wb}^* is the net radiation at wet-bulb temperature and is estimated by:

$$Q_{wb}^* = R_s (1 - \alpha) + \left(R_{il} - R_{ol}^{wb}\right) \quad \text{(S11.31)}$$

and where R_{ol}^{wb} is the outgoing longwave radiation (MJ m^{-2} day^{-1}) at wet-bulb temperature and is estimated as follows:

$$R_{ol}^{wb} = \sigma (T_a + 273.15)^4 + 4\sigma (T_a + 273.15)^3 (T_{wb} - T_a) \quad \text{(S11.32)}$$

The change in heat storage, G_w, is calculated from (McJannet et al. (2008b, Equation 31):

$$G_w = \rho_w c_w h_w (T_w - T_{w0}) \quad \text{(S11.33)}$$

Thus, for the time-step in question, T_w and G_w are now known and E_{McJ} in Equation (S11.22) can be computed.

The McJannet et al. (2008b) model operates at a daily time-step.

Based on the above approach, McJannet et al. (2008b) applied gridded climate data to estimate average daily (and monthly) evaporation for a range of water bodies from an irrigation canal to five large lakes. Overall, the modelled estimates are within 10% of the independent evaporation estimates (McJannet et al., 2008b, Section 5.7), however, the correlation coefficient between monthly modelled and observed evaporation values is very low for two of the lake studies.

A worked example is provided in **Appendix S19**.

The differences between Finch (2001) and McJannet et al. (2008b) procedures to estimate lake evaporation are:

Finch (2001)	McJannet et al. (2008b)
Adopted Penman (1948) equation	Adopted Penman-Monteith equation
Wind function depends on wind speed	Wind function depends on wind speed and lake area
Adjusted water level for daily rainfall and daily evaporation loss	No adjustment of water level for rainfall or evaporation
Tested on one 10 m lake in UK	Tested on three shallows lakes, a weir, an irrigation channel and two deep reservoirs

Lake evaporation by lake-specific vertical temperature profiles

Sometimes for a lake, monthly or seasonal vertical water temperature profiles are available that can be used to estimate the vertical water body heat flux (G_w in Equations (S11.1) and (11.22)). Fennessey (2000) provides an example for a shallow lake in Massachusetts, U.S as follows:

G_w is defined more precisely as a function of time

$$G_w(t) = \frac{dH(t)}{dt} \tag{S11.34}$$

where $H(t)$ is the total heat energy content of the lake per unit area of the lake surface at time t (MJ m^{-2}) and is computed by:

$$H(t) = \frac{\rho_w c_w}{A_s} \sum_{i=1}^{m} \left[\frac{T_w(z_{i+1}) + T_w(z_i)}{2}\right] V_i \tag{S11.35}$$

where the lake is segregated into m horizontal layers, each layer being $(z_{i+1} - z_i)$ thick (m) , ρ_w is the density of water (kg m^{-3}), c_w is the specific heat of water (MJ kg^{-1} K^{-1}), A_s is the surface area of the lake (m^2), $T_w(z_i)$ and $T_w(z_{i+1})$ are respectively the water temperature at z_i and z_{i+1}, and V_i is the volume (m^3) of each layer defined by:

$$V_i = \frac{(A_{i+1} + A_i)(z_{i+1} - z_i)}{2} \tag{S11.36}$$

Thus, $G_w(t)$ can be incorporated in the Penman based equation of Finch (2001) (Equation S11.1) or in the Penman-Monteith based equation of McJannet et al. (2008b) (Equation S11.22).

Supplementary Material

Appendix S12 Estimating evaporation from lakes covered by vegetation

Brezny et al. (1973, Table 1) measured the evaporation rate of cattail, *Typha augustfolia L.*, in 0.36 m^2 tanks in Rajashan, India. Over approximately 75 days, they found that the evaporation from tanks with plants was 52% more than the evaporation from tanks without plants. In contrast, based on a comparison of measured evaporation from Barren Box Swamp (a lake covered with cattail, *Typha orientalis* PRESL., in NSW, Australia) compared with a lake devoid of vegetation, Linacre et al. (1970, Table IV) observed over three days 34% less evaporation from the swamp compared to a nearby lake without vegetation. Linacre et al. (1970, page 385) attributed the lower observed evaporation from swamp compared with the lake evaporation to lower albedo of the clear water in the lake, to the shelter provided by the reeds in the swamp, and to the internal resistance to water movement of the reeds. These contrasting results illustrate the difficulty in assessing the impact of vegetation on evaporation from lakes.

There is an extensive body of literature addressing the question of evaporation from lakes covered by vegetation. Abtew and Obeysekera (1995) summarise the results of 19 experiments which, overall, show that the transpiration of macrophytes is greater than open surface water. However, most experiments were not carried out *in situ*. On the other hand, Mohamed et al. (2008) lists the results of 11 *in situ* studies (estimating evaporation by eddy correlation or Bowen Ratio procedures) in which wetland evaporation is overall less than open surface water.

Based on theoretical considerations and a literature survey, Idso (1981) offered the following observations. Firstly, reliable experiments assessing the relative rates of evaporation from vegetated water bodies and open surface water must be conducted *in situ* (Idso (1981, page 46). Secondly, for extensive water bodies covered by vegetation, evaporation will most likely be lower than the open surface water estimate (Idso (1981, page 47). It is noted that Anderson and Idso (1987, page 1041) concluded that canopy surface geometry is important in the evaporative process and, therefore, for small or narrow canopies (e.g., macrophytes along stream reaches where advective energy is significant), evaporative water losses greater than open water can occur.

Drexler et al. (2004, page 2072) in a review of models and methods to estimate wetland evapotranspiration offered the following comments.

1. For many wetland types, the physical processes are poorly characterised.
2. Generalisation is difficult because of variable nature of the results, even within well-studied vegetation types.
3. The wetland environment is very varied, making it particularly difficult to measure ET.
4. Seasonal variation of ET is also an important consideration.

A number of models – Penman (**Appendix S4**), Penman-Monteith (**Appendix S5**), the Shuttleworth-Wallace variation of Penman-Monteith (**Appendix S5**), and Priestley-Taylor (Section 2.1.3) – have been used in several studies (Wessel and Rouse, 1994; Abtew and Obeysekera, 1995; Souch et al. 1998; Bidlake, 2000; Lott and Hunt, 2001; Jacobs et al., 2002; Drexler et al., 2004) to estimate the rate of evaporation from a lake covered by vegetation. **Table S7** summarises seven comparisons and suggests that the weighted Penman-Monteith method which is able to account for variations of r_a and r_s for different vegetation surface performs satisfactorily. For this model, and based on one experiment, the mean model estimate of lake evaporation compared to a mean measured value was 1.10.

Readers are referred to a very recent review by Clulow et al (2012) in which they discuss, inter alia, under what conditions Penman, Priestley-Taylor and Penman-Monteith models can be used to estimate actual evaporation from a lake covered by vegetation.

Supplementary Material

Appendix S13 Estimating potential evaporation in rainfall-runoff modelling

Several procedures including Penman-Monteith, Priestley-Taylor and Morton have been used in daily and monthly rainfall-runoff modelling at a daily or monthly time-step to estimate potential evaporation/evapotranspiration. In the Penman-Monteith model the aerodynamic and surface roughness coefficients (r_a and r_s respectively) need to be specified in Equation (5). Some typical values of r_a and r_s are listed in **Table S2**. In a sensitivity analysis in which the Penman-Monteith equation was incorporated into the SHE model (Abbott et al., 1986a, b), Beven (1979, page 176 and Figure 5) adopted constant values of r_a = 46 s m^{-1} for grass and 4 s m^{-1} for pine forest. However, values varied from mid-day (r_s = 50 s m^{-1} for grass and 100 s m^{-1} for pine forest) to mid-night (r_s = 200 s m^{-1} for grass and 400 s m^{-1} for pine forest). Beven concluded that the evapotranspiration estimates were very dependent on the values of the aerodynamic and canopy resistance parameters.

In using the Priestley-Taylor algorithm (Equation (6)) for estimating catchment potential evapotranspiration, the parameter α_{PT} needs to be specified. Zhang et al (2001, Equation 4) adopted 1.28 and Raupach et al. (2001, page 1152) recommended 1.26. It should be noted that the α_{PT} 'constant' is commonly set to 1.26 although optimised values vary greatly depending on the moisture and advective conditions in which the measurements are made (see **Table S8**). This is not surprising as the Priestley-Taylor algorithm was developed assuming non-advective conditions and without recourse to measurement of the aerodynamic component.

One of the advantages of Morton's (1983a) CRAE method to estimate potential evapotranspiration is that it does not require wind data as input and, therefore, has been used extensively in Australia to estimate historical monthly potential evapotranspiration in rainfall-runoff modelling (Chiew and Jayasuria, 1990; Chiew and McMahon, 1993; Chiew et al., 1993; Jones et al., 1993; Siriwardena et al., 2006). In many water engineering applications, analysis depends on measured or estimated monthly runoff and potential evaporation over an extended period, often more than 100 years.

There are at least two options available to analysts to estimate Morton's ET_{Wet} in Australia. One approach is to use the mean monthly areal potential values (equivalent to wet environment areal evapotranspiration using Morton's nomenclature) produced jointly by the CRC for Catchment Hydrology and the Bureau of Meteorology in 2001 (see http://www.bom.gov.au/climate/averages and Wang et al. (2001) with detailed methodology described in Chiew et al. (2002)). For daily modelling, the mean monthly values can be disaggregated into equal daily values. A major disadvantage with this approach is that there is no variation in potential evapotranspiration from year to year. However, Chapman (2003, Section 5) applied four rainfall-runoff models to 15 catchments in Australia and concluded that, in terms of modelling daily streamflow, equally good results could be obtained by using average monthly potential evapotranspiration data in the place of daily potential evapotranspiration values. Rather than adopting average monthly values, Oudin et al. (2005) used average daily values in an application of four rainfall-runoff models to 308 catchments in Australia, France and the United States. They concluded that the average daily potential evaporation values resulted in modelled runoffs that were little different to those produced using daily varying potential evaporation (Oudin et al., 2005, Tables 3 and 4).

The second option is to estimate Morton's wet environmental evapotranspiration from climate data using Equation (18). Chiew and Jayasuria (1990) reviewed Morton's wet environmental evapotranspiration and compared, for three locations in south-eastern Australia, daily estimates of Morton's wet environmental evapotranspiration with Penman's free-water evaporation. They concluded that (i) Morton's model can estimate successfully daily global and net radiation (Chiew and Jayasuria, 1990, page 293); (ii) Morton's wet environment evaporation can be used to represent potential evapotranspiration in rainfall-runoff modelling (Chiew and Jayasuria, 1990, page 293); (It should be noted that this assessment was based on Penman rather than the more appropriate Penman-Monteith model.) (iii) Morton's ET_{Wet} cannot estimate low potential evapotranspiration values accurately and underestimates high values (Chiew and Jayasuria, 1990, page 291).

Based on data for 19 climate stations in Australia from 1970 to 1989, Chapman (2001) demonstrated that overall pan evaporation data are a better estimate of potential evapotranspiration than maximum air temperature. Furthermore, he developed the following simple relationship (applicable only to Australia) that could be used if no other data were available to estimate potential evaporation for catchment modelling purposes:

$$ET_{eqPM} = A_p E_{Pan} + B_p \tag{S13.1}$$

where ET_{eqPM} is the daily equivalent Penman-Monteith potential evaporation (mm day^{-1}), E_{Pan} is the daily Class-A pan evaporation (mm day^{-1}), and A_p and B_p are given by:

$$A_p = 0.17 + 0.011 Lat \tag{S13.2}$$

$$B_p = 10^{(0.66 - 0.211\, Lat)} \tag{S13.3}$$

where Lat is the latitude of the catchment in degrees South.

Supplementary Material

Appendix S14 Estimating evaporation of intercepted rainfall

It is recognised that interception is variable in space and in time. According to Klaassen et al. (1998) the interception storage of water in dense forests is an important process and varies seasonally (Gerrits et al., 2010) and across vegetation types. Crockford and Richardson (2000) note that because interception is dependent on rainfall and other meteorological variables it is difficult to make conclusions about interception losses for specific vegetation types.

Because potential evaporation rates are higher in the hotter months of a year and lower during colder months, interception is seasonal. Other factors such as rainfall intensity, wind, and snow also impact interception storage and, hence, interception evaporation (Gerrits et al., 2010). Gerrits et al. (2010) note that although interception storage can be very variable; for the beech forest they studied in Luxembourg, its size played a minor role in evaporation. Stewart (1977) has shown that the evaporation of transpired water is very different to the evaporation of intercepted water and, hence, it is important that these two components are considered separately.

Although Herbst et al. (2008) state that the Gash model (Gash, 1979) is the most widely and successfully used interception model, Gerrits et al. (2010) adopted the Rutter model (Rutter et al., 1971, 1975) in their analysis. In his model, Gash (1979) incorporated the Penman-Monteith equation which was found by Herbst et al. (2008) to give estimates of wet canopy evaporation equivalent to those estimates from the eddy covariance energy balance approach. In the 1971 Rutter model the authors (Rutter et al., 1971) incorporated the Penman (1956) equation to estimate potential evaporation.

Teklehaimanot and Jarvis (1991) concluded from their experiments that evaporation rates from a wet canopy could be satisfactorily modelled by the Penman (1948) equation. Moreover, they further showed that the actual evaporation from a partially wet canopy could be modelled by multiplying the Penman evaporation by C_{ret}/S_{can} , where C_{ret} is the amount of water retained on the canopy (mm) and S_{can} is the storage capacity of the canopy (mm).

Readers are referred to a recent and comprehensive review by Muzylo et al. (2009), who addressed the theoretical basis of 15 interception models including their evaporation components, who identified inadequacies and research questions, and who noted there were few comparative studies and little information about uncertainty in measured and modelled parameters.

Modelling evapotranspiration-interception in an urban area

Grimmond and Oke (1991) developed a hydrologic model of an urban area at an hourly time-step to estimate evaporation over a range of meteorological conditions. The model includes the Penman (1948) equation modified by Monteith (1965) for vegetation surface and the Rutter et al. (1971) interception model modified by Shuttleworth (1978) to provide a smooth transition between wet and dry vegetation canopies. In addition, anthropogenic heat flux and stored heat flux were also modelled. The model was tested for a small urban area in Vancouver, Canada and according to the authors the model showed promise.

Supplementary Material

Appendix S15 Estimating bare soil evaporation

Following Philip (1957), Ritchie (1972, page 1205) proposed a two-stage model to estimate bare soil evaporation. Salvucci (1997) developed further the Ritchie approach defining the evaporation loss for stage-1 by:

$$E_{stage\ 1} = \bar{E}_{Penman} \times t_1 \tag{S15.1}$$

where $E_{stage\ 1}$ is the cumulative stage-1 bare soil evaporation (mm) which, according to Allen et al. (1998, page 145), should not exceed the readily evaporable water (REW) which they define as the maximum depth of water that can be evaporated from the top-soil without restriction. Typical REW values are: sand 2 – 7 mm, loam 8 – 10 mm and clay 8 – 12 mm. t_1 is the length of the stage-1 atmosphere-controlled evaporation period (day) which is defined as:

$$t_1 = \frac{REW}{\bar{E}_{Penman}} \tag{S15.2}$$

$\bar{E}_{Penman}$ is the daily average stage-1 actual evaporation (mm day^{-1}) and is assumed to be at or near the rate of Penman evaporation. McVicar et al. (2012, page 183) prefers to use the term energy-limited rather than stage-1. Alternatively, a more rigorous procedure to estimate t_1 is recommended by Dingman (1992, page 293) who suggests the end of stage-1 is readily observed from ground or satellite observations of albedo.

Discussing evaporation from bare soil, Monteith (1981, pages 10 and 11) observes that "When bare soil is thoroughly wetted, the soil surface behaves like water in so far as the relative humidity of the air in contact with the surface is 100%". Monteith (1981, page 11) further adds that as a matter of observation the rate of evaporation "…is usually very close to the rate for adjacent short vegetation, despite differences in radiative and aerodynamic properties".

Stage-2 evaporation (the water-limited stage, McVicar et al. (2012, page 183)), is dependent on stage-1 and two limiting cases need to be considered.

1. Where the unsaturated hydraulic conductivity (mm day^{-1}), $K_{us} << \bar{E}_{Penman}$. This would occur with relatively low permeability soils.
2. Where $K_{us} >> \bar{E}_{Penman}$ and, therefore, the cumulative drainage is much greater than the cumulative actual evaporation.

Salvucci (1997, Equations 18 and 19 respectively) developed the following empirical equations for the two cases:

For $K_{us} << \bar{E}_{Penman}$

$$E_{bsoil}(t) = E_{stage\ 1}\left[-0.621 + 1.621\left(\frac{t}{t_1}\right)\right]^{0.5},\ t \geq t_1 \tag{S15.3}$$

For $K_{us} >> \bar{E}_{Penman}$

$$E_{bsoil}(t) = E_{stage\ 1}\left[1 + 0.811 ln\left(\frac{t}{t_1}\right)\right],\ t \geq t_1 \tag{S15.4}$$

where $E_{bsoil}(t)$ is the cumulative bare soil evaporation up to time t.

As a check on the total evaporable water (TEW), typical values for a range of soils are provided by Allen et al. (1998, Table 19). For example, sand = 6 – 12 mm, loam = 16 – 22 mm and clay = 22 – 29 mm. TEW is defined by Allen et al. (1998, Equation 73) as:

$$TEW = 10(\theta_{FC} - 0.5\theta_{WP})z_e \tag{S15.5}$$

where θ_{FC} is the soil moisture content (%) at field capacity, θ_{WP} is the soil moisture content (%) at wilting point, z_e is the depth of the surface soil layer that is subject to drying from evaporation. If this is unknown, Allen et al. (1998, page 144) recommend $z_e = 0.10 – 0.15$ m.

It is interesting to note that Penman (1948, page 137) observed from his experiments that freshly wetted bare soil evaporated at about 90% of the rate observed for open surface water for the same weather conditions.

Based on FAO56 methodology (Allen et al., 1998), Allen et al. (2005) developed a two-stage strategy (energy limited and water limited stages) to estimate bare soil evaporation. Mutziger et al (2005) applied the methodology to seven data sets and concluded that model accuracy was about ±15%.

Supplementary Material

Appendix S16 Class-A pan evaporation equations and pan coefficients

Although some researchers, e.g., Watts and Hancock (1984, page 295), are critical of an evaporative pan as a reliable climatic instrument (they list 10 potential problems), it should be noted that Roderick et al. (2009b, Section 4) comment "…that the pan evaporation record provides the only direct measurement of changing evaporative demand…" which is crucial in climate change studies. In Australia, 60 stations have been identified as high quality Class-A pan evaporation stations (Jovanovic et al., 2008).

Equations: Kohler et al. (1955)

Kohler et al. (1955) (see Dingman (1992, Equation 7.41)) developed the following empirical equations to estimate daily open-water evaporation, E_{fw} (mm day^{-1}) from Class-A pan evaporation data:

$$E_{fw} = 0.7[E_{Pan} + 0.064p\alpha_{Pan}(0.37 + 0.00255u_{Pan})|T_{Pan} - T_a|^{0.88}] \text{ for } T_{Pan} > T_a \tag{S16.1}$$

$$E_{fw} = 0.7[E_{Pan} - 0.064p\alpha_{Pan}(0.37 + 0.00255u_{Pan})|T_{Pan} - T_a|^{0.88}] \text{ for } T_{Pan} < T_a \tag{S16.2}$$

where E_{Pan} is the daily evaporation measured by an unguarded Class-A pan (mm day^{-1}), p is the atmospheric pressure (kPa), α_{Pan} is the proportion of energy exchanged through the sides of the pan and is specified in Equation (S16.3), u_{Pan} is the average daily wind speed at a height of 150 mm above the pan (km day^{-1}), and T_{pan} and T_a are respectively the mean daily pan water and air temperature (°C).

$$\alpha_{Pan} = 0.34 + 0.0117T_{Pan} - 3.5\times10^{-7}(T_{Pan} + 17.8)^3 + 0.00135u_{Pan}^{0.36} \tag{S16.3}$$

Wind run for anemometers not at 150 mm above the pan should be adjusted using Equation (S4.4). Based on an intercontinental comparison, Burman (1976) concluded that the Kohler et al. (1955) equations were superior to empirical methods proposed by Christiansen (1968) and Oliver (1961) which are not included here.

Equations: Chiew & McMahon (1992)

Chiew and McMahon (1992, Appendix) developed daily, 3-day, weekly and monthly pan coefficients as simple linear regressions of the form:

$$E_{Pen,j} = I_j + G_jE_{Pan,j} \tag{S16.4}$$

where for month j, $E_{Pen,j}$ is the Penman(1948) estimate of evaporation for a land environment *rather than open water*, $E_{Pan,j}$ is the evaporation from a Class-A pan, and I_j and G_j are respectively the intercepts and the gradients of daily, 3-day, weekly and monthly totals. Values of I_j and G_j for 26 climate stations in Australia are given in Chiew and McMahon (1992).

Equations: Allen et al (1998)

Equations for estimating Reference Crop evapotranspiration, E_{RC}, are presented by Allen et al. (1998, page 55, Table 7) taking into account the site of the pan in terms of the upwind fetch as follows:

$$ET_{RC} = K_{Pan}E_{Pan} \tag{S16.5}$$

where K_{Pan} is the pan coefficient given by:

for a green vegetated fetch (1 to 1000 m) within a dry area at least 50 m wide

$$K_{Pan} = 0.108 - 0.0286u_2 + 0.0422ln(FET) + 0.1434ln(RH_{mean}) - 0.000631[ln(FET)]^2 ln(RH_{mean}) \quad \text{(S16.6)}$$

for a dry fetch (1 to 1000 m) within a green vegetated area at least 50 m wide

$$K_{Pan} = 0.61 + 0.00341RH_{mean} - 0.000162u_2RH_{mean} - 0.00000050u_2FET + 0.00327u_2ln(FET) - 0.00289u_2ln(86.4u_2) - 0.0106ln(86.4u_2)ln(FET) + 0'00063[ln(FET)]^2 ln(86.4u_2) \quad \text{(S16.7)}$$

where FET is the fetch or length of the identified surface (m), u_2 is the daily wind speed at 2 m height, and RH_{mean} is the mean daily relative humidity (%). According to Allen et al. (1998, Table 7), Equations (S16.6) and (S16.7) should not be used outside the following ranges 1 m ≤ FET ≤ 1000 m, 30% ≤ RH_{mean} ≤ 84%, and 1 ms^{-1} ≤ u_2 ≤ 8 m s^{-1}.

A range of pan coefficients based on Equations (S16.6) and (S16.7) are displayed in **Table S9** which illustrates the importance of appropriately specifying the microclimate around a pan in order to have a representative estimate of Reference Crop evapotranspiration. Because $E_{Pan} = \frac{ET_{RC}}{f_{Pan}}$, we are able to use the table to explore how the evaporating power (in this case being represented by pan evaporation E_{Pan}) is affected quantitatively by the characteristics of a site. For example, the pan evaporation under a light wind, low humidity and a green vegetated fetch will be reduced by ~14% for a 10 m fetch compared with a 1000 m one; for a dry fetch under the same conditions, the pan evaporation will increase by ~20%.

Equations: Snyder et al. (2005)

Based on pan data in California, Snyder et al. (2005, Equations 6, 8 and 9) proposed the following set of empirical equations to estimate reference crop evaporation.

$$ET_{RC} = 10sin\left[\left(\frac{E_{pa}}{19.2}\right)\frac{\pi}{2}\right] \quad \text{(S16.8)}$$

$$E_{pa} = E_{pan}F_{100} \quad \text{(S16.9)}$$

$$F_{100} = -0.0035[ln(F)]^2 + 0.0622[ln(F)] + 0.79 \quad \text{(S16.10)}$$

where ET_{RC} is the reference crop evapotranspiration (mm day^{-1}), E_{pan} is the Class-A pan evaporation (unscreened) (mm day^{-1}) and F is the upwind grass fetch (m). The method is suitable for semi-arid conditions but would require calibration for humid or windier climates (Snyder et al., 2005, page 252).

Ghare et al. (2006) introduced modifications to the Snyder equations but field testing in Italy and Serbia by Trajkovic and Kolakovic (2010) showed that the original Snyder model performed better.

Computed monthly and annual Class-A pan coefficients

Although it is not possible to check independently that pan coefficients are correct, one can compare computed values with those found in the literature. Published results of estimating the pan coefficients for the two Penman wind functions (Equations S4.5 and S4.6) are presented in **Table S10** along with pan coefficients for Reference Crop evapotranspiration and the Priestley-Taylor potential evaporation. The exceptionally low pan coefficients for Priestley-Taylor are based on 16 climate stations in Jordon. The coefficients are plotted against mean annual unscreened Class-A pan evaporation in **Figure S2** which illustrates, at least for this arid environment, that adopting a spatially constant pan coefficient may be unwise. This observation is consistent with McVicar et al. (2007, Figure 10) who observed for the Coarse Sandy Hill catchments in north-central China both spatial and seasonal variations in pan coefficients.

Published monthly and annual open-water pan coefficients are often extrapolated to other locations. Care needs to be taken as several local factors will impact pan coefficients including relative humidity (Alvarez et al., 2007; Hoy and Stephens, 1979; Kohler et al., 1955), reservoir dimensions (Alvarez et al., 2007), degree of stratification (Hoy and Stephens, 1979), presence of aquatic plants (Winter, 1981), and lake turbidity and salinity (Grayson et al., 1996). Locally calibrated coefficients are preferred.

Australian pan coefficients

In Australia, in order to prevent the consumption of water by birds and animals, bird guards (wire screens) were installed progressively on the Class-A evaporation pans during the late 1960s and early 1970s, and by 1975 most pans were operating with screens which reduce the evaporation. van Dijk (1985) compared the evaporation recorded from evaporation pans with and without bird guards at four Australian locations between 1967 to 1971. The average monthly effect at the four locations ranged from 4.1% to 8.2% reduction in measured evaporation, with an average of 6.6%. These reductions are less than the values of 13% for humid areas and 10% for semi-arid regions noted in a review by Lincare (1994). Based on the findings of van Dijk (1985), the Australian Bureau of Meteorology (2007) recommends an annual conversion factor of +7%. Jovanovic et al. (2008) have developed a high-quality monthly pan evaporation data set that includes 60 locations across Australia covering the period from about 1970 to present for monitoring evaporation trends.

In Australia, the associated climate data required to estimate open-water evaporation (E_{fw}) (mm/unit time) using Equation (S16.1) or (S16.2) are not available at many pan evaporation sites and, as a consequence, monthly (or annual) pan coefficients are developed using:

$$E_{fw,j} = K_j E_{Pan,j} \tag{S16.11}$$

where j is the specific month and K_j is the average monthly pan coefficient. Traditionally, K_j is assumed constant, although Linacre (1994, Figure 1) using Stanhill's (1976) data for 12 sites world-wide found that for very high evaporation rates K_j decreased from the nominal 0.7 value.

Hoy and Stephens (1977; 1979) calculated the monthly pan coefficients of seven Australian reservoirs by comparing the evaporation of a Class-A pan with the heat budget method over several years. The average monthly pan estimates are listed in **Table S11**. Annual pan coefficients were estimated for a greater number of Australian reservoirs by Hoy and Stephens (1977; 1979) and these results are listed in **Table S12**.

We have computed monthly pan coefficients for 68 sites across Australia by correlating monthly evaporation values from Class-A evaporation pans with corresponding Penman evaporation estimates using his 1956 wind function, based on measured daily climate data at the same or a nearby location, thus yielding open-water evaporation. Thirty-nine of the 68 sites are part of the high quality evaporation pan network (Jovanovic et al., 2008, Table 1);

another 29 stations with monthly pan coefficients have been included in the analysis for spatial completeness. Pan coefficients are presented in **Table S6**. At least 10 monthly values are used in calculating 79.4% of the computed monthly pan coefficients. The analysis of the results in the table shows that mean monthly pan coefficients (weighted for length of record) across the 68 Australian stations is 0.80. This average value compares with 0.76 (based on published data in **Table S10** for Penman (1956) and Penman (1948) the latter adjusted by Equation (S4.8) to be equivalent to Penman (1956)). It should be noted that in computing the monthly solar radiation term in the Penman model, the coefficients a_s and b_s in Equation (S3.9) were optimised to 0.05 and 0.65 respectively (**Appendix S6**).

For many practical problems, annual evaporation estimates need to be disaggregated into monthly values or monthly evaporation values into daily values. This process is not straightforward, when there is no concurrent at-site climate data which could be used to provide guidance as to how the annual or monthly values should be partitioned.

For annual evaporation, a standard approach is to use monthly pan coefficients if available. Another approach, that is available to Australian analysts, is to apply the average monthly values of point potential evapotranspiration for the given location and pro rata the values to sum to the annual evaporation. Maps for each calendar month are available in Wang et al. (2001). This approach is based on the recent analysis by Kirono et al. (2009, Figure 3) who found that, for 28 locations around Australia, Morton's potential evapotranspiration ET_{Pot} correlated satisfactorily (R^2 = 0.81) with monthly Class-A pan evaporation although over-estimating pan evaporation by 8%.

For monthly disaggregation to daily data in Australia one could utilize the analysis of Rayner (2005) who reports on synthetic gridded daily Class-A pan evaporation data based on solar radiation and vapour pressure deficit (Jeffrey et al., 2001). The grids are at a spatial resolution of 0.05°(~5 km) and cover the period 1919 to present. McVicar et al. (2007, page 211) note, however, that if pan coefficients are spatially averaged across a range of climates the averaged value will tend to be damped.

Modifying pan data for estimating evaporation from a deep lake

To estimate deep lake evaporation from pan data, Webb (1966, Equation 3) proposed an alternative approach based on vapour pressure to estimate monthly lake evaporation by summing daily values as follows:

$$E_{L,d} = 1.50\frac{v_L^* - v_4}{v_P^* - v_4}E'_{pan} \tag{S16.12}$$

where $E_{L,d}$ is the daily estimate of lake evaporation (mm day^{-1}), E'_{pan} is the daily pan evaporation (mm day^{-1}), v_L^* is the afternoon average lake saturation vapour pressure (mbar), v_P^* is the afternoon maximum pan saturation vapour pressure (mbar), and v_4 is the afternoon average vapour pressure 4 m above the ground surface (mbar). The monthly evaporation value is the sum of the daily values. The empirical coefficient of 1.50 was established from Lake Hefner data.

Supplementary Material

Appendix S17 Comparing published evaporation estimates

A detailed review of the literature identified 27 papers in which comparisons were made between model estimates of potential or actual evaporation or evapotranspiration and field measurements (water balance studies, Bowen Ratio or eddy correlation), lysimeter observation or comparisons between evaporation equations. Detailed discussion of field measurements of evaporation are outside the scope of this paper. We refer readers to Harbeck (1958), Grant (1975), Myrup et al. (1979), Brutsaert (1982), Dingman (1992, Sections 7.8.2 and 7.8.3), Lenters et al. (2005), and Ali et al. (2008) for applications of the techniques. Details for each of the 27 studies are listed **Table 5**. For each study two items of information are generally provided in the table – the ratio of the average model values (daily, monthly or annual) to a base value, and a measure of error generally as a root mean square error or standard error of estimate. For four studies, multiple sets of results are available.

The bias results (ratios in **Table 5**) are consolidated in **Table 6** under six headings. Under the first two headings each model result is compared with measured observations. For the six lake studies a water balance, eddy correlation or Bowen Ratio estimate were the basis of the comparison. For the seven non-lake studies, the base estimates were from eddy correlation or Bowen Ratio experiments. The third comparison of four studies is based on lysimeter observations. The remaining three sets of comparisons are between various models and Penman-Monteith, Priestley-Taylor or Hargreaves-Samani estimates. The results are summarised in **Figure 3** where each model ratio value includes at least two studies.

In interpreting these results, readers should note the comment of Winter and Rosenberry (1995, page 983) who stated that “Regardless of their intended use, it is not uncommon for equations developed for determination of potential evapotranspiration from vegetation to be used for determination of evaporation from open water”.

The information in **Figure 3** requires some interpretation. Firstly, the ratios in column (1) “Lakes”, column (2) “Lysimeter” and column (3) “Land” may be regarded as absolute estimates in the sense that the modelled estimates are compared against measured evaporation. Secondly, ratios in columns (4) “Relative to PM” and (5) “Relative to PT” are relative to Penman-Monteith and Priestley-Taylor set to a ratio value of 1.00. Thirdly, the values in columns (1) and (2) are for open-water (“Lakes”) or “Lysimeter” measurements, in which water is not limiting in either comparison. On the other hand, values in column (3) will have been influenced by the availability of soil moisture to the plants and by the vegetation type and, therefore, will not be evaporating or transpiring at a potential rate. This would explain why Turc (Tu) and the Priestley-Taylor (PT) values differ markedly between columns (2) and (3).

Table 5 also contains error information mainly as a root mean square error (RMSE) or as a standard error of estimate (SEE). We have summarised the relevant results in **Table 7** which lists the root mean square error (mm day^{-1}) or the standard error of estimate (mm day^{-1}). Because the values of RMSE or SEE were available for Priestley-Taylor in all comparisons, relative errors (as the ratio of RMSE or SEE for the particular model to that for PT) have been computed. These results are summarised as the median for each method. As a guide, the median RMSE for the six Priestley-Taylor analyses is 0.97 mm day^{-1} and 0.66 mm day^{-1} for the eight SEE values.

Supplementary Material

Appendix S18 Comparing evaporation estimates based on measured climate data for six Australian automatic weather stations

Table S13 shows the results of estimating annual evaporation for 14 daily and monthly evaporation/evapotranspiration models based separately on daily and monthly climate data recorded at six widely distributed Australian automatic weather stations over the period January 1979 to March 2010. The latitude and longitude of each station are listed in the table along with the mean annual rainfall estimated for the concurrent period used in the computation of evaporation estimates. Annual values are the sum of 12 monthly means. The number of days and complete months of data available at each station is as follows: Perth Airport (6238 days, 192 months), Darwin Airport (11307 days, 334 months), Alice Springs Airport (11288 days, 320 months), Brisbane Airport (3674 days, 111 months), Melbourne Airport (3842 days, 116 months), and Grove (Companion) (9622 days, 241 months). The authors advise that care needs to be exercised in extending more widely any conclusions arising from this analysis of only six stations.

The results in the table are listed under four main groups: those that estimate actual open-water evaporation (i) Penman 1956 (P56), Priestley-Taylor (PT), Makkink (Ma); (ii) those that estimate reference crop evaporation – FAO-56 Reference Crop (FAO-56 RC), Blaney-Criddle (BC), Hargreaves-Samani (HS), modified Hargreaves (mod H), Turc (Tu); (iii) models that estimate actual evapotranspiration – Morton (Mo), Brutsaert-Strickler (BS), Granger-Gray (GG), Szilagyi-Jozsa SJ); and (iv) three additional methods that include Thornthwaite's monthly potential estimates (Th), PenPan modelled estimates of actual Class-A pan evaporation (PP), and actual evaporation measured by a Class-A evaporation pan. In interpreting these results readers should note that we have applied each method as set out in the relevant reference except we adopted a time-step of both one day and one month. For some models the recommended time-step for analysis is longer than one day. This information is provided where the model is discussed in the paper.

For the daily data in each group, the ratio of the annual evaporation to the value for a key method is calculated and listed as the "Daily ratio". Also for each station, the ratio of annual estimates based on monthly and daily data (M to D ratio) are compared. Several observations follow:

1. Relative to the key procedure in each group, the evaporation estimates in **Table S13** are reasonably consistent, excepted for Blaney-Criddle, across the six sites which have very different climates. As noted in **Appendix S9** the Blaney-Criddle procedure was developed for application in the dry western United States and, therefore, may not perform successfully in regions subject to a different climate (like Melbourne or Grove) where the procedure appears to perform inadequately. See also item 9 below.
2. On averaging the daily ratios for the open water group, the actual evaporation estimates for Priestley-Taylor and Makkink are 0.88× and 0.59× the Penman 1956 estimate. This is consistent with our summary of published data presented in **Table 6** and **Figure 3**.
3. For the reference crop group, Hargreaves-Samani and Turc are 1.10× and 0.90× the FAO-56 Reference Crop average, again consistent with the lysimeter data listed in **Table 6** and **Figure 3**.
4. The PenPan estimates for the six stations are consistent with the values plotted in **Figure S3** which are based on 68 Australian stations.
5. The results in **Table S13** show that for Penman 1956, Priestley-Taylor, Makkink, FAO-56 Reference Crop, Turc, Granger-Gray and PenPan there is less than ~2% difference in

annual evaporation estimates using a daily or a monthly time-step. However, for Szilagyi-Jozsa and Brutsaert-Strickler, the monthly values are respectively 7% and 10% higher than the daily values whereas for Hargreaves-Samani and Blaney-Criddle the monthly values are 14% and 22% lower than the daily estimates.

6. In the analysis we observed that Brusaert-Strickler and Szilagyi-Jozsa generated negative daily evapotranspiration (12.7% and 15.9% of days respectively). This inadequacy was noted by Brutsaert and Strickler (1979, page 448) in the analysis of their model results. In our analysis the negative evaporations occurred mainly in winter (May through to August).
7. It was also observed that for Grove using Szilagyi-Jozsa model, unrealistically high equilibrium temperatures (say > 100°C) were computed for 2.8% of days. These unrealistic temperatures appeared to occur mainly on days when the difference between maximum and minimum humidity is around zero.
8. On average, mean annual actual evaporation estimates at a site should be less than mean annual rainfall at the site. Brusaert-Strickler, Granger-Gray and Szilagyi-Jozsa meet this criterion for four, three and three of the six sites respectively. On the other hand, all Morton's estimates were less than the mean annual rainfalls for all sites.
9. Blaney and Criddle also generated many negative daily evapotranspiration estimates, even for Alice Springs which climate-wise is semi-arid and not too dissimilar to the dry western United States.

Supplementary Material

Appendix S19 Worked examples

This set of worked examples is based on data from the Automatic Weather Station 015590 Alice Springs Airport (Australia). The daily data and other relevant information for the worked examples are for the 20 July 1980 as follows:

Station: Alice Springs Airport
Station reference number: 015590
Latitude: 23.7951 °S
Elevation: 546 m
Maximum daily air temperature: 21.0 °C
Minimum daily air temperature: 2.0 °C
Maximum relative humidity: 71%
Minimum relative humidity: 25%
Daily sunshine hours: 10.7 hours
Wind run at 2 m height: 51 km day^{-1} (=51×1000/(24×60×60) = 0.5903 m s^{-1})

General constants used in worked examples:
Solar constant (G_{sc}) = 0.0820 MJ m^{-2} min^{-1}
Stefan-Boltzmann (σ) = 4.903×10^{-9} MJ m^{-2} day^{-1} °K^{-4}
von Kármán constant (k) = 0.41
Latent heat of vaporization (λ) = 2.45 MJ kg^{-1}
Mean density of air (ρ_a) = 1.20 kg m^{-3} at 20°C
Specific heat of air (c_a) = 0.001013 MJ kg^{-1} K^{-1}
Mean density of water (ρ_w) = 997.9 kg m^{-3} at 20°C
Specific heat of water (c_w) =0.00419 MJ kg^{-1} K^{-1}

Specific constants used in worked examples:
Albedo for water = 0.08 (adopted from **Table S3**)
Albedo for reference crop α = 0.23 (adopted from **Table S3**)
Priestley-Taylor α_{PT} = 1.26 for PT equation
Priestley-Taylor α_{PT} = 1.28 for BS equation

Worked example 1: Intermediate calculations for daily analysis

Estimate the values of the intermediate variables associated with computing daily evaporation.

Mean daily temperature ($\boldsymbol{T_{mean}}$***)***

$$T_{mean} = \frac{T_{max}+T_{min}}{2} \text{ (see Equation (S2.1))} \quad \text{(S19.1)}$$

$$T_{mean} = \frac{21.0+2.0}{2} = 11.5°\text{C} \quad \text{(S19.2)}$$

Saturation vapour pressure at $\boldsymbol{T_{max}}$ ***(***$\boldsymbol{v^*_{Tmax}}$***)***

$$v^*_{Tmax} = 0.6108exp\left[\frac{17.27T_{max}}{T_{max}+237.3}\right] \text{ (see Equation (S2.5))} \quad \text{(S19.3)}$$

$$v^*_{Tmax} = 0.6108exp\left[\frac{17.27\times21.0}{21.0+237.3}\right] = 2.4870 \text{ kPa} \quad \text{(S19.4)}$$

Saturation vapour pressure at T_{min} (v^*_{Tmin})

$v^*_{Tmin} = 0.6108 exp\left[\frac{17.27 T_{min}}{T_{min}+237.3}\right]$ (see Equation (S2.5)) (S19.5)

$v^*_{Tmin} = 0.6108 exp\left[\frac{17.27 \times 2.0}{2.0+237.3}\right]$ = 0.7056 kPa (S19.6)

Daily saturation vapour pressure (v^*_a)

$v^*_a = \frac{v^*_{Tmax}+v^*_{Tmin}}{2}$ (see Equation (S2.6)) (S19.7)

$v^*_a = \frac{2.4870 + 0.7056}{2}$ = 1.5963 kPa

Mean daily actual vapour pressure (v_a)

$v_a = \frac{v^*_{Tmin}\frac{RH_{max}}{100}+v^*_{Tmax}\frac{RH_{min}}{100}}{2}$ (see Equation (S2.7)) (S19.8)

$v_a = \frac{0.7056\frac{71}{100}+2.4870\frac{25}{100}}{2}$ = 0.5614 kPa (S19.9)

Slope of saturation vapour pressure at T_{mean} (Δ)

$\Delta = 4098\left(0.6108 Exp\left(\frac{17.27 T_{mean}}{T_{mean}+237.3}\right)\right)/(T_{mean}+237.3)^2$ (see Equation (S2.4))(S19.10)

$\Delta = 4098\left(0.6108 Exp\left(\frac{17.27 \times 11.5}{11.5+237.3}\right)\right)/(11.5+237.3)^2$ = 0.0898 kPa °C^{-1} (S19.11)

Atmospheric pressure

$p = 101.3\left(\frac{293-0.0065 Elev}{293}\right)^{5.26}$ (see Equation (S2.10)) (S19.12)

$p = 101.3\left(\frac{293-0.0065 \times 546}{293}\right)^{5.26}$ = 95.01027 kPa (S19.13)

Psychrometric constant

$\gamma = 0.00163\frac{p}{\lambda}$ (see Equation (S2.9)) (S19.14)

$\gamma = 0.00163\frac{95.01027}{2.45}$ = 0.0632 kPa °C^{-1} (S19.15)

Day of Year

1980 is a leap year, therefore

DoY = 31 + 28+ 31 +30 + 31 +30 + 20 +1 = 202 (see Equations (S3.21 to S3.23)) (S19.16)

Inverse relative distance Earth to Sun (d_r)

$d_r^2 = 1 + 0.033 cos\left(\frac{2\pi}{365} DoY\right)$ (see Equation (S3.6)) (S19.17)

$d_r^2 = 1 + 0.033 cos\left(\frac{2\pi}{365} 202\right)$ = 0.9688 (S19.18)

Solar declination (δ)

$\delta = 0.409 sin\left(\frac{2\pi}{365} DoY - 1.39\right)$ (see Equation (S3.7)) (S19.19)

$\delta = 0.409 sin\left(\frac{2\pi}{365} 202 - 1.39\right)$ = 0.3557 (S19.20)

***Sunset hour angle* (ω_s)**

$\omega_s = arcos[-\tan(lat)\tan(\delta)]$ (see Equation (S3.8)) (S19.21)

Latitude (lat) is in radians, hence $lat = \pi \frac{-23.7951}{180}$ = -0.4153 radians (S19.22)

noting the negative value as Alice Springs is in the southern hemisphere.

$\omega_s = arcos[-\tan(-0.4153)\tan(0.3557)]$ = 1.4063 (S19.23)

***Maximum daylight hours* (*N*)**

$N = \frac{24}{\pi}\omega_s$ (see Equation (S3.11)) (S19.24)

$N = \frac{24}{\pi}1.4063$ = 10.7431 hours (S19.24)

Worked example 2: Estimate R_n for daily analysis

***Extraterrestrial radiation* (R_a)**

$R_a = \frac{1440}{\pi} G_{sc} d_r^2 [\omega_s sin(lat) sin(\delta) + cos(lat) cos(\delta) sin(\omega_s)]$ (see Equation (S3.5))(S19.26)

where G_{sc} is the solar constant

$$R_a = \frac{24x60}{\pi} 0.082 \times 0.9688 \begin{bmatrix} 1.4063 sin(-0.4153) sin(0.3557) \\ + cos(-0.4153) cos(0.3557) sin(1.4063) \end{bmatrix}$$ (S19.27)

= 23.6182 MJ m^{-2} day^{-1}

***Clear sky radiation* (R_{so})**

$R_{so} = (0.75 + 2 \times 10^{-5} Elev) R_a$ (see Equation (S3.4)) (S19.28)

$R_{so} = (0.75 + 2 \times 10^{-5} \times 546) 23.6182$ = 17.9716 MJ m^{-2} day^{-1} (S19.29)

***Incoming solar radiation* (R_s)**

$R_s = \left(a_s + b_s \frac{n}{N}\right) R_a$ (see Equation (S3.9)) (S19.30)

Adopting a_s = 0.23 and b_s = 0.50 (see **Appendix S3**) and noting there were 10.7 hours of sunshine for the day being analysed

$R_s = \left(0.23 + 0.5 \frac{10.7}{10.7431}\right) 23.6182$ = 17.1940 MJ m^{-2} day^{-1} (S19.31)

Note: If measured values of solar radiation (R_s) were available, the daily analysis would begin here.

***Net longwave radiation* (R_{nl})**

$R_{nl} = \sigma(0.34 - 0.14 \bar{v}_a^{0.5}) \left(\frac{(T_{max}+273.2)^4 + (T_{min}+273.2)^4}{2}\right) \left(1.35 \frac{R_s}{R_{so}} - 0.35\right)$ (see Equation (S3.3)) (S19.32)

where σ is the Stefan-Boltzmann constant

$R_{nl} = 4.903 \times 10^{-9} (0.34 - 0.14 \times 0.5614^{0.5}) \left(\frac{(21+273.2)^4 + (2+273.2)^4}{2}\right) \left(1.35 \frac{17.194}{17.9716} - 0.35\right.$ (S19.33)

$R_{nl} = 7.1784$ MJ m^{-2} day^{-1}

Net incoming shortwave radiation $(\boldsymbol{R_{ns}})$

$R_{ns} = (1-\alpha)R_s$ (see Equation (S3.2)) (S19.34)

where α is the albedo for the evaporating surface, which will depend on the evaporating surface. In the worked examples that follow, water and reference crop surfaces are considered:

water α *= 0.08*

$R_{ns} = (1-\alpha)R_s = (1-0.08)17.1940 = 15.8184$ MJ m^{-2} day^{-1} (S19.35)

reference crop α *= 0.23*

$R_{ns} = (1-\alpha)R_s = (1-0.23)17.1940 = 13.2393$ MJ m^{-2} day^{-1} (S19.36)

Net radiation $(\boldsymbol{R_n})$

$R_n = R_{ns} - R_{nl}$ (see Equation (S3.1)) (S19.37)

Thus for water $R_n = R_{ns} - R_{nl} = 15.8184 - 7.1784 = 8.6401$ MJ m^{-2} day^{-1} (S19.38)

For reference crop $R_n = R_{ns} - R_{nl} = 13.2393 - 7.1784 = 6.0610$ MJ m^{-2} day^{-1}

(S19.39)

Worked example 3: Estimate daily open-water evaporation using Penman equation

$$E_{PenOW} = \frac{\Delta}{\Delta+\gamma}\frac{R_{nw}}{\lambda} + \frac{\gamma}{\Delta+\gamma}E_a \text{ (see Equation (S4.1))} \quad \text{(S19.40)}$$

$$\frac{\Delta}{\Delta+\gamma} = \frac{0.0898}{0.0898 + 0.0632} = 0.5870 \quad \text{(S19.41)}$$

$$\frac{\gamma}{\Delta+\gamma} = \frac{0.0632}{0.0898 + 0.06325} = 0.4130 \quad \text{(S19.42)}$$

Adopting the Penman 1956 wind function gives:

$$E_a = f(u)(v_a^* - v_a) \text{ (see Equations (S4.2) and (S4.3))} \quad \text{(S19.43)}$$

$$E_a = (1.313 + 1.381\times 0.5903)(1.5963 - 0.5614) = 2.2025 \text{ mm day}^{-1} \quad \text{(S19.44)}$$

$$E_{PenOW} = 0.5870\frac{8.6401}{2.45} + 0.4130\times 2.2025 = 2.9797 \text{ mm day}^{-1} \quad \text{(S19.45)}$$

Worked example 4: Estimate daily reference crop evapotranspiration for short grass using the FAO-56 Reference Crop procedure

$$ET_{RCsh} = \frac{0.408\Delta(\mathrm{R_n}-\mathrm{G})+\gamma\frac{900}{\mathrm{T}+273}\mathrm{u_2}(v_a^*-v_a)}{\Delta+\gamma(1+0.34\mathrm{u_2})} \text{ (see Equation (S5.18))} \quad \text{(S19.46)}$$

In this example we assume the soil flux, G, is zero which according to Allen et al., (1998, page 54; Shuttleworth, 1992, page 4.10) is a reasonable assumption for daily analysis.

$$ET_{RCsh} = \frac{0.408\times 0.0898\,(6.0610-0)+0.0632\frac{900}{11.5+273}0.5903(1.5963-0.5614)}{0.0898+0.0632(1+0.34\times 0.5903)} \quad \text{(S19.47)}$$

$$ET_{RCsh} = \frac{0.22206+0.10538}{0.16578} = 2.0775 \text{ mm day}^{-1} \quad \text{(S19.48)}$$

Worked example 5: Estimate daily reference crop evapotranspiration for rye grass at Alice Springs using the Matt-Shuttleworth model

There are five steps in the procedure which includes Equations (S5.34) – (S5.37). The first step is to estimate the average height and surface resistance ($(r_s)_c$) for rye grass, which from Shuttleworth and Wallace (2009) Table 3, is 0.30 m and 66 s m^{-1} respectively. Next, the climatological resistance is computed.

$$r_{clim} = 86400\,\frac{\rho_a c_a (VPD)}{\Delta R_n} \text{ (see Equation (S5.34))} \tag{S19.49}$$

$$r_{clim} = 86400\,\frac{1.20\times 0.001013(1.5963-0.5614)}{0.0898\times 6.0610} = 199.9 \text{ s m}^{-1} \tag{S19.50}$$

The third step is to estimate $\frac{VPD_{50}}{VPD_2}$ from Equation (S5.35)

$$\frac{VPD_{50}}{VPD_2} = \left(\frac{302(\Delta+\gamma)+70\gamma u_2}{208(\Delta+\gamma)+70\gamma u_2}\right) + \frac{1}{r_{clim}}\left[\left(\frac{302(\Delta+\gamma)+70\gamma u_2}{208(\Delta+\gamma)+70\gamma u_2}\right)\left(\frac{208}{u_2}\right) - \left(\frac{302}{u_2}\right)\right] \tag{S19.51}$$

where $\left(\frac{302(\Delta+\gamma)+70\gamma u_2}{208(\Delta+\gamma)+70\gamma u_2}\right) = \left(\frac{302(0.0898+0.0632)+70\times 0.0632\times 0.5903}{208(0.0898+0.0632)+70\times 0.0632\times 0.5903}\right) = 1.4177$ (S19.52)

$$\frac{VPD_{50}}{VPD_2} = 1.4177 + \frac{1}{199.9}\left[1.4177\left(\frac{208}{0.5903}\right) - \left(\frac{302}{0.5903}\right)\right] = 1.3574 \tag{S19.53}$$

Next, r_c^{50} is estimated from Equation (S5.36)

$$r_c^{50} = \frac{1}{(0.41)^2} ln\left[\frac{(50-0.67h_c)}{(0.123h_c)}\right] ln\left[\frac{(50-0.67h_c)}{(0.0123h_c)}\right] \frac{ln\left[\frac{(2-0.08)}{0.0148}\right]}{ln\left[\frac{(50-0.08)}{0.0148}\right]} \tag{S19.54}$$

for h_c = 0.3 m

$$r_c^{50} = \frac{1}{(0.41)^2} ln\left[\frac{(50-0.67\times 0.3)}{(0.123\times 0.3)}\right] ln\left[\frac{(50-0.67\times 0.3)}{(0.0123\times 0.3)}\right] \frac{ln\left[\frac{(2-0.08)}{0.0148}\right]}{ln\left[\frac{(50-0.08)}{0.0148}\right]} = 244.2 \text{ s m}^{-1} \tag{S19.55}$$

The final step is to calculate ET_c from Equation (S5.37)

$$ET_c = \frac{1}{\lambda}\frac{\Delta R_n + \frac{\rho_a c_p u_2 (VPD_2)}{r_c^{50}}\left(\frac{VPD_{50}}{VPD_2}\right)}{\Delta + \gamma\left(1+\frac{(r_s)_c u_2}{r_c^{50}}\right)} \tag{S19.56}$$

$$ET_c = \frac{1}{2.45}\frac{0.0898\times 6.6061 + \frac{1.20\times 0.001013\times 0.5903(1.5963-0.5614)}{244.2}(1.3574)}{0.0898+0.0632\left(1+\frac{66\times 0.5903}{244.2}\right)} = 1.4847 \text{ mm day}^{-1} \tag{S19.57}$$

Worked example 6: Estimate daily actual evapotranspiration using the Advection-Aridity (Bruitsaert-Strickler) model

$$ET_{Act}^{BS} = (2\alpha_{PT} - 1)\frac{\Delta}{\Delta+\gamma}\frac{R_n}{\lambda} - \frac{\gamma}{\Delta+\gamma} f(u_2)(v_a^* - v_a) \text{ (see Equation (S8.2))} \tag{S19.58}$$

Note for BS equation, α_{PT} = 1.28 for rural catchments, and for this example R_n is based on an albedo value of 0.23 (Equation (S19.36)). The 1948 Penman wind function is adopted (Equation S4.11).

$$ET_{Act}^{BS} = (2\times1.28-1)\frac{0.0898}{0.0898+0.0632}\frac{6.0610}{2.45} - \frac{0.0632}{0.0898+0.0632}(2.626+1.381\times0.5903)(1.5963-0.5614) \quad \text{(S19.59)}$$

$$ET_{Act}^{BS} = 2.2651 - 1.4711 = 0.7940 \text{ mm day}^{-1} \quad \text{(S19.60)}$$

Worked example 7: Estimate daily actual evapotranspiration using the Granger-Gray model

$$ET_{Act}^{GG} = \frac{\Delta G_g}{\Delta G_g+\gamma}\frac{R_n-G}{\lambda} + \frac{\gamma G_g}{\Delta G_g+\gamma}E_a \text{ (see Equation (S8.4))} \quad \text{(S19.61)}$$

For this worked example we set G = 0, and note that Granger and Gray (1989, page 26) adopted the Penman (1948) wind function. Granger-Gray procedure estimates evapotranspiration rates for non-saturated lands. To illustrate the procedure, R_n is based on an albedo value of 0.23 (Equation S19.36)).

E_a is estimated from:

$$E_a = f(u)(v_a^* - v_a) \text{ (see Equation (S4.2))} \quad \text{(S19.62)}$$

$$E_a = (2.626+1.381\times0.5903)(1.5963-0.5614) = 3.5614 \text{ mm day}^{-1} \quad \text{(S19.63)}$$

$$D_p = \frac{E_a}{E_a+\frac{R_n-G}{\lambda}} \text{ (see Equation (S8.6))} \quad \text{(S19.64)}$$

$$D_p = \frac{3.5614}{3.5614+\frac{6.0610-0}{2.45}} = 0.5901 \quad \text{(S19.65)}$$

$$G_g = \frac{1}{0.793+0.20e^{4.902D_p}} + 0.006D_p \text{ (see Equation (S8.5))} \quad \text{(S19.66)}$$

$$G_g = \frac{1}{0.793+0.20e^{4.902\times0.5901}} + 0.006\times0.5901 = 0.2307 \quad \text{(S19.67)}$$

$$ET_{Act}^{GG} = \frac{0.0898\times0.2307}{0.0898\times0.2307+0.0632}\frac{6.0610-0}{2.45} + \frac{0.0632\times0.2307}{0.0898\times0.2307+0.0632}3.5614 \quad \text{(S19.68)}$$

$$ET_{Act}^{GG} = 0.6107 + 0.6188 = 1.2295 \text{ mm day}^{-1} \quad \text{(S19.69)}$$

Worked example 8: Estimate daily actual evapotranspiration using the Szilagyi-Jozsa model

$$ET_{Act}^{SJ} = 2E_{PT}(T_e) - E_{Pen} \text{ (see Equation (S8.7))} \quad \text{(S19.70)}$$

$$\frac{R_n}{\lambda E_{Pen}} = 1 + \gamma\frac{T_e-T_a}{v_e^*-v_a} \text{ (see Equation (S8.8))} \quad \text{(S19.71)}$$

For this example procedure R_n is based on an albedo value of 0.23 (Equation S19.34)) and, therefore, E_{Pen} needs to be recomputed incorporating R_n = 6.0610 MJ m^{-2} day^{-1} and Penman's 1948 wind function resulting in E_{Pen} = 2.9221 mm day^{-1}.

To estimate T_e (the equilibrium temperature) from Equation (S19.69), a numerical solution is required as v_e^* is a function of T_e. Equation (S19.69) is rearranged as follows:

$$T_e = T_a - \frac{1}{\gamma}\left[1-\frac{R_n}{\lambda E_{Pen}}\right](v_e^* - v_a) \quad \text{(S19.72)}$$

noting from Equation (S2.5) that $v_e^* = 0.6108exp\left[\frac{17.27T_e}{T_e+237.3}\right]$ (S19.73)

Using Microsoft Excel Goal Seek, T_e = 9.900 °C (for T_a = 11.5 °C, R_n = 6.0610 MJ m^{-2} day^{-1}, E_{Pen} = 2.923 mm day^{-1}, and v_e^* = 1.2197 kPa). To compute E_{Act}^{SJ}, we need $E_{PT}(T_e)$. From Equation (6) and setting G = 0, and Δ for T_e = 9.900 °C is equal to 0.0818, and α_{PT} = 1.31 (see penultimate paragraph in **Appendix S8** under heading Szilagyi-Jozsa model), we obtain;

$$E_{PT}(T_e) = \alpha_{PT}\left[\frac{\Delta}{\Delta+\gamma}\frac{R_n}{\lambda}\right] \quad \text{(S19.74)}$$

$$E_{PT}(9.900\ °\text{C}) = 1.31\left[\frac{0.0818}{0.0818+0.0632}\times\frac{6.0610}{2.45}\right] = 1.8285 \text{ mm day}^{-1} \quad \text{(S19.75)}$$

$$E_{Act}^{SJ} = 2\times 1.8285 - 2.923 = 0.7340 \text{ mm day}^{-1} \quad \text{(S19.76)}$$

Worked example 9: Estimate daily Class-A pan evaporation using the PenPan model

$$E_{PenPan} = \frac{\Delta}{\Delta+a_p\gamma}\frac{R_{NPan}}{\lambda} + \frac{a_p\gamma}{\Delta+a_p\gamma}f_{Pan}(u)(v_a^* - v_a) \text{ (see Equation (S6.1))} \quad \text{(S19.77)}$$

where a_p is an empirical constant = 2.4

$$P_{rad} = 1.32 + 4\times 10^{-4} lat + 8\times 10^{-5} lat^2 \text{ (see Equation (S6.6))} \quad \text{(S19.78)}$$

Noting φ is in absolute value of latitude in degrees

$$P_{rad} = 1.32 + 4\times 10^{-4}\times 23.7951 + 8\times 10^{-5}\times(23.7951)^2 = 1.3748 \quad \text{(S19.79)}$$

$$f_{dir} = -0.11 + 1.31\frac{R_S}{R_a} \text{ (see Equation (S6.5))} \quad \text{(S19.80)}$$

$$f_{dir} = -0.11 + 1.31\frac{17.1940}{23.6182} = 0.8437 \quad \text{(S19.81)}$$

$$R_{SPan} = [f_{dir}P_{rad} + 1.42(1 - f_{dir}) + 0.42\alpha_{ss}]R_S \text{ (see Equation (S6.4))} \quad \text{(S19.82)}$$

where α_{SS} = 0.26 (assuming short grass **Table S3**)

$$R_{SPan} = [0.8437\times 1.3748 + 1.42(1 - 0.8437) + 0.42\times 0.26]17.1940 \quad \text{(S18.83)}$$

$$R_{SPan} = 25.6375 \text{ MJ m}^{-2} \text{ day}^{-1} \quad \text{(S19.84)}$$

$$R_{NPan} = (1 - \alpha_A)R_{SPan} - R_{nl} \text{ (see Equation (S6.3))} \quad \text{(S19.85)}$$

where α_A = 0.14 (**Appendix S6**)

$$R_{NPan} = (1 - 0.14)25.6375 - 7.1784 = 14.8699 \text{ MJ m}^{-2} \text{ day}^{-1} \quad \text{(S19.86)}$$

$$f_{Pan}(u) = 1.201 + 1.621\, u_2 \text{ (see Equation (S6.2))} \quad \text{(S19.87)}$$

$$f_{Pan}(u) = 1.201 + 1.621\times 0.5903 = 2.1578 \quad \text{(S19.88)}$$

$$E_{PenPan} = \frac{0.0898}{0.0898+2.4\times 0.0632}\frac{14.8699}{2.45} + \frac{2.4\times 0.0632}{0.0898+2.4\times 0.0632}2.1578(1.5963 - 0.5614) \quad \text{(S19.89)}$$

$$E_{PenPan} = 2.2570 + 1.4027 = 3.6587 \text{ mm day}^{-1} \quad \text{(S19.90)}$$

For a screened Class-A pan, E_{PenPan} = 0.93* 3.6597 = 3.4035 mm day^{-1}.

A discussion regarding the screen factor of 0.93 can be found in **Appendix S16**.

Worked example 10: Estimate daily potential evaporation using the Makkink model

$$E_{Mak} = 0.61\left(\frac{\Delta}{\Delta+\gamma}\frac{R_s}{2.45}\right) - 0.12 \text{ (see Equation (S9.6))} \quad \text{(S19.91)}$$

$$E_{Mak} = 0.61\left(\frac{0.0898}{0.0898+0.0632}\frac{17.1940}{2.45}\right) - 0.12 = 2.3928 \text{ mm day}^{-1} \quad \text{(S19.92)}$$

Worked example 11: Estimate daily reference crop evapotranspiration using the Blaney-Criddle model

$$ET_{BC} = \left(0.0043RH_{min} - \frac{n}{N} - 1.41\right) + b_{var}p_y(0.46T_a + 8.13) \quad \text{(S19.93)}$$

(see Equation (S9.7))

$$b_{var} = e_0 + e_1RH_{min} + e_2\frac{n}{N} + e_3u_2 + e_4RH_{min}\frac{n}{N} + e_5RH_{min}u_2 \quad \text{(S19.94)}$$

(see Equation (S9.8))

$$b_{var} = 0.81917 - 0.0040922\times25 + 1.0705\times\frac{10.7}{10.7431} + 0.065649\times0.5903 - 0.0059684\times25\frac{10.7}{10.7431} - 0.0005967\times25\times0.5903 = 1.6644 \quad \text{(S19.95)}$$

p_y is the percentage of actual day-light hours for the day compared to the number of day-light hour during the entire year (N_{year}). The latter can be computed from Equation (S3.11) as follows:

$$N_{year} = \sum_{J=1}^{365,366}\left(\frac{24}{\pi}\omega_s\right) \text{ (see Equation (S3.11))} \quad \text{(S19.96)}$$

For non-leap years and leap years N_{year} = 4380 and 4393 respectively.

Thus $p_y = 100\frac{n}{N_{year}} = 100\frac{10.7}{4393} = 0.2436$

$$ET_{BC} = \left(0.0043\times25 - \frac{10.7}{10.7431} - 1.41\right) + 1.6644\times0.2436(0.46\times11.5 + 8.13) \quad \text{(S19.97)}$$

$$ET_{BC} = -2.2985 + 5.4411 = 3.1426 \text{ mm day}^{-1} \quad \text{(S19.98)}$$

Worked example 12: Estimate daily reference crop evapotranspiration using the Turc model

Turc (1961) proposed two equations, one for humid days and another for non-humid days (see **Appendix S9**). As the average humidity for Alice Springs on 7 July 1980 was 48%, the equation for non-humid days is adopted.

$$ET_{Turc} = 0.013(23.88R_s + 50)\left(\frac{T_a}{T_a+15}\right)\left(1 + \frac{50-RH}{70}\right) \quad \text{(S19.99)}$$

(see Equation (S9.11))

$$ET_{Turc} = 0.013(23.88\times17.1940 + 50)\left(\frac{11.5}{11.5+15}\right)\left(1 + \frac{50-36.5}{70}\right) = 2.6727 \text{ mm day}^{-1} \quad \text{(S19.100)}$$

Worked example 13: Estimate daily reference crop evapotranspiration using the Hargreaves-Samani model

$$ET_{HS} = 0.0135 C_{HS} \frac{R_a}{\lambda} (T_{max} - T_{min})^{0.5} (T_a + 17.8) \quad \text{(S19.101)}$$

(see Equation (S9.12))

$$C_{HS} = 0.00185 (T_{max} - T_{min})^2 - 0.0433 (T_{max} - T_{min}) + 0.4023 \quad \text{(S19.102)}$$

(see Equation (S9.13))

$$C_{HS} = 0.00185 (21 - 2)^2 - 0.0433 (21 - 2) + 0.4023 = 0.2475 \quad \text{(S19.103)}$$

$$ET_{HS} = 0.0135 \times 0.2475 \frac{23.6182}{2.45} (21 - 2)^{0.5} (11.5 + 17.8) = 4.1129 \text{ mm day}^{-1}$$

Worked example 14: Estimate monthly reference crop evapotranspiration using the modified Hargreaves model

The modified Hargreaves method operates at a monthly time-step. The appropriate data for Alice Springs for July 1980 is as follows:

Mean maximum daily temperature: 19.500 °C
Mean minimum daily temperature: 4.119 °C
Mean monthly temperature: 11.810 °C
Maximum humidity: 77.968%
Minimum humidity: 33.032%
Daily sunshine hours: 8.34 hours
Wind run at 2 m height: 74.677 km day^{-1} (=74.677×1000/(24×60×60) = 0.8643 m s^{-1})
Rainfall for month: 10.8 mm
Mean diurnal temperature range for July: (19.500 – 4.119) = 15.381°C

$$ET_{Harg,j} = 0.0013 S_O (T_j + 17.0)(\overline{TD}_j - 0.0123 P_j)^{0.76} \quad \text{(S19.104)}$$

(see Equation (S9.14))

$$S_0 = 15.392 d_r^2 (\omega_s sin(lat) sin(\delta) + cos(lat) cos(\delta) sin(\omega_s)) \quad \text{(S19.105)}$$

(see Equation (S9.15))

$$S_0 = 15.392 \times 0.9688 \begin{pmatrix} 1.4063 sin(-0.4153) sin(0.3557) \\ + cos(-0.4153) cos(0.3557) sin(1.4063) \end{pmatrix} = 9.6710 \quad \text{(S19.106)}$$

$$ET_{Harg,j} = 0.0013 \times 9.6710 (11.810 + 17.0)(15.381 - 0.0123 \times 10.8)^{0.76} \quad \text{(S19.107)}$$

$$ET_{Harg,j} = 2.8721 \text{ mm day}^{-1} = 2.8721 \times 31 = 89.035 \text{mm month}^{-1} \quad \text{(S19.108)}$$

Worked example 15: Estimate daily potential evaporation using the Priestley-Taylor model

$$E_{PT} = \alpha_{PT} \left[\frac{\Delta}{\Delta + \gamma} \frac{R_n}{\lambda} - \frac{G}{\lambda} \right] \quad \text{(see Equation (6))} \quad \text{(S19.109)}$$

Assuming G = 0.0, $\frac{\Delta}{\Delta+\gamma}$ = 0.5870, R_n = 8.6401 MJ m^{-2} day^{-1} (for water), and adopting α_{PT} = 1.26 (see Section 2.1.3), we obtain

$$E_{PT} = 1.26 \left[0.5870 \frac{8.6401}{2.45} - \frac{0.0}{2.45} \right] = 2.6083 \text{ mm day}^{-1}$$

Worked example 16: Estimate monthly potential evapotranspiration using the Thornthwaite equation

Use the Thornthwaite equation to estimate the average monthly potential evapotranspiration for July at Alice Springs. The Thornthwaite estimates are computed from mean daily temperatures and mean daily day-light hours for each month. At Alice Springs, the mean daily temperature (°C) for each month, based on the whole record, are:

Jan 29.11; Feb 28.32; Mar 25.18; Apr 20.85; May 15.70; Jun 12.43

Jul 11.90; Aug 14.56; Sep 19.86; Oct 23.22; Nov 26.40; Dec 28.07

The mean daily hours of day-light are estimated from Equation (S19.24) and for July the value is 10.68 hours.

$$\bar{E}_{Th,j} = 16\left(\frac{\overline{hrday}}{12}\right)\left(\frac{daymon}{30}\right)\left(\frac{10\bar{T}_J}{I}\right)^{a_{Th}} \text{ (see Equation (S9.2))} \tag{S19.110}$$

Thus the average potential evapotranspiration for the month of July is estimated as:

$$I = \sum_{j=1}^{12}\left(\frac{\bar{T}_j}{5}\right)^{1.514} = 111.1827 \tag{S19.111}$$

$$a = 6.75\times10^{-7}I^3 - 7.71\times10^{-5}I^2 + 0.01792I + 0.49239 \tag{S19.112}$$

$$a = 6.75\times10^{-7}\times(111.1827)^3 - 7.71\times10^{-5}\times(111.1827)^2 + 0.01792\times111.1827 + 0.49239 = 2.4594 \tag{S19.113}$$

$\overline{hrday}$ is the mean daily day-light hours in a given month. From observed data for the month of July at Alice Springs $\overline{hrday}$ = 10.68 hours.

$$\bar{E}_{Th,Jul} = 16\left(\frac{\overline{hrday}}{12}\right)\left(\frac{daymon}{30}\right)\left(\frac{10\bar{T}_J}{I}\right)^{a_{Th}} \tag{S19.114}$$

$$\bar{E}_{Th,Jul} = 16\left(\frac{10.68}{12}\right)\left(\frac{31}{30}\right)\left(\frac{10\times11.90}{111.1827}\right)^{2.4594} = 17.391 \text{ mm month}^{-1} \tag{S19.115}$$

Worked example 17: Estimating deep lake evaporation using Kohler and Parmele model

Use the Kohler and Parmele (1967) model to estimate the monthly evaporation for September 1999 for a hypothetical deep lake near Melbourne. The following data are available:

Lake area at full supply level (FSL) (A_L): 1.74 km^2
Lake capacity: 26.8 GL
Average water depth ($\bar{h}$): 27.0 m
Catchment area of lake at full supply level: 3.5 km^2 (The lake is an off-stream reservoir)
Contents at beginning of September 1999 (V_1): 25.000 GL
Lake water temperature at beginning of September 1999 (T_{L1}): 10.5 °C
Contents at end of September 1999 (V_2): 24.1194GL
Lake water temperature at end of September 1999 (T_{L2}): 11.6 °C
Average lake temperature during September 1999 (T_w): 10.8 °C
Rainfall for September 1999 (P_d): 60 mm (2.0 mm day^{-1})

Average temperature of rain falling on reservoir in September 1999 (T_p): 10 °C
Average air temperature for September 1999 (T_a): 13.37 °C
Atmospheric pressure (p): 1004.22 (hPa) (= 100.422 kPa)
Wind run for September 1999 (u): 329.1 km day^{-1}
Surface water inflow for September 1999 (SW_{in}): assume 0.40 mm day^{-1} at FSL
Average temperature of surface water inflow for September 1999 (T_{swin}): 11 °C
Surface water outflow for September 1999 (SW_{out}): 1.00 GL (equivalent to 19.16 mm at FSL)
Average temperature of surface water outflow for September 1999 (T_{swout}): 10.8 °C
Assume no groundwater inflow or outflow

Specific constants for Worked Examples 17 and 18:
Density of air (ρ_a): 1.2 kg m^{-3}
Density of water (ρ_w): 997.9 kg m^{-3}
Effective emissivity of water (ε_w): 0.95
Specific heat of water (c_w): 4.19 kJ kg^{-1} °C^{-1}
Height at which the wind speed and vapour pressure are measured (z_m): 2.0 m
Zero-plane displacement (z_d): ~0.000 m
Roughness height of surface (z_0): 0.001 m for water
Latent heat of vaporization (λ): 2.45 MJ kg^{-1}
Stefan-Boltzmann constant (σ): 4.903×10^{-9} MJ m^{-2} day^{-1} K^{-4}
Slope of the vapour pressure curve based on an average September 1999 air temperature of 13.37°C (Δ): 0.10008 kPa °C^{-1}
Psychrometric constant for Melbourne (γ): 0.0665 kPa °C^{-1}

To estimate the monthly evaporation for the hypothetical deep lake based on Kohler and Parmele (1967) we apply the following equations at a daily time-step:

$$E_{DL} = E_{PenOW} + \alpha_{KP}(A_w - \frac{\Delta Q}{\Delta t}) \text{ (see Equation (S10.1))} \quad \text{(S19.116)}$$

$$\alpha_{KP} = \frac{\Delta}{\Delta + \gamma + \frac{4\varepsilon_w \sigma (T_w + 273.2)^3}{\rho_w \lambda K_E u}} \text{ (see Equation (S10.2))} \quad \text{(S19.117)}$$

$$A_w = \frac{c_w \rho_w}{\lambda}(P_d T_p + SW_{in} T_{swin} - SW_{out} T_{swout} + GW_{in} T_{gwin} - GW_{out} T_{gwout})$$
(see Equation (S10.3)) (S19.118)

$$\Delta Q = \frac{c_w \rho_w}{A_L \lambda}(V_2 T_{L2} - V_1 T_{L1}) \text{ (see Equation (S10.4))} \quad \text{(S19.119)}$$

$$K_E = 0.622 \frac{\rho_a}{p \rho_w} \frac{1}{6.25\left[ln\left(\frac{z_m - z_d}{z_0}\right)\right]^2} \text{ (see Equation (S10.5))} \quad \text{(S19.120)}$$

$$K_E = 0.622 \frac{1.2}{\left(\frac{1004.22}{10}\right) \times 997.9} \times \frac{1}{6.25\left[ln\left(\frac{2.0 - 0.000}{0.001}\right)\right]^2} = 2.0627 \times 10^{-8} \quad \text{(S19.121)}$$

$$\alpha_{KP} = \frac{0.10008}{0.10008 + 0.0665 + \frac{4 \times 0.95 \times 4.903 \times 10^{-9} (10.8 + 273.2)^3}{997.9 \times 2.45 \times 2.0627 \times 10^{-8} \times (329.1 \times 1000)}} = 0.52045 \quad \text{(S19.122)}$$

$$A_w = \left(\frac{4.19}{1000}\right)\frac{997.9}{2.45}\left[\left(\frac{2.0}{1000}\right) \times 10 + \left(\frac{0.4}{1000}\right) \times 11 - \left(\frac{19.16}{1000}\right) \times 10.8 + 0 - 0\right] = -0.3115 \text{ mm day}^{-1}$$
(S19.123)

$$\Delta Q = \left(\frac{4.19}{1000}\right)\frac{997.9}{(1.74\times10^6)2.45}(24.1194\times10^6\times11.6 - 25.000\times10^6\times10.5)\frac{1}{30} \qquad \text{(S19.124)}$$

$= 0.5651$ mm day^{-1}

E_{Pen} for September 1999 at the lake near Melbourne has been computed (separately from this worked example) as 117.2 mm (3.91 mm day^{-1})

$$E_{DL} = 3.91 + 0.5204\left(-0.3115 - \frac{0.5651}{1}\right) \qquad \text{(S19.125)}$$

$= 3.91 - 0.4562 = 3.45$ mm day^{-1} = 103.5 mm evaporation for September 1999.

Worked example 18: Estimating deep lake evaporation using Vardavas and Fountoulakis model

This worked example is for the same hypothetical deep lake described in Worked Example 17. The exercise is to estimate lake evaporation for September 1999. Vardavas and Fountoulakis (1996, Section 1) adopted a monthly time-step.

$$E_{DL} = \left(\frac{\Delta}{\Delta+\gamma}\right)E_s + \left(\frac{\gamma}{\Delta+\gamma}\right)E_a \quad \text{(see Equation (S10.7))} \qquad \text{(S19.126)}$$

$$E_s = \frac{1}{\lambda}\left(R_n + \Delta H_{j,j-1}\right) \quad \text{(see Equations (S10.8) and (S10.9))} \qquad \text{(S19.127)}$$

$$\Delta H_{j,j-1} = -48.6\bar{h}\frac{\Delta T_{wl}}{t_m} \quad \text{(see Equation (S10.9))} \qquad \text{(S19.128)}$$

From the data in worked example 16:

$$\Delta H_{j,j-1} = -48.6\times27.0\frac{11.6-10.5}{30} = -48.114 \text{ W m}^{-2} \qquad \text{(S19.129)}$$

Convert this from W m^{-2} to MJ m^{-2} day^{-1} (1 W = 1 J sec^{-1})

$$\Delta H_{j,j-1} = -48.114\times0.0864 = -4.1570 \text{ MJ m}^{-2}\text{ day}^{-1} \qquad \text{(S19.130)}$$

Assume for September 1999 R_n = 9.3469 MJ m^{-2} day^{-1}

$$E_s = \frac{1}{2.45}(9.3469 + (-4.1570)) = 2.1183 \text{ mm day}^{-1} \qquad \text{(S19.131)}$$

$$E_a = C_u\bar{u}[v_a^*(T_a) - v_a(T_a)] \quad \text{(see Equations (S10.10) and (S10.11))} \qquad \text{(S19.132)}$$

noting that the vapour pressure deficit $v_a^*(T_a) - v_a(T_a)$ is in units of mbar (Vardavas, 1987, page 249).

First we need to estimate u_* from

$$\bar{u} = \frac{u_*}{k}ln\left(\frac{z_2u_*}{0.135\upsilon}\right) \quad \text{(see Equation (S10.16))} \qquad \text{(S19.133)}$$

where k is the von Kármán constant of 0.41

$$\upsilon = 2.964\times10^{-7}\frac{T_a^{3/2}}{p} \quad \text{(see Equation (S10.15))} \qquad \text{(S19.134)}$$

$$\upsilon = 2.964\times10^{-7}\frac{(13.37+273.2)^{3/2}}{\frac{1004.22}{10}} = 1.4318\times10^{-5} \text{ m}^2\text{s}^{-1} \qquad \text{(S19.135)}$$

Thus for a wind speed of 3.809 m s^{-1}, Equation (S19.133) is

$$3.809 = \frac{u_*}{0.41}\ln\left(\frac{2.0u_*}{0.135\times1.4318\times10^{-5}}\right) \qquad \text{(S19.136)}$$

Using Microsoft Excel Goal Seek, $u_* = 0.132$ m s^{-1} (S19.137)

$$C_u = \frac{3966}{T_a ln\left(\frac{z_2}{z_{ov}}\right) ln\left(\frac{z_1}{z_{om}}\right)} \text{ (see Equation (S10.12))} \quad (S19.138)$$

$$z_{om} = 0.135\frac{\upsilon}{u_*} = 0.135\frac{1.4318\times10^{-5}}{0.132} = 1.4643\times10^{-5} \quad (S19.139)$$

$$z_{ov} = 0.624\frac{\upsilon}{u_*} = 0.624\frac{1.4318\times10^{-5}}{0.132} = 6.7685\times10^{-5} \quad (S19.140)$$

$$C_u = \frac{3966}{(13.37+273.2) ln\left(\frac{2.0}{6.7685\times10^{-5}}\right) ln\left(\frac{2.0}{1.4643\times10^{-5}}\right)} \quad (S19.141)$$

$= 0.1137$ mm day^{-1}/(m s^{-1} mbar)

which is within the range 0.11 to 0.13 mm day^{-1}/(m s^{-1} mbar) estimated for Australian reservoirs as noted by Vardavas (1987, page 264).

Assume for this hypothetical example the vapour pressure deficit = 0.6152 kPa

$$E_a = C_u\bar{u}[v_a^*(T_a) - v_a(T_a)] = 0.1137\times3.809\times(0.6152\times10) \quad (S19.142)$$

where the factor 10 in the last set of brackets converts kPa to mbar

$= 2.664$ mm day^{-1}

$$E_{DL} = \left(\frac{0.10008}{0.10008+0.0665}\right)2.1183 + \left(\frac{0.0665}{0.10008+0.0665}\right)2.664 \quad (S19.143)$$

$= 2.336$ mm day^{-1} $= 70.1$ mm evaporation for September 1999.

Worked example 19: Estimating lake evaporation based on the equilibrium temperature by McJannet et al. (2008)

Estimate for a hypothetical lake near Alice Springs, the evaporation for 20 July 1980. The following details are available:

Average lake area: 5 km^2
Average lake depth: 10 m
Latitude: 23.7951 °S
Elevation: 546 m
Lake water temperature for 19 July was 10.8734 °C.

The meteorological data for 20 July 1980 are listed at the beginning of this appendix. For the purposes of this example, the fraction of cloud cover (C_f) is based on Equation (S3.18) where $K_{ratio} = \frac{R_s}{R_{so}} = \frac{17.1940}{17.9716} = 0.9567$ and hence $C_f = 2(1 - K_{ratio}) = 0.08654$.

Adjust wind speed to equivalent of 10 m height.

$$u_{10} = u_2\frac{\ln\left(\frac{10}{z_0}\right)}{\ln\left(\frac{2}{z_0}\right)} \quad (S19.144)$$

where $z_0 = 0.0002$ m (adopted from **Table S2** for open sea)

$$u_{10} = 0.5903\frac{\ln\left(\frac{10}{0.0002}\right)}{\ln\left(\frac{2}{0.0002}\right)} = 0.6934 \quad (S19.145)$$

Estimate the values of the intermediate variables associated with computing daily evaporation in addition to those in Worked Example 1.

Dew point temperature (T_d)

$$T_d = \frac{116.9+237.3\ln(v_a)}{16.78-\ln(v_a)} \text{ (see Equation (S2.3))} \quad \text{(S19.146)}$$

From Equation S19.9 v_a = 0.5614 kPa

$$T_d = \frac{116.9+237.3\ln(0.5614)}{16.78-\ln(0.5614)} = -1.1579\ °\text{C} \quad \text{(S19.147)}$$

Wet-bulb temperature (T_{wb})

$$T_{wb} = \frac{0.00066\times 100 T_a + \frac{4098 v_a}{(T_d+237.3)^2} T_d}{0.00066\times 100 + \frac{4098 v_a}{(T_d+237.3)^2}} \text{ (see Equation (S2.2))} \quad \text{(S19.148)}$$

$$T_{wb} = \frac{0.00066\times 100\times 11.5 + \frac{4098\times 0.5614}{(-1.1579+237.3)^2}(-1.1579)}{0.00066\times 100 + \frac{4098\times 0.5614}{(-1.1579+237.3)^2}} = 6.6311\ °\text{C} \quad \text{(S19.149)}$$

Slope of saturation vapour pressure curve at wet-bulb temperature (Δ_{wb})

$$\Delta_{wb} = \frac{4098\left[0.6108 exp\left(\frac{17.27 T_{wb}}{T_{wb}+237.3}\right)\right]}{(T_{wb}+237.3)^2} \text{ (see Equation (S2.4))} \quad \text{(S19.150)}$$

where Δ_{wb} is the slope of the saturation vapour pressure curve at wet-bulb temperature

$$\Delta_{wb} = \frac{4098\left[0.6108 exp\left(\frac{17.27\times 6.6311}{6.6311+237.3}\right)\right]}{(6.6311+237.3)^2} = 0.06727\text{ kPa }°\text{C}^{-1} \quad \text{(S19.151)}$$

Wind function ($f(u)$)

$$f(u) = \left(\frac{5}{A}\right)^{0.05}(3.80 + 1.57 u_{10}) \text{ (see Equation (S11.24))} \quad \text{(S19.152)}$$

$$f(u) = \left(\frac{5}{5}\right)^{0.05}(3.80 + 1.57\times 0.6934) = 4.8887 \quad \text{(S19.153)}$$

Aerodynamic resistance (r_a)

$$r_a = \frac{\rho_a c_a}{\gamma\left(\frac{f(u)}{86400}\right)} \text{ (see Equation (S11.23))} \quad \text{(S19.154)}$$

$$r_a = \frac{1.20\times 0.001013}{0.0632\left(\frac{4.8887}{86400}\right)} = 339.9\text{ s m}^{-1} \quad \text{(S19.155)}$$

The next step is to compute the net radiation. For 20 July 1980, R_s and R_{ns} were estimated respectively as 17.1940 MJ m^{-2} day^{-1} (Equation (S19.31)) and 15.8184 MJ m^{-2} day^{-1} (Equation (S19.35)) noting that albedo for water is 0.08. Incoming longwave radiation is estimated from:

$$R_{il} = \left(C_f + (1-C_f)\left(1-\left(0.261\, exp(-7.77\times 10^{-4} T_a^2)\right)\right)\right)\sigma(T_a+273.15)^4 \text{ (see Equation (S11.26))} \quad \text{(S19.156)}$$

$$R_{il} = \left(0.08654 + (1-0.08654)\left(1-\left(0.261\, exp(-7.77\times 10^{-4} 11.5^2)\right)\right)\right)$$

$$\times\ 4.903\times 10^{-9}(11.5+273.15)^4 = 25.2641\text{ MJ m}^{-2}\text{ day}^{-1} \quad \text{(S19.157)}$$

Outgoing longwave radiation as a function of wet-bulb temperature is estimated from:

$R_{ol}^{wb} = \sigma(T_a + 273.15)^4 + 4\sigma(T_a + 273.15)^3(T_{wb} - T_a)$ (see Equation (S11.32)) (S19.158)

$R_{ol}^{wb} = 4.903{\times}10^{-9}(11.5 + 273.15)^4 + 4{\times}4.903{\times}10^{-9}(11.5 + 273.15)^3$
$(6.6311 - 11.5)$ = 29.9866 MJ m^{-2} day^{-1} (S19.157)

$Q_{wb}^{*} = R_s(1-\alpha) + \left(R_{il} - R_{ol}^{wb}\right)$ (see Equation (S11.31)) (S19.160)

$Q_{wb}^{*} = 15.8184 + 25.2641 - 29.9866$ = 11.0959 MJ m^{-2} day^{-1} (S19.161)

We now need to calculate the time constant (τ) and the equilibrium temperature (T_e).

$\tau = \frac{\rho_w c_w h_w}{4\sigma(T_{wb}+273.15)^3 + f(u)(\Delta_{wb}+\gamma)}$ (see Equation (S11.29)) (S19.162)

$\tau = \frac{997.9 \times 0.00419 \times 10}{4{\times}4.903{\times}10^{-9}(6.6311+273.15)^3+4.8887(0.06727+0.0632)}$ = 39.1739 days (S19.163)

$T_e = T_{wb} + \frac{Q_{wb}^{*}}{4\sigma(T_{wb}+273.15)^3 + f(u)(\Delta_{wb}+\gamma)}$ (see Equation (S11.30)) (S19.164)

$T_e = 6.6311 + \frac{11.0959}{4{\times}4.903{\times}10^{-9}(6.6311+273.15)^3+4.8887(0.06727+0.0632)}$ = 17.0269 °C (S19.165)

The next step is to estimate today's water temperature given yesterday's water temperature (assume T_{w0} = 10.8734)

$T_w = T_e + (T_{w0} - T_e)\exp\left(-\frac{1}{\tau}\right)$ (see Equation (S11.28)) (S19.166)

$T_w = 17.0269 + (10.8734 - 17.0269)\exp\left(-\frac{1}{39.1739}\right)$ = 11.0285 °C (S19.167)

As we have an estimate of the water temperature, we can now estimate the change in heat storage (G_w), the slope of the saturation vapour pressure curve at water temperature (Δ_w), the saturation vapour pressure at water temperature (v_w^{*}), and the lake evaporation (E_{McJ}).

$G_w = \rho_w c_w h_w(T_w - T_{w0})$ (see Equation (S11.33)) (S19.168)

$G_w = 997.9 \times 0.00419 \times 10(11.0285 - 10.8734)$ = 6.4850 MJ m^{-2} day^{-1} (S19.169)

$\Delta_w = \frac{4098\left[0.6108 exp\left(\frac{17.27 T_w}{T_w+237.3}\right)\right]}{(T_w+237.3)^2}$ (see Equation (S2.4)) (S19.170)

$\Delta_w = \frac{4098\left[0.6108 exp\left(\frac{17.27\times 11.0285}{11.0285+237.3}\right)\right]}{(11.0285+237.3)^2}$ = 0.08740 kPa °C^{-1} (S19.171)

$v_w^{*} = 0.6108 exp\left[\frac{17.27 T_w}{T_w+237.3}\right]$ (see Equation (S2.5)) (S19.170)

$v_w^{*} = 0.6108 exp\left[\frac{17.27\times 11.0285}{11.0285+237.3}\right]$ = 1.3152 kPa (S19.173)

The penultimate step is to recompute the net radiation given the water temperature.

R_{ns} and R_{il} will not change as they are essentially unaffected by the surface temperature. However, the outgoing longwave radiation (R_{ol}) is a function of water temperature which is now known.

$R_{ol} = 0.97\,\sigma(T_w + 273.15)^4$ (see Equation (S11.27)) (S19.174)

$R_{ol} = 0.97 \times 4.903 \times 10^{-9} (11.0285 + 273.15)^4$ = 31.0169 MJ m^{-2} day^{-1} (S19.175)

Thus,

$Q^* = R_s(1-\alpha) + (R_{il} - R_{ol})$ (see Equation (S11.25)) (S19.176)

$Q^* = 15.8184 + (25.2641 - 31.0169)$ = 10.0656 MJ m^{-2} day^{-1}

$E_{McJ} = \frac{1}{\lambda}\left(\frac{\Delta_w(Q^* - G_w) + \frac{86400\rho_a c_a (v_w^* - v_a)}{r_a}}{\Delta_w + \gamma}\right)$ (see Equation (S11.22)) (S19.177)

$$E_{McJ} = \frac{1}{2.45}\left(\frac{0.087340(10.0656 - 6.4850) + \frac{86400 \times 1.2 \times 0.001013(1.3152 - 0.5614)}{339.9}}{0.08732 + 0.0632}\right) \quad \text{(S19.178)}$$

E_{McJ} = 1.4796 mm day^{-1} (S19.179)

Supplementary Material

Appendix S20 Listing of Fortran 90 version of Morton's WREVAP program

The following program listing called Program WREVAP, which is a slightly modified version of Morton's WREVAP model, is written in Fortran 90 and follows closely the steps set out in Appendix C of Morton (1983a). The deep lake sub-routine is based on Morton (1986, Section 3).

The program uses a monthly time-step and requires the following input data: for each month, average daily temperature (°C), average daily relative humidity (%), and average daily sunshine hours. Other data required as input are mean annual precipitation (mm), latitude (decimal degree and negative for the southern hemisphere), and elevation of the station (m). For deep lake evaporation, lake salinity (ppm) and average lake depth (m) are also required. The outputs from the CRAE sub-model are monthly net solar radiation (mm), monthly potential evapotranspiration (mm), monthly wet areal evapotranspiration (mm) and monthly actual areal evapotranspiration (mm); from the CRWE sub-model are net radiation at the water surface, potential evaporation and actual shallow lake evaporation; and from CWLE sub-model are net radiation at the water surface, potential evaporation and actual deep lake evaporation.

Structure of Program WREVAP

Program WREVAP calculates the actual evapotranspiration from a landscape (catchment) environment, evaporation from a shallow lake and evaporation from a deep lake based on Morton's (1983a,b; 1986) WREVAP program. The program WREVAP is a slightly modified version of Morton's WREVAP and consists of one module (WREVAP data) and five subroutines (crae, crwe, crle1, crle2 and sub1). crae, crwe and crle represent Morton's three program CRAE, CRWE and CRLE. Two versions of CRLE are include: crle1 calculates lake evaporation assuming the water depth in the lake is constant, and crle2 calculates lake evaporation assuming the water depth in the lake varies on a monthly basis.

The structure of Program WREVAP is shown in the figure below where:

WREVAP data	Variable declarations and constants
crae	Calculates the actual evapotranspiration from landscape
crwe	Calculates evaporation from shallow lake
crle1	Calculates evaporation from deep lake (constant depth)
crle2	Calculates evaporation from deep lake (variable depth)
sub1	Calculates the solar radiation

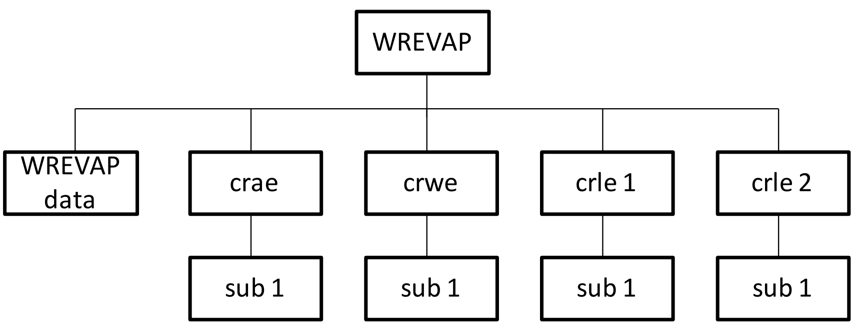

Input data: latitude (degrees), station height (m), mean annual precipitation (mm year^{-1}), number of months, monthly temperature (°C), relative humidity (%), sunshine hours (h), lake depth (m), salinity (ppm).

The input data is supplied to the program via two files: a parameter file and a data file.
Parameter file: WREVAP.par
*Example***:**

Melbourne.dat	File containing the climate and other data	
Melbourne.out	Output file	
1	Flag	1 – evapotranspiration from landscape
		2 – evaporation from shallow lake
		3 – evaporation from deep lake (constant depth)
		4 – evaporation from deep lake (variable depth)

Data file:
Record

1	Station header
2	Latitude, station height, mean annual rainfall and number of months
3	Data header
4	year, month, number of days, temperature, relative humidity and sunshine hours
.	" " "
.	" " "

Example: Melbourne.dat (for crae and crwe)

```
86282  86     MELBOURNE AIRPORT
-37.666  113.4  660 201
Year  Month Day   Temperature  RH     SH
1993  5     31      12.54      72.58  8.88
1993  6     30      10.12      76.73  7.08
1993  7     31       9.90      75.74  10.03
1993  8     31      11.62      69.44  -9999
1993  9     30      12.12      75.97  9.63
1993  10    31      13.16      70.58  11.20
1993  11    30      15.15      71.00  10.95
1993  12    31      16.80      68.94  9.53
  .
  .
```

Example: ThomsonReservoir.dat (for crle1)

```
Thomson Reservoir
-37.752  415.0  1090   36  22.95  23
Year  Month Day   Temperature  RH     SH
2007     3  31      16.59      69.96  8.02
2007     4  30      13.45      74.71  7.31
2007     5  31      12.56      73.88  5.20
2007     6  30       6.94      85.04  3.91
2007     7  31       6.98      79.93  4.45
2007     8  31       9.33      72.12  6.58
2007     9  30       9.77      69.64  7.03
```

2007	10	31	12.77	64.85	7.86
2007	11	30	15.43	75.45	8.42
2007	12	31	17.28	69.95	8.43

.
.

Example: ThomsonReservoirVD.dat (for crle2)

Thomson Reservoir

-37.752 415.0 1090 36 23

Year	Month	Day	Temperature	RH	SH	Depth
2007	3	31	16.59	69.96	8.02	22.52
2007	4	30	13.45	74.71	7.31	21.99
2007	5	31	12.56	73.88	5.20	21.69
2007	6	30	6.94	85.04	3.91	21.79
2007	7	31	6.98	79.93	4.45	23.39
2007	8	31	9.33	72.12	6.58	24.26
2007	9	30	9.77	69.64	7.03	24.86
2007	10	31	12.77	64.85	7.86	25.26
2007	11	30	15.43	75.45	8.42	25.52
2007	12	31	17.28	69.95	8.43	25.62

.
.

Program WREVAP (Fortran 90)

Lines designated as !C-1 to !C-39 identify the equivalent equations in Morton (1983a, Appendix C) and those designated as ! (3) to ! (8) are from Morton (1986). A list of variables is provided at the end of the program.

```
Module WREVAPdata
   implicit none
   save
   character(len=80) :: fn
   integer :: year, month, nd, ios, j, im, nm, nn(12)
   real :: phid, h, p, pa, pps, azd, td, t, s, v, vd, delta, &
           theta, tc, c0, c1, c2, w, phi, rh
   real :: alpha(2) = (/17.27, 21.88/), beta(2) = (/237.3, 265.5/),&
           pi = 3.14159254, gamma(2), ftz(2), fz(2), az, azz, cz, &
           cosz, comega, eta, ge, z, tmp, a0, g0, b, rt, rtc, &
           zeta, ft, lambda, et, etp, tau, rho, delp, delt, vp, &
           tp, es, d, salt, omega, taua, g, a, b0, rtp, etw, b1, &
           b2, ltheat, xm(4,12), gdew, rw, ep, ew
end Module WREVAPdata

program WREVAP
!  Calculates Morton's ET
!  05 April 2012
   use WREVAPdata
   implicit none
   integer :: flag
   open (10, file = 'WREVAP.par', status = 'old')
   read (10, 100) fn; 100 format(a)
   open (11, file = fn, status = 'old')

!  Input data file
   read (10, 100) fn
   open (21, file = fn)
!  Output file
   read (11, 100) fn
   write (21, 100) fn
   read (10, *) flag
   if (flag == 1) then
!     b0 = 1.; b1 = 14.; b2 = 1.20; fz(1) = 28.     !Morton's values
      b0 = 1.; b1 = 13.4; b2 = 1.13; fz(1) = 29.2     ! QJ's values
      es = 5.22e-8
      write (21, '("fz, b1, and b2", 3f8.2)'), fz(1), b1, b2
      read (11, *) phid, h, pa, nm
      write (21, 200) phid, h, pa, nm
      200 format('Latitude =', f7.2, '  Station height =', f8.2, &
      ' m  Mean annual precipitation =', f8.1, ' mm'/  &
      '#  of months =', i5 )
      write (21, 201)
      201 format(' Year Month  Temp     Rel Hum  Sunshine’  &
          ‘Net Rad     PET        WET        AET      ft'/ &
           '             (oC)       (%)     (Ratio)   (mm)’ &
          ’       (mm)       (mm)       (mm)')
   else
      b0 = 1.12
```

```
      b1 = 13.
      b2 = 1.12
      es = 5.5e-8
      fz(1) = 25.
      if (flag == 2) then
         read (11, *) phid, h, pa, nm
         write (21, 200) phid, h, pa, nm
      else if (flag == 3 ) then
         read (11, *) phid, h, pa, nm, d, salt
         write (21, 202) phid, h, pa, d, salt, nm
         202 format('Latitude =', f7.2, '  Station height =', &
             f8.2, ' m', '  Mean annual precipitation =', &
             f8.1, ' mm'/ ' Lake depth =', f7.2, ' m',    &
             '  Salt =', f8.1, ' ppm', ' #  of months =', i5 )
      else if (flag == 4 ) then
         read (11, *) phid, h, pa, nm, salt
         write (21, 203) phid, h, pa, salt, nm
         203 format('Latitude =', f7.2, '  Station height =', &
             f8.2, ' m', '  Mean annual precipitation =', &
             f8.1, ' mm'/ '  Salt =', f8.1, ' ppm',       &
             ' #  of months =', i5 )
      end if
   end if
   read (11, *)
!  Skip a line
   phi = phid*pi/180.
!  Compute the ratio of atmospheric pressure at the station to that
!  at sea level
   pps = ((288. - 0.0065*h)/288)**5.256                       !C-1
   p = pps*1013.
!  Estimate the zenith value of the dry season snow free clear sky
!  albedo
   azd = 0.26 - 0.00012*pa*(1 + abs(phid/42) +       &
           (phid/42)**2)*pps**0.5                             !C-2
   if (azd < 0.11) azd = 0.11
   if (azd > 0.17) azd = 0.17
   gamma(1) = 0.66*pps
   gamma(2) = gamma(1)/1.15
   fz(2) = fz(1)*1.15
   ftz(1) = fz(1)*sqrt(1./pps)
   ftz(2) = ftz(1)*1.15
   nn = 0 ; xm =0.
   if (flag == 1) then
      call crae(1)
   else if (flag == 2) then
      write (21, 204)
      204 format(' Year Month  Temp     Rel Hum  Sunshine  ‘,  &
          ‘Net Rad     PET        AET'/ &
          ‘             (oC)       (%)    (Ratio)   (mm)’,  &
          ’       (mm)       (mm)’)
      call crwe(2)
   else if (flag == 3) then
      write (21, 204)
      call crle1(3)
   else if (flag == 4) then
```

```
      write (21, 205)
      205 format(‘ Year Month  Temp     Rel Hum  Sunshine’,  &
                ’    Depth   Net Rad     PET        AET’/ &
                ‘              (oC)       (%)    (Ratio)’, &
                ‘      (m)     (mm)       (mm)       (mm)')
      call crle2(4)
   end if
end program WREVAP

subroutine crae(flag)
!    Calculates the actual evapotranspiration from landscape
     use WREVAPdata
     implicit none
     integer :: flag
     do im = 1, nm
        read (11, *, iostat = ios) year, month, nd, t, rh, s
        if (ios < 0) exit
        if (s < 0. .OR. rh < 0. .OR. t < -999.) cycle
        call sub1(flag)
!       Estimate the net radiation for soil-plant surfaces at air
!       temperature (rt), the stability factor (sf), the vapour
!       pressure coefficient (ft) and the heat transfer
!       coefficient (lambda)
        rt = (1. - a)*g - b                                   !C-27
        rtc = rt                                              !C-28
        if (rtc < 0.) rtc = 0.                                !C-28a
        zeta = 1./(0.28*(1. + vd/v) + delta*rtc*pps**0.5/ &
              (gamma(j)*b0*fz(j)*(v - vd)))                   !C-29
        if (zeta < 1.) zeta = 1.                              !C-29a
        ft = fz(j)/zeta/pps**0.5                              !C-30
        lambda = gamma(j) + 4.*es*(t + 273)**3/ft             !C-31
!       Estimate the final values from the following quickly
!       converging iterative solution of the vapour transfer
!       and energy balance equations
        tp = t
        vp = v
        delp = delta
        do
           delt = (rt/ft + vd - vp +lambda*(t - tp))/  &
              (delp + lambda)                                 !C-32
           tp = tp + delt                                     !C-33
           vp = 6.11*exp(alpha(j)*tp/(tp + beta(j)))          !C-34
           delp = alpha(j)*beta(j)*vp/(tp + beta(j))**2       !C-35
           if (abs(delt) < 0.01) exit
        end do

!       Estimate the potential evapotranspiration (etp), the net
!       radiation for soil-plant surfaces at equilibrium temperature
!       (rtp) and the wet-environment areal evapotranspiration (etw)
        etp = rt - lambda*ft*(tp - t)                         !C-36
        rtp = etp + gamma(j)*ft*(tp - t)                      !C-37
        etw = b1 + b2*rtp/(1. + gamma(j)/delp)                !C-38
        if (etw < etp/2.) etw = etp/2.                        !C-38a
        if (etw > etp) etw = etp                              !C-38a
!       Estimate the areal evapotranspiration (et) from the
```

```
!        complementary relationship
         et = 2.*etw - etp                                         !C-39
         ltheat = 28.5
         if (t < 0.) ltheat = 28.5*1.15
         et = nd*et/ltheat
         rt = nd*rt/ltheat
         etp = nd*etp/ltheat
         etw = nd*etw/ltheat
         write (21, 201) year, month, t, rh, s, rt, etp, etw, et, ft
         201 format(i5, i3, 8f10.2)
         xm(1,month) = xm(1,month) + rt
         xm(2,month) = xm(2,month) + etp
         xm(3,month) = xm(3,month) + etw
         xm(4,month) = xm(4,month) + et
         nn(month) = nn(month) + 1
      end do
      write (21, 202)
      202 format(/10x,'Mean Values'/'Month   Net Rad      PET'  &
                 '       WET       AET  # of months')
      do month = 1, 12
         xm(:,month) = xm(:,month)/nn(month)
         write (21, 203) month, (xm(j,month), j = 1, 4), nn(month)
         203 format(i5, 4f10.2, i5)
      end do
      write (21, 204) (sum(xm(j,:)), j = 1, 4)
      204 format('Annual', f9.1, 3f10.2)
end subroutine crae

subroutine sub1(flag)
   use WREVAPdata
   implicit none
   integer :: flag
   if (t < 0.) then
      j = 2
   else
      j = 1
   end if
!  Compute the saturation vapour pressure at td (vd), at t (v) and
!  the slope of the saturation vapour pressure at t (delta)
   v = 6.11*exp(alpha(j)*t/(t + beta(j)))                         !C-4
!  Calculate dew point temperature from relative humidity
!  (Lawrence 2005)
   gdew = 17.625*t/(243.04 + t) + log(rh/100.)
   td = 243.04*gdew/(17.625 - gdew)
   vd = 6.11*exp(17.27*td/(td + 237.3))
   delta = alpha(j)*beta(j)*v/(t + beta(j))**2                    !C-5
!  Compute various angles and functions leading up to an estimate
!  of the extra-atmospheric global radiation (ge)
   theta = 23.2*sin((29.5*month - 94.)*pi/180.)*pi/180.       !C-6
   z = phi - theta
   cosz = cos(z)                                                  !C-7
   if (cosz < 0.001) cosz = 0.001                                 !C-7a
   if (cosz > 1.) cosz = 1.
   z = acos(cosz)
   comega = 1. - cosz/cos(phi)/cos(theta)                         !C-8
```

```
   if (comega < -1.) comega = -1.                           !C-8a
   omega = acos(comega)
   cz = cosz + (sin(omega)/omega - 1.)*cos(phi)*cos(theta)    !C-9
   eta = 1. + sin((29.5*month - 106)*pi/180.)/60.            !C-10
   ge = 1354*omega*cz/pi/eta/eta                              !C-11
!  Estimate the zenith value of snow-free clear-sky albedo (azz),
!  zenith value of clear-sky albedo (az) and the clear sky
!  albedo (a0)
   if (flag > 1) then
      azz = 0.05
   else
      azz = azd                                               !C-12
      if (azz > 0.5*(0.91 - vd/v)) azz = 0.5*(0.91 - vd/v)   !C-12a
   end if
   c0 = v - vd                                                !C-13
   if (c0 < 0.) c0 = 0.                                      !C-13a
   if (c0 > 1.) c0 = 1.                                      !C-13a
   az = azz + (1. - c0*c0)*(0.34 - azz)                       !C-14
   a0 = az*(exp(1.08) - (2.16*cosz/pi +   &
   sin(z))*exp(0.012*z*180./pi))/1.473/(1. - sin(z))          !C-15
!  Estimate precipitable water (w) and a turbidity coefficient (tc)
   w = vd/(0.49 + t/129.)                                     !C-16
   c1 = 21 - t                                                !C-17
   if (c1 < 0.) c1 = 0.                                      !C-17a
   if (c1 > 5.) c1 = 5.                                      !C-17a
   tc  = (0.5 + 2.5*cz*cz)*exp(c1*(pps - 1.))                 !C-18
!  Compute the transmittancy of clear skies to direct beam
!  solar radiation (tau)
   tau = exp(-0.089*(pps/cz)**0.75 - 0.083*(tc/cz)**0.90 - &
          0.029*(w/cz)**0.60)                                 !C-19
!  Estimate the part of tau that is the result of absorption (taua)
   taua = exp(-0.0415*(tc/cz)**0.90 - (0.0029**0.5)*  &
             (w/cz)**0.3)                                     !C-20
   tmp = exp(-0.0415*(tc/cz)**0.90 - 0.029*(w/cz)**0.6)
   if (taua < tmp) taua = tmp                                !C-20a
!  Compute the clear-sky global radiation (g0) and the incident
!  global radiation (g)
   g0 = ge*tau*(1. + (1. - tau/taua)*(1. + a0*tau))           !C-21
   s = s*pi/24./omega
   if (s > 1.) s = 0.999
   g = s*g0 + (0.08 + 0.30*s)*(1. - s)*ge                     !C-22
!  Estimate the average albedo (a)
   a = a0*(s + (1. - s)*(1. - z*180/pi/330))                  !C-23
!  Estimate the proportional increase in atmospheric radiation
!  due to clouds (rho)
   c2 = 10.*(vd/v - s - 0.42)                                 !C-24
   if (c2 < 0.) c2 = 0.                                      !C-24a
   if (c2 > 1.) c2 = 1.                                      !C-24a
   rho = 0.18*((1. - c2)*(1. - s)**2 + c2*(1. - s)**0.5)/pps  !C-25
!  Calculate the net long-wave radiation loss for soil-plant
!  surface at air temperature (b)
   b = es*(t + 273)**4*(1. - (0.71 + 0.007*vd*pps)*(1. + rho))!C-26
   tmp = 0.05*es*(t + 273)**4
   if ( b < tmp) b = tmp                                     !C-26a
end subroutine sub1
```

```
subroutine crwe(flag)
!  Calculates Morton's ET - Shallow lake evaporation
!  05 April 2012
   use WREVAPdata
   implicit none
   integer :: flag
   do im = 1, nm
      read (11, *, iostat = ios) year, month, nd, t, rh, s
      if (ios < 0) exit
      if (s < 0. .OR. rh < 0. .OR. t < -999.) cycle
      call sub1(flag)
!     Estimate the net radiation for water surface at air
!     temperature (rw),
!     the stability factor (sf), the vapour pressure
!     coefficient (ft) and the heat transfer coefficient (lambda)
      rw = (1. - a)*g - b
      rtc = rw
      if (rtc < 0.) rtc = 0.
      zeta = 1./(0.28*(1. + vd/v) + delta*rtc*pps**0.5/  &
             (gamma(j)*b0*fz(j)*(v - vd)))
      if (zeta < 1.) zeta = 1.
      ft = fz(j)/zeta/pps**0.5
      lambda = gamma(j) + 4.*es*(t + 273)**3/ft
!     Estimate the final values from the following quickly
!     converging iterative solution of the vapour transfer
!     and energy balance equations
      tp = t
      vp = v
      delp = delta
      do
         delt = (rw/ft + vd - vp +lambda*(t - tp))/(delp + lambda)
         tp = tp + delt
         vp = 6.11*exp(alpha(j)*tp/(tp + beta(j)))
         delp = alpha(j)*beta(j)*vp/(tp + beta(j))**2
         if (abs(delt) < 0.01) exit
      end do

!     Estimate the potential evaporation (ep), the net radiation
!     for soil-plant surfaces at equilibrium temperature (rtp)
!     and the shallow lake evaporation (ew)
      ep = rw - lambda*ft*(tp - t)
      rtp = ep + gamma(j)*ft*(tp - t)
      ew = b1 + b2*rtp/(1. + gamma(j)/delp)
      if (ew < ep/2.) ew = ep/2.
      if (ew > ep) ew = ep
      ltheat = 28.5
      if (t < 0.) ltheat = 28.5*1.15
      ep = nd*ep/ltheat
      rw = nd*rw/ltheat
      ew = nd*ew/ltheat
      write (21, 201) year, month, t, rh, s, rw, ep, ew
      201 format(i5, i3, 6f10.2)
      xm(1,month) = xm(1,month) + rw
      xm(2,month) = xm(2,month) + ep
```

```
      xm(3,month) = xm(3,month) + ew
      nn(month) = nn(month) + 1
   end do
   write (21, *) ' Mean values'
   write (21, *) 'Month  Net Rad     PET        AET'
   do month = 1, 12
      xm(:,month) = xm(:,month)/nn(month)
      write (21, 203) month, (xm(j,month), j = 1, 3)
      203 format(i5, 4f10.2)
   end do
   write (21, 204) (sum(xm(j,:)), j = 1, 3)
   204 format('Annual', f9.1, 3f10.2)
end subroutine crwe

subroutine crle1(flag)
!  Calculates Morton's ET - Deep lake evaporation
!  05 April 2012
   use WREVAPdata
   implicit none
   integer, parameter :: nmx = 360
   integer :: ic, iy(nmx), mon(nmx), tnd(nmx), flag
   real ::  tgw(nmx), tv(nmx), tvd(nmx), ts(nmx), gl(nmx), &
              tt(nmx), trh(nmx), tdelta(nmx)
   do im = 1, nm
      read (11, *, iostat = ios) year, month, nd, t, rh, s
      if (ios < 0) exit
      if (s < 0. .OR. rh < 0. .OR. t < -999.) cycle
      call sub1(flag)
      tgw(im+12) = (1. - a)*g - b
      tt(im) = t
      trh(im) = rh
      ts(im) = s
      tv(im) = v
      tvd(im) = vd
      tdelta(im) = delta
      iy(im) = year
      tnd(im) = nd
      mon(im) = month
   end do
   call deepLake(nmx, nm, tgw, gl, d, salt)
   do im = 1, nm
      t = tt(im)
      rh = trh(im)
      s = ts(im)
      v = tv(im)
      vd = tvd(im)
      delta = tdelta(im)
!     Estimate the net radiation for water surface at air
!     temperature (rw),
!     the stability factor (sf), the vapour pressure coefficient
!     (ft) and the heat transfer coefficient (lambda)
      rw = gl(im)
      rtc = rw
      if (rtc < 0.) rtc = 0.
      zeta = 1./(0.28*(1. + vd/v) + delta*rtc*pps**0.5/   &
```

```
               (gamma(j)*b0*fz(j)*(v - vd)))                         !C-29
          if (zeta < 1.) zeta = 1.                                   !C-29a
          ft = fz(j)/zeta/pps**0.5                                   !C-30
          lambda = gamma(j) + 4.*es*(t + 273)**3/ft                  !C-31
!         Estimate the final values from the following quickly
!         converging iterative solution of the vapour transfer
!         and energy balance equations
          tp = t
          vp = v
          delp = delta
          ic = 0
          do
             delt = (rw/ft + vd - vp +lambda*(t - tp))/   &
                        (delp + lambda)                              !C-32
             tp = tp + delt                                          !C-33
             vp = 6.11*exp(alpha(j)*tp/(tp + beta(j)))               !C-34
             delp = alpha(j)*beta(j)*vp/(tp + beta(j))**2            !C-35
             if (abs(delt) < 0.01) exit
             ic = ic + 1
             if (ic > 100) then
                print *, 'Did not converge for month', im
                exit
             end if
          end do
!         Estimate the potential evaporation (ep), the net radiation
!         for soil-plant surfaces at equilibrium temperature (rtp) and
!         the deep lake evaporation (ew)
          ep = rw - lambda*ft*(tp - t)
          rtp = ep + gamma(j)*ft*(tp - t)
          ew = b1 + b2*rtp/(1. + gamma(j)/delp)
          if (ew < ep/2.) ew = ep/2.
          if (ew > ep) ew = ep
          ltheat = 28.5
          if (t < 0.) ltheat = 28.5*1.15
          nd = tnd(im)
          ep = nd*ep/ltheat
          rw = nd*rw/ltheat
          ew = nd*ew/ltheat
          write (21, 201) iy(im), mon(im), t, rh, s, rw, ep, ew
          201 format(i5, i3, 6f10.2)
          xm(1,mon(im)) = xm(1,mon(im)) + rw
          xm(2,mon(im)) = xm(2,mon(im)) + ep
          xm(3,mon(im)) = xm(3,mon(im)) + ew
          nn(mon(im)) = nn(mon(im)) + 1
       end do
       write (21, *) ' Mean values'
       write (21, *) 'Month  Net Rad     PET        AET'
       do month = 1, 12
          xm(:,month) = xm(:,month)/nn(month)
          write (21, 203) month, (xm(j,month), j = 1, 3)
          203 format(i5, 4f10.2)
       end do
       write (21, 204) (sum(xm(j,:)), j = 1, 3)
       204 format('Annual', f9.1, 3f10.2)
    end subroutine crle1
```

```
subroutine deepLake(nmx, nm, tgw, gl, d, salt)
!  Calculates the available solar and waterborne heat(gl) using
!  Morton 1986
   implicit none
   integer :: im, nmx, nm, ti, t1, i, i1, ii
   real :: gw(nmx), tgw(nmx), gl(nmx), t0, t, glb, gle, &
   salt, d, f, k
   t0 = 0.96 + 0.013*d                                           !(6)
   if (t0 < 0.039*d) t0 = 0.039*d
   if (t0 > 0.13*d) t0 = 0.13*d
   t = t0/(1. + salt/27000)**2                                   !(7)
   if (t > 6.) t = 6.
   k = t0/(1. + (d/93)**7)                                       !(8)
!  Calculates the delayed solar and waterborne energy (gw)
   ti = int(t)
   t1 = ti + 1
   f = t - ti
   i = 12
   tgw(1:12) = tgw(13:24)
   do im = 1, nm
      i = i + 1
      i1 = i - t1
      ii = i - ti
      gw(im) = tgw(ii) + f*(tgw(i1) - tgw(ii))                  !(3)
   end do
!  Calculates the available solar and waterborne heat(gl)
   glb = 50.
   do i = 1, 2
      do im = 1, 12
         gle = glb + (gw(im) - glb)/(k + 0.5)                   !(4)
         gl(im) = (glb + gle)/2.                                !(5)
         glb = gle
      end do
   end do
   do im = 1, nm
      gle = glb + (gw(im) - glb)/(k + 0.5)                      !(4)
      gl(im) = (glb + gle)/2.                                   !(5)
      glb = gle
   end do
end subroutine deepLake

subroutine crle2(flag)
!  Calculates Morton's ET - Deep lake evaporation
!  05 April 2012
   use WREVAPdata
   implicit none
   integer, parameter :: nmx = 360
   integer :: ic, iy(nmx), mon(nmx), tnd(nmx), flag
   real ::  tgw(nmx), tv(nmx), tvd(nmx), ts(nmx), gl(nmx), &
            tt(nmx), trh(nmx), tdelta(nmx), da(nmx)
   do im = 1, nm
      read (11, *, iostat = ios) year, month, nd, t, rh, s, da(im)
      if (ios < 0) exit
      if (s < 0. .OR. td < 0. .OR. t < -999.) cycle
```

```
      call sub1(flag)
      tgw(im+12) = (1. - a)*g - b
      tt(im) = t
      trh(im) = rh
      ts(im) = s
      tv(im) = v
      tvd(im) = vd
      tdelta(im) = delta
      iy(im) = year
      mon(im) = month
      tnd(im) = nd
   end do
   call deepLakeVD(nmx, nm, tgw, gl, da, salt)
   do im = 1, nm
      t = tt(im)
      rh = trh(im)
      s = ts(im)
      v = tv(im)
      vd = tvd(im)
      delta = tdelta(im)
!     Estimate the net radiation for water surface at air
!     temperature (rw),
!     the stability factor (sf), the vapour pressure coefficient
!     (ft) and the heat transfer coefficient (lambda)
      rw = gl(im)
      rtc = rw
      if (rtc < 0.) rtc = 0.
      zeta = 1./(0.28*(1. + vd/v) + delta*rtc*pps**0.5/  &
              (gamma(j)*b0*fz(j)*(v - vd)))              !C-29
      if (zeta < 1.) zeta = 1.                           !C-29a
      ft = fz(j)/zeta/pps**0.5                           !C-30
      lambda = gamma(j) + 4.*es*(t + 273)**3/ft          !C-31
!     Estimate the final values from the following quickly
!     converging iterative solution of the vapour transfer and
!     energy balance equations
      tp = t
      vp = v
      delp = delta
      ic = 0
      do
         delt = (rw/ft + vd - vp +lambda*(t - tp))/(delp + lambda)
                                                         !C-32
         tp = tp + delt                                  !C-33
         vp = 6.11*exp(alpha(j)*tp/(tp + beta(j)))       !C-34
         delp = alpha(j)*beta(j)*vp/(tp + beta(j))**2    !C-35
         if (abs(delt) < 0.01) exit
         ic = ic + 1
         if (ic > 100) then
            print *, 'Did not converge for month', im
            exit
         end if
      end do

!     Estimate the potential evaporation (ep), the net radiation
!     for soil-plant
```

```
!      surfaces at equilibrium temperature (rtp) and the deep lake
!      evaporation (ew)
!
       ep = rw - lambda*ft*(tp - t)
       rtp = ep + gamma(j)*ft*(tp - t)
       ew = b1 + b2*rtp/(1. + gamma(j)/delp)
       if (ew < ep/2.) ew = ep/2.
       if (ew > ep) ew = ep
       ltheat = 28.5
       if (t < 0.) ltheat = 28.5*1.15
       nd = tnd(im)
       ep = nd*ep/ltheat
       rw = nd*rw/ltheat
       ew = nd*ew/ltheat
       write (21, 201) iy(im), mon(im), t, rh, s, da(im), rw, ep, ew
       201 format(i5, i3, 7f10.2)
       xm(1,mon(im)) = xm(1,mon(im)) + rw
       xm(2,mon(im)) = xm(2,mon(im)) + ep
       xm(3,mon(im)) = xm(3,mon(im)) + ew
       nn(mon(im)) = nn(mon(im)) + 1
   end do
   write (21, *) ' Mean values'
   write (21, *) 'Month  Net Rad     PET        AET'
   do month = 1, 12
       xm(:,month) = xm(:,month)/nn(month)
       write (21, 203) month, (xm(j,month), j = 1, 3)
       203 format(i5, 4f10.2)
   end do
   write (21, 204) (sum(xm(j,:)), j = 1, 3)
   204 format('Annual', f9.1, 3f10.2)
end subroutine crle2

subroutine deepLakeVD(nmx, nm, tgw, gl, da, salt)
!  Calculates the available solar and waterborne heat(gl) using
!  Morton 1986
   implicit none
   integer :: im, nmx, nm, ti, t1, i, i1, ii
   real :: gw(nmx), tgw(nmx), gl(nmx), t0, t, glb, gle, salt, &
             d, f, da(nmx), k
   tgw(1:12) = tgw(13:24)
   i = 12
   do im = 1, nm
       d = da(im)
       t0 = 0.96 + 0.013*d                                    !(6)
       if (t0 < 0.039*d) t0 = 0.039*d
       if (t0 > 0.13*d) t0 = 0.13*d
       t = t0/(1. + salt/27000)**2                            !(7)
       if (t > 6.) t = 6.
       k = t0/(1. + (d/93)**7)                                !(8)
!  Calculates the delayed solar and waterborne energy (gw)
       ti = int(t)
       t1 = ti + 1
       f = t - ti
       i = i + 1
       i1 = i - t1
```

```
      ii = i - ti
      gw(im) = tgw(ii) + f*(tgw(i1) - tgw(ii))                   !(3)
   end do
!  Calculates the available solar and waterborne heat(gl)
   glb = 50.
   do i = 1, 2
      do im = 1, 12
         gle = glb + (gw(im) - glb)/(k + 0.5)                    !(4)
         gl(im) = (glb + gle)/2.                                 !(5)
         glb = gle
      end do
   end do
   do im = 1, nm
      gle = glb + (gw(im) - glb)/(k + 0.5)                       !(4)
      gl(im) = (glb + gle)/2.                                    !(5)
      glb = gle
   end do
end subroutine deepLakeVD
```

Key variables used in Program WREVAP

Variable	Description
a	average albedo
a0	clear-sky albedo
alpha	constant used in estimating vapour pressure - changes at 0^o C
az	zenith value of clear-sky albedo
azd	zenith value of the dry season snow free clear sky albedo
azz	zenith value of snow-free clear-sky albedo
b	net longwave radiation loss for soil-plant surface at air temperature
beta	constant used in estimating vapour pressure - changes at 0^o C
cosz	cosine of the noon angular zenith distance of the sun
cz	cosine of the average angular zenith distance of the sun
delt	correction to tp in iteration process
delta	slope of the saturation vapour pressure at t
es	surface emissivity times the Stefan-Boltzmann constant
et	areal evapotranspiration
eta	radius vector of the sun
etp	potential evapotranspiration
etw	wet-environment areal evapotranspiration
ft	vapour pressure coefficient
g	incident global radiation
g0	clear-sky global radiation
gamma	psychrometric constant - changes at 0^o C
ge	extra-atmospheric global radiation in Wm^{-2}
gl	available solar and waterborne heat
glb	value of gl at the beginning
gle	value of gl at the end
gw	delayed solar and waterborne heat
h	station height
iy	array to store year
k	storage constant
lambda	heat transfer coefficient
ltheat	latent heat of vaporisation water
mon	array to store month
nd	number of days in a month
nm	number of months
omega	angle in radians the earth rotates between sunrise and noon
p	atmospheric pressure
pa	mean annual rainfall
phi	latitude in radians
phid	latitude in degrees
pps	ratio of atmospheric pressure at the station to that at sea level
rho	proportional increase in atmospheric radiation due to clouds
rt	net radiation for soil-plant surfaces at air temperature
rtp	net radiation for soil-plant surfaces at equilibrium temperature
rw	net radiation for water surface at air temperature
s	ratio of observed to maximum possible sunshine duration
sf	the stability factor

t	average air temperature
t	lake delay time in months
tau	transmittancy of clear skies to direct beam soar radiation
taua	part of tau that is the result of absorption
tc	turbidity coefficient
td	average dew point temperature
tdelta	array to store delta
theta	declination of sun
tnd	array to store nd
to	soft water delay time in months
tp	potential evapotranspiration equilibrium temperature
trh	array to store rh
ts	array to store s
tt	array to store t
tv	array to store v
tvd	array to store vd
v	saturation vapour pressure at t
vd	saturation vapour pressure at td
vp	saturation vapour pressure at tp
w	precipitable water
xm	variable to calculate mean monthly values

Supplementary Material

Appendix S21 Worked example of Morton's CRAE, CRWE and CRLE models within the WREVAP framework

List of variables that are used in this appendix are taken from Morton (1983a, Appendix D) and from Morton (1986))

(Note these variables are different to those adopted in **Appendix S20** and in the main text and other appendices.)

Variable	Description	Units
a	Average albedo	dimensionless
a_0	Clear-sky albedo	dimensionless
a_z	Zenith value of clear-sky albedo	dimensionless
a_{zd}	Zenith value of the dry-season snow-free clear sky albedo	dimensionless
a_{zz}	Zenith value of clear-sky snow-free albedo	dimensionless
B	Net longwave radiation loss for soil-plant surface at air temperature	W m^{-2}
b_0	Constant	undefined
b_1	Constant	W m^{-2}
b_2	Constant	undefined
c_0	$v - v_D$	mbar
c_1	Working variable	°C
c_2	Working variable	dimensionless
E_P	Potential evaporation	W m^{-2}, mm $month^{-1}$
E_T	Actual areal evapotranspiration	W m^{-2}, mm $month^{-1}$
E_{TP}	Potential evapotranspiration	W m^{-2}, mm $month^{-1}$
E_{TW}	Wet-environment areal evapotranspiration	W m^{-2}, mm $month^{-1}$
E_W	Shallow lake evaporation	W m^{-2}, mm $month^{-1}$
f_T	Vapour transfer coefficient	W m^{-2} $mbar^{-1}$
f_z	Constant used in estimating f_T	W m^{-2} $mbar^{-1}$
G	Incident global radiation	W m^{-2}
G_E	Extra-atmospheric global radiation	W m^{-2}
G_L	Available (routed) solar and waterborne energy	W m^{-2}
G_{LB}	Available solar and waterborne heat energy at the beginning	W m^{-2}

	of the month	
G_{LE}	Available solar and waterborne heat energy at the end of the month	W m^{-2}
G_o	Clear-sky global radiation	W m^{-2}
G_W^0	Solar plus waterborne heat input	W m^{-2}
G_W^t	Delayed solar and waterborne energy inputs	W m^{-2}
$G_W^{[t]}$, $G_W^{[t+1]}$	Value of G_W^0 computed $[t_L]$ and $[t_L + 1]$ months	W m^{-2}
$\bar{h}$	Average depth of lake	m
H	Site elevation	m
i	Month number	dimensionless
j	Turbidity coefficient	undefined
P_A	Mean annual rainfall	mm year^{-1}
p	Atmospheric pressure at station	mbar
p_s	Atmospheric pressure at mean sea level	mbar
$\frac{p}{p_s}$	Ratio of atmospheric pressure at station to atmospheric pressure at mean sea level	dimensionless
RH	Mean daily relative humidity	%
R_{nl}	Net longwave radiation	W m^{-2}
R_s	Measured incoming solar radiation	W m^{-2}
R_T	Net radiation at soil-plant surface at air temperature	W m^{-2}
R_{TC}	R_T with $R_{TC} \geq 0$	W m^{-2}
R_{TP}	Net radiation at the soil-plant surface for equilibrium temperature	W m^{-2}
R_W	Net radiation for water surface at air temperature	W m^{-2}
s	Average lake salinity	ppm
S	Ratio of observed to maximum possible sunshine duration	dimensionless
S_c	Storage coefficient	months
t_0	Soft water delay time	months
t_L	Lake lag or delay time	months
$[t_L]$	Integral component of the lake lag	months
T	Mean daily air temperature for month	°C
T_D	Mean daily dew point temperature for month	°C
T_P	Equilibrium temperature	°C
T_P'	Trial value of T_P in iteration process	°C

W	Precipitable water vapour	mm
Z	Noon angular zenith distance of sun	radian
z	Average angular zenith distance of the Sun	radian
α	Constant Equations (S21.12 and S21.78); albedo Equation (S21.97)	°C; dimensionless
β	Constant Equations (S21.12 and S21.78)	°C
γ	Psychrometric constant	mbar $°C^{-1}$
δh	Water borne heat input	W m^{-2}
Δ	Saturation vapour pressure curve at T	mbar $°C^{-1}$
Δ_P	Slope of saturation vapour pressure curve at T_P	mbar $°C^{-1}$
Δ'_T	Slope of saturation vapour pressure curve at T'_P	mbar $°C^{-1}$
$[\delta T_P]$	Adjustment to T_P in iteration process	°C
ε	Surface emissivity	dimensionless
ξ	Stability factor	undefined
η	Radius vector of sun	undefined
θ	Declination of sun	radians
λ	Heat transfer coefficient	mbar $°C^{-1}$
ρ	Proportional increase in atmospheric radiation due to clouds	dimensionless
σ	Stefan-Boltzmann constant	W m^{-2} K^{-4}
τ	Transmittancy of clear sky to direct beam radiation	undefined
τ_a	Proportion of τ that is the result of absorption	undefined
υ	Mean daily saturation vapour pressure at air temperature for month	mbar
υ_D	Mean daily saturation vapour pressure at dew point temperature for month	mbar
υ_P	Mean daily saturation vapour pressure at equilibrium temperature for month	mbar
υ'_P	Trial value of υ_P in iteration process	mbar
Ø	Latitude	degree, radians
ω	Angle the earth rotates between sunrise and noon	radian

CRAE: Estimate actual evaporation

Use Morton's CRAE model to estimate the potential and actual evaporation for July 1980 at Alice Springs (Bureau of Meteorology, Australia station number 15590). Although the general methodology is presented in **Appendix S7**, the following procedure follows the detailed steps in Morton (1983a, Appendix C) and the Fortran program in **Appendix S20**. The symbols adopted here are those used by Morton and are different to those used in the Morton Fortran program (**Appendix S20**) and in the other appendices.

The site conditions at Alice Spring automatic weather station are as follows:

Latitude (Ø)	-23.7951 °S (negative for southern hemisphere)
	-0.4153 radian
Site elevation (H)	546 m
Mean annual rainfall (P_A)	285.8 mm year^{-1}

The meteorological data for July 1980 is:

Mean daily air temperature (T)	11.8 °C day^{-1}
Mean daily relative humidity (RH)	55.5 % day^{-1}
Mean daily sunshine hours	8.35 hour day^{-1}

Because Morton assumes dew point temperature is available to estimate saturation vapour pressure rather than relative humidity, we carry out the following preliminary calculations to estimate dew point temperature (T_D) as follows (Lawrence, 2005, Equation 8):

$$T_D = \frac{243.04\left[ln\left(\frac{RH}{100}\right)+\frac{17.625\,T}{243.04+T}\right]}{17.625-ln\left(\frac{RH}{100}\right)-\frac{17.625\,T}{243.04+T}} \qquad \text{(S21.1)}$$

where T is air temperature (°C), RH is the relative humidity (%).

For July 1980, Alice Springs

$$T_D = \frac{243.04\left[ln\left(\frac{55.5}{100}\right)+\frac{17.625\times11.8}{243.04+11.8}\right]}{17.625-ln\left(\frac{55.5}{100}\right)-\frac{17.625\times11.8}{243.04+11.8}} = 3.1755\ °C \qquad \text{(S21.2)}$$

To maintain consistency with Morton's (1983a) procedure, we adopt the units he used in his Appendix C namely W m^{-2} for radiation, mbar for vapour pressure and °C for temperature. We also adopt Morton's nomenclature and record below Morton's equation numbers in italics.

The following two equations refer to the site conditions.

Equation C-1: Compute the ratio ($\frac{p}{p_s}$) of atmospheric pressure at Alice Springs station (p) to that at sea level (p_s):

$$\frac{p}{p_s} = [(288 - 0.0065H)/288)]^{5.256} \qquad \text{(S21.3)}$$

$$\frac{p}{p_s} = [(288 - 0.0065 \times 546)/288)]^{5.256} = 0.9369 \qquad \text{(S21.4)}$$

Equation C-2: Estimate the zenith value of the dry-season snow-free clear sky albedo (a_{zd}):

$$a_{zd} = 0.26 - 0.00012P_A\left(\frac{p}{p_s}\right)^{0.5}\left[1 + \left|\frac{Ø}{42}\right| + \left(\frac{Ø}{42}\right)^2\right] \qquad \text{(S21.5)}$$

where Ø is the latitude in decimal degree (negative for the southern hemisphere).

$$a_{zd} = 0.26 - 0.00012 \times 285.8(0.9369)^{0.5}\left[1 + \left|\frac{-23.7951}{42}\right| + \left(\frac{-23.7951}{42}\right)^2\right] \qquad \text{(S21.6)}$$

$$= 0.1973$$

Equation C-2a: $0.11 \le a_{zd} \le 0.17$ (S21.7)

Hence, given Equation C-2a, adopt a_{zd} = 0.17.

The following sequential operations are carried out for each month.

Initially, we need to compute the mean maximum daylight hours for July at Alice Springs. The procedure is described earlier in **Appendix S19** – see Equation (S3.11). The value is 10.68 hours. The mean daily sunshine for July 1980 was recorded as 8.34 hour day^{-1} giving a ratio of observed to maximum possible sunshine duration (S) of 0.7818.

Equation C-3: Compute the saturation vapour pressure (υ_D) at dew point temperature (°C)

$$\upsilon_D = 6.11 exp\left[\frac{17.27T_D}{T_D+237.3}\right] \quad \text{(S21.8)}$$

$$\upsilon_D = 6.11 exp\left[\frac{17.27\times 3.1755}{3.1755+237.3}\right] = 7.6751 \text{ mbar} \quad \text{(S21.9)}$$

Equation C-4: Compute the saturation vapour pressure (υ) at air temperature (°C)

$$\upsilon = 6.11 exp\left[\frac{17.27T}{T+237.3}\right] \quad \text{(S21.10)}$$

$$\upsilon = 6.11 exp\left[\frac{17.27\times 11.8}{11.8+237.3}\right] = 13.8463 \text{ mbar} \quad \text{(S21.11)}$$

Equation C-5: Compute the slope of the saturation vapour pressure (Δ) curve at T °C.

$$\Delta = \frac{\alpha\beta\upsilon}{(T+\beta)^2} \quad \text{(S21.12)}$$

α = 17.27 °C when T ≥ 0 °C, otherwise α = 21.88 °C (Morton, 1983a, page 60)

β = 237.3 °C when T ≥ 0 °C, otherwise β = 265.5 °C (Morton, 1983a, page 60)

$$\Delta = \frac{17.27\times 237.3\times 13.8463}{(11.8+237.3)^2} = 0.9145 \text{ mbar} \quad \text{(S21.13)}$$

Equation C-6: Compute angles and functions for estimating extra-terrestrial global radiation.

$$\theta = 23.2 sin(29.5i - 94) \quad \text{(S21.14)}$$

where i is month of year, for July i = 7, and θ is in degrees (Morton, 1983a, Item (1)).

$$\theta = \left(23.2\sin\left((29.5\times 7 - 94)\frac{\pi}{180}\right)\right)\frac{\pi}{180} = 0.3741 \text{ radian} \quad \text{(S21.15)}$$

As Morton's equations are based on degrees, the inner $\frac{\pi}{180}$ converts degrees to radians and the outer converts the resulting angle in degrees to radians.

Equation C-7:

$$cos\ Z = \cos(\emptyset - \theta) \quad \text{(S21.16)}$$

$$cos\ Z = \cos(-0.4153 - 0.3741) = 0.7043 \quad \text{(S21.17)}$$

$$Z = arcos(0.7043) = 0.7894 \text{ radian} \quad \text{(S21.18)}$$

Equation C-7a: $cos\ Z \geq 0.001$ (S21.19)

Hence Equation C-7a is satisfied

Equation C-8:

$$cos\ \omega = 1 - \frac{cos\ Z}{cos\ \emptyset\ \cos\theta} \quad \text{(S21.20)}$$

$$cos\ \omega = 1 - \frac{0.7043}{cos\ (0.3741)\ \cos(-0.4153)} = 0.1731 \quad \text{(S21.21)}$$

$$\omega = arcos\ (0.1731) = 1.3968 \text{ radian} \quad \text{(S21.22)}$$

Equation C-8a: $cos\ \omega \geq -1$

Hence Equation C-8a is satisfied

Equation C-9:

$$cos\ z = cos\ Z + \left[\frac{180}{\pi}\frac{sin\ \omega}{\omega} - 1\right] cos\ \emptyset \cos\theta \tag{S21.23}$$

$$cos\ z = 0.7043 + \left[\frac{sin\ (1.3968)}{1.3968} - 1\right] cos\ (-0.4153\ )\cos{(0.3741)} = 0.4531 \tag{S21.24}$$

Note: $\frac{180}{\pi}$ in Equation (S21.23) (from Morton, 1983a, Equation C-9) is deleted as ω is in radian.

Equation C-10: Compute the radius vector of the sun (η)

$$\eta = 1 + \frac{1}{60}\sin{(29.5\ i - 106)} \tag{S21.25}$$

$$\eta = 1 + \frac{1}{60}\sin{\left((29.5 \times 7 - 106)\frac{\pi}{180}\right)} = 1.0164 \tag{S21.26}$$

Equation C-11: Compute of extra-terrestrial global radiation (G_E)

$$G_E = \frac{1354}{\eta^2}\frac{\omega}{180} cos\ z \tag{S21.27}$$

$$G_E = \frac{1354}{(1.0164)^2}\frac{1.3968}{\pi} 0.4531 = 264.0388 \text{ W m}^{-2} \tag{S21.28}$$

Note: The division by π rather than 180 in Equation S21.28 is because ω is in radian.

Equation C-12: Estimate the zenith value of snow-free clear sky albedo (a_{zz})

$$a_{zz} = a_{zd} = 0.17 \tag{S21.29}$$

Equation C-12a: $0.11 \leq a_{zz} \leq 0.5\left(0.91 - \frac{v_D}{v}\right)$ (S21.30)

$$0.11 \leq a_{zz} \leq 0.5\left(0.91 - \frac{7.6751}{13.8463}\right),\ 0.11 \leq a_{zz} \leq 0.1778 \tag{S21.31}$$

Hence Equation C-12a is satisfied.

Equation C-13:

$$c_0 = v - v_D \tag{S21.32}$$

$$c_0 = 13.8463 - 7.6751 = 6.1712 \text{ mbar} \tag{S21.33}$$

Equation C-13a: $0 \leq c_0 \leq 1$ (S21.34)

Equation C-13a not satisfied, adopt $c_0 = 1$. This constraint will be effective during snow cover when the vapour pressure deficit is less than one mbar.

Equation C-14: Estimate the zenith value of the clear-sky albedo (a_z)

$$a_z = a_{zz} + (1 - c_0^2)(0.34 - a_{zz}) \tag{S21.35}$$

$$a_z = 0.17 + (1 - 1)(0.34 - 0.17) = 0.17 \tag{S21.36}$$

Equation C-15: Estimate the clear-sky albedo (a_0)

$$a_0 = \frac{a_z\left[exp(1.08) - \left(\frac{2.16 cos\ Z}{\pi} + sin\ Z\right) exp(0.021\ Z)\right]}{1.473(1 - sin\ Z)} \tag{S21.37}$$

$$a_0 = \frac{0.17\left[exp(1.08) - \left(\frac{2.16 \times 0.7043}{\pi} + sin\ 0.7894\right) exp\left(0.021 \times 0.7894 \frac{180}{\pi}\right)\right]}{1.473(1 - sin\ 0.7894)} = 0.3540 \quad \text{(S21.38)}$$

Note: $\frac{180}{\pi}$ in Equation (S21.38) is to adjust Z from radian to degree.

Equation C-16: Estimate the precipitable water (W) in mm.

$$W = \frac{v_D}{0.49 + \frac{T}{129}} \quad \text{(S21.39)}$$

$$W = \frac{7.6751}{0.49 + \frac{11.8}{129}} = 13.1994 \text{ mm} \quad \text{(S21.40)}$$

Equation C-17:

$$c_1 = 21 - T \quad \text{(S21.41)}$$

$$c_1 = 21 - 11.8 = 9.2 \quad \text{(S21.42)}$$

Equation C-17a: $0 \le c_1 \le 5$ (S21.43)

Equation C-17a is not satisfied, adopt $c_1 = 5$.

Equation C-18: Compute the turbidity coefficient (j)

$$j = (0.5 + 2.5\ cos^2 z) exp\left[c_1 \left(\frac{p}{p_s} - 1\right)\right] \quad \text{(S21.44)}$$

$$j = (0.5 + 2.5\ (0.4531)^2) exp[5(0.9369 - 1)] = 0.7391 \quad \text{(S21.45)}$$

Equation C-19: Compute the transmittancy of clear sky to direct beam radiation (τ)

$$\tau = exp\left[-0.089 \left(\frac{p}{p_s} \frac{1}{\cos z}\right)^{0.75} - 0.083 \left(\frac{j}{cos\ z}\right)^{0.90} - 0.029 \left(\frac{W}{cos\ z}\right)^{0.60}\right] \quad \text{(S21.46)}$$

$$\tau = exp\left[-0.089 \left(0.9369 \frac{1}{0.4531}\right)^{0.75} - 0.083 \left(\frac{0.7391}{0.4531}\right)^{0.90} - 0.029 \left(\frac{13.1994}{0.4531}\right)^{0.60}\right] \quad \text{(S21.47)}$$

$\tau = 0.6055$

Equation C-20: Estimate the proportion of τ that is the result of absorption (τ_a)

$$\tau_a = exp\left[-0.0415 \left(\frac{j}{\cos z}\right)^{0.90} - (0.0029)^{0.5} \left(\frac{W}{cos\ z}\right)^{0.3}\right] \quad \text{(S21.48)}$$

$$\tau_a = exp\left[-0.0415 \left(\frac{0.7391}{0.4531}\right)^{0.90} - (0.0029)^{0.5} \left(\frac{13.1994}{0.4531}\right)^{0.3}\right] = 0.8085 \quad \text{(S21.49)}$$

Equation C-20a: $\tau_a \ge exp\left[-0.0415 \left(\frac{j}{\cos z}\right)^{0.90} - 0.029 \left(\frac{W}{cos\ z}\right)^{0.6}\right]$ (S21.50)

Checking Equation C-20a constraint

$$\tau_a \ge exp\left[-0.0415 \left(\frac{0.7391}{0.4531}\right)^{0.90} - 0.029 \left(\frac{13.1994}{0.4531}\right)^{0.6}\right] \ge 0.7530 \quad \text{(S21.51)}$$

Equation C-20a constraint is satisfied.

Equation C-21: Compute clear-sky global radiation (G_o)

$$G_o = G_E \tau \left[1 + \left(1 - \frac{\tau}{\tau_a}\right)(1 + a_0 \tau)\right] \quad \text{(S21.52)}$$

$$G_o = 264.0388 \times 0.6055 \left[1 + \left(1 - \frac{0.6055}{0.8085}\right)(1 + 0.3540 \times 0.6055)\right] \quad \text{(S21.53)}$$

G_o = 208.6217 W m^{-2}

Equation C-22: Compute the incident global radiation (G)

$$G = SG_o + (0.08 + 0.30S)(1 - S)G_E \quad \text{(S21.54)}$$

$$G = 0.7818 \times 208.6217 + (0.08 + 0.30 \times 0.7818)(1 - 0.7818)264.0388 \quad \text{(S21.55)}$$

G = 181.2221 W m^{-2}

Equation C-23: Estimate the average albedo (a)

$$a = a_0\left[S + (1 - S)\left(1 - \frac{Z}{330}\right)\right] \quad \text{(S21.56)}$$

$$a = 0.3540\left[0.7818 + (1 - 0.7818)\left(1 - \frac{0.7894}{330}\frac{180}{\pi}\right)\right] = 0.3434 \quad \text{(S21.57)}$$

Equation C-24:

$$c_2 = 10\left(\frac{v_D}{v} - S - 0.42\right) \quad \text{(S21.58)}$$

$$c_2 = 10\left(\frac{7.6751}{13.8463} - 0.7818 - 0.42\right) = -6.4749 \quad \text{(S21.59)}$$

Equation C-24a: $0 \leq c_2 \leq 1$

Constraint Equation C-24a is not satisfied, hence set c_2 = 0

Equation C-25: Estimate the proportional increase in atmospheric radiation due to clouds (ρ)

$$\rho = 0.18[(1 - c_2)(1 - S)^2 + c_2(1 - S)^{0.5}]\frac{p_S}{p} \quad \text{(S21.60)}$$

$$\rho = 0.18[(1 - 0)(1 - 0.7818)^2 + 0(1 - 0.7818)^{0.5}]\frac{1}{0.9369} = 0.009147 \quad \text{(S21.61)}$$

Equation C-26: Compute net longwave radiation loss for soil-plant surface at air temperature (B)

$$B = \varepsilon\sigma(T + 273)^4\left[1 - \left(0.71 + 0.007v_D\frac{p}{p_S}\right)(1 + \rho)\right] \quad \text{(S21.62)}$$

From Morton (1983a, page 64), ε (emissivity) = 0.92, σ (Stefan-Boltzmann constant) = 5.67×10^{-8} W m^{-2} K^{-4}. Thus,

$$B = 0.92 \times 5.67 \times 10^{-8}(11.8 + 273)^4\left[\begin{matrix}1 - (0.71 + 0.007 \times 7.6751 \times 0.9369) \\ (1 + 0.009147)\end{matrix}\right] \quad \text{(S21.63)}$$

B = 79.8629 W m^{-2}

Equation C-26a: $B \geq 0.05\varepsilon\sigma(T + 273)^4$ (S21.64)

Constraint = $0.05 \times 0.92 \times 5.67 \times 10^{-8}(11.8 + 273)^4$ = 17.1594 (S21.65)

and thus Equation C-26a constraint is satisfied.

Equation C-27: Estimate net radiation at soil-plant surface at air temperature

$$R_T = (1 - a)G - B \quad \text{(S21.66)}$$

$R_T = (1 - 0.3434)181.2221 - 79.8629$= 39.1275 W m^{-2} (S21.67)

Equation C-28: $R_{TC} = R_T$ = 39.1275 W m^{-2} (S21.68)

Equation C-28a: $R_{TC} \geq 0$, and constraint is satisfied.

Equation C-29: Compute stability factor (ξ)

$$\frac{1}{\xi} = 0.28\left(1+\frac{\upsilon_D}{\upsilon}\right) + \frac{\Delta R_{TC}}{\gamma p\left(\frac{p_s}{p}\right)^{0.5} b_0 f_z(\upsilon-\upsilon_D)} \tag{S21.69}$$

From Morton (1983a, page 64), b_0 = 1 for the CRAE model, and noting that γp = $\gamma p_s\left(\frac{p}{p_s}\right)$, f_z and γp_s are respectively 28.0 W m^{-2} mbar^{-1} and 0.66 mbar °C^{-1} for T ≥ 0 °C. For T < 0, f_z = 28.0×1.15 W m^{-2} mbar^{-1} and γp_s = 0.66/1.15 mbar °C^{-1}.

$$\frac{1}{\xi} = 0.28\left(1+\frac{7.6751}{13.8463}\right) + \frac{0.9145\times 39.1275}{0.66*0.9369(1/0.9369)^{0.5}1\times 28.0(13.8463-7.6751\,)} = 0.7594 \tag{S21.70}$$

Equation C-29a: $\frac{1}{\xi} \leq 1$. Constraint is satisfied.

Equation C-30: Estimate the vapour transfer coefficient (f_T)

$$f_T = \frac{1}{\xi}\left(\frac{p_s}{p}\right)^{0.5} f_z \tag{S21.71}$$

$$f_T = 0.7594\left(\frac{1}{0.9369}\right)^{0.5} 28.0 = 21.9676 \tag{S21.72}$$

Equation C-31: Estimate the heat transfer coefficient (λ)

$$\lambda = \gamma p + \frac{4\varepsilon\sigma(T+273)^3}{f_T} \tag{S21.73}$$

$$\lambda = 0.66\times 0.9369 + \frac{4\times 0.92\times 5.67\times 10^{-8}(11.8+273)^3}{21.9676} = 0.8378 \tag{S21.74}$$

The penultimate step in estimating Morton CRAE evaporations is to estimate the potential evapotranspiration equilibrium temperature. This can be found by using Morton's (1983a, Equations C-32 to C-35) converging iterative process. The four equations are as follows:

Equation C-32: $$[\delta T_P] = \frac{\left[\frac{R_T}{f_T}+\upsilon_D-\upsilon_P'+\lambda(T-T_P')\right]}{(\Delta_P'+\lambda)} \tag{S21.75}$$

Equation C-33: $$T_P = T_P' + [\delta T_P] \tag{S21.76}$$

Equation C-34: $$\upsilon_P = 6.11\, exp\left[\frac{\alpha T_P}{(T_P+\beta)}\right] \tag{S21.77}$$

Equation C-35: $$\Delta_P = \frac{\alpha\beta\upsilon_P}{(T_P+\beta)^2} \tag{S21.78}$$

Initial values of T_P', υ_P' and Δ_P' are chosen equal to T, υ and Δ and intermediate values of T_P, υ_P and Δ_P are calculated from Equations C-33, C-34 and C-35 and $[\delta T_P]$ from Equation C-32. The intermediate values then replace the initial values in Equations C-33, C-34 and C-35, again calculating $[\delta T_P]$. This process is repeated until $[\delta T_P]$ ≤ 0.01 °C. As the table below shows, only two iterations were required to solve for T_P for our example.

Initial values	Initial pass	2nd pass
T_P' = 11.8	T_P = 9.2947	T_P = 9.1963
υ_P' = 13.8463	υ_P =11.7150	υ_P =11.6376
Δ_P' = 0.9145	Δ_P = 0.7895	Δ_P = 0.7849
$[\delta T_P]$ = -2.5053	$[\delta T_P]$ = -0.0982	$[\delta T_P]$ = -0.0001

Equation C-36: Estimate potential evapotranspiration (E_{TP})

$$E_{TP} = R_T - \lambda f_T(T_P - T) \tag{S21.79}$$

$$E_{TP} = 39.1275 - 0.8378 \times 21.9676(9.1963 - 11.8) \tag{S21.80}$$

E_{TP} = 87.0472 W m^{-2}

Equation C-37: Estimate net radiation (R_{TP}) at the soil-plant surface for equilibrium temperature.

$$R_{TP} = E_{TP} + \gamma p f_T(T_P - T) \tag{S21.81}$$

$$R_{TP} = 87.0472 + 0.66 \times 0.9369 \times 21.9676(9.1963 - 11.8) \tag{S21.82}$$

R_{TP} = 51.6792 W m^{-2} (S21.83)

Equation C-38: Estimate wet-environment areal evapotranspiration (E_{TW})

$$E_{TW} = b_1 + \frac{b_2}{\left(1+\frac{\gamma p}{\Delta_P}\right)} R_{TP} \tag{S21.84}$$

Morton (1983a, page 65) recommended values for b_1 and b_2 as 14 W m^{-2} and 1.20 respectively.

$$E_{TW} = 14 + \frac{1.20}{\left(1+\frac{0.66\times0.9369}{0.7849}\right)} 51.6792 = 48.6877 \text{ W m}^{-2} \tag{S21.85}$$

Equation C-38a: Constraint is $\frac{1}{2}E_{TP} \leq E_{TW} \leq E_{TP}$. The constraint is satisfied.

Equation C-39: Estimate actual areal evapotranspiration (E_T)

$$E_T = 2E_{TW} - E_{TP} \tag{S21.86}$$

$$E_T = 2 \times 48.6877 - 87.0472 = 10.3282 \text{ W m}^{-2} \tag{S21.87}$$

The final step is to convert evaporation in power unit of W m^{-2} to evaporation units of mm day^{-1} by dividing by the latent heat of vaporization which for $T \geq 0$°C is 28.5 W day kg^{-1} and for T < 0°C, it is 28.5×1.15 W day kg^{-1}. Hence,

$$E_{TP} = 87.0472 \text{ W m}^{-2} = \frac{87.0472}{28.5} = 3.0543 \text{ mm day}^{-1} \tag{S21.88}$$

$$E_{TW} = 48.6877 \text{ W m}^{-2} = \frac{48.6877}{28.5} = 1.7083 \text{ mm day}^{-1} \tag{S21.89}$$

$$E_T = 10.3282 \text{W m}^{-2} = \frac{10.3282}{28.5} = 0.3624 \text{ mm day}^{-1} \tag{S21.90}$$

In conclusion, the July 1980 evaporation rates at Alice Springs are as follows:

E_{TP} (potential evapotranspiration) = 3.0543×31 = 94.7 mm month^{-1}

E_{TW} (wet-environment areal evapotranspiration) = 1.7083×31 = 53.0 mm month^{-1}

E_T (actual areal evapotranspiration) = 0.3624×31 = 11.2 mm month^{-1}

CRWE: Estimate shallow lake evaporation

To estimate shallow lake evaporation, the CRWE model, which is a slightly modified version of CRAE, may be used. The modifications are listed in Morton (1983a, Section 2.6) as follows:

1. The snow-free clear-sky albedo (a_{zz}) is set to a constant value of 0.05. This allows Equations C-2, C-12 and their constraints to be deleted.
2. The emissivity (ε) in Equations C-26, C26a and C31 is set to 0.97. Hence, $\varepsilon\sigma$ becomes 5.5×10^{-8} W m^{-2} K^{-4}.
3. In Equations C-29 and C-30, f_z is 25.0 W m^{-2} mbar^{-1} for $T \geq 0$, and 28.75 W m^{-2} mbar^{-1} for $T < 0$.
4. In Equation C-29, $b_0 = 1.12$.
5. Values for b_1 and b_2 are 13 W m^{-2} and 1.12 respectively.
6. To reflect the change in the type of evaporation that is taking place in Equations C-27, C-36 and C-38, R_T becomes R_W, E_{TP} becomes E_P and E_{TW} becomes E_W (shallow lake evaporation).

Applying these modifications to the CRAE model for July 1980 at Alice Springs yields the following results:

Morton equation number	Variable	Result	Morton equation number	Variable	Result	Morton equation number	Variable	Result
C-1	$\frac{p}{p_s}$	0.9369	C16	W	13.199	C-29	$\frac{1}{\xi}$	1.0935
C-3	v_D	7.6751	C-17	c_1	9.2	C-30	f_T	28.243
C-4	v	13.8463	C-18	j	0.7391	C-31	λ	0.7983
C-5	Δ	0.9145	C-19	τ	0.6055	C-32	$[\delta T_P]$	0.0000
C-6	θ	0.3741	C-20	τ_a	0.8085	C-33	T_P	9.6680
C-7	$cos\ Z$	0.7043	C-21	G_o	202.55	C-34	v_P	12.013
C-8	$cos\ \omega$	0.1731	C-22	G	176.47	C35	Δ_P	0.8072
C-9	$cos\ z$	0.4531	C-23	a	0.1010	C-36	E_P	122.352
C-10	η	1.0164	C-24	c_2	-6.475	C-37	R_{TP}	85.282
C-11	G_E	264.04	C-25	ρ	0.00913	C-38	E_W	71.946
C-13	c_0	6.1712	C-26	B	84.203		E_W (lake evaporation)	2.52 mm day^{-1} or 78.3 mm month^{-1}
C-14	a_z	0.05	C-27	R_W	74.446			
C-15	a_0	0.1041	C-28	R_{TC}	74.446			

CRLE: Incorporating water borne energy input and available solar plus water borne energy routing for deep lake evaporation

Estimate the March 2008 evaporation for the Thomson Reservoir, a deep lake 120 km east of Melbourne (latitude 37.75 °S, elevation 415 m, average depth ($\bar{h}$) 22.95 m, and average salinity (s) 23 ppm).

The method is based on Morton (1986). The soft water delay time, the lake delay time and the storage coefficient are computed first:

$$t_0 = 0.96 + 0.013\bar{h} \;\text{ with } 0.039\bar{h} \le t_0 \le 0.13\bar{h} \;\text{ (see Equation (S7.15))} \qquad \text{(S21.91)}$$

where t_0 is soft water delay time.

$$t_0 = 0.96 + 0.013 \times 22.95 = 1.2584 \text{ months} \qquad \text{(S21.92)}$$

t_0 is within the range $0.039\bar{h}$ = 0.8950 and $0.13\bar{h}$ = 2.9835

$$t_L = \frac{t_0}{\left(1+\frac{s}{27000}\right)^2} \;\text{ with } t \le 6.0 \;\text{ (see Equation (S7.16))} \qquad \text{(S21.93)}$$

where t_L is lake lag or delay time and s is lake salinity in ppm

$$t_L = \frac{1.2584}{\left(1+\frac{23}{27000}\right)^2} = 1.2563 \text{ months (which is less than 6.0)} \qquad \text{(S21.94)}$$

$$S_c = \frac{t_0}{\left[1+\left(\frac{\bar{h}}{93}\right)^7\right]} \;\text{ (see Equation (S7.14))} \qquad \text{(S21.95)}$$

where S_c is storage constant (months)

$$S_c = \frac{1.2584}{\left[1+\left(\frac{22.95}{93}\right)^7\right]} = 1.2583 \text{ months} \qquad \text{(S21.96)}$$

The sequential steps in the computation of monthly deep lake evaporation are as follows:

Step 1: Estimate and add together solar and water borne heat input, thus

$$G_W^0 = (1-\alpha)R_s - R_{nl} + \delta h \;\text{ (see Equation (S7.10))} \qquad \text{(S21.97)}$$

where G_W^0 is the solar input (the superscript refers to the current month) plus waterborne heat input (δh) and α is the albedo for water.

In this example, because the Thomson Reservoir is very large and there is no waterborne input, δh = 0. Values of G_W^0 and G_{LE} (see step 3 below) for January 2008 and February 2008 are:

	January 2008	February 2008	March 2008
G_W^0 (W m^{-2})	187	152	120
G_{LE} (W m^{-2})	160	175	Not required

Step 2: Estimate the delayed solar and waterborne energy inputs (see **Appendix S7**).

$$G_W^t = G_W^{[t_L]} + (t_L - [t_L])\left(G_W^{[t_L+1]} - G_W^{[t_L]}\right) \;\text{ (see Equation (S7.11))} \qquad \text{(S21.98)}$$

where $[t_L]$ and $(t_L - [t_L])$ are the integral and fractional components of the lake lag or delay time, t_L, (months), $G_W^{[t_L]}$ and $G_W^{[t_L+1]}$ are respectively the value (W m^{-2}) of G_W^0 computed $[t_L]$ and $[t_L + 1]$ months previously. In this example, from Equation (S21.94) t_L = 1.2563 months and, therefore, $[t_L]$ = 1 month and $(t_L - [t_L])$ = 0. 2563 months.

Thus to estimate G_W^t for March 2008, Equation (S21.98) becomes

$$G_W^{Mar08} = G_W^{[Feb08]} + (t_L - [t_L])\left(G_W^{[Jan08]} - G_W^{[Feb08]}\right) \quad \text{(S21.99)}$$

$$G_W^{Mar08} = 152 + (0.2563)(187 - 152) = 160.71 \text{ W m}^{-2} \quad \text{(S21.100)}$$

Step 3: Compute the available and water borne energy.

$$G_{LE} = G_{LB} + \frac{G_W^t - G_{LB}}{0.5 + S_c} \text{ (see Equation (S7.12))} \quad \text{(S21.101)}$$

$$G_L = 0.5(G_{LE} + G_{LB}) \text{ (see Equation (S7.13))} \quad \text{(S21.102)}$$

where G_{LB} and G_{LE} are respectively the available solar and waterborne heat energy (W m^{-2}) at the beginning and end of the month

$$G_{LE}^{Mar08} = G_{LE}^{Feb08} + \frac{G_W^{Mar08} - G_{LE}^{Feb08}}{0.5 + S_c} \quad \text{(S21.103)}$$

$$G_{LE}^{Mar08} = 175 + \frac{160.71 - 175}{0.5 + 1.2583} = 166.87 \text{ W m}^{-2} \quad \text{(S21.104)}$$

$$G_L^{Mar08} = 0.5\left(G_{LE}^{Mar08} + G_{LE}^{Feb08}\right) \quad \text{(S21.105)}$$

$$G_L^{Mar08} = 0.5(166.87 + 175) = 170.94 \text{ W m}^{-2} \quad \text{(S21.106)}$$

Step 4: Convert the available energy per month to a monthly lake evaporation rate by applying the sequence of steps set out in the worked example *CRAE: Estimate actual evaporation* after Equation S21.87 where

$$R_{TC} = G_L^{Mar08} = 170.94 \text{ W m}^{-2} \quad \text{(S21.107)}$$

These calculations yield the March 2008 lake evaporation for Thomson Reservoir as 186 mm.

References for Supplementary Material

Abbott, M.B., Bathurst, C., Cunge, J.A., O'Connell, P.E., and Rasmussen, J., 1986a. An introduction to the European Hydrological System - Systeme Hydrologique Europeen, SHE. 1. History and philosophy of a physically-based, distributed modelling system. *Journal of Hydrology*, **87**, 45-59.

Abbott, M.B., Bathurst, C., Cunge, J.A., O'Connell, P.E., and Rasmussen, J., 1986b. An introduction to the European Hydrological System - Systeme Hydrologique Europeen, SHE. 1. Structure of a physically-based, distributed modelling system. *Journal of Hydrology*, **87**, 61-77.

Abtew, W. and Obeysekera, J., 1995. Lysimeter study of evapotranspiration of Cattails and comparison of three methods. *Transactions American Society of Agricultural Engineers* **38** (1), 121-129.

Adam, J.C., Clark, E.A., Lettenmaier, D.P., and Wood, E.F., 2006. Correction of global precipitation products for orographic effects. *Journal of Climate* **19**, 15-38.

Al-Rawi, M.N.A., 1991. A simple, accurate and reliable method for measuring the Sun's elevation and orientation. *Renewable Energy* **1** (2), 231-235.

Alexandris, S., Stricevic, R., and Petkovic, S., 2008. Comparative analysis of reference evapotranspiration from the surface of rainfed grass in central Serbia, calculated by six empirical methods against the Penman-Monteith formula. *European Water* **21/22**, 17-28.

Ali, S., Ghosh, N.C., and Singh, R., 2008. Evaluating best evaporation estimate model for water surface evaporation in semi-arid India. *Hydrological Processes* **22**, 1093-1106.

Allen, J.B. and Crow, F.T, 1971. Predicting lake evaporation by performance of evaporation, ponds, pans and tanks. *Transactions of the American Society of Agricultural Engineers* **14** (3), 458-463.

Allen, R. G. and Brockway, C. E., 1983 Estimating Consumptive Use on a Statewide Basis. *Proceedings of the 1983 Irrigation Specialty Conference*, ASCE, Jackson, Wyo., 79-89.

Allen, R.G. and Pruitt, W.O., 1986. Rational Use of The FAO Blaney-Criddle Formula. *Journal Irrigation and Drainage Engineering* **112** (2), 139-155.

Allen, R.G., Pereira, L.S., Raes, D., and Smith, M., 1998. *Crop evapotranspiration Guidelines for computing crop water requirements* FAO Irrigation and Drainage Paper **56**. Food and Agriculture Organization of the United Nations.

Allen, R.G., Pruitt, W.O., Raes, D., Smith, M., and Pereira, L.S., 2005. Estimating evaporation from bare soil and the crop coefficient for the initial period using common soils information. *Journal of Irrigation and Drainage Engineering* **131** (1), 14-23.

Alvarez, M.V., Gonzalez-Real, M.M., Baille, A., and Molina Martinez, J.M., 2007. A novel approach for estimating the pan coefficient of irrigation water reservoirs: Application to South Eastern Spain. *Agricultural Water Management*, **92**: 29 - 40.

Amatya, D.M., Skaggs, R.G., and Gregory, J.D., 1995. Comparison of methods for estimating REF-ET. *Journal of Irrigation and Drainage Engineering* **121** (6), 427-435.

Amer, K.H. and Hatfield, J.L., 2004. Canopy resistance as affected by soil and meteorological factors in potato. *Journal of Agronomy* **96** (4), 978-985.

Anderson, M.G. and Idso, S.B., 1987. Surface geometry and stomatal conductance effects on evaporation from aquatic macrophytes. *Water Resources Research* **23** (6), 1037-1042.

ASCE, 2005. *The ASCE Standardized Reference Evapotranspiration Equation.* Eds Allen, R.G., Walter, I.A., Elliott, R., Howell, T., Itenfisu, D., and Jensen, M., American Society of Civil Engineers. . *The ASCE standardized reference evapotranspiration equation. Task Committee on Standardized Reference Evapotranspiration.*, EWRI-American Society Civil Engineers 59pp.

Australian Bureau of Meteorology, 2007. *Australian daily evaporation*. Technical Notes, National Climate Centre. Product Code IDCJCO.

Bahel, V., Srinivasan, R., and Bakhsh, H., 1986. Solar radiation for Dhahran, Saudi Arabia. *Energy* **11**, 985–989.

Barton, I.J., 1979. A parameterization of the evaporation from nonsaturated surfaces. *Journal of Applied Meteorology* **18**, 43-47.

Benson, R.B., Paris, M.V., Sherry, J.E., and Justus, C.G., 1984. Estimation of daily and monthly direct, diffuse and global solar radiation from sunshine duration measurements. *Solar Energy* **32**, 523–535.

Berger, A., Loutre, M-F., and Tricot, C., 1993. Insolation and Earth’s orbital periods. *Journal of Geophysical Research* **90** (D6), 10341-10362.

Beven, K., 1979. A sensitivity analysis of the Penman-Monteith actual evapotranspiration estimates. *Journal of Hydrology* **44**, 169-190.

Bidlake, W.R., 2000. Evapotranspiration from a bulrush-dominated wetland in the Klamath Basin, Oregon. *Journal of the American Water Resources Association* **36** (6), 1309-1320.

Black, T.A., 1979. Evapotranspiration from Douglas-fir stands exposed to soil water deficits. *Water Resources Research* **15** (1), 164-170.

Black, P.E., 2007 Revisiting the Thornthwaite and Mather water balance. *Journal of the American Water Resources Association* **43** (6), 1604-1605.

Blaney, H.F., 1959. Monthly consumptive use requirements for irrigated crops. *Journal of Irrigation and Drainage Division, American Society of Civil Engine*ers **85** (IR1), 1-12.

Bowen, I.S., 1926. The ratio of heat loss by conduction and by evaporation from any water surface. *Physical Review* **27**, 779-787.

Brezny, O., Mehta, I., and Sharma, R.K., 1973. Studies on evapotranspiration of some aquatic weeds. *Weed Science* **21** (3), 197-204.

Bristow, K.L. and Campbell, G.S., 1984. On the relationship between incoming solar radiation and daily maximum and minimum temperature. *Agricultural and Forest Meteorology* **31** (2), 159–166.

Brown, T.C., Hobbins, M.T., and Ramírez, J.A., 2008. Spatial distribution of water supply in the coterminous United States. *Journal of the American Water Resources Association* **44** (6), 1474-1487.

Brutsaert, W., 1982. *Evaporation into the atmosphere.* Dordrecht, Holland: D. Reidel Publishing Company.

Brutsaert, W. and Strickler, H., 1979. An advection-aridity approach to estimate actual regional evapotranspiration. *Water Resources Research* **15**, 443-449.

Burman, R.D. 1976. Intercontinental comparison of evaporation estimates *Journal of the Irrigation and Drainage Division*, **102** (1), 109-118.

Cabral, O.M.R., Rocha, H.R., Gash, J.H.C., Ligo, M.A.V., Freitas, H.C., and Tatsch, J.D., 2010. The energy and water balance of a *Eucalyptus* plantation in southeast Brazil. *Journal of Hydrology* **388**, 208-216.

Calder, I.R. and Neal, C., 1984. Evaporation from saline lakes: a combination equation approach. *Hydrological Sciences Journal* **29**, 89-97.

Carlson, T., 2007. An overview of the "triangle method" for estimating surface evapotranspiration and soil moisture from satellite imagery. *Sensors* **7 (**8)**,** 1612-1629. doi: 10.3390/s7081612**.**

Chapman, T.G., 2001. Estimation of daily potential evaporation for input to rainfall-runoff models. In Ghassemi, F., Post, D., Sivapalan, M., and Vertessy, R. (Eds), *MODSIM2001: Integrating models for Natural Resources Management across Disciplines, Issues and Scales*. MSSANZ, **1**, 293-298.

Chapman, T.G., 2003. *Estimation of evaporation in rainfall-runoff models.* MODSIM 2003 International Congress on Modelling and Simulation, Townsville, Queensland, Australia.

Chen, R., Ersi, K., Yang, J., Lu, S., and Zhao, W., 2004. Validation of five global radiation models with measured daily data in China. *Energy Conversion and Management* **45**, 1759–1769.

Chiew, F.H.S. and Jayasuria, L.N.N., 1990. *Applicability of Morton’s complementary relationship method of estimating evapotranspiration in rainfall-runoff modelling*. Conference on Agricultural Engineering, Toowoomba. The Institution of Engineers Australia.

Chiew, F.H.S. and Leahy, C.P., 2003. Comparison of evapotranspiration variables in evapotranspiration maps for Australia with commonly used evapotranspiration variables. *Australian Journal of Water Resources* **7**, 1–11.

Chiew, F.H.S. and McMahon, T.A., 1991. The applicability of Morton’s and Penman’s evapotranspiration estimates in rainfall-runoff modelling. *Water Resources Bulletin* **27** (4), 611-620.

Chiew, F.H.S. and McMahon, T.A., 1992. An Australian comparison of Penman potential evapotranspiration estimates and Class A evaporation pan data. *Australian Journal of Soil Science* **30**, 101-112.

Chiew, F.H.S. and McMahon, T.A., 1993. *Complete set of daily rainfall, potential evaporation and streamflow for twenty-eight unregulated Australian catchments*. Centre for Environmental Hydrology, The University of Melbourne.

Chiew, F.H.S., Stewardson, M.J., and McMahon, T.A., 1993. Comparison of six rainfall-runoff modelling approaches. *Journal of Hydrology* **147**, 1-36.

Chiew, F.H.S., Kamaladasa, N.N., Malano, H.M., and McMahon, T.A. 1995. Penman-Monteith, FAO-24 reference crop evapotranspiration and class-A pan data in Australia. *Agricultural Water Management* **28**, 9-21.

Chiew, F, Wang, Q.J., McConachy, F., James, R., Wright, W, and de Hoedt, G., 2002. Evapotranspiration maps for Australia. *Proceedings of 27th Hydrology and Water Resources Symposium, Institution of Engineers Australia*, CDROM (ISBN 0-8582-5778-5).

Chin, D.A., 2011. Thermodynamic consistency of potential evapotranspiration estimates in Florida. *Hydrological Processes* **25**, 288-301.

Christiansen, J.E., 1968. Pan evaporation and evapotranspiration from climatic data. *Journal of the Irrigation and Drainage Division, ASCE* **94** (IR2), Paper 5988.

Cogley, J.G., 1979. The albedo of water as a function of latitude. *Monthly Weather Review* **107**, 775-781.

Cohen, S., Ianetz, A., and Stanhill, G., 2002. Evaporative climate changes at Bet Dagan, Israel, 1964-1998. *Agricultural and Forest Meteorology* **111**, 83-91.

Clulow, A.D., Everson. C.S., Mengistu, M.G., Jarmain, C., Jewitt, G.P.W., Price, J.S., and Grundling, P.-L., 2012. Measurement and modelling of evaporation from a coastal wetland in Maputaland, South Sfrica. *Hydrology and Earth System Sciences* **16**, 3233-3247.

Crockford, R.H. and Richardson, D.P., 2000. Partitioning of rainfall into throughfall, stemflow and interception: effect of forest type, ground cover and climate. *Hydrological Processes* **14**, 2903-2920.

Davenport, A.G., 1960. Rationale for determining design wind velocities. *Journal American Society of Civil Engineers* **ST-86**, 39-68.

Davies, J.A. and Allen, C.D., 1973. Equilibrium, potential and actual evaporation from cropped surfaces in southern Ontario. *Journal of Applied Meteorology* **12,** 649-657.

de Bruin, H.A.R., 1978. A simple model for shallow lake evaporation. *Journal of Applied Meteorology* **17**, 1132-1134.

de Bruin, H.A.R., 1981. The determination of (reference crop) evapotranspiration from routine weather data. Proceedings of Technical Meeting 38. *Committee for Hydrological Research TNO*, Evaporation in relation to hydrology. Proceedings and Informations **28**, 25-37.

de Bruin, H.A.R., 1982. Temperature and energy balance of a water reservoir determined from standard weather data of a land station. *Journal of Hydrology* **59**, 261-274.

de Bruin, H.A.R., 1987. From Penman to Makkink. Proceedings of Technical Meeting 44. *Committee for Hydrological Research TNO*, J.C. Hooghart (Ed.) Evaporation and weather. Proceedings and Informations **39**, 5-31.

de Bruin, H.A.R. and Holtslag, A.A.M., 1982. A simple parameterization of the surface fluxes of sensible and latent heat during daytime compared with the Penman-Monteith concept. *Journal of Applied Meteorology* **21**, 1610-1621.

Dingman, S.L., 1992. *Physical Hydrology*. Prentice Hall.

Donohue, R.J., Roderick, M.L. and McVicar, T.R., 2008. Deriving consistent long-term vegetation information from AVHRR reflectance data using a cover-triangle-based framework. *Remote Sensing of Environment* **112** (6), 2938-2949.

Donohue, R.J., McVicar, T.R., and Roderick, M.L., 2009. Climate-related changes in Australian vegetation cover as inferred from satellite observations for 1981-2006. *Global Change Biology* **15** (4), 1025-1039.

Donohue, R.J., McVicar, T.R., Li, L.T., and Roderick, M.L., 2010a. A data resource for analysing dynamics in Australian ecohydrological conditions. *Austral Ecology* **35** (5), 593-594, doi: 10.1111/j.1442-9993.2010.02144.x.

Donohue, R.J., McVicar, T.R., and Roderick, M.L., 2010b. Assessing the ability of potential evaporation formulations to capture the dynamics in evaporative demand within a changing climate. *Journal of Hydrology* **386**, 186-197.

Doorenbos, J. and Pruitt, W.O., 1992. *Guidelines for predicting crop water requirements*. FAO Irrigation and Drainage Paper **24**. Food and Agriculture Organization of the United Nations.

Douglas, E.M., Beltrán-Przekurat, A., Niyogi, D., Pielke, R.A., and Vörösmarty, C.J., 2009. The impact of agricultural intensification and irrigation on land-atmosphere interactions and Indian monsoon precipitation – A mesoscale modeling perspective. *Global and planetary Change* **67**, 117-128.

Drexler, J.D., Snyder, R.L., Spano, D., and Paw U, K.T., 2004. A review of models and micrometeorological methods used to estimate wetland evapotranspiration. *Hydrological Processes* **18**, 2071-2101.

Droogers, P. and Allen, R.G., 2002. Estimating reference evapotranspiration under inaccurate data conditions, *Irrigation and Drainage Systems* **16,** 33-45.

Dunin, F.X. and Greenwood, E.A.N., 1986. Evaluation of the ventilated chamber for measuring evaporation from a forest. *Hydrological Processes* **1**, 47-62.

Dunne, T. and Leopold, L.B., 1978. *Water in Environmental Planning*. W. H. Freeman and Company, New York, NY, USA.

Duru, J.O., 1984. Blaney-Morin-Nigeria evapotranspiration model. *Journal of Hydrology* **70**, 71-83.

Edinger, J.E., Duttweiler, D.W., and Geyer, J.C., 1968. The response of water temperature to meteorological conditions. *Water Resources Research* **4** (5), 1137-1143.

Elhaddad, A., Garcia, L.S., and Chávez, J.L., 2011. Using a surface energy balance model to calculate spatially distributed actual evapotranspiration. *Journal of Irrigation and Drainage Engineering, ASCE,* **137** (1), 17-26.

Elsawwaf, M., Willems, P., and Feyen, J., 2010. Assessment of the sensitivity and prediction uncertainty of evaporation models applied to Nasser Lake, Egypt. *Journal of Hydrology* **395**, 10-22.

Federer, C. A., Vörösmarty, C., and Fekete, B., 1996. Intercomparison of Methods for Calculating Potential Evaporation in Regional Global Water Balance Models, *Water Resources Research* **32** (7), 2315-2321.

Fennessey, N.M, 2000. Estimating average monthly lake evaporation in the Northeast United States. *Journal American Water Resources Association* **36** (4), 759-769.

Ficke, J.F., 1972. Comparison of evaporation computation method, Pretty Lake. *United States Geological Survey Professional Paper* **686-A**, 48 pp.

Finch, J.W., 2001. A comparison between measured and modelled open water evaporation from a reservoir in south-east England. *Hydrological Processes* **15**, 2771-2778.

Finch, J.W. and Gash, J.H.C., 2002. Application of a simple finite difference model for estimating evaporation from open water. *Journal of Hydrology* **255**, 253-259.

Fisher, J.B., de Biase, T.A., Qi, Y., Xu, M., and Goldstein, A.H., 2005. Evapotranspiration models compared on a Sierra Nevada forest ecosystem. *Environmental Modelling & Software* **20,** 783-796.

Fleming, P.M., Brown, J.A.H., and Aitken, A.P., 1989. Evaporation in Botswana and Australia, the transference of equations and techniques between continents. Hydrology and Water Resources Symposium 1989, *The Institution of Engineers, Australia National Conference Publication* **89** (19), 58-65.

Flint, A.L. and Childs, S.W., 1991. Use of the Priestley-Taylor evaporation equation for soil water limited conditions in a small forest clearcut. *Agricultural and Forest Meteorology* **56**, 247-260.

Fraedrich, K., Behlau, A., Kerath, G., and Weber, G., 1977. A simple model for estimating the evaporation from a shallow water reservoir. *Tellus*, **29**, 428-434.

Frevert, D.K., Hill, R.W., and Braaten, B.C., 1983. Estimation of FAO evapotranspiration coefficients. *Journal of Irrigation and Drainage ASCE* **109** (IR2), 265-270.

Gash, J.H.C., 1979. An analytical model of rainfall interception by forests. *Quarterly Journal of the Royal Meteorological Society* **105**, 43-55.

Gerrits, A.W.J., Pfister, L., and Savenije, H.H.G., 2010. Spatial and temporal variability of canopy and forest floor interception in a beech forest. *Hydrological Processes* **24**, 3011-3025.

Ghare, A.D., Porey, P.D., and Ingle, R.N., 2006. “Discussion of ‘Simplified estimation of reference evapotranspiration from pan evaporation data in California’ by Snyder. R.L., Orang, M., Matyac, S., and Grismer, M.E.” *Journal of Irrigation and Drainage Engineering* **132** (5), 519-520.

Giles, D.G., Black, T.A., and Spittlehouse, D.L., 1984. Determination of growing season soil water deficits on a forested slope using water balance analysis. *Canadian Journal of Forest Research* **15**, 107-114.

Glenn, E., Huete, A., Nagler, P, Hirschboeck, K., and Brown, P., 2007. Integrating remote sensing and ground methods to estimate evapotranspiration. *Critical Reviews in Plant Sciences*, **26**, 139-168.

Glenn, E. P., Nagler, P. L., and Huete, A.R., 2010. Vegetation Index Methods for Estimating Evapotranspiration by Remote Sensing. *Surveys in Geophysics* **31 (**6), 531-555**.** doi: 10.1007/s10712-010-9102-2**.**

Granger, R.J, 1998. Partitioning of energy during the snow-free season at the Wolf Creek Research Basin. In *Proceedings of a Workshop held in Whitehorse*. Pomeroy, J.W. and Granger, R.J. (eds), Yukon , 5-7 March, 33-43.

Granger, R.J. and Gray, D.M., 1989. Evaporation from natural nonsaturated surfaces. *Journal of Hydrology* **111**, 21-29.

Granier, A., Huc., R., and Barigah, S.T., 1996. Transpiration of natural rain forest and its dependence on climatic factors. *Agricultural and Forest Meteorology* **78**, 19–29.

Grant, D.R., 1975. Comparison of evaporation measurements using different methods. *Quarterly Journal of the Royal Meteorological Society* **101**, 543–550.

Grayson, R.B., Argent, R.M., Nathan, R.J., McMahon, T.A., and Mein, R.G., 1996. *Hydrological Recipes - Estimation Techniques in Australian Hydrology*. Cooperative Research Centre for Catchment Hydrology, Clayton, Australia.

Grimmond, C.S.B. and Oke, T.R., 1991. An evapotranspiration-interception model for urban areas. *Water Resources Research* **27** (1), 1739-1755.

Guerschman, J.P., Van Dijk, A.I.J.M., Mattersdorf, G., Beringer, J., Hutley, L.B., Leuning, R., Pipunic, R.C., and Sherman, B.S., 2009. Scaling of potential evapotranspiration with MODIS data reproduces flux observations and catchment water balance observations across Australia. *Journal of Hydrology* **369**, 107–119.

Harbeck, G.E., 1958. Lake Hefner water-loss investigations. *International Association Scientific Hydrology*, **45**, 437-443.

Harbeck, G.E., 1962. *A practical field technique for measuring reservoir evaporation utilizing mass-transfer theory*. U.S. Geological Survey Professional Paper **272-E**.

Hargreaves, G.H. and Samani, Z.A., 1985. Reference crop evapotranspiration from temperature. *Applied Engineering in Agriculture* **1** (2), 96-99.

Harmsen, E.W., Pérez, A.G., and Winter, A., 2003. *Estimating long-term average monthly evapotranspiration from pan evaporation data at seven locations in Puerto Rico.* NOAA-CREST/NASA-EPSCoR Joint Symposium for Climate Studies, University of Puerto Rico – Mayaguez Campus. 7pp.

Herbst, M., Rosier, P.T.W., McNeil, D.D., and Harding, R.J., 2008. Seasonal variability of interception evaporation from the canopy of a mixed deciduous forest. *Agricultural and Forest Meteorology* **148**, 1655-1667.

Hobbins, M.T., Ramírez, J.A., Brown, T.C., and Claessens, L.H.J.M., 2001a. The complementary relationship in estimation of regional evapotranspiration: The Complementary Relationship Areal Evapotranspiration and Advection-Aridity models. *Water Resources Research* **37** (5), 1367-1387.

Hobbins, M.T., Ramírez, J.A., and Brown, T.C. 2001b. Complementary relationship in the estimation of regional evapotranspiration: An enhanced Advection-Aridity model. *Water Resources Research* **37** (5), 1388–1401.

Hounam, C.E., 1973. Comparison between pan and lake evaporation. *World Meteorological Organisation* Technical Note **126**, 52pp.

Hoy, R.D., 1977. Pan and lake evaporation in northern Australia. Hydrology Symposium 1977. The Institution of Engineers Australia, National Conference Publication No. **77**/5, 57-61.

Hoy, R.D. and Stephens, S.K. 1977. Field study of evaporation – Analysis of data from Eucumbene, Cataract, Manton and Mundaring. A.W.R.C. Technical Paper **21**, 195pp.

Hoy, R.D. and Stephens, S.K., 1979. *Field study of lake evaporation – analysis of data from phase 2 storages and summary of phase 1 and phase2*. Australian Water Resources Council Technical Report paper No. **41**.

Hoyt, D.V., 1977. Percent of possible sunshine and the total cloud cover. *Monthly Weather Review* **105**, 648-652.

Idso, S.B., 1981. Relative rates of evaporative water losses from open and vegetation covered water bodies. *Water Resources Bulletin* **17** (1), 46-48.

Jacobs, J.M., Mergelsberg, S.L., Lopera, A.F., and Myers, D.A., 2002. Evapotranspiration from a wet prairie wetland under drought conditions: Paynes Prairie, Florida, USA. *Wetlands* **22** (2), 374-385.

Jarvis, P.G. and McNaughton, K.G., 1986. Stomatal control of transpiration: scaling up from leaf to region. *Advances in Ecological Research* **15**, 1-49.

Jeffrey, S.J., Carter, J.O., Moodie, K.B., and Beswick, A.R., 2001. Using spatial interpolation to construct a comprehensive archive of Australian climate data. *Environmental Modelling and Software* **16** (4), 309-330.

Jensen, M.E., 2010 *Estimating evaporation from water surfaces*. Presentation at CSU/ARS Evapotranspiration Workshop, Fort Collins. (15 March 2010).

Jensen, M.E., Burman, R.D., and Allen, R.G., (Eds), 1990. Evapotranspiration and irrigation water requirements. *ASCE Manuals and Reports on Engineering Practice* **70.**

Jia, L., X G., Liu, S., Huang, C., Yan, Y., and Liu, G., 2009. Regional estimation of daily to annual regional evapotranspiration with MODIS data in the Yellow River Delta wetland. *Hydrology and Earth System Sciences* **13**, 1775-1787.

Johnson, F., and Sharma, A., 2010. A comparison of Australian open water body evaporation trends for current and future climates estimated from Class A evaporation pans and general circulation models. *Journal of Hydrometeorology* **11**, 105-121.

Jones, D.A., Wang, W., and Fawcett, R., 2009. High-quality spatial climate data-sets for Australia. *Australian Meteorological and Oceanographic Journal* **58**, 233-248.

Jones, R.N., Bowler, J.M., and McMahon, T.A., 1993. Modelling water budgets of closed lakes, western Victoria. *Quaternary Australasia Papers* **11** (1), 50-60.

Jovanovic, B., Jones, D., and Collins, D., 2008. A high-quality monthly pan evaporation dataset for Australia. *Climatic Change* **87**, 517-535.

Jury, W.A. and Tanner, C.B., 1975. Advection modification of the Priestley and Taylor evapotranspiration formula. *Agronomy Journal* **67**, 840-842.

Kalma, J.D., McVicar, T.R., and McCabe, M.F., 2008. Estimating land surface evaporation: A review of methods using remotely sensed surface temperature data. *Surveys in Geophysics* **29**, 421-469.

Keijman, J.Q., 1974. The estimation of the energy balance of a lake from simple weather data. *Boundary-Layer Meteorology* **7**, 399-407.

Keijman, J.Q. and Koopmans, R.W.R., 1973. A comparison of several methods of estimating the evaporation of Lake Flevo. *International Association of Hydrological Sciences Symposium on Hydrology of Lakes*, 225-232.

Kelliher, F.M., Leuning, R. and Schulze, E.D., 1993. Evaporation and canopy characteristics of coniferous forests and grasslands. *Oecologia* **95** (2), 153-163.

Kelliher, F.M., Leuning, R., Raupach, M.R. and Schulze, E.D., 1995. Maximum conductances for evaporation from global vegetation types. *Agricultural and Forest Meteorology* **73**, 1-16.

Kirono, D.G.C., Jones, R.N., and Cleugh, H.A., 2009. Pan-evaporation measurements and Morton-point potential evaporation estimates in Australia: are their trends the same? *International Journal of Climatology* **29**: 711–718.

Klaassen, W., Bosveld, F., and de Water, E., 1998. Water storage and evaporation as constituents of rainfall interception. *Journal of Hydrology* **212-213**, 36-50.

Kohler M.A., Nordenson, T.J., and Fox, W.E., 1955. *Evaporation from pans and lakes*. Weather Bureau research Paper **38**, US Department of Commerce, Washington.

Kohler, M.A. and Parmele, L.H., 1967. Generalized estimates of free-water evaporation. *Water Resources Research* **3** (4), 997-1005.

Komatsu, H., 2005. Forest categorization according to dry-canopy evaporation rates in the growing season: comparison of the Priestley-Taylor coefficient values from various observation sites. *Hydrological Processes* **19**, 3873-3896.

Kotwicki, V., 1994. *The nature of evaporation from Lake Alexandrina*. Water Down Under ’94, Adelaide.

Kumagai, T., Saitoh, T.M., Sato, Y., Morooka, T., Manfroi, O.J., Kuraji. K., and Suzuki, M., 2004. Transpiration, canopy conductance and the decoupling coefficient of a lowland mixed dipterocarp forest in Sarawk, Borneo: dry spell effects. *Journal of Hydrology* **287**, 237-251.

Lavery, B., Joung, G., and Nicholls, N., 1997. An extended high-quality historical rainfall dataset for Australia. *Australian Meteorological Magazine* **46**, 27-38.

Lawrence, M.G., 2005. The relationship between relative humidity and the dewpoint temperature in moist air: a simple conversion and applications. *Bulletin American Meteorological Society* **86**, 225-233.

Lenters, J., Kratz, T.K., and Bowser, C.J., 2005. Effects of climate variability on lake evaporation: results from a long-term energy budget of Sparkling Lake, northern Wisconsin (USA). *Journal of Hydrology* **308**, 168-195.

Linacre, E.T., 1968. Estimating the net-radiation flux. *Agricultural Meteorology* **5**, 49-63.

Linacre, E.T., 1992. *Climate Data and Resources*. Routledge, Boca Raton, Fla.

Linacre, E.T., 1993. Data-sparse estimation of lake evaporation, using a simplified Penman equation. *Agricultural and Forest Meteorology* **64**, 237-256.

Linacre, E.T., 1994. Estimating U.S. Class-A pan evaporation from few climate data. *Water International* **19**, 5-14.

Linacre, E.T., Hicks, B.B., Sainty, G.R., and Grauze, G., 1970. The evaporation from a swamp. *Agricultural Meteorology* **7**, 375-386.

Lott, R.B. and Hunt, R.J., 2001. Estimating evapotranspiration in natural and constructed wetlands. *Wetlands* **21** (4), 614-628.

Louche, A., Notton, G., Poggi, P., and Simonnot, G., 1991. Correlations for direct normal and global horizontal irradiation on a French Mediterranean site. *Solar Energy* **46**, 261–266.

Lu, J., Sun, G., McNulty, S.G., and Amatya, D.M., 2005. A comparison of six potential evapotranspiration methods for regional use in the Southeastern United States," *Journal American Water Resources Association* **41**, 621-633.

Magnani, F., Leonardi, S., Tognetti, R., Grace, J., and Borghetti, M, 1998. Modelling the surface conductance of a broad-leaf canopy: effects of partial decoupling from the atmosphere. *Plant Cell and Environment* **21**, 867-879.

Maidment, D.R. 1992. *Handbook of Hydrology.* McGraw-Hill Inc., New York.

Martinez-Lonano, J.A., Tena, F., Onrubia, J.E., and Rubia, J., 1984. The historical evolution of the Ångström formula and its modifications: review and bibliography. *Agricultural and Forest Meteorology* **33**, 109-128.

McArthur, A.J., 1992. The Penman form equations and the value of Delta: a small difference of opinion or a matter of fact? *Agricultural and Forest Meteorology* **57**, 305-308.

McCullough, E.C., 1968. Total daily radiant energy available extraterrestrially as a harmonic series in the day of the year. *Arch. Met. Geoph. Biokl*., Ser. B, **16**, 129-143.

McCullough, E.C. and Porter, W.P., 1971. Computing clear day solar radiation spectra for the terrestrial ecological environment. *Ecology* **52** (6), 1008-1015.

McJannet, D., Cook, F., and Burn, S., 2008a. *Evaporation reduction by manipulation of surface area to volume ratios: overview, analysis and effectiveness.* CSIRO: Water for a Healthy Country National Research Flagship. Urban Water Security Research Alliance Technical Report No. 8.

McJannet, D.L., Webster. I.T., Stenson, M.P., and Sherman, B.S., 2008b. *Estimating open water evaporation for the Murray-Darling Basin.* A report to the Australian Government from the CSIRO Murray-Darling Basin Sustainable Yields Project.

McJannet, D.L., Webster, I.T., and Cook, F.J., 2012 An area-dependent wind function for estimating open water evaporation using land-based meteorological data. *Environmental Modelling & Software* doi:10.1016/j.envsoft.2011.11.017.

McLeod, A.J. and Webster, I.T., 1996. *A heat budget method of estimating evaporation from irrigation channels*. Proceedings 23rd Hydrology and Water Resources Symposium. The Institution of Engineers Australia **2**, 373-379.

McNaughton, K.G. and Black, T.A., 1973. A study of evapotranspiration from a Douglas Fir forest using the energy balance approach. *Water Resources Research* **9**, 1579-1590.

McNaughton, K.G. and Jarvis, P.G., 1991. Effects of spatial scale on stomatal control of transpiration. *Agricultural and Forest Meteorology* **54**, 279-301.

McVicar, T.R. and Jupp, D.L.B., 2002. Using covariates to spatially interpolate moisture availability in the Murray–Darling basin – a novel use of remotely sensed data. *Remote Sensing of Environment* **79** (2–3), 199–212.

McVicar, T.R., Van Niel, T.G., Li, L-T., Hutchinson, M.F., Mu, X-M., and Liu, Z-H. 2007. Spatially distributing monthly reference evapotranspiration and pan evaporation considering topographical influences. *Journal of Hydrology* **338**, 196-220.

McVicar, T.R., Van Niel, T.G., Li, L.T., Roderick, M.L., Rayner, D.P. Ricciardulli, L., and Donohue, R.J., 2008. Wind speed climatology and trends for Australia, 1975-2006:

Capturing the stilling phenomenon and comparison with near-surface reanalysis output. *Geophysical Research Letters*, **35**, L20403, doi:10.1029/2008GL035627.

McVicar, T.R., Roderick, M.L., Donohue, R.J., Li, L.T., Van Niel, T.G., Thomas, A., Grieser, J., Jhajharia, D., Himri, Y., Mahowald, N.M., Mescherskaya, A.V., Kruger, A.C., Rehman, S., and Dinpashoh, Y., 2012. Global review and synthesis of trends in observed terrestrial near-surface wind speeds: Implications for evaporation. *Journal of Hydrology* **416-417**, 182-205 doi:10.1016/j.jhydrol.2011.10.024.

Meinzer, F.C., Andrade, J.L., Goldstein, G., Holbrook, N.M., Cavelier, J., and Jackson, P., 1997. Control of transpiration from the upper canopy of a tropical forest: the role of stomatal, boundary layer and hydraulic architecture components. *Plant Cell and Environment* **20**, 1242–1252.

Menges, H.O., Ertekin, C, and Sonmete, M.H., 2006. Evaluation of global solar radiation models for Konya, Turkey. *Energy Conversion and Management* **47**, 3149-3173.

Meyer, W.S., 1999. *Standard reference evaporation calculation for inland south eastern Australia*. CSIRO Land and Water, Technical Report **35/98**.

Milly, P.C.D., 1991. A refinement of the combination equations for evaporation. *Surveys in Geophysics* **12**, 145-154.

Mohamed, Y.A., Bastiaanssen, W.G.M., Savenije, H.H.G., van den Hurk, B.J.J.M., and Finlayson, C.M., 2008. *Evaporation from wetland versus open water: a theoretical explanation and an application with satellite data over the Sudd wetland*. Manuscript.

Monteith, J.L., 1965. Evaporation and environment. In G.E. Fogg (Ed), The state and movement of water in living organisms. *Symposium Society Experimental Biology* **19**, 205-234., Cambridge University Press, London.

Monteith, J.L., 1981. Evaporation and surface temperature. *Quarterly Journal of the Royal Meteorological Society* **107** (451), 1-27.

Morton, F.I., 1979. Climatological estimates of lake evaporation. *Water Resources Research* **15** (1), 64-76.

Morton, F.I., 1983a. Operational estimates of areal evapotranspiration and their significance to the science and practice of hydrology. *Journal of Hydrology*, **66**, 1-76.

Morton, F.I., 1983b. Operational estimates of lake evaporation. *Journal of Hydrology,* **66**, 77-100.

Morton, F.I., 1986. Practical estimates of lake evaporation. *Journal of Climate & Applied Meteorology* **25**, 371-387.

Morton, F.I., Richard, F., and Fogarasi, S., 1985. *Operational estimates of areal evapotranspiration and lake evaporation – Program WREVAP*. NHRI Paper **24**, Inland Waters Directorate, Environment Canada, Ottawa.

Mukammal, E.I. and Neumann, H.H., 1977. Application of the Priestley-Taylor evaporation model to assess the influence of soil moisture on the evaporation from a large weighing lysimter and class A pan. *Boundary-Layer Meteorology* **12**, 243-256.

Mutziger, A.J., Burt, C.M., Howes, D.J., and Allen, R.G., 2005. Comparison of measured and FAO-56 modeled evaporation from bare soil. *Journal of Irrigation and Drainage Engineering* **131**,(1), 59-72.

Muzylo, A., Llorens, P., Valente, F., Keize, J.J., Domingo, F., and Gash, J.H.C., 2009. A review of rainfall interception modelling. *Journal of Hydrology* **370**, 191-206.

Myrup, L.O., Powell, T.M., Godden, D.A., and Goldman, C.R., 1979. Climatological estimate of the average monthly energy and water budgets of Lake Tahoe, California-Nevada. *Water Resources Research* **15** (6), 1499-1508.

Nandagiri, L. and Kovoor, G.M., 2006. Performance Evaluation of Reference Evapotranspiration Equations across a Range of Indian Climates *Journal of Irrigation and Drainage Engineering*, **132**, (3), 238-249.

New, M., Lister, D., Hulme, M., and Makin, I., 2002. A high-resolution data set of surface climate over global land areas. *Climate Res.*, **21**, 1-25.

Neuwirth, F., 1973. Experiences with evaporation pans at a shallow steppe-lake in Austria. *International Association of Hydrological Science* 'Hydrology of Lakes', Helsinki, 290-297.

Nimmo, W.R., 1964. Measurement of evaporation by pans and tanks. *Australian Meteorological Magazine* **46**, 17-53.

Nordenson, T.J. and Baker, D.R., 1962. Comparative evaluation of evaporation instruments. *Journal of Geophysical Research* **67**, 671-679.

Oliver,H., 1961. *Irrigation and Climate*. Edward Arnold Ltd., London, 250 pp.

Oudin, L., Michel, C., and Andtil, F., 2005. Which potential evapotranspiration input for a lumped rainfall-runoff model? Part 1 – Can rainfall-runoff models effectively handle detailed potential evapotranspiration inputs? *Journal of Hydrology* **303**, 275-289

Page, J.K., 1961. The estimation of monthly mean values of daily total short wave radiation on vertical and inclined surfaces from sunshine records for latitudes 40_N–40_S. In: *Proceedings of UN conference on new sources of energy*, 378–90.

Paw U, K.T., 1992. A discussion of the Penman form equations and comparisons of some equations to estimate latent energy flux density. *Agricultural and Forest Meteorology* **57**, 297-304.

Paw U, K.T. and Gao, W., 1988. Applications of solutions to non-linear energy budget equations. *Agricultural and Forest Meteorology* **43**, 121-145.

Payne, R.E., 1972. Albedo of sea water. *Journal of Atmospheric Research* **29**, 959-970.

Penman, H.L., 1948. Natural evaporation from open water, bare soil and grass. *Proceedings Royal Society London*, **A193**, 120-145.

Penman, H.L. 1956. Evaporation: An introductory survey. *Netherlands Journal Agricultural Science* **4**: 9-29.

Philip, J.R., 1957. Evaporation and moisture and heat fields in the soil. *Journal of Meteorology* **14**, 354-366.

Price, J.S., 1994. Evapotranspiration from a lakeshore *Typha* marsh on Lake Ontario. *Aquatic Botany* **48**, 261-272.

Priestley, C.H.B. and Taylor, R.J., 1972. On the assessment of surface heat flux and evaporation using large scale parameters. *Monthly Weather Review* **100**, 81-92.

Raupach, M.R., 2001. Combination theory and equilibrium evaporation. *Quarterly Journal of the Royal Meteorological Society* **127**, 1149-1181.

Raupach, M.R., Kirby, J.M., Barrett, D.J., Briggs, P.R., Lu, H., and Zhang, H., 2001. Balances of Water, Carbon, Nitrogen and Phosphorus in Australian Landscapes: (2) Model Formulation and Testing. *CSIRO Land and Water Technical Report* **41**/01.

Rayner, D., 2005. *Australian synthetic daily Class A pan evaporation*. Queensland Department of Natural resources and Mines Technical Report.

Ritchie, J.T., 1972. Model for predicting evaporation from row crop with incomplete cover. *Water Resources Research* **8**, 1204-1213.

Roderick, M.L., 1999 Estimating the diffuse component from daily and monthly measurements of global radiation *Agricultural and Forest Meteorology* **95**, 169-185.

Roderick, M.L., Rotstayn, L.D., Farquhar, G.D. and Hobbins, M.T., 2007. On the attribution of changing pan evaporation. *Geophysical Research Letters* **34**, L17403, doi:10.1029/2007GL031166.

Roderick, M.L., Hobbins, M.T., and Farquhar, G.D., 2009a. Pan evaporation trends and the terrestrial water balance. 1. Principles and observations. *Geography Compass* **3** (2), 746-760.

Roderick, M.L., Hobbins, M.T., and Farquhar, G.D., 2009b. Pan evaporation trends and the terrestrial water balance. 1. Energy balance and interpretation. *Geography Compass* **3** (2), 761-780.

Rosenberry, D.O., Stannard, D.I., Winter, T.C., and Martinez, M.L., 2004. Comparison of 13 equations for determining evapotranspiration from a prairie wetland, Cottonwood Lake Area, North Dakota, USA. *Wetlands* **24** (3), 483.

Rotstayn, L.D., Roderick, M.L., and Farquhar, G.D., 2006. A simple pan-evaporation model for analysis of climate simulation: Evaluation over Australia. *Geophysical Research Letters* **33**, L17715, doi:10.1029/2006GL027114, 206.

Rutter, A.J., Kershaw, K.A., Robbins, P.C., and Morton. A.J., 1971. A predictive model of rainfall interception in forests. I. Derivation of the model from observations in a plantation of Corsican pine. *Agricultural Meteorology* **9**, 367-384.

Rutter, A.J., Morton, A.J., and Robins, P.C., 1975. A predictive model of rainfall interception in forests. II. Generalization of the model and comparison with observations in some coniferous and hardwood stands. *Journal of Applied Ecology* **12**, 367-380.

Sacks, L.A., Lee, T.M., and Radell, M.J., 1994. Comparison of energy-budget evaporation losses from two morphometrically different Florida seepage lakes. *Journal of Hydrology* **156**, 311-334.

Salvucci, G.D., 1997. Soil and moisture independent estimation of stage-two evaporation from potential evaporation and albedo or surface temperature. *Water Resources Research* **33** (1), 111-122.

Samani, Z., 2000. Estimating Solar Radiation and Evapotranspiration Using Minimum Climatological Data. *Journal of Irrigation and Drainage Engineering* **126**, 265-278.

Saunders, R.W., 1990. The determination of broad-band surface albedo from AVHRR visible and near-infrared radiances. *International Journal of Remote Sensing* **11** (1), 49–67.

Scozzafava, M. and Tallini, M., 2001. Net infiltration in the Gran Sasso Massif of central Italy using the Thornthwaite water budget and curve number method. *Hydrogeology Journal* **9**, 461-475.

Sharma, M.L., 1984. Evapotranspiration from an Eucalytus community. *Agricultural Water Management* **8**, 41-56.

Shaw, E.M., 1994. *Hydrology in Practice*. Chapman & Hall, London, 3rd Edition, 569 pp.

Shuttleworth, W.J., 1992. In: Maidment, D.R. (Ed.), *Evaporation*. McGraw-Hill, New York, pp. 4.1-4.53 (Chapter 4).

Shuttleworth, W.J. 1978. A simplified one dimensional theoretical description of the vegetation-atmosphere interaction. *Boundary Layer Meteorology* **14**, 3-27.

Shuttleworth, W.J. 1988. Evaporation from Amazonian rainforest. *Proceedings Royal Society London B* **233**, 321-246.

Shuttleworth, W.J. and Calder, I.R., 1979. Has the Priestley-Taylor equation any relevance to forest evaporation? Journal of *Applied Meteorology* **18**, 639-646.

Shuttleworth, W.J. and Wallace, J.S. 1985. Evaporation from sparse crops – an energy combination theory. *Quarterly Journal of the Royal Meteorological Society* **111**, 839-855.

Shuttleworth, W.J. and Wallace, J.S., 2009. Calculating the water requirements of irrigated crops in Australia using the Matt-Shuttleworth approach. *Transactions of the American Society of Agricultural and Biological Engineers* **52** (6), 1895-1906.

Silberstein, R.P., Sivapalan, M., Viney, N.R., Held, A., and Hatton, T.J., 2003. Modelling the energy balance of a natural jarrah (*Eucalyptus marginata)* forest. *Agricultural and Forest Meteorology* **115**, 210-230.

Simpson, J.P. and Paulson, C.A., 1979. Mid-ocean observations of atmospheric radiation. *Quarterly Journal of Royal Meteorological Society*, **103**, 487-502.

Siriwardena, L., Finlayson, B.L. and McMahon, T.A., 2006. The impact of land use change on catchment hydrology in large catchments: The Comet River, Central Queensland, Australia. *Journal of Hydrology* **326**, 199-214.

Slatyer, R.O. and McIlroy, I.C., 1961. *Practical Microclimatology*. Commonwealth Scientific and Industrial Organisation, Australia, UNESCO.

Snyder. R.L., Orang, M., Matyac, S., and Grismer, M.E., 2005. Simplified estimation of reference evapotranspiration. From pan evaporation data in California. *Journal of Irrigation and Drainage Engineering* **131** (3), 249-253.

Sobrino, J.A., Gómez, M., Jiménez-Muñoz, J.C., Olioso, A., and Chehbouni, G., 2005. A simple algorithm to estimate evapotranspiration from DAIs data: Application to the DAISEX campaigns. *Journal of Hydrology* **315**, 117-125.

Souch, C., Grimmond, C.S.B., and Wolfe, C.P., 1998. Evapotranspiration rates from wetlands with different disturbance histories: Indiana Dunes National Lakeshore. *Wetlands* **18** (2), 216-229.

Stanhill, G., 1963. Evaporation in Israel. *Bulletin of Research Council of Israel* **11G**, 160-172.

Stanhill, G., 1969. Evaporation from Lake Tiberias: an estimate by the combined water balance-mass transfer approach. *Israel Journal of Earth Science* **18**, 101-108.

Stanhill, G. 1976. *The CIMO International Evaporimeter Comparisons*. World Meteorological Organisation, Geneva Publication **449**, 38pp.

Stanhill, G., 2002. Is the Class A evaporation pan still the most practical and accurate method for determining irrigation water requirements? *Agricultural and Forest Meteorology* **112**, 233-236.

Stannard, D.I., 1993. Comparison of Penman-Monteith, Shuttleworth-Wallace, and modified Priestley-Taylor Evapotranspiration models for wildland vegetation in semiarid rangeland. *Water Resources Research* **29** (5), 1379-1392.

Stewart, J.B., 1977. Evaporation from the wet canopy of a pine forest. *Water Resources Research* **13** (6), 915-921.

Stewart, R.B., Rouse, W.R., 1976. A simple method for determining the evaporation from shallow lakes and ponds. *Water Resources Research* **12** (4), 623-628.

Stewart, R.B. and Rouse, W.R., 1977. Substantiation of the Priestley and Taylor parameter alpha = 1.26 for potential evaporation in high latitudes. *Journal of Applied Meteorology* **16**, 649-650.

Stitger, C.J., 1980. Solar radiation as statistically related to sunshine duration: a comment using low-latitude data. *Agricultural Meteorology* **21**, 173-178.

Sumner, D.M. and Jacobs, J.M., 2005. Utility of Penman-Monteith, Priestley-Taylor, reference evapotranspiration, and pan evaporation methods to estimate pasture evapotranspiration. *Journal of Hydrology* **308**, 81-104.

Sweers, H.E., 1976. A nomograph to estimate the heat-exchange coefficient at the air-water interface as a function of wind speed and temperature; a critical survey of some literature. *Journal of Hydrology* **30**, 375-401.

Szeicz, G., Endrödi, G., and Tajchman, S., 1969. Aerodynamic and surface factors in evaporation. *Water Resources Research* **5** (2), 380-396.

Szilagyi, J., 2001. Modeled areal evaporation trends over the conterminous United States. *Journal of Irrigation and Drainage Engineering* **127** (4), 196-200.

Szilagyi, J., 2007. On the inherent asymmetric nature of the complementary relationship of evaporation. *Geophysical Research Letters* **34**, L02405, doi:10.1029/2006GL028708.

Szilagyi, J. and Jozsa, J., 2008. New findings about the complementary relationship-based evaporation estimation methods. *Journal of Hydrology* **354**, 171-186.

Szilagyi, J., Hobbins, M.T., and Jozsa, J., 2009. Modified Advection-Aridity model of evapotranspiration. *Journal of Hydrologic Engineering* **14** (6), 569-574.

Tang, R., Li, Z-L., and Tang, B., 2010. An application of the T-s-VI triangle method with enhanced edges determination for evapotranspiration estimation from MODIS data in and semi-arid regions: Implementation and validation *Remote Sensing of Environment* **114** (3), 540-551, doi: 10.1016/j.rse.2009.10.012.

Teklehaimont, Z. and Jarvis, P.G., 1991. Direct measurement of evaporation of intercepted water from forest canopies. *Journal of Applied Ecology* **28**, 603-618.

Thom, A.S., Thony, J.-L., and Vauclin, M, 1981. On the proper employment of evaporation pans and atmometers in estimating potential transpiration. *Quarterly Journal of the Royal Meteorological Society* **107**, 711-736.

Thornthwaite, C.W. 1948. An approach toward a rational classification of climate. *Geographical Review* **38** (1), 55-94.

Thornthwaite, C.W. and Mather, J.R. 1957 Instructions and Tables for the Computing Potential Evapotranspiration and the Water Balance, *Drexel Institute of Technology Publications in Climatology* **10**, 185-311.

Tiris, M., Tiris, C., and Erdalli, Y., 1997. *Water heating systems by solar energy*. Marmara Research Centre, Institute of Energy Systems and Environmental Research, NATO TU-COATING, Gebze, Kocaeli, Turkey [in Turkish].

Trajkovic, S. and Kolakovic. S., 2009. Evaluation of reference evapotranspiration equations under humid conditions. *Water Resources Management* **23**, 3057-3067.

Trajkovic, S.and Kolakovic, S., 2010. Comparison of simplified pan-based equations for estimating reference evapotranspiration. *Journal of Irrigation and Drainage Engineering* **136** (2), 137-140.

Trajković, S. and Stojnić, V., 2007. Effect of wind speed on accuracy of Turc method in a humid climate. *Facta Universitstis, Architecture and Civil Engineering* **5** (2), 107-113.

Turc, L., 1954. Le bilan d'eau des sols. Relations entre les précipitations, l'evaporation et l'écoulement. *Annual Agronomy* **5**, 491-596.

Turc, L., 1955. Le bilan d'eau des sols. Relations entre les précipitations, l'evaporation et l'écoulement. *Annual Agronomy* **6**, 5-131.

Turc, L., 1961. Estimation of irrigation water requirements, potential evapotranspiration: A simple climatic formula evolved up to date (in French). *Annual Agronomy* **12**, 13–49.

Ulgen, K. and Hepbasli. A., 2004. Solar radiation models. Part 1: a review. *Energy Sources* **26**, 507-520.

Valiantzas, J.D., 2006. Simplified versions for the Penman evaporation equation using routine weather data. *Journal of Hydrology* **331**, 690-702.

van Bavel, C.H.M., 1966. Potential evaporation: The combination concept and its experimental verification. *Water Resources Research* **2** (3), 455-467.

van Dijk, M.H., 1985. Reduction in evaporation due to the bird screen used in the Australian class-A pan evaporation network. *Australian Meteorological Magazine* **33**, 181-183.

Vardavas, I.M., 1987. Modelling the seasonal variation of net all-wave radiation flux and evaporation in a tropical wet-dry region. *Ecological Modelling* **39**, 247-268.

Vardavas, I.M. and Fountoulakis, A., 1996. Estimation of lake evaporation from standard meteorological measurements: application to four Australian lakes in different climatic regions. *Ecological Modelling* **84**, 139-150.

Wallace, J. and McJannet, D., 2010. Processes controlling transpiration in the rainforests of north Queensland, Australia. *Journal of Hydrology* **384**, 107-117.

Wang, Q.J., Chiew, F.H.S., McConachy, F.L.N., James, R., de Hoedt, G.C., and Wright, W.J. 2001. *Climatic Atlas of Australia Evapotranspiration*. Bureau of Meteorology, Commonwealth of Australia.

Watts, P.J. and Hancock, N.H., 1984. Evaporation and potential evaporation – A practical approach for agricultural engineers. Conference on Agricultural Engineering, Bundaberg, *The Institution of Engineers Australia*, *National Conference Publication* **84** (6), 290-297.

Webb, E.K., 1966. A pan-lake evaporation relationship: J*ournal of Hydrology*, **4**:1-11.

Weeks, W.D., 1982. Evaporation: a case study using data from a lake in Eastern Queensland. Hydrology and Water resources Symposium, Melbourne, *The Institution of Engineers*, *Australia*, *National Conference Publication* **82**(3), 189-193.

Weiβ, M. and Menzel, L., 2008. A global comparison of four potential evapotranspiration equations and their relevance to stream flow modelling in semi-arid environments. *Advances in Geoscience* **18**, 15-23.

Wessel, D.A. and Rouse, W.R., 1994. Modelling evaporation from wetland tundra. *Boundary-Layer Meteorology* **68**, 109-130.

Wieringa, J., 1986. Roughness-dependent geographical interpolation of surface wind speed averages. *Quarterly Journal of Royal Meteorological Society* **112**, 867-889.

Winter, T.C., 1981. Uncertainties in estimating the water balance of lakes. *Water Resources Bulletin*, 17: 82 - 115.

Winter, T.C. and Rosenberry, D.O., 1995. Evaluation of 11 equations for determining evaporation for a small lake in the north central United States. *Water Resources Research* **31** (4), 983-993.

Xu, C.-Y. and Chen, D. 2005. Comparison of seven models for estimation of evapotranspiration and groundwater recharge using lysimeter measurement data in Germany. *Hydrological Processes* **19**, 3717-3734.

Xu, C.-Y.and Singh, V.P., 2001. Evaluation and generalisation of temperature-based methods for calculating evaporation. *Hydrological Processes* **15**, 305-319.

Yang, K., Koike, T., and Ye, B., 2006. Improving estimation of hourly, daily, and monthly solar radiation by importing global data sets. *Agricultural and Forest Meteorology* **137**, 43–55.

Yang, J. and Wang, Y., 2011. Estimating evapotranspiration fraction by modeling two-dimensional space of NDVI/albedo and day-night surface temperature difference: A comparative study. *Advances in Water Resources* **34**, 512-518.

Yin, Z.-Y. and Brook, G.A., 1992. Evapotranspiration in the Okefenokee Swamp watershed: a comparison of temperature-based and water balance methods. *Journal of Hydrology* **131**, 293-312.

Young, A.A., 1947. Some recent evaporation investigations. *Transactions of the American Geophysical Union* **28**, 279-284.

Zhang, L., Dawes, W.R., and Walker G. R, 2001, Response of mean annual evapotranspiration to vegetation changes at catchment scale. *Water Resources Research* **37** (3), 701-708.

Table S1 Values of specific constants

Constant	Symbol	Value	Reference
Atmospheric pressure	p	$101.3\left(\frac{293-0.0065Elev}{293}\right)^{5.26}$ kPa*	Dingman (1992, p. 224)
Density of water	ρ_w	997.9 kg m^{-3} at 20°C	Dingman (1992, p. 542)
Mean air density	ρ_a	1.20 kg m^{-3} at 20°C	Shaw (1994, p. 6)
Emissivity of water	ε_w	0.95	Dingman (1992, p. 583)
Surface emissivity	ε_s	0.92 (adopted by Morton)	Morton (1983b, p. 64)
Specific heat of water	c_w	4.19 kJ kg^{-1} °C^{-1}	Maidment (1992, p. 7.23) Morton (1979, p.72)
Specific heat of air	c_a	1013 J kg^{-1} K^{-1}	Allen et al. (1998, Equation 8); McJannet et al. (2008, page 43)
Latent heat of vaporization	λ	2.45 MJ kg^{-1} at 20°C 28.5 W days kg^{-1}	Dingman (1992, p. 547) Allen et al. (1998, p. 31) Morton (1983b, p. 65)
Psychrometric constant	γ	$\gamma = 0.00163\frac{p}{\lambda}$ kPa°C^{-1}	Dingman (1992, p. 225)
Stefan-Boltzmann constant	σ	4.90×10^{-9} MJ m^{-2} day^{-1} K^{-4} 5.67×10^{-8} W m^{-2} K^{-4}	Dingman (1992, p. 582) Morton (1983a, p.64)
von Kármán constant	k	0.41	Szeicz et al., 1969) p. 380)

* $Elev$ is elevation (m)

Table S2 Roughness height, aerodynamic and surface resistance of typical surfaces

Surface	Location	Height of surface condition (m)	Zero-plane displacement (m)	Roughness length (m)	Aerodynamic resistance, r_a, (s m^{-1})	Average surface resistance, r_s, (s m^{-1})
Open sea, fetch >5 km				0.0002 o	see **Appendix S4**	
Open water		0.01 n		0.001 n		0 n
Open flat terrain: grass				0.03 o		
Desert		0.001 e	0.1 c	0.05 c		200 e
Semi-desert			0.5 c	0.1 c		
Arid land						250 j
Cultivation				0.005 e		91 f
Hypothetical reference crop		0.12 a			104 a	70 a
Well watered production crops						50 j
Short grass			0.2 c	0.02 c		
Tall grass			1 c	0.1 c		
Low crops				0.10 o		
High crops				0.25 o		
Grassland	Based on 7 sites in northern hemisphere	0.5* e, g (0.05 – 0.85) 0.5e		0.01 e, g	37 e, g (14 - 71)	40 e, g (5 – 143) 125
Uncut lucerne		1.0 n		0.1 n	22 n	60 n
Evergreen shrub			1 c	0.1 c		
Deciduous shrub			1 c	0.1 c		
Parkland, bushes				0.5 o		
Non-forest wetland		0.3 e				152 e
Savannah/xeric shrub		8.0 e				189 e
Coniferous forest	Based on 8 references world-wide	8 e, g (5 – 20) 25			7 e, g (5 – 14)	50 e, g (30 - 125) 189
Evergreen needleleaf forest			15 c	1.0 c		

Deciduous needleleaf forest			20 c	1.0 c		
Beech	Northern Apennines, Italy					200 i
Evergreen broadleaf forest			20 c	2.0 c		
Deciduous broadleaf forest			15 c	0.8 c		
Eucalyptus plantation	São Paulo State, Brazil	12-21 b			summer 19±14 b winter 9±2	summer 19±14 b winter 167±292
Eucalyptus maculata	Kioloa State Forest,NSW, Australia					60 d
Eucalyptus forest	Collie, Western Australia				5 l	50 l
Lower montane rainforest	Nth Q'ld, Australia	25 & 32 m				summer 71 & 163 m winter 56 & 119
Pristine lowland rain forest	Nth Q'ld, Australia	27 m				summer 171 m winter 115
Upper montane cloud rainforest	Nth Q'ld, Australia	8 m				summer 317 m winter 160
Mixed woodland			20 c	0.8 c		
Tropical rainforest	French Guiana	~28 d				140 – 170 d
Tropical trees	Panama					250 – 500 k
Lowland mixed dipterocarp forest	Sarawak, Borneo	50 h			10 h	84 h
Regular large obstacle coverage (suburb, forest)				1.0 o		

a: Allen et al. (1998, page 23), b: Cabral et al. (2010), c: Douglas et al. (2009), d: Dunin and Greenwood (1986, page 51), e: Federer et al. (1996), f: Granier et al. (1996), g: Kelliher et al.(1993), h: Kumagai et al. (2004), i: Magnani et al. (1998, page 870), j: McNaughton and Jarvis (1991), k: Meinzer et al. (1997), l: Sharma (1984, page 49), m : Wallace & McJannet (2010), n: Watt & Hancock (1984), o: Wieringa (1986, Table 1) based on Davenport (1960)

*Value is median of a range shown in parenthesis # clonal *Eucalyptus grandis* × *Eucalyptus urophylla*

Table S3 Albedo values

Surface	Albedo, α	Reference
Water*	0.08	Maidment (1992)
Desert (bare ground)	0.30	McVicar et al. (2007)
Semi-desert	0.25	Douglas et al. (2009)
Tundra	0.20	Douglas et al. (2009)
Short grass	0.26	Watts & Hancock (1984)
Pasture (short grass)	0.26	McVicar et al. (2007), Douglas et al. (2009)
Reference (short) crop	0.23	Allen et al. (1998, page 51)
Long grass (1 m)	0.16	Watts & Hancock (1984)
Irrigated crop	0.18	Douglas et al. (2009)
Crop/mixed farming	0.20	Douglas et al. (2009)
Evergreen shrub	0.10	Douglas et al. (2009)
Deciduous shrub	0.20	Douglas et al. (2009)
Sparse forest	0.18	McVicar et al. (2007)
Rain forest	0.15	Dingman (1992)
Eucalypts	0.20	Dingman (1992)
Evergreen needleleaf forest	0.10	Douglas et al. (2009)
Deciduous needleleaf forest	0.20	Douglas et al. (2009)
Evergreen broadleaf forest	0.15	Douglas et al. (2009)
Deciduous broadleaf forest	0.20	Douglas et al. (2009)
Forest (mixed woodland)	0.15	McVicar et al. (2007), Douglas et al. (2009)
Urban area	0.25	McVicar et al. (2007)

* Based on Cogley (1979), Jensen (2010, Table 1) provides a table of albedo values for water. Jensen's table shows that albedo for water has a seasonal pattern being high in winter and low in summer and increases from an average value of 0.065 at the equator to values varying from 0.11 to 0.36 at 60° – 70°N latitude.

Table S4 Median, 10th and 90th percentile monthly evaporation based on data recorded at the 68 Australian AWSs for three Penman wind functions, and for FAO-56 Reference Crop and Priestley-Taylor algorithms expressed as a percentage of the Penman (1948) median estimate

Parameter	Penman (1948) wind function	Penman Penman (1956) wind function	Linacre (1993)	FAO-56 Reference Crop	Priestley-Taylor
Median	100%	-9.9%	-15.8%	-26.4%	-17.1%
10th percentile	-63.0%	-67.5%	-72.0%	-74.3%	-75.7%
90th percentile	57.4%	45.5%	33.4%	22.3%	29.2%

Table S5 Guideline for defining shallow and deep lakes and the methods to estimate lake evaporation

Shallow lake	Average depth (m)	***Deep lake***	Average depth (m)
Morton recommendations			
Morton CRWE		Morton CRLE	
Seasonal heat storage changes (Morton, 1983b, page 84) and water advection are not important	undefined	For depths less than 1.5 m use CRWE (Morton, 1986, page 385)	1.5
Deep lakes are considered shallow if one is interested only in annual or mean annual evaporation (Morton, 1983b, page 84)	undefined	Seasonal heat storage changes and water advection are important	undefined
Recommendations of other authors			
Shallow lake without seasonal heat storage analysis		***Deep lake***	
Sacks et al (1994, Abstract)	3	Vardavas & Fountoulakis (1996)	3 – 23
Penman equation can be applied without adjusting for heat storage Monteith (1981, page 9)	less than "…a metre or so…"	Kohler & Parmele (1967)	undefined
de Bruin (1978, Section 2)	3		
Shallow lake with seasonal heat storage analysis			
McJannet et al. (2008b)	1 – 6	McJannet et al. (2008b)	25 - 30
Finch & Gash (2002)	10	Finch & Gash (2002)	10
Finch (2001)	10		
Fennessey (2000)	2		
Sacks et al (1994, page 312)	< 5		
Fraedrich et al. (1977, Section 6)	8		
Stewart & Rouse (1976, page 624)	0.6		
Keijman and Koopmans (1973)	3.0		

Table S6 Mean monthly screened Class-A evaporation pan coefficients for estimating Penman open-water evaporation (1956 wind function) at 68 Australian locations

For each station, the second row of values specifies the number of months used to compute the mean monthly pan coefficients. Asterisk denotes high quality Class-A evaporation pan. nd is no data

BOM ref.	Station name	Lat °S	Long °E	Jan	Feb	Mar	Apr	May	Jun	Jul	Aug	Sep	Oct	Nov	Dec	Year
2012	Halls Creek Airport*	-18.23	127.66	0.735	0.880	0.753	0.696	0.702	0.711	0.702	0.696	0.671	nd	0.709	0.697	0.723
				3	2	2	3	2	2	2	1	1	0	1	1	
3003	Broome Airport*	-17.95	122.24	0.822	0.842	0.866	0.816	0.742	0.743	0.768	0.788	0.859	0.897	0.882	0.837	0.822
				9	12	7	13	16	14	14	14	16	15	16	11	
7178	Paraburdoo	-23.20	117.67	0.607	0.571	0.591	0.614	0.564	0.654	0.594	0.644	0.635	0.587	0.608	0.591	0.605
				2	1	2	1	3	3	1	2	3	3	3	2	
9021	Perth Airport*	-31.93	115.98	0.825	0.821	0.782	0.818	0.827	0.850	0.915	0.984	0.979	0.960	0.903	0.862	0.877
				16	16	16	16	16	15	15	16	15	15	16	16	
9034	Perth Reg. Office*	-31.96	115.87	0.912	0.866	0.837	0.837	0.818	0.807	0.869	0.931	0.942	0.966	0.942	0.945	0.889
				14	11	11	11	13	11	10	11	11	9	12	12	
9538	Dwellingup	-32.71	116.06	0.880	0.867	0.864	0.921	0.813	0.789	0.748	0.912	0.933	1.028	0.963	0.923	0.887
				10	11	13	13	9	11	9	6	9	12	14	12	
9592	Permberton	-34.45	116.04	0.950	0.941	0.883	0.920	0.981	0.890	nd	nd	0.892	0.980	0.983	0.962	0.938
				3	4	2	2	1	1	0	0	1	1	1	2	
9741	Albany Airport*	-34.94	117.80	0.827	0.822	0.809	0.856	0.859	0.830	0.882	0.938	0.970	0.987	0.917	0.856	0.879
				16	15	12	15	17	16	15	17	13	15	18	15	
13017	Giles Met. Office*	-25.03	128.30	0.650	0.656	0.650	0.686	0.727	0.765	0.755	0.747	0.718	0.694	0.678	0.659	0.699
				28	26	25	27	28	30	29	28	27	28	27	28	
14015	Darwin Airport*	-12.42	130.89	0.775	0.771	0.866	0.855	0.779	0.744	0.766	0.812	0.836	0.853	0.838	0.779	0.806
				10	12	13	25	24	29	26	29	30	25	17	16	
14198	Jabiru Airport	-12.66	132.89	0.842	0.856	0.827	0.812	0.766	0.709	0.734	0.740	0.732	0.773	0.788	0.848	0.786
				2	3	4	3	6	4	5	5	7	7	4	2	
14508	Gove Airport*	-12.27	136.82	0.859	0.831	0.899	0.889	0.888	0.863	0.889	0.921	0.935	0.944	0.922	0.864	0.892
				18	16	17	19	17	19	19	20	21	22	15	18	

14513	Wallaby Beach	-12.19	136.71	nd	0.773	nd	0.846	0.862	0.811	0.751	0.873	0.873	0.920	0.890	0.782	0.838
				0	1	0	3	3	3	3	3	5	5	4	3	
14612	Larrimah	-15.57	133.21	0.756	0.878	0.850	0.780	0.792	0.739	0.793	0.798	0.756	0.709	0.697	0.577	0.760
				4	3	4	3	1	3	2	2	6	1	3	3	
14703	Centre Island	-15.74	136.82	nd	nd	0.825	0.912	0.816	0.872	0.905	1.060	0.923	0.975	0.870	0.950	0.911
				0	0	1	2	1	2	2	1	2	3	2	2	
14704	McArthur River Mine	-16.44	136.08	0.700	0.721	0.773	0.734	0.694	0.666	0.671	0.701	0.703	0.688	0.700	0.660	0.701
				4	9	6	4	4	9	5	7	4	4	5	4	
15135	Tennant Creek Airport*	-19.64	134.18	0.644	0.667	0.632	0.601	0.623	0.648	0.657	0.649	0.627	0.632	0.633	0.646	0.638
				24	21	27	28	30	29	28	27	28	28	29	24	
15590	Alice Springs Airport*	-23.80	133.89	0.668	0.669	0.657	0.690	0.737	0.781	0.783	0.756	0.724	0.712	0.684	0.675	0.711
				24	27	25	21	26	24	25	25	28	26	26	24	
15666	Rabbit Flat	-20.18	130.01	0.721	0.789	0.765	0.764	0.779	0.797	0.762	0.761	0.731	0.756	0.715	0.808	0.762
				4	8	7	7	7	6	6	8	7	9	7	3	
16001	Woomera Aerodrome*	-31.16	136.81	0.695	0.687	0.691	0.715	0.731	0.790	0.788	0.777	0.766	0.759	0.725	0.711	0.736
				24	28	28	28	28	25	27	30	25	28	27	29	
17043	Oodnadatta Airport	-27.56	135.45	0.630	0.633	0.652	0.669	0.713	0.754	0.750	0.762	0.739	0.744	0.656	0.636	0.695
				5	5	5	4	5	6	5	4	4	3	5	4	
18012	Ceduna AMO*	-32.13	133.70	0.828	0.816	0.793	0.773	0.781	0.834	0.831	0.848	0.841	0.835	0.823	0.821	0.819
				23	27	28	29	29	28	29	28	27	28	28	29	
23034	Adelaide Airport	-34.95	138.52	0.827	0.808	0.789	0.786	0.800	0.833	0.858	0.866	0.890	0.886	0.862	0.831	0.836
				27	24	21	25	22	21	20	22	23	23	25	23	
23090	Adelaide (Kent Town)*	-34.92	138.62	0.905	0.895	0.922	0.890	0.912	0.925	0.937	0.979	0.969	0.995	0.938	0.920	0.932
				10	10	9	8	8	9	9	9	9	9	9	9	
23321	Nuriootpa Comparison*	-34.48	139.00	0.803	0.791	0.787	0.844	0.887	0.925	0.992	0.971	0.980	0.935	0.857	0.815	0.882
				19	20	18	16	20	19	18	19	18	19	16	20	
23373	Nuriootpa Viticultural*	-34.48	139.01	0.804	0.783	0.780	0.820	0.814	0.908	0.924	0.944	1.043	0.947	0.880	0.836	0.874
				9	8	4	6	7	5	5	5	5	9	7	6	
24024	Loxton Res. Centre	-34.44	140.60	0.785	0.790	0.797	0.849	0.858	0.899	0.940	0.929	0.933	0.892	0.834	0.804	0.859
				18	18	24	21	21	22	21	18	22	16	20	18	

26021	Mount Gambier Aero*	-37.75	140.77	0.920	0.907	0.876	0.918	0.949	1.013	1.031	1.024	1.039	1.044	0.991	0.945	0.972
				31	30	29	30	28	29	28	28	30	30	27	30	
27045	Weipa Aero*	-12.68	141.92	0.774	0.838	0.861	0.890	0.844	0.779	0.788	0.794	0.823	0.836	0.856	0.831	0.826
				4	5	3	9	14	15	13	16	10	13	8	8	
29126	Mount Isa Mine	-20.74	139.48	0.689	0.720	0.679	0.674	0.662	0.705	0.710	0.705	0.674	0.664	0.674	0.686	0.687
				11	10	10	10	10	11	11	9	11	12	12	3	
29127	Mount Isa Aero*	-20.68	139.49	0.745	0.752	0.729	0.706	0.726	0.736	0.749	0.745	0.723	0.709	0.718	0.727	0.730
				23	20	26	26	28	29	27	29	28	27	21	21	
31011	Cairns Aero*	-16.87	145.75	0.851	0.835	0.858	0.873	0.838	0.835	0.831	0.857	0.847	0.850	0.835	0.832	0.845
				12	10	11	16	22	24	24	24	25	26	22	19	
32040	Townsville Aero*	-19.25	146.77	0.824	0.821	0.812	0.773	0.771	0.762	0.777	0.794	0.809	0.814	0.812	0.827	0.800
				18	11	22	24	24	26	28	27	28	25	22	16	
40223	Brisbane Aero	-27.42	153.11	0.848	0.822	0.830	0.836	0.858	0.857	0.860	0.844	0.859	0.848	0.845	0.841	0.846
				11	8	9	11	14	13	14	13	14	12	13	11	
40428	Brian Pastures*	-25.66	151.75	0.773	0.794	0.786	0.772	0.752	0.738	0.755	0.787	0.806	0.813	0.806	0.772	0.779
				22	22	18	22	24	21	24	18	22	21	21	19	
40842	Brisbane aero	-27.39	153.13	0.857	0.856	0.847	0.858	0.856	0.849	0.856	0.885	0.880	0.863	0.877	0.844	0.861
				8	6	9	9	9	6	10	9	9	10	7	9	
48027	Cobar aero*	-31.48	145.83	0.736	0.727	0.725	0.765	0.802	0.863	0.882	0.873	0.843	0.815	0.768	0.732	0.794
				26	28	28	26	23	25	26	25	28	25	28	24	
53048	Moree Comparison*	-29.48	149.84	0.809	0.822	0.795	0.813	0.846	0.878	0.915	0.946	0.899	0.866	0.843	0.811	0.854
				16	15	17	16	15	14	14	15	15	16	15	15	
53115	Moree Aero*	-29.49	149.85	0.791	0.783	0.786	0.777	0.797	0.862	0.886	0.883	0.867	0.838	0.811	0.788	0.822
				9	10	12	13	14	13	12	15	14	14	12	14	
55024	Gunnedah Res. Centre*	-31.03	150.27	0.713	0.687	0.708	0.675	0.667	0.649	0.558	nd	nd	nd	0.763	0.710	0.681
				1	2	3	3	1	3	1	0	0	0	3	3	
55054	Tamworth Airport	-31.09	150.85	0.806	0.795	0.809	0.802	0.858	0.904	0.912	0.962	0.896	0.876	0.863	0.830	0.859
				11	10	12	12	12	14	12	9	10	11	9	10	
56018	Inverell Res. Centre	-29.78	151.08	0.873	0.857	0.837	0.871	0.810	0.783	0.799	0.888	0.908	0.906	0.921	0.879	0.861
				8	8	6	7	10	9	10	11	11	10	11	8	

59040	Coffs Harbour MO*	-30.31	153.12	0.839	0.850	0.835	0.838	0.842	0.827	0.844	0.865	0.890	0.889	0.869	0.886	0.856
				19	20	15	24	18	21	23	25	27	28	23	21	
61078	Williamtown RAAF*	-32.79	151.84	0.810	0.805	0.836	0.819	0.820	0.770	0.808	0.848	0.858	0.839	0.829	0.816	0.821
				25	23	23	22	24	20	25	25	26	26	24	25	
61089	Scone SCS*	-32.06	150.93	0.862	0.853	0.841	0.870	0.879	0.895	0.908	0.933	0.953	0.937	0.891	0.851	0.889
				12	13	14	13	14	14	13	15	14	12	13	12	
66037	Sydney Airport AMO*	-33.95	151.17	0.835	0.835	0.827	0.826	0.846	0.805	0.828	0.847	0.862	0.873	0.857	0.842	0.840
				27	22	28	23	19	26	25	26	24	22	26	26	
67033	Richmond RAAF	-33.60	150.78	0.839	0.837	0.846	0.842	0.899	0.880	0.869	0.850	0.849	0.848	0.854	0.825	0.853
				15	12	15	13	16	15	13	14	14	14	15	13	
68076	Nowra RAN Air Station	-34.94	150.55	0.783	0.774	0.796	0.764	0.735	0.685	0.771	0.786	0.790	0.784	0.789	0.785	0.770
				15	15	19	17	16	17	17	15	13	15	17	13	
70014	Canberra Airport Comparison*	-35.30	149.20	0.785	0.791	0.770	0.801	0.820	0.849	0.881	0.879	0.873	0.883	0.852	0.811	0.833
				30	28	28	30	29	29	29	27	28	31	28	29	
70015	Canberra Forestry	-35.30	149.10	nd	nd	0.677	0.812	0.860	0.973	0.943	0.994	0.933	nd	nd	nd	0.885
				0	0	1	1	1	1	1	1	1	0	0	0	
72060	Khancoban SMHEA	-36.23	148.14	0.869	0.867	0.867	0.958	1.022	1.221	1.227	1.164	1.040	1.028	0.949	0.873	1.007
				13	12	14	14	11	14	12	13	12	13	13	12	
72150	Wagga Wagga AMO*	-35.16	147.46	0.815	0.813	0.810	0.865	0.944	0.984	1.069	1.097	1.053	0.988	0.893	0.843	0.931
				24	25	23	21	23	22	22	22	24	22	20	23	
76031	Mildura Airport*	-34.24	142.09	0.793	0.785	0.785	0.819	0.840	0.882	0.921	0.925	0.889	0.864	0.838	0.811	0.846
				19	21	20	17	19	19	19	20	20	21	20	19	
82039	Rutherglen Research*	-36.10	146.51	0.821	0.819	0.806	0.862	0.897	0.904	0.989	0.993	1.025	1.056	0.919	0.804	0.908
				16	16	17	13	15	12	16	11	13	9	14	13	
85072	East Sale Airport*	-38.12	147.13	0.887	0.872	0.879	0.911	0.912	0.900	0.913	0.966	0.954	0.987	0.935	0.903	0.918
				25	26	26	26	28	25	29	26	29	23	25	27	
85103	Yallourn SEC	-38.19	146.33	0.885	0.820	0.917	0.935	1.070	0.914	0.959	1.007	1.101	1.029	1.033	0.940	0.968
				7	6	7	7	2	4	4	7	2	4	2	2	
86282	Melbourne Airport	-37.67	144.83	0.835	0.816	0.799	0.795	0.847	0.868	0.872	0.892	0.859	0.887	0.895	0.838	0.850
				9	9	9	9	9	10	8	8	10	11	11	11	

87031	Laverton RAAF	-37.86	144.76	0.812	0.789	0.765	0.771	0.788	0.846	0.881	0.880	0.907	0.896	0.864	0.825	0.835
				16	20	20	21	20	19	20	17	17	15	19	18	
88023	Lake Eildon*	-37.23	145.91	1.015	1.010	1.034	1.139	1.281	1.444	1.546	1.405	1.281	1.229	1.145	1.028	1.213
				26	26	22	19	22	24	20	23	24	22	19	23	
90103	Hamilton Res. Station	-37.83	142.06	0.784	0.725	0.692	0.739	0.713	0.681	0.717	0.776	0.862	0.935	0.907	0.841	0.781
				15	14	9	11	7	7	11	9	12	9	9	12	
91104	Launceston Airport Companion*	-41.54	147.20	0.880	0.882	0.858	0.908	0.967	0.961	1.062	1.110	1.079	1.043	0.979	0.893	0.968
				20	20	20	20	18	15	15	19	18	22	19	19	
91219	Scottsdale	-41.17	147.49	1.008	1.024	1.009	1.065	1.007	0.936	0.952	1.062	1.105	1.137	1.101	1.027	1.036
				24	22	17	14	15	15	17	17	16	18	21	24	
92038	Swansea Post Office	-42.12	148.07	0.903	0.903	0.916	0.987	1.085	0.982	0.969	1.010	1.036	1.049	0.961	0.941	0.979
				2	2	2	2	2	2	2	2	2	2	2	1	
94008	Hobart Airport	-42.83	147.50	0.888	0.897	0.889	0.879	0.863	0.916	0.913	0.970	0.987	0.978	0.950	0.912	0.920
				19	22	20	20	20	21	21	22	21	21	20	19	
94029	Hobart (Ellerslie Road)	-42.89	147.33	0.972	0.932	0.941	0.936	0.944	0.993	0.991	0.974	1.022	1.079	1.007	0.968	0.980
				15	16	16	15	15	16	13	15	14	15	15	14	
94069	Grove (Comparison)*	-42.98	147.08	0.873	0.854	0.864	0.858	0.823	0.855	0.876	0.852	0.926	0.949	0.945	0.920	0.883
				18	20	21	21	16	18	13	14	19	20	18	20	
96033	Liawenee	-41.90	146.67	1.057	nd	1.075	nd	nd	nd	nd	nd	nd	nd	1.132	1.068	1.083
				3	0	1	0	0	0	0	0	0	0	2	2	
97053	Strathgordon Village*	-42.77	146.05	0.973	0.955	0.947	0.870	0.946	0.765	0.708	0.748	0.890	0.989	1.023	0.947	0.897
				6	7	7	4	4	7	4	8	6	5	8	6	

Table S7 Comparison of equations to estimate evaporation from a lake covered with vegetation
(Adv. and Disadv. are abbreviations for advantage and disadvantage, respectively.)

Reference	Application	Penman (Section 2.1.1)	Penman-Monteith (Section 2.1.2)	Weighted Penman-Monteith (Equation S5.30)	Shuttleworth-Wallace (Equation S5.22)	Priestley-Taylor (Section 2.1.3)
Wessel & Rouse (1994) Table III	Wetland tundra		Adv: accurate if r_s is available Disadv: inadequate for complex surfaces	Adv: handle any surfaces Weight components by surface area	Disadv: Cannot model area with no canopy. Not recommended	
	Bowen Ratio		0.75 (1.21)#	1.10 (1.41)	1.35 (1.65)	
Abtew & Obeysekera (1995) Figures 7 to 9	South Florida	The two coefficients in the wind function were found by calibration	Monteith (1965) r_a from Equation S5.3. r_s varied from 25 s m^{-1} during high ET season and 90 s m^{-1} for rest of year.			α = 1.18 by calibration
	Lysimeter within wetland complex	P=0.03+1.01Meas (see = 0.57 mm day^{-1})	PM=1.17+0.75Meas (see = 0.39 mm day^{-1})			PT=1.15 +070Meas (see = 0.53 mm day^{-1})
Souch et al. (1998) Table 3	Indiana, USA Undisturbed site	Penman modified by Shuttleworth (1992)	r_a from Shuttleworth (1992, Equation 4.2.25); r_s = 0 for standing water & r_s = 5 s m^{-1} for vegetation			Assumed vapour pressure deficits depressed, α = 1
	Eddy correlation	1.03 (0.67)	0.98 (0.44)			1.03 (0.67)
Bidlake (2000) Table 4	Wetland in Oregon, USA (semi-arid)		Several calibrations were based on r_s. Chosen best option			Calibrated with α overall <1

	Eddy correlation		0.98* (1.04)			0.92* (1.00)
Lott & Hunt (2001) Table 2	Wisconsin, USA	Adopted Dunne & Leopold (1978) to compute E_a				
	Lysimeter and water table fluctuations	Natural wetland 0.70 Constructed wetland 1.01				
Jacobs et al. (2002) Table 3	Highland marsh Florida, USA	Penman (1956)	r_a = Monin-Obukhov similarity for neutral conditions			α = 1.26
	Eddy correlation	1.31 (1.83)	1.14 (1.62)			1.39 (1.59)
Drexler et at. (2004)		Adv: Minimal data Disadv: does not account for r_s	Adv: Minimal data, accounts for r_s Disadv: Can't handle mixed vegetation, hence r_a and r_s difficult to estimate	Adv: can handle r_a and r_s for different surfaces including standing water	Disadv: Does not handle standing water	Disadv: No wind component nor r
	No quantitative comparisons					

Value is ratio of mean model estimate to mean measured estimate. Values in parentheses are root mean square error in mm day^{-1}. * Value is based on the slope of the regression between the model and the measured values.

Table S8 Measured values of Priestley-Taylor coefficient (α_{PT})

(Partly adapted from Flint and Childs (1991) and Fisher et al. (2005))

α_{PT}	Surface	Daily (24 hr) or day-time (day-light hour)	Reference
1.57	Strongly advective conditions	na	Jury and Tanner (1975)
1.29	Grass (soil at field capacity)	daily	Mukammal and Neumann (1977)
1.27	Irrigated ryegrass	daily	Davies and Allen (1973)
1.26	Saturated surface	daily	Priestley and Taylor (1972)
1.26	Open-surface water	daily	Priestley and Taylor (1972)
1.26	Wet meadow	daily	Stewart and Rouse (1977)
1.18	Wet Douglas-fir forest	daily	McNaughton and Black (1973)
1.12	Short grass	day-time	De Bruin and Holtslag (1982)
1.09	Boreal broad-leaf deciduous N = 1	daily	Komatsu (2005)
1.05	Douglas-fir forest	daily	McNaughton and Black (1973)
1.04	Bare soil surface	day-time	Barton (1979)
0.90	Mixed reforestation (water limited)	daily	Flint and Childs (1991)
0.87	Ponderosa pine (water limited)	day-time	Fisher et al. (2005)
0.85	Temperate broad-leaf deciduous N = 9	day-time	Komatsu (2005)
0.84	Douglas-fir forest (unthinned)	daily	Black (1979)
0.82	Tropical broad-leaf evergreen N = 7	day-time	Komatsu (2005)
0.80	Douglas-fir forest (thinned)	daily	Black (1979)
0.76	Temperate broad-leaf evergreen N = 5	day-time	Komatsu (2005)
0.73	Douglas-fir forest	day-time	Giles et al. (1984)
0.72	Spruce forest	day-time	Shuttleworth and Calder (1979)
0.65	Temperate coniferous evergreen N = 35	day-time	Komatsu (2005)
0.55	Boreal coniferous evergreen N = 8	day-time	Komatsu (2005)
0.53	Boreal coniferous deciduous N = 2	day-time	Komatsu (2005)

na: not known; N is the number of experimental sites

Table S9 Effect of type and length fetch, wind speed and humidity on Class-A pan coefficients without bird-guard*

Wind	Fetch length (m)	Green vegetated fetch in a dry area		Dry fetch in a green vegetated area	
		Low humidity < 40%	High humidity > 70%	Low humidity < 40%	High humidity > 70%
Light	10	0.65	0.85	0.60	0.80
< 2 m s^{-1}	1000	0.75	0.85	0.50	0.70
Strong	10	0.55	0.65	0.50	0.65
5 - 8 m s^{-1}	1000	0.60	0.75	0.40	0.55

*Results were extracted from Allen et al. (1998, Table 5)

Table S10 Published references listing annual Class-A pan coefficients based on the Penman equation with wind functions of Penman (1948) and Penman (1956), Reference Crop equation and Priestley-Taylor equation

Reference	Location	Number of sites	Time-step D or M	Penman (1948)	Penman (1956)	Reference Crop	Priestley-Taylor
Screened pan							
Weeks (1982)	Callide Dam, Queensland	1	M	0.88			
Fleming et al. (1989)	South Lake Wyangan, Vic, Aus	1	M		0.76		
Chiew et al. (1995)	Australia	16	D & M			0.67 (FAO 24)	
Cohen et al. (2002)		1	M		1.03	0.77	
Coefficients adjusted to a screened pan coefficient							
Young (1947)*				0.82			
Penman (1948)*	Rothamsted, UK	several	6Ds & M	0.83			
Kohler et al. (1955)*				0.64 – 0.88			
Harbeck (1958)*				0.74			
Nordenson & Baker (1962)*				0.79			
Nimmo (1964)*				0.65– 0.85			
Stanhill (1969)*				0.75			
Allen & Crow (1971)*				0.80 – 0.83			
Ficke (1972)*				0.81			
Hounam (1973)*				0.77, 0.86			
Neuwirth (1973)*				0.77			
Hoy (1977)*				0.83			
Duru (1984)*				0.83			
Stanhill (2002)	World-wide	18	na	Penman ?? 0.68			
Harmsen et al. (2003)	Puerto Rico	7	M			0.84	
Sumner & Jacobs (2005)	Florida, USA	1	D			0.75	
Weiβ and Menzel (2008)	Jordon						0.43 (0.24 -0.72)

D: daily time-step, M: monthly time-step; na: not available * References from Linacre (1994)

Table S11 Monthly Class-A evaporation pan coefficients for selected Australian lakes*

Station name	Lat °S	Long °E	Jan	Feb	Mar	Apr	May	Jun	Jul	Aug	Sep	Oct	Nov	Dec
Lake Eucumbene	36.083	148.667	0.82	0.95	0.91	1.03	2.07	2.19	1.65	1.56	0.47	0.47	0.52	0.67
Cataract Reservoir	34.333	150.833	0.98	1.07	1.11	1.14	1.22	1.25	1.12	0.75	0.76	0.80	0.88	0.93
Manton Reservoir	12.833	131.083	1.13	1.09	1.06	1.01	0.94	0.85	0.79	0.75	0.83	0.88	0.91	1.10
Mundaring Reservoir	31.916	116.166	1.02	1.06	1.12	1.18	1.15	1.18	1.01	0.91	0.81	0.78	0.79	0.94
Blue Lagoon	38.183	146.366	0.92	0.95	0.94	0.91	0.88	0.88	0.7	0.77	0.94	0.94	1.06	0.96
Lake Wyangan	34.283	146.033	0.86	0.86	0.87	0.82	0.78	0.69	0.66	0.68	0.82	0.97	0.85	0.83
Rifle Creek reservoir	20.950	139.583	0.76	0.66	0.79	0.82	0.66	0.56	0.52	0.52	0.57	0.65	0.65	0.83

*All pan coefficients are extracted from Hoy and Stephens (1979)

Table S12 Annual Class-A evaporation pan coefficients for selected Australian lakes*

Station name	Lat °S	Long °E	Annual pan coefficient
Lake Menindee	32.333	142.333	0.76
Lake Pamamaroo	32.300	142..466	0.71
Lake Cawdilla	32.466	142.233	0.76
Stephens Creek Reservoir	31.833	141.500	0.74
Lake Albacutya	35.750	141.966	0.85
Lake Hindmarsh	36.083	141.916	0.79
Lake Eucumbene	36.083	148.667	0.87
Cataract Reservoir	34.333	150.833	0.98
Manton Reservoir	12.833	131.083	0.93
Mundaring Reservoir	31.916	116.166	1.00
Blue Lagoon	38.183	146.366	0.94
Lake Wyangan South	34.283	146.033	0.82
Rifle Creek Reservoir	20.950	139.583	0.68
Lake Albert	35.633	139.333	0.87
Callide Dam	24.400	150.617	0.87
Lake Alexandrina	35.750	139.283	0.66

*All pan coefficients are extracted from Hoy and Stephens (1979) except for Callide Dam and Lake Alexandrina which are taken from Weeks (1982) and Kotwicki (1994, Table 2) respectively.

Table S13 Comparison of annual estimates of evaporation (mm day^{-1}) at six Australian locations by 13 daily and monthly models plus Class-A pan and mean annual rainfall for period January 1979 to March 2010*. (P56: Penman 1956; PT: Priestley-Taylor; Ma: Makkink; FAO56 RC: FAO-56 Reference Crop; BC: Blaney-Criddle; HS: Hargreaves-Samani; mod H: modified Hargreaves; Tu: Turc; Mo: Morton CRAE; BS: Brutsaert-Strickler; GG: Granger-Gray; SJ: Szilagyi-Jozsa; Th: Thornthwaite; PP; PenPan (adjusted for bird screen)

		Pen56	PT	Ma	FAO56 RC	BC	HS	mod H	Tu	Mo	BS	GG	SJ	Th	PP	Class-A pan
9021 Perth Airport (31.9275°S, 115.9764°E) rain: 708 mm	Daily (D)	1908	1609	1123	1567	1182	1629		1385		736	799	701		2398	2090
	Daily ratio	**1.00**	0.84	0.59	**1.00**	0.75	1.04		0.85		**1.00**	1.09	0.95		**1.00**	0.87
	Monthly (M)	1908	1626	1126	1571	1072	1383	1537	1349	600	773	794	738	896	2378	
	M to D ratio	**1.000**	**1.011**	**1.003**	**1.003**	**0.907**	**0.849**		**0.974**		**1.050**	**0.994**	**1.053**		**0.992**	
14015 Darwin Airport (12-4239°S, 130.8925°E) rain: 1723 mm	Daily (D)	2240	2195	1382	1823	1332	1639		1674		1515	1140	1531		2699	2548
	Daily ratio	**1.00**	0.98	0.62	**1.00**	0.73	0.90		0.92		**1.00**	0.75	1.01		**1.00**	0.94
	Monthly (M)	2238	2200	1381	1821	1238	1620	1259	1664	1247	1529	1136	1545	1966	2690	
	M to D ratio	**0.999**	**1.002**	**0.999**	**0.999**	**0.929**	**0.988**		**0.994**		**1.009**	**0.996**	**1.009**		**0.997**	
15590 Alice Springs Airport (23.7951°S, 133.8890°E) rain: 296 mm	Daily (D)	2299	1785	1321	2012	1703	2396		1854		537	805	360		3085	3210
	Daily ratio	**1.00**	0.78	0.57	**1.00**	0.85	1.19		0.92		**1.00**	1.50	0.67		**1.00**	1.04
	Monthly (M)	2313	1814	1326	2031	1573	2019	2048	1811	90.3	584	801	407	1152	3079	
	M to D ratio	**1.006**	**1.016**	**1.004**	**1.009**	**0.924**	**0.843**		**0.977**		**1.088**	**0.995**	**1.131**		**0.998**	
40842	Daily	1819	1709	1130	1427	930	1355		1366		1070	912	1107		2157	1937

Brisbane Aero (27.3917°S, 153.1292°E) rain: 1168 mm	(D)															
	Daily ratio	**1.00**	0.94	0.62	**1.00**	0.65	0.95		0.96		**1.00**	0.85	1.03		**1.00**	0.90
	Monthly (M)	1821	1720	1132	1433	797	1285	1247	1363	894	1090	910	1125	991	2154	
	M to D ratio	**1.001**	**1.006**	**1.002**	**1.004**	**0.857**	**0.948**		**0.998**		**1.019**	**0.998**	**1.016**		**0.999**	
86282 Melbourne Airport 37.6655°S, 144.8321°E) rain: 482 mm	Daily (D)	1652	1217	826	1361	559	1361		1000		349	624	328		2123	1757
	Daily ratio	**1.00**	0.74	0.50	**1.00**	0.41	1.00		0.73		**1.00**	1.79	0.94		**1.00**	0.83
	Monthly (M)	1611	1231	828	1317	409	1057	1165	993	447	422	609	400	744	2022	
	M to D ratio	**0.975**	**1.012**	**1.002**	**0.968**	**0.732**	**0.777**		**0.993**		**1.209**	**0.976**	**1.220**		**0.952**	
94069 Grove (42.9831°S, 147.0772°E) rain: 693 mm	Daily (D)	1014	991	656	770	116	1173		777		630	589	704		1108	987
	Daily ratio	**1.00**	0.98	0.65	**1.00**	0.15	1.52		1.01		**1.00**	0.93	1.12		**1.00**	0.89
	Monthly (M)	1004	996	657	758	34	899	1005	777	391	653	597	744	654	1082	
	M to D ratio	**0.990**	**1.005**	**1.002**	**0.984**	**0.293**	**0.766**		**1.000**		**1.037**	**1.014**	**1.057**		**0.977**	

*All annual estimates are based on the sum of the average monthly values for the concurrent period of observation at each station.

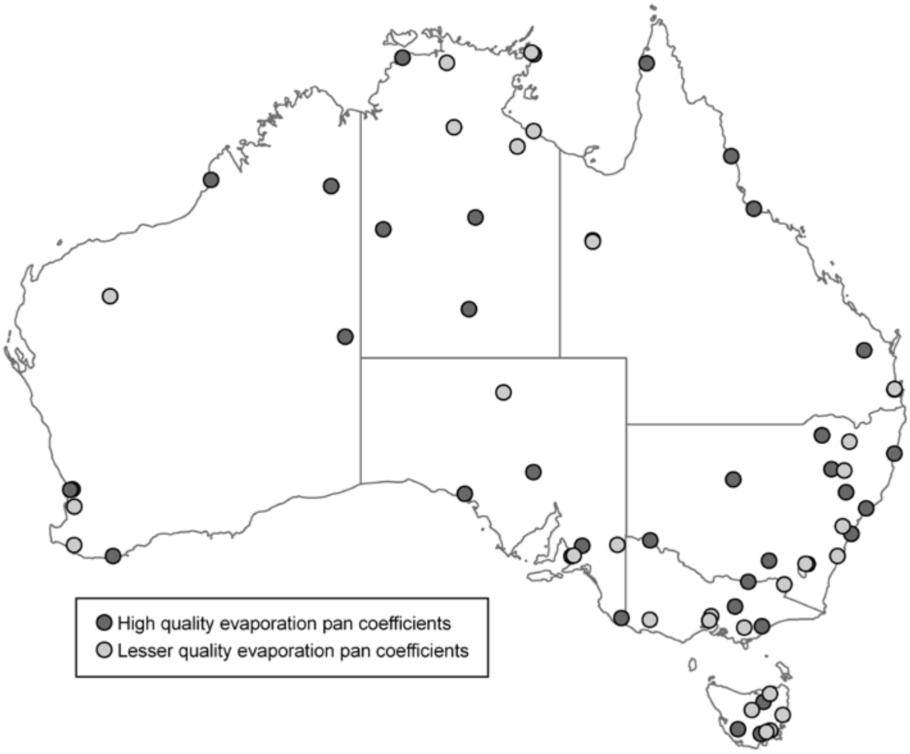

Figure S1 Location of the 68 Automatic Weather Stations and Class-A evaporation pans (of which 39 pans are high quality) used in the analyses

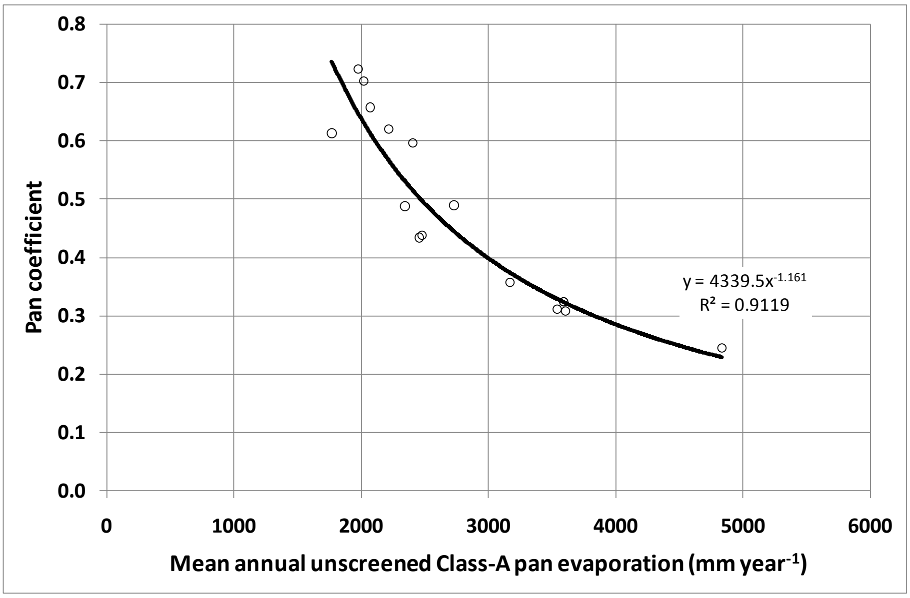

Figure S2 Plot showing Priestley-Taylor pan coefficients against mean annual unscreened Class-A pan evaporation based on six years of climate station data in Jordon (Weiβ and Menzel, 2008)

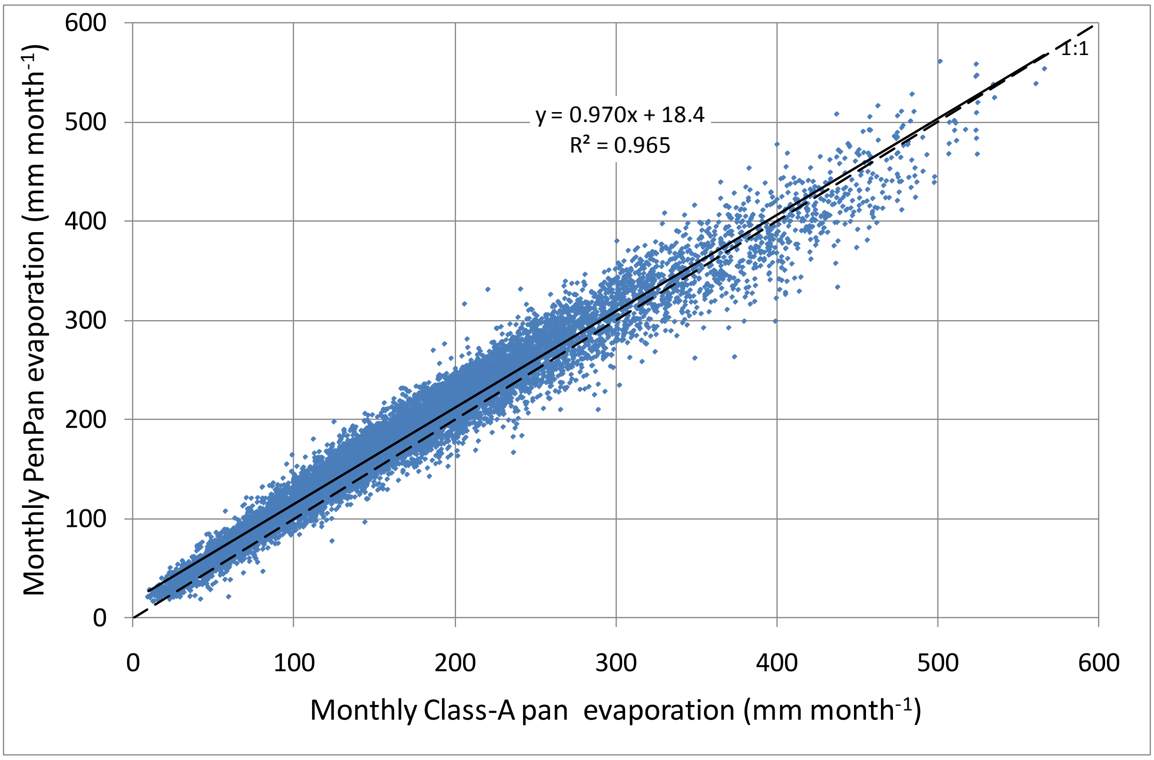

Figure S3 Comparison of monthly PenPan evaporation and Class-A pan evaporation for 68 Australian climate stations